Study of nuclear excitations via proton inelastic scattering and related topics at RCNP

A. Tamii

Research Center for Nuclear Physics, Osaka University

Yomeimon Gate at Toshogu Temple in Nikko, Japan in 17th century

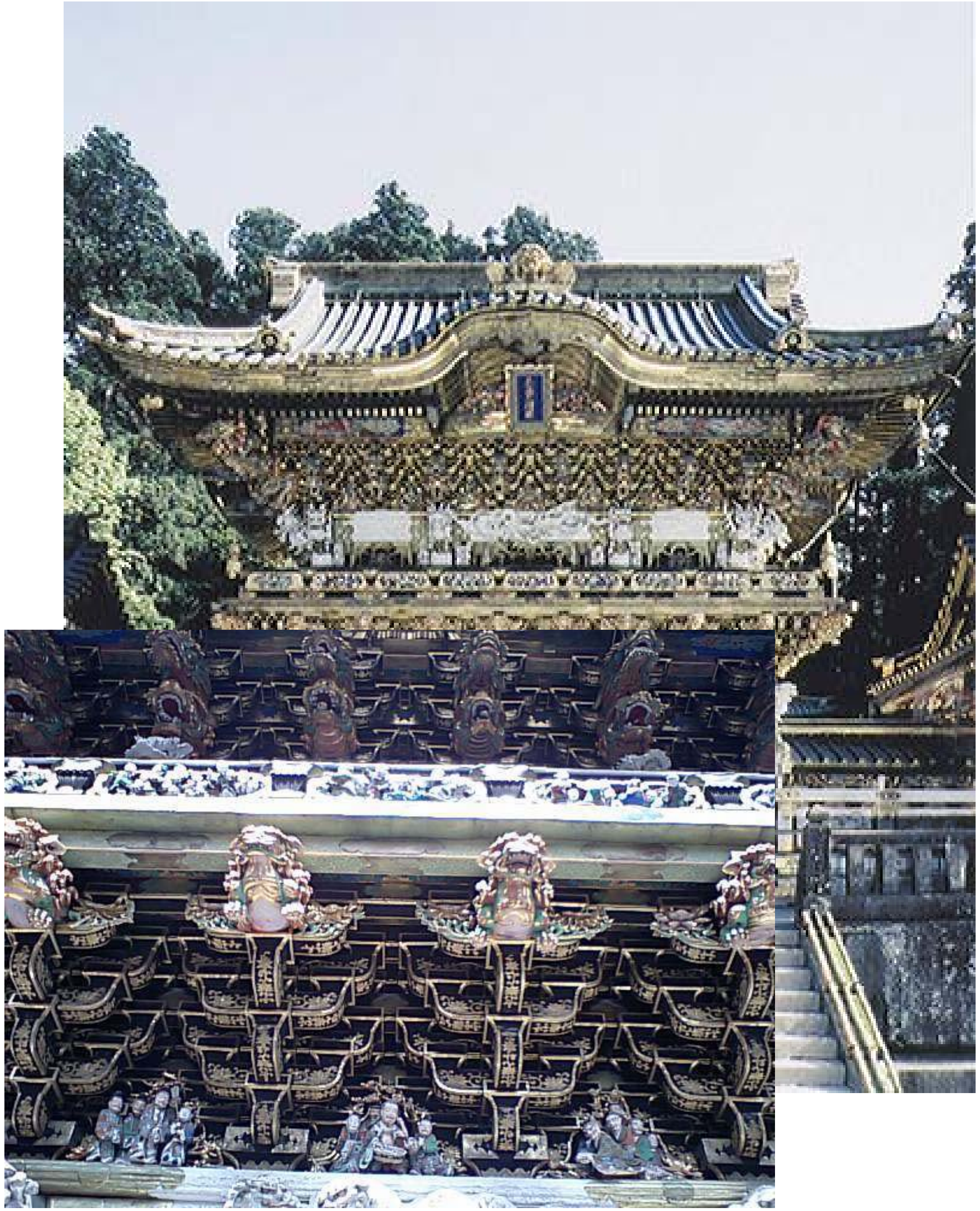

The gate looks fully symmetric.
But...

There is intentional error in the symmetry.
Why?

People were afraid that God did not like a perfect work made by human-being.

It seems that God likes symmetry breaking...

This is the part in my talk related to symmetries. The rest of my talk is related to spin, nuclear spin excitations.

Outline

- Overview of the RCNP cyclotron facility
- High resolution proton inelastic scattering experiment at zero degrees
- Summary

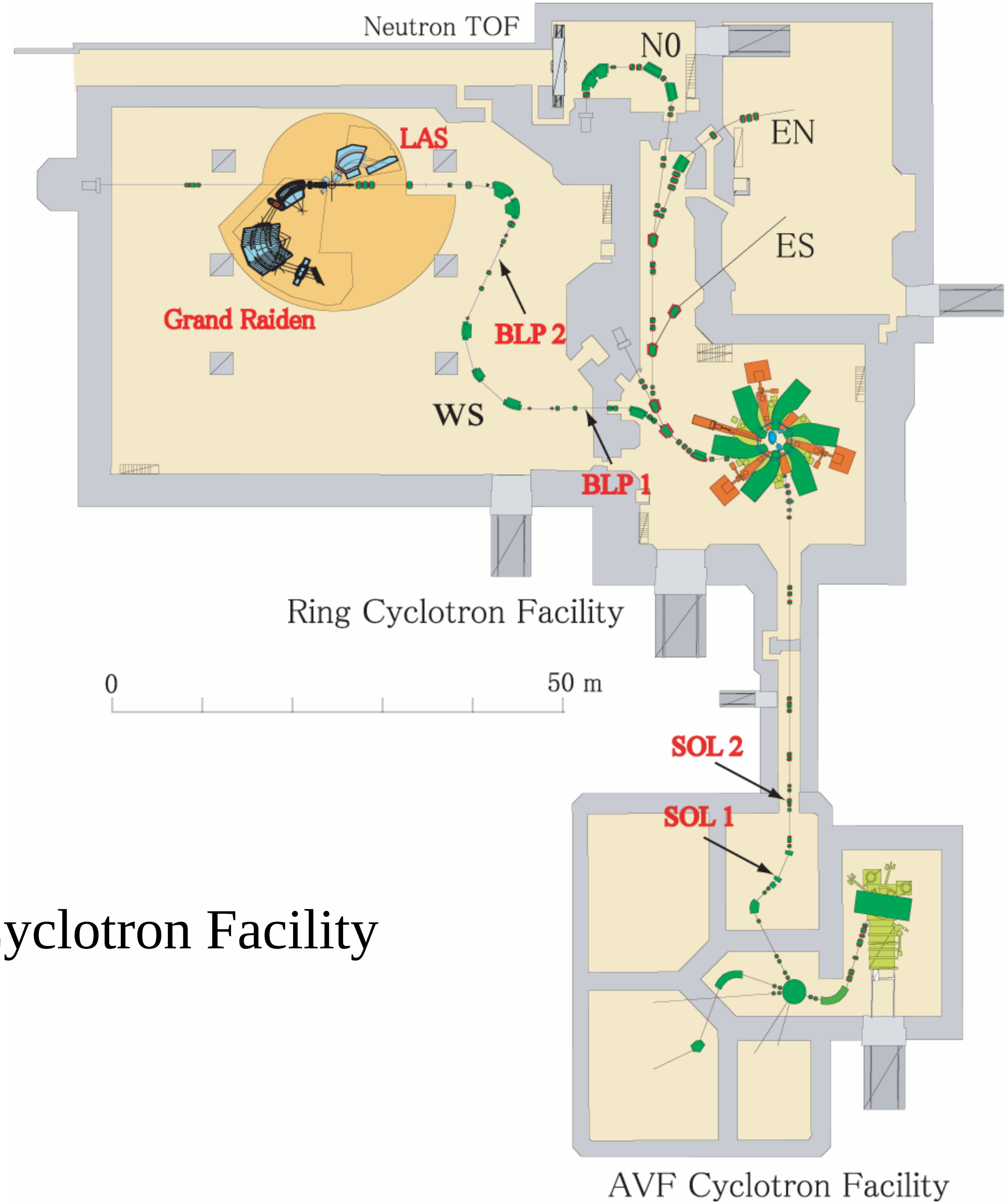

RCNP Cyclotron Facility

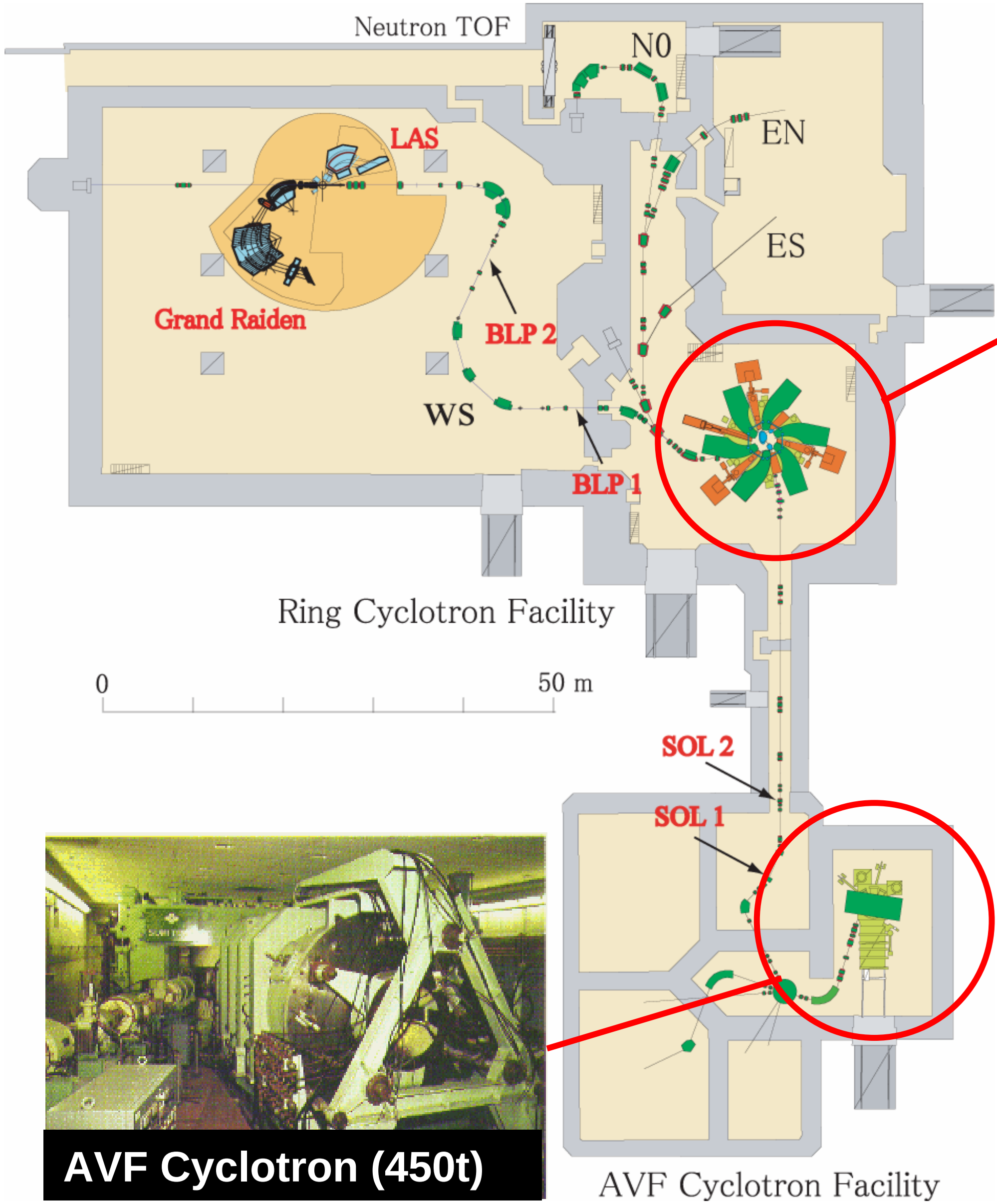

AVF Cyclotron (450t)

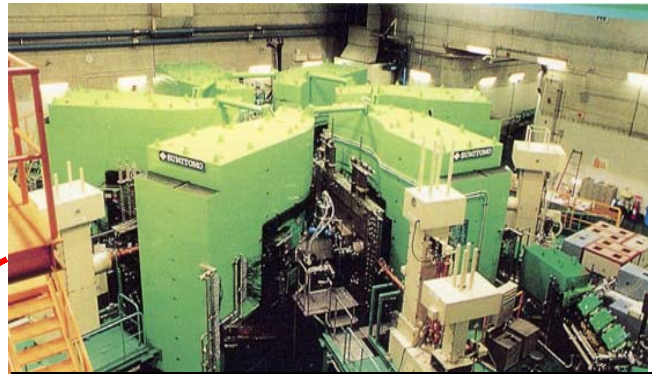

RING Cyclotron (2,200t)

K=400

- proton beams
  < 400 MeV, ~ 1μA
- 3He beams
  < 150 MeV/A
- d, α, ^{6}Li
  < 100 MeV/A
- Heavy ion beams

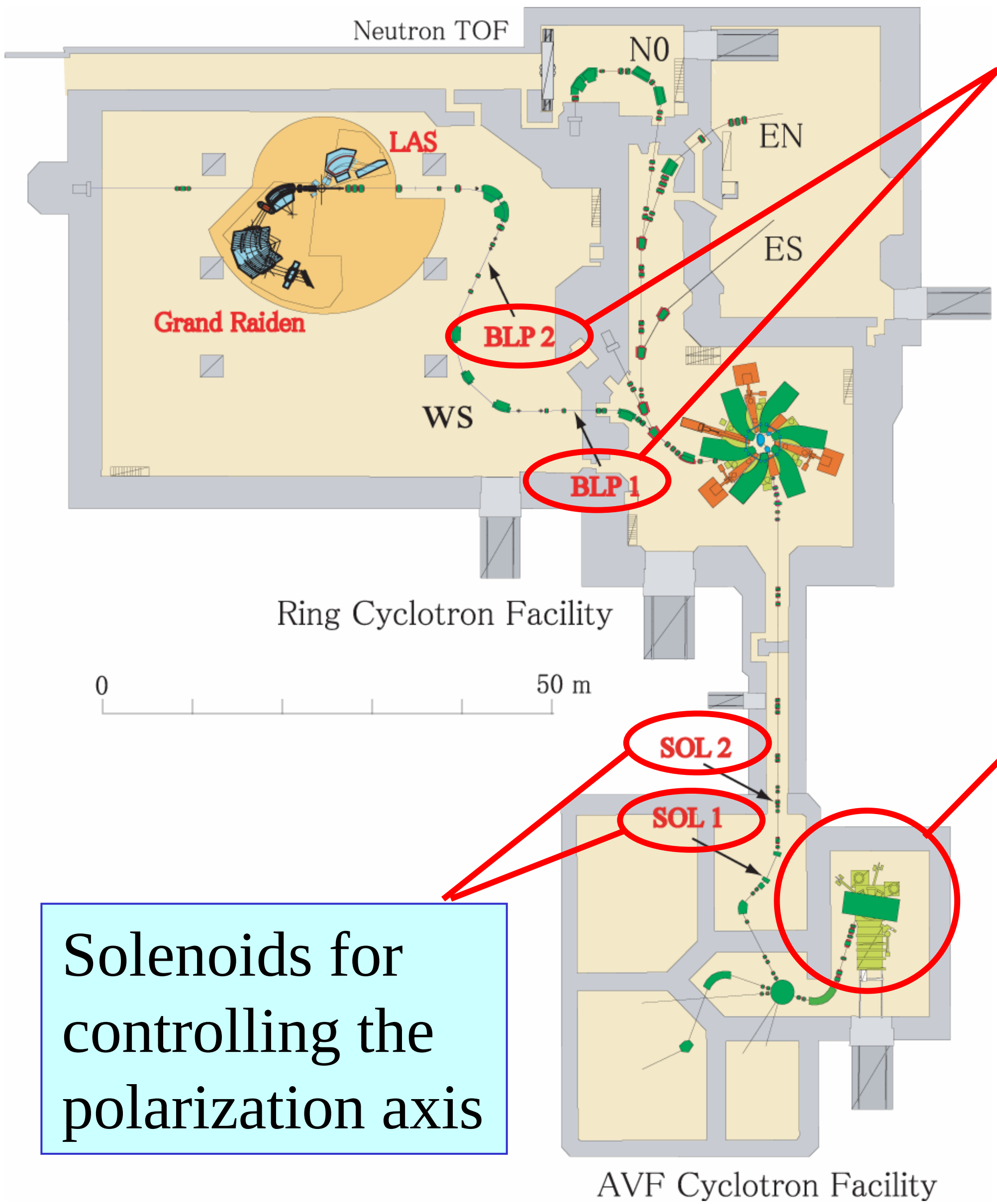

Beam line polarimeters for pol. measurement

Solenoids for controlling the polarization axis

Ion Sources

- Polarized p/d Ion Source
  pol. ~ 70%
- Neomafios
  light ions
- 18GHz SC ECRIS
  heavy ions

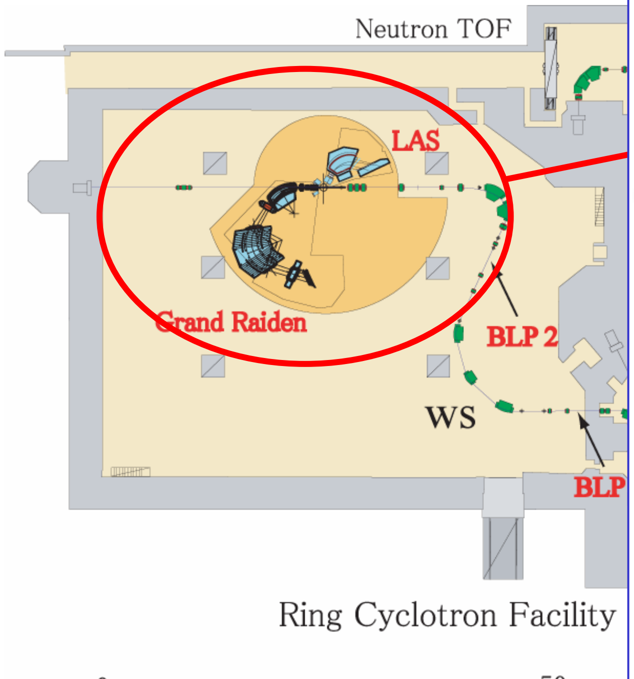

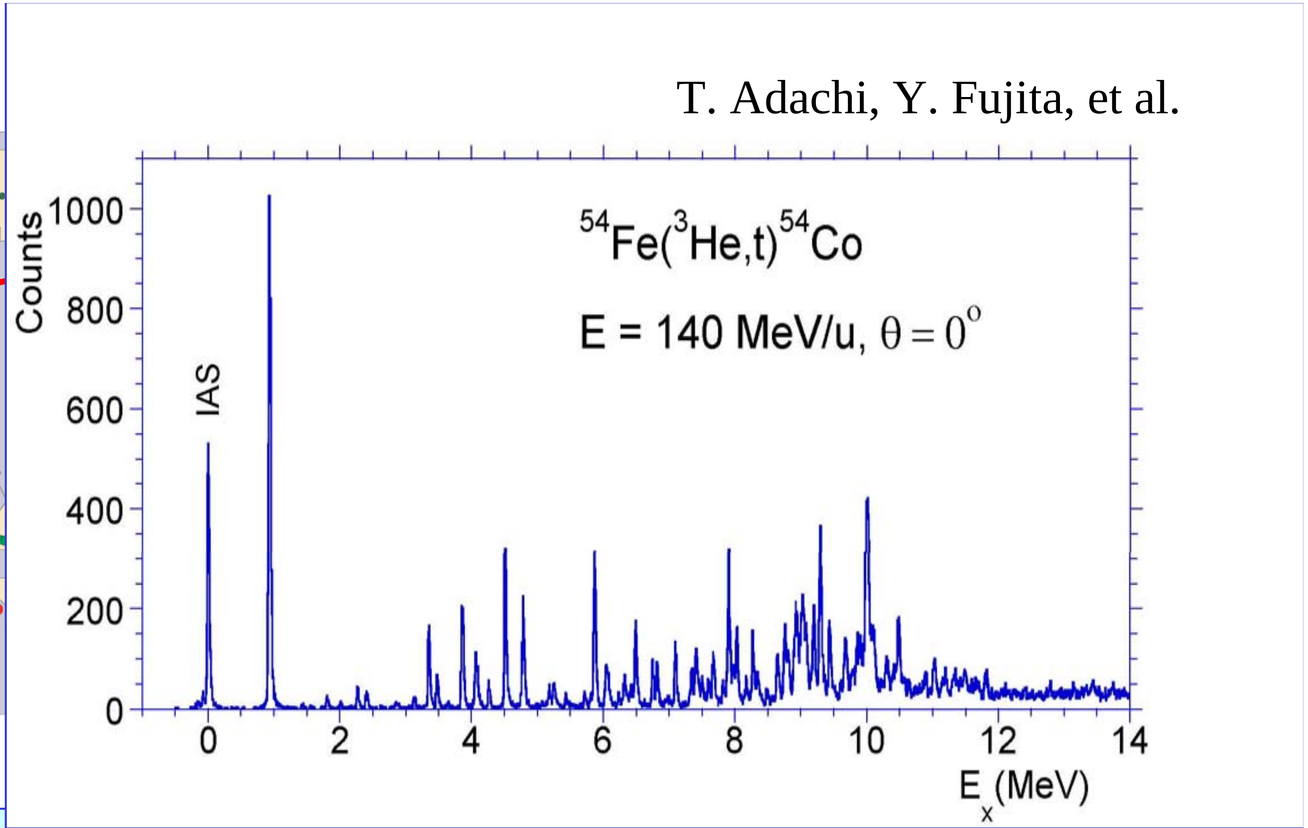

Grand Raiden & Large Acceptance Spectrometer (LAS)
(high-resolution and/or coincidence measurements)

- elastic/inelastic scattering: (p,p’), (d,d’), (α,α’), ...
- charge exchange reactions: (^{3}He,t), (^{7}Li,^{7}Be), ...
- transfer/pick-up reactions: (p,d), (p,t), (d,^{3}He), ...
- coincidence measurements: (p,pp), (p,pd), ...

100m n-TOF course

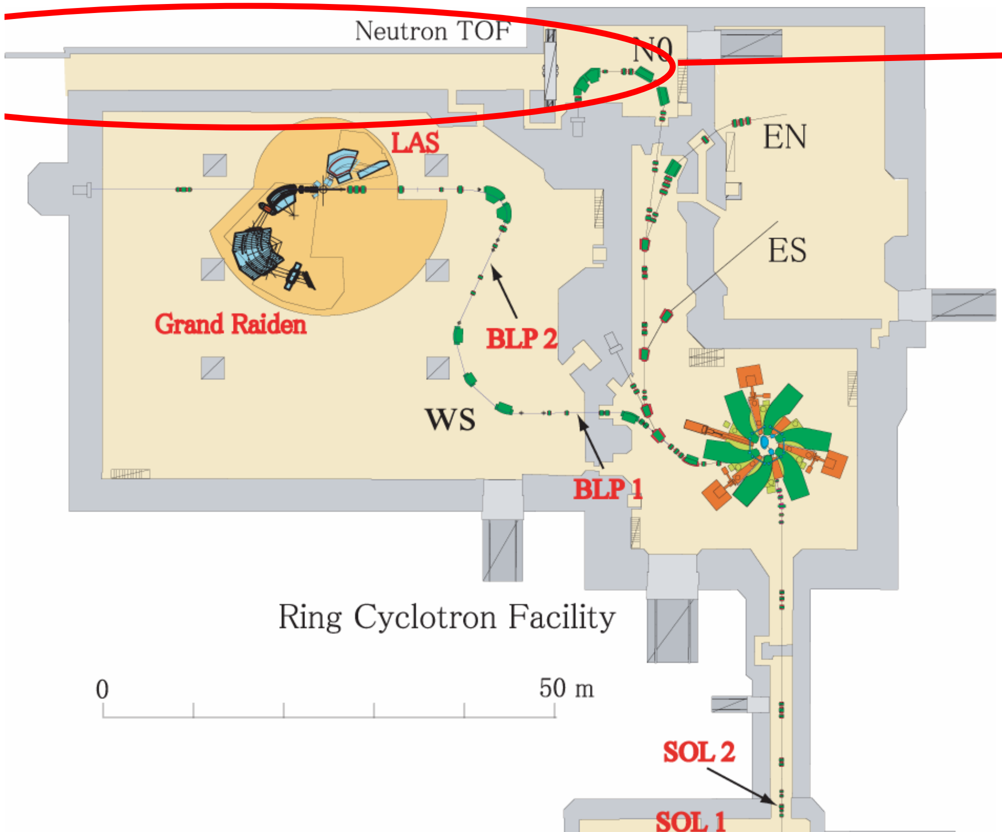

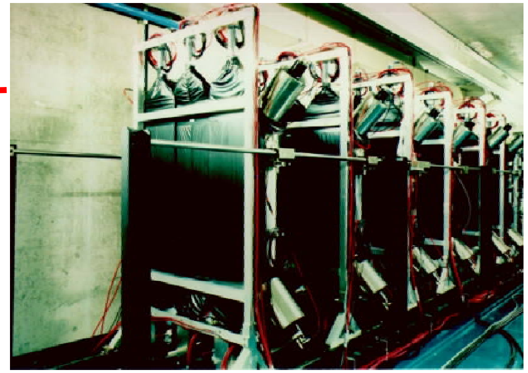

Neutron Polarimeter (NPOL-2)

T. Wakasa et al., K. Yako et al.

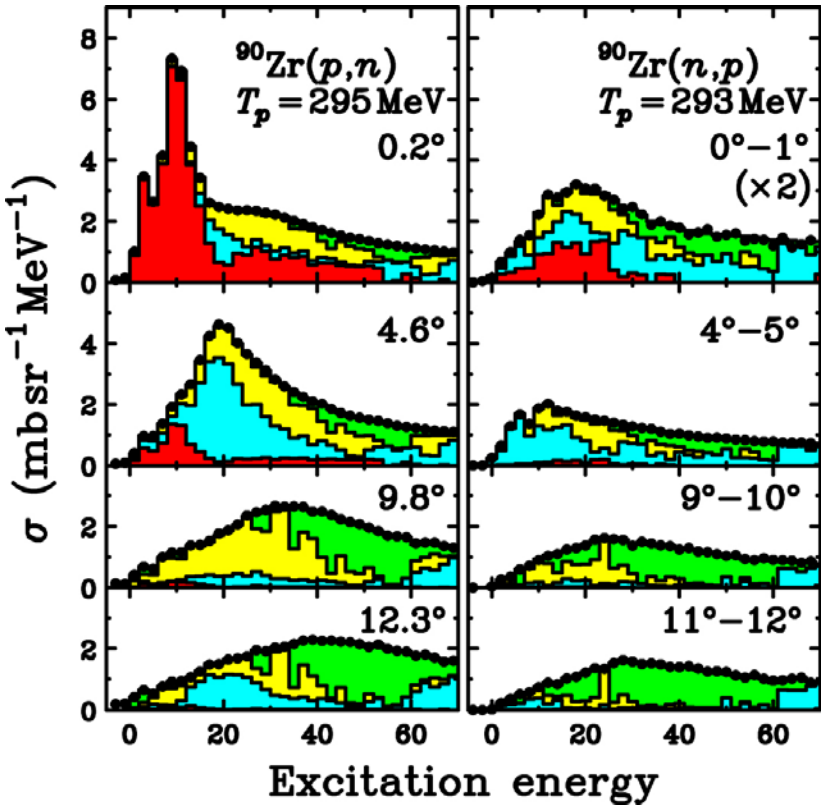

Neutron TOF course and Neutron Polarimeter (NPOL-2,3)

- (p,n) measurements for any spin-transfer coefficient

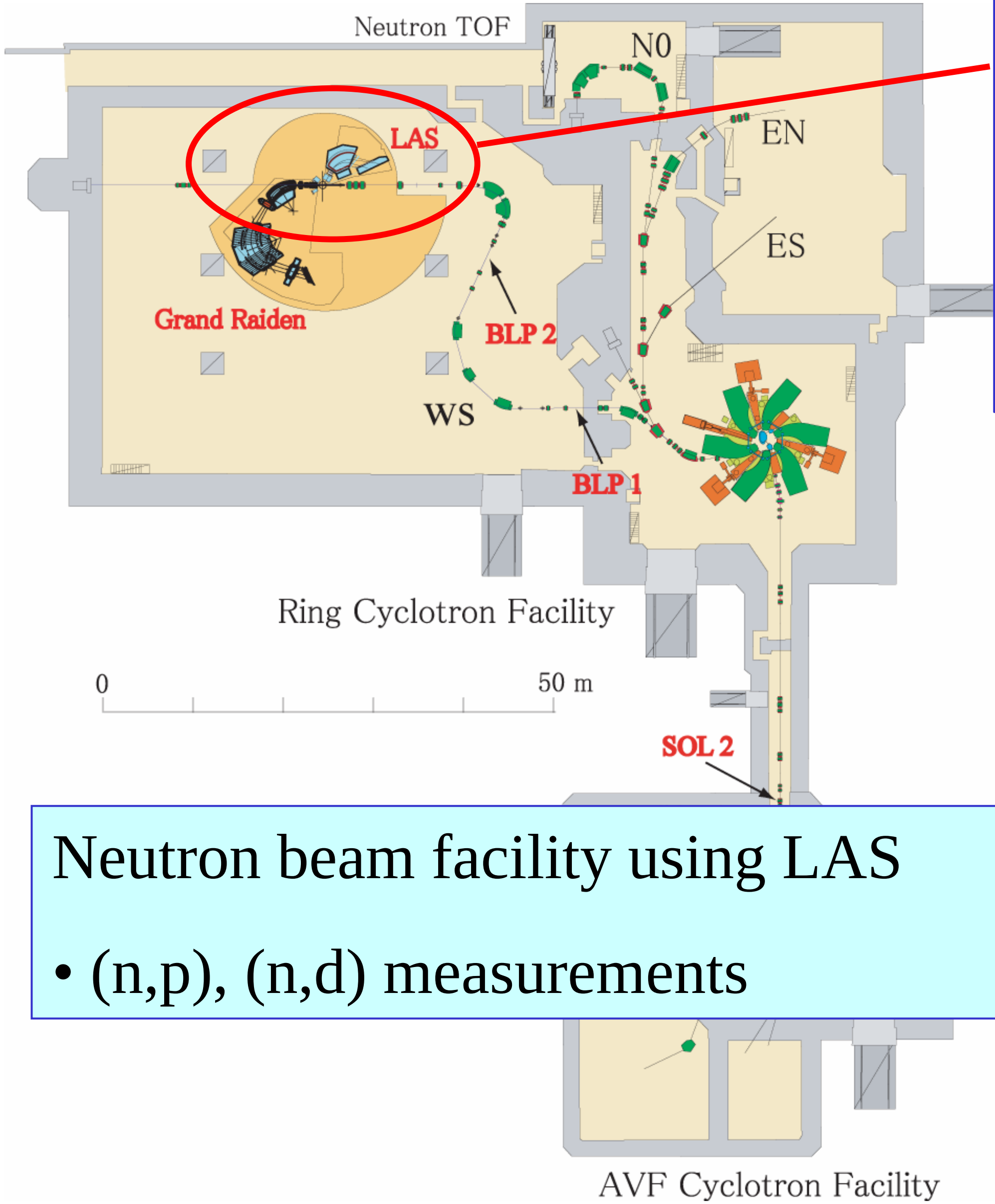

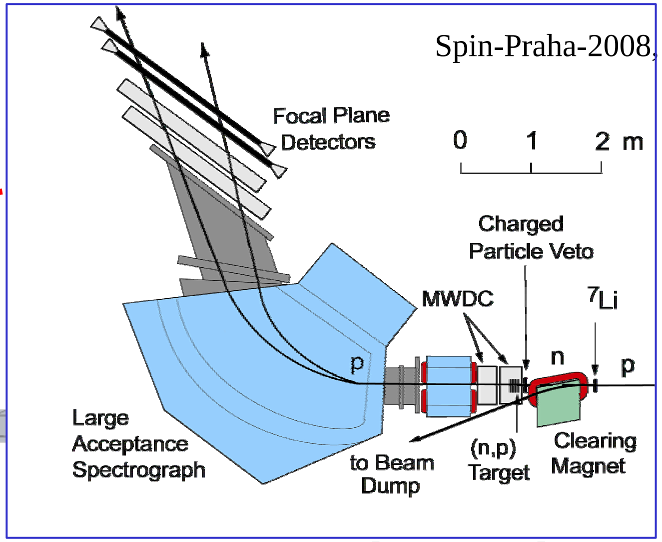

Neutron beam facility

T. Wakasa et al., K. Yako et al.

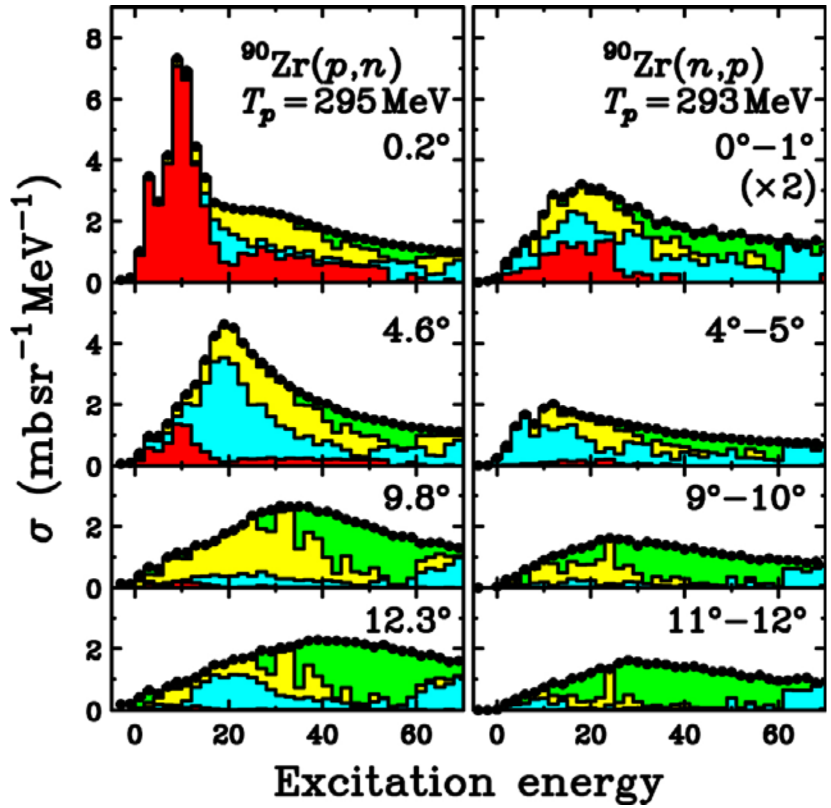

Neutron beam facility using LAS

- (n,p), (n,d) measurements

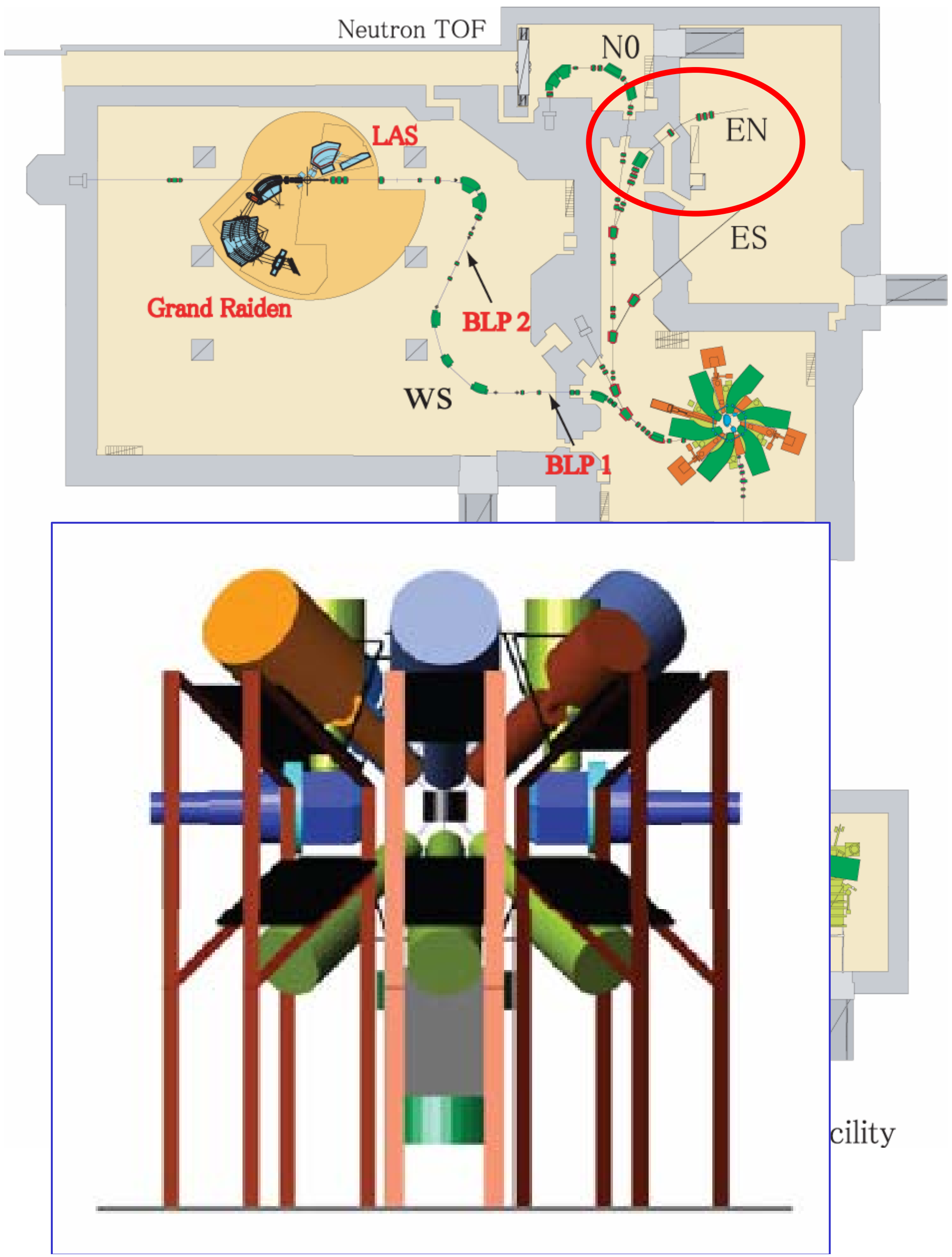

Experiments with unstable nuclei

- High-spin shape isomer search
  HPGe array
  (11 HPGe's, 25-35% thick)
- magnetic moment of unstable nuclei (β-NMR)

A. Odahara, T. Shimoda, et al.
K. Matsuta, et al.

Y. Masuda, K. Hatanaka, et al.

Test of a ultra-cold neutron source

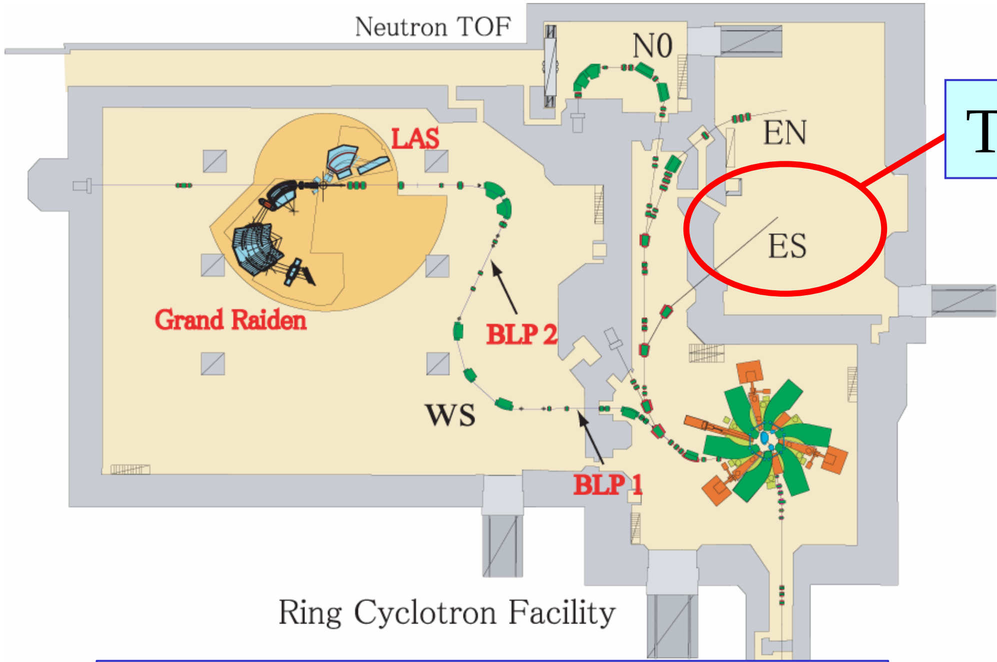

Spallation UCN source

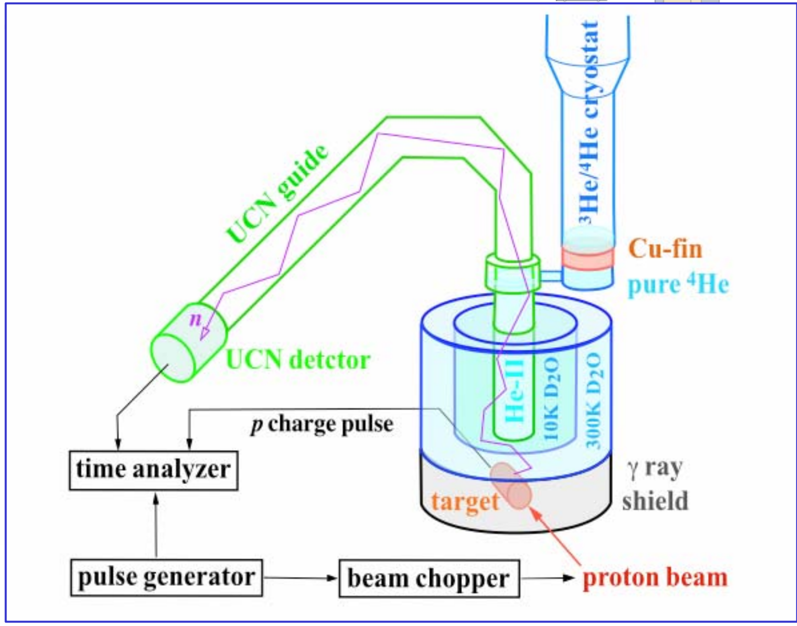

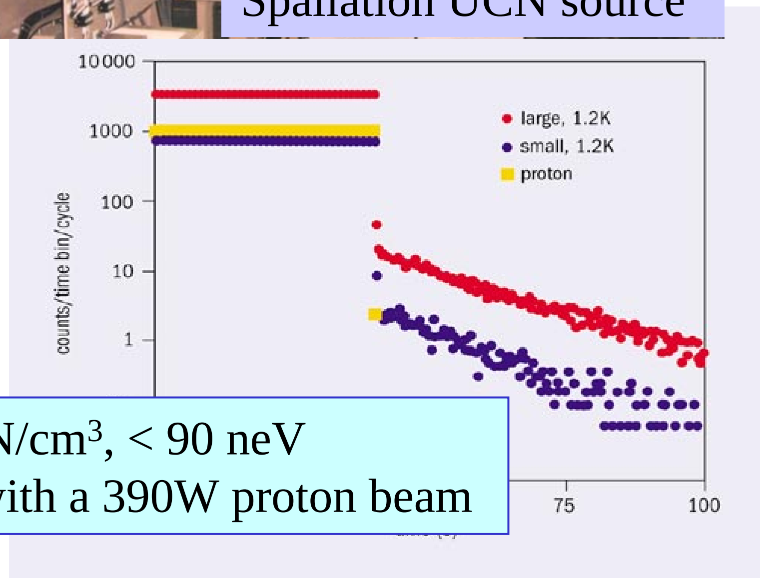

15 UCN/cm^3, < 90 neV
at 1K with a 390W proton beam

High-Resolution Proton Inelastic-Scattering experiment at zero degrees

Collaborators

RCNP, Osaka University

A. Tamii, H. Matsubara, T. Adachi, K. Fujita, H. Hashimoto,
K. Hatanaka, Y. Tameshige and M. Yosoi

Dep. of Phys., Osaka University

Y. Fujita

Dep. of Phys., Kyoto University

H. Sakaguchi and J. Zenihiro

CNS, Univ. of Tokyo

T. Kawabata, K. Nakanishi,
Y. Shimizu and Y. Sasamoto

CYRIC, Tohoku University

M. Itoh and Y. Sakemi

Dep. of Phys., Kyushu University

M. Dozono

Dep. of Phys., Niigata University

Y. Shimbara

KVI, Univ. of Groningen

L.A. Popescu

IFIC-CSIC, Univ. of Valencia

B. Rubio and A.B. Perez-Cerdan

Sch. of Science Univ. of Witwatersrand

J. Carter and H. Fujita

iThemba LABS

F.D. Smit

IKP, TU-Darmstadt

P. von Neumann-Cosel, A. Richter,
I. Poltoratska, V. Ponomarev
and K. Zimmer

Experimental Setup

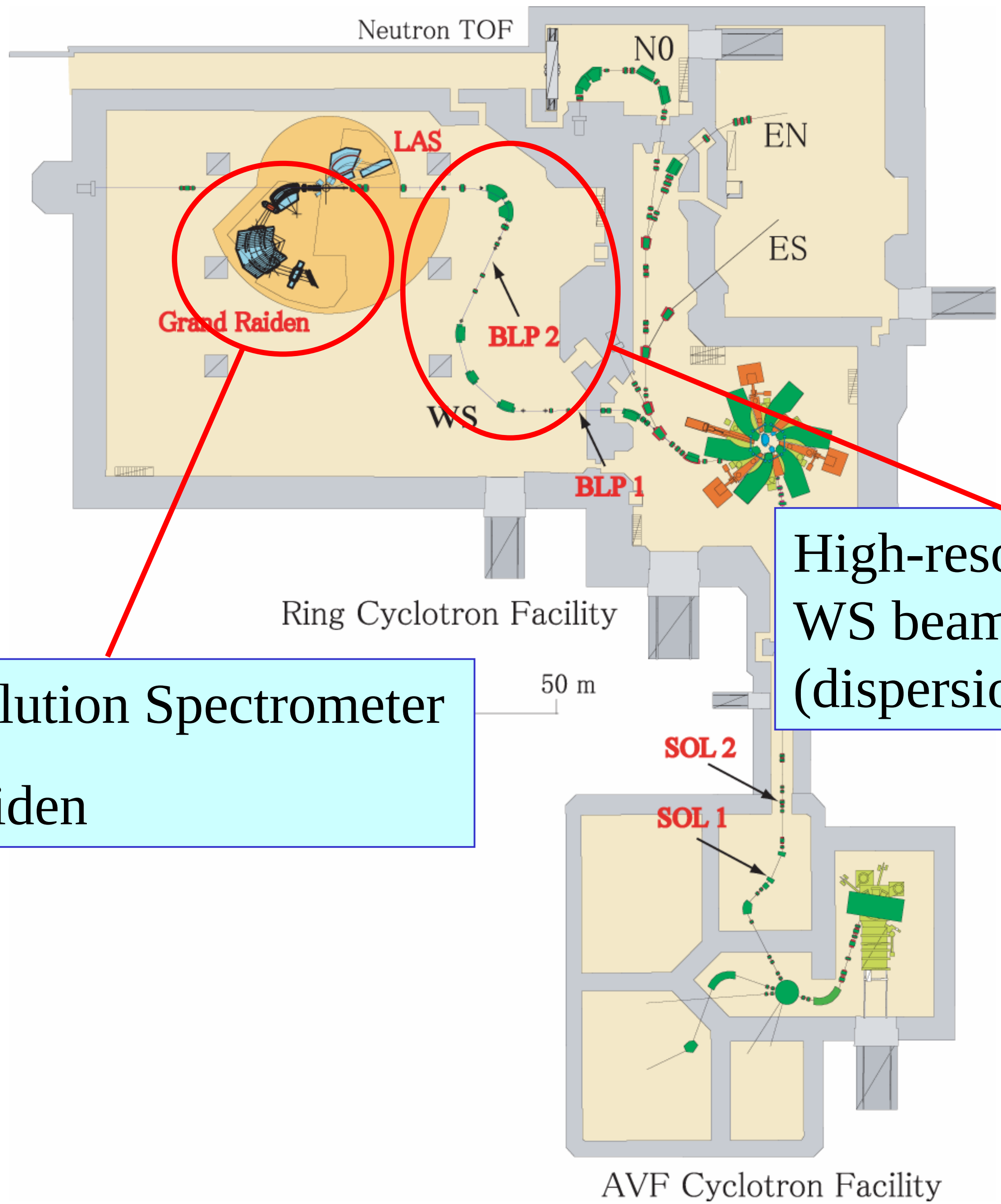

High-resolution Spectrometer

Grand Raiden

High-resolution
WS beam-line
(dispersion matching)

Spectrometers in the 0-deg. experiment setup

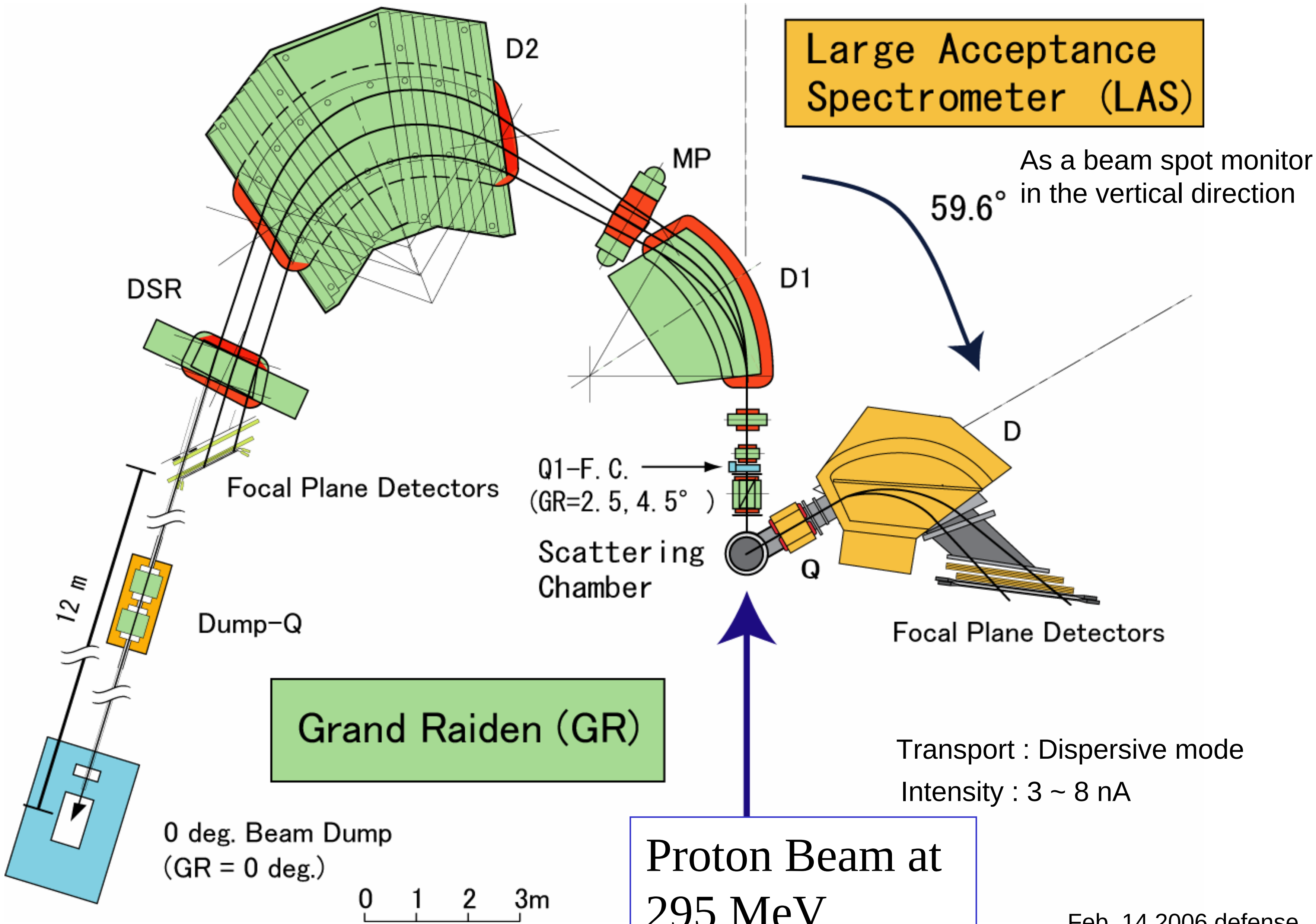

Transport : Dispersive mode

Intensity : 3 ~ 8 nA

Proton Beam at 295 MeV

Feb. 14 2006 defense

Grand Raiden in the 0deg Measurement Setup

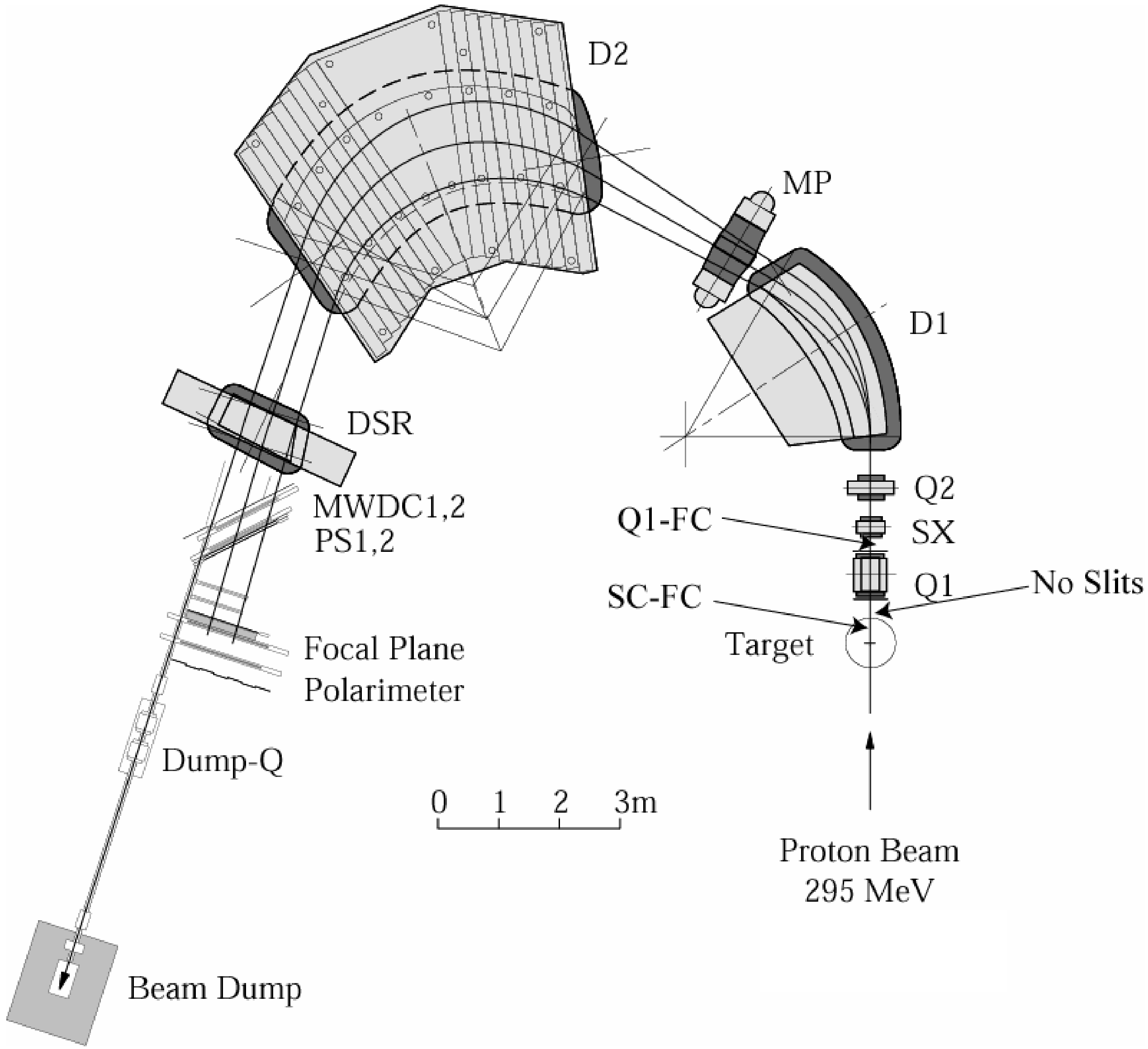

Grand Raiden in the 0deg Measurement Setup

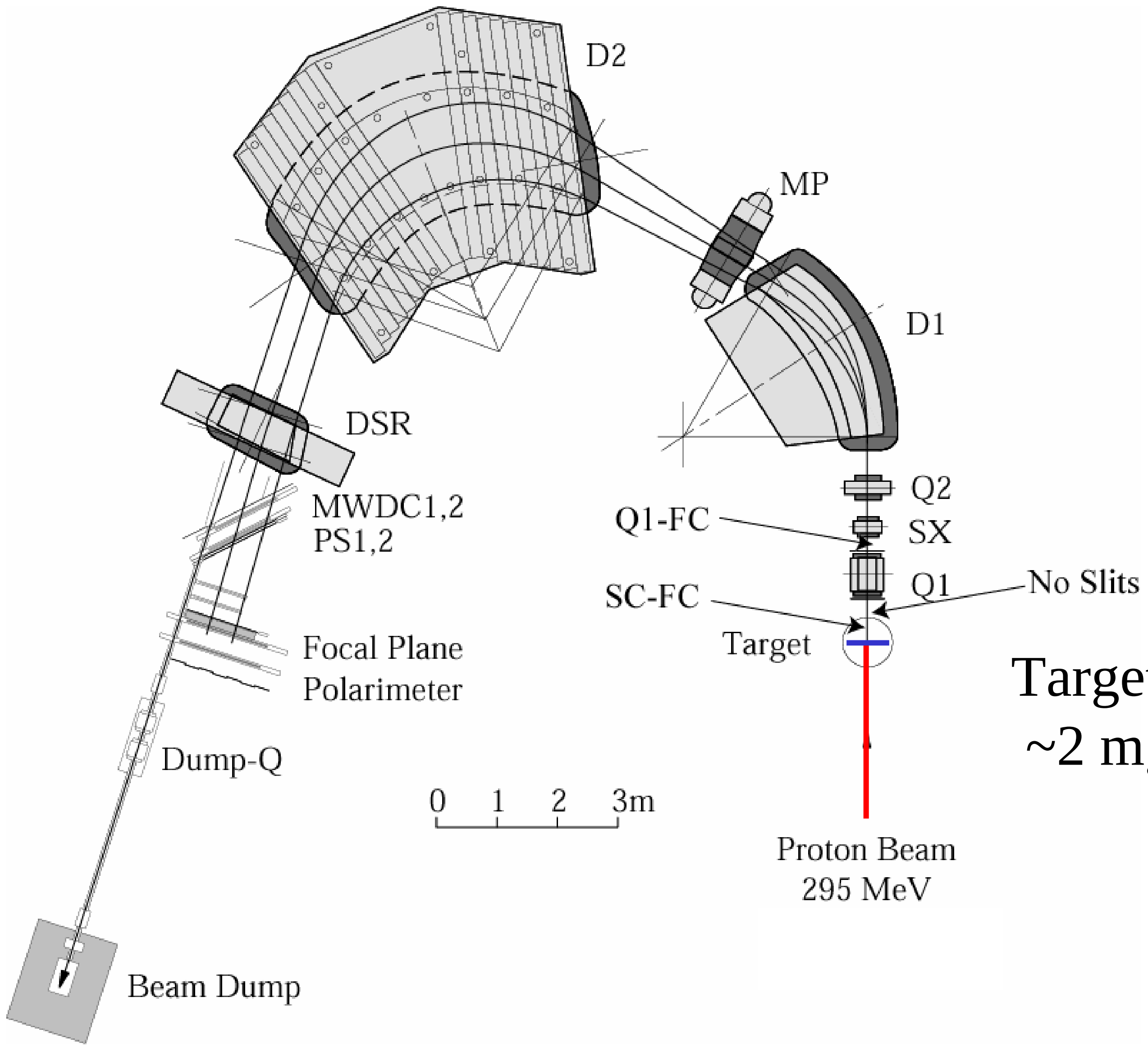

Target foil:
~2 mg/cm^2

Grand Raiden in the 0deg Measurement Setup

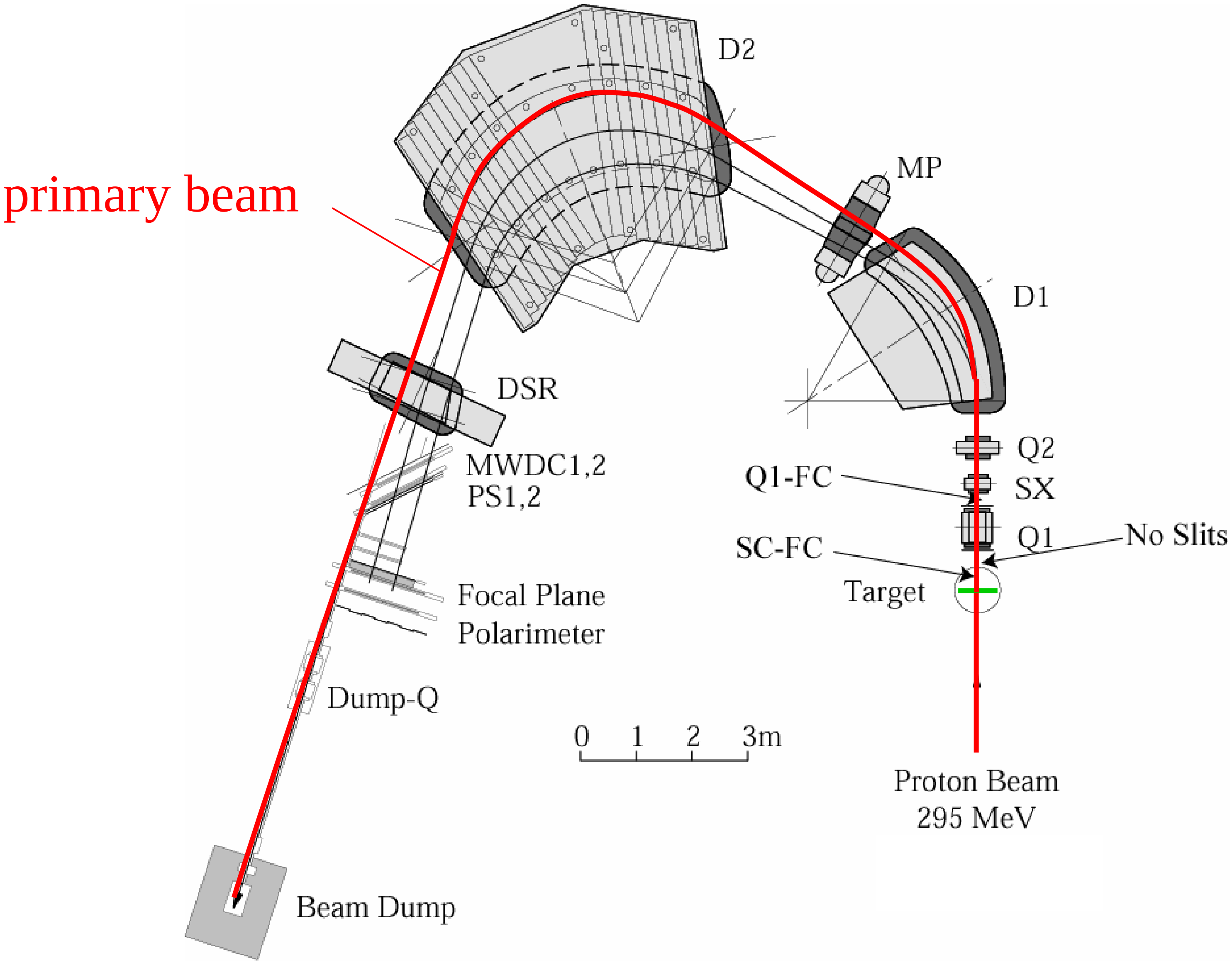

Grand Raiden in the 0deg Measurement Setup

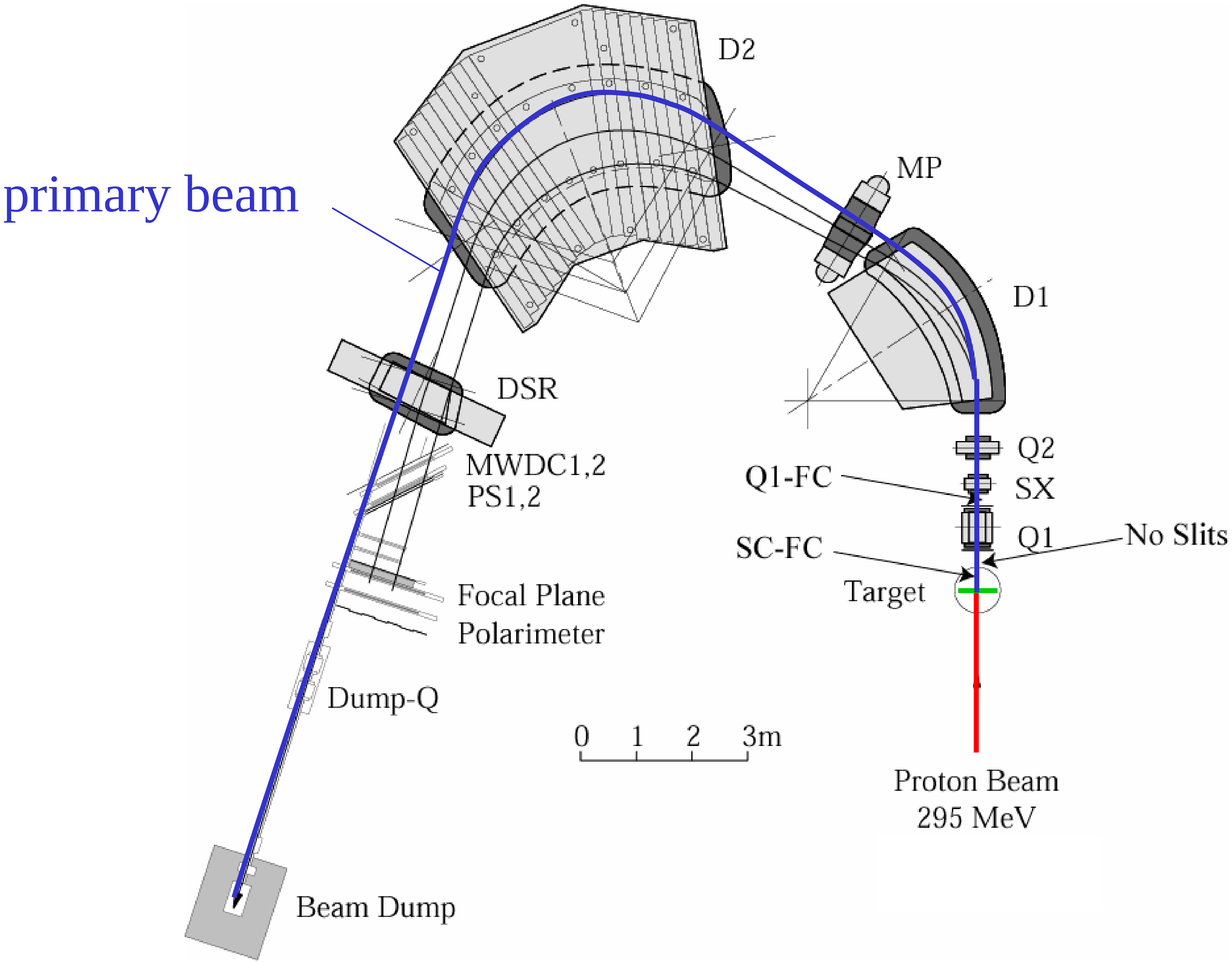

Grand Raiden in the 0deg Measurement Setup

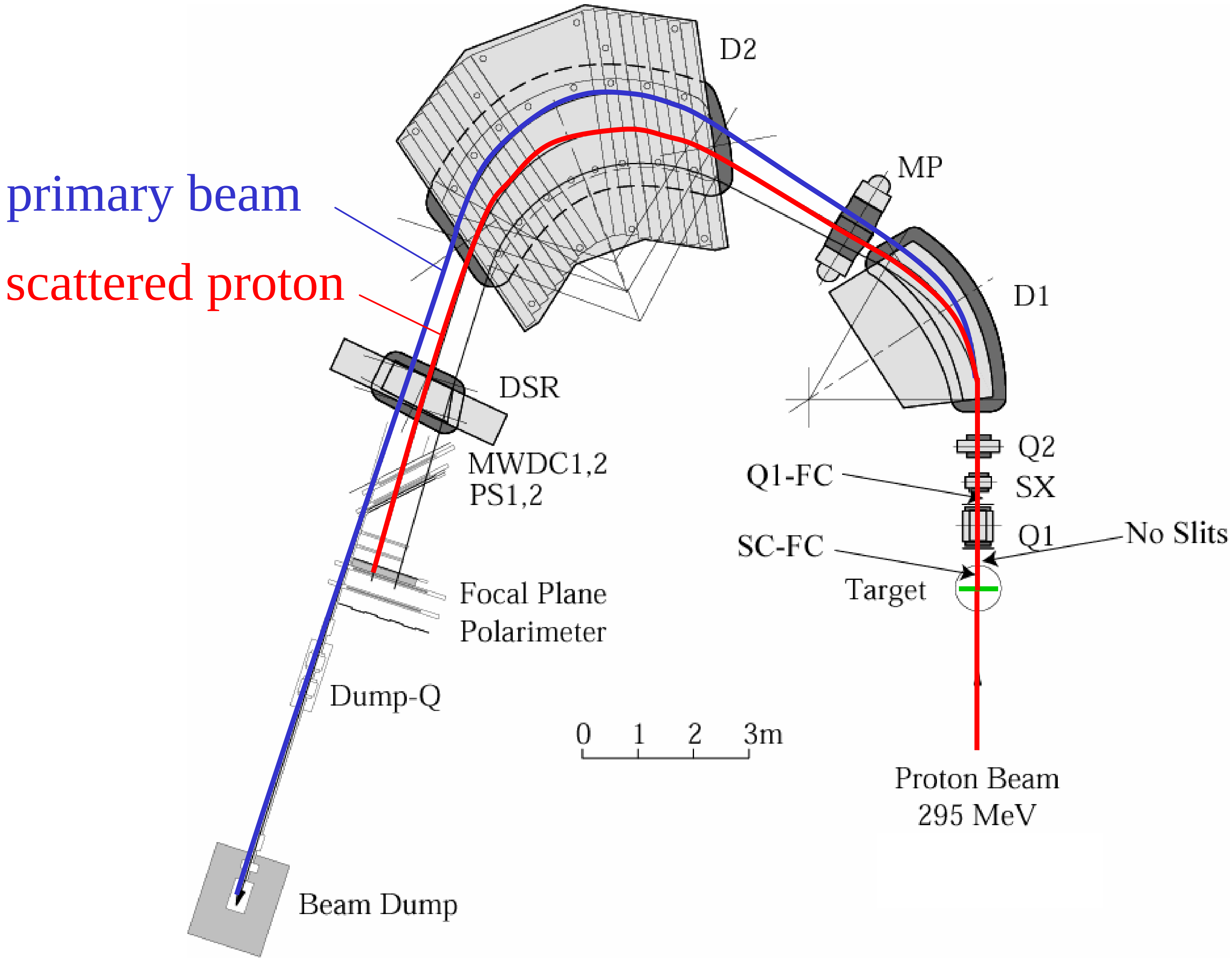

Grand Raiden in the 0deg Measurement Setup

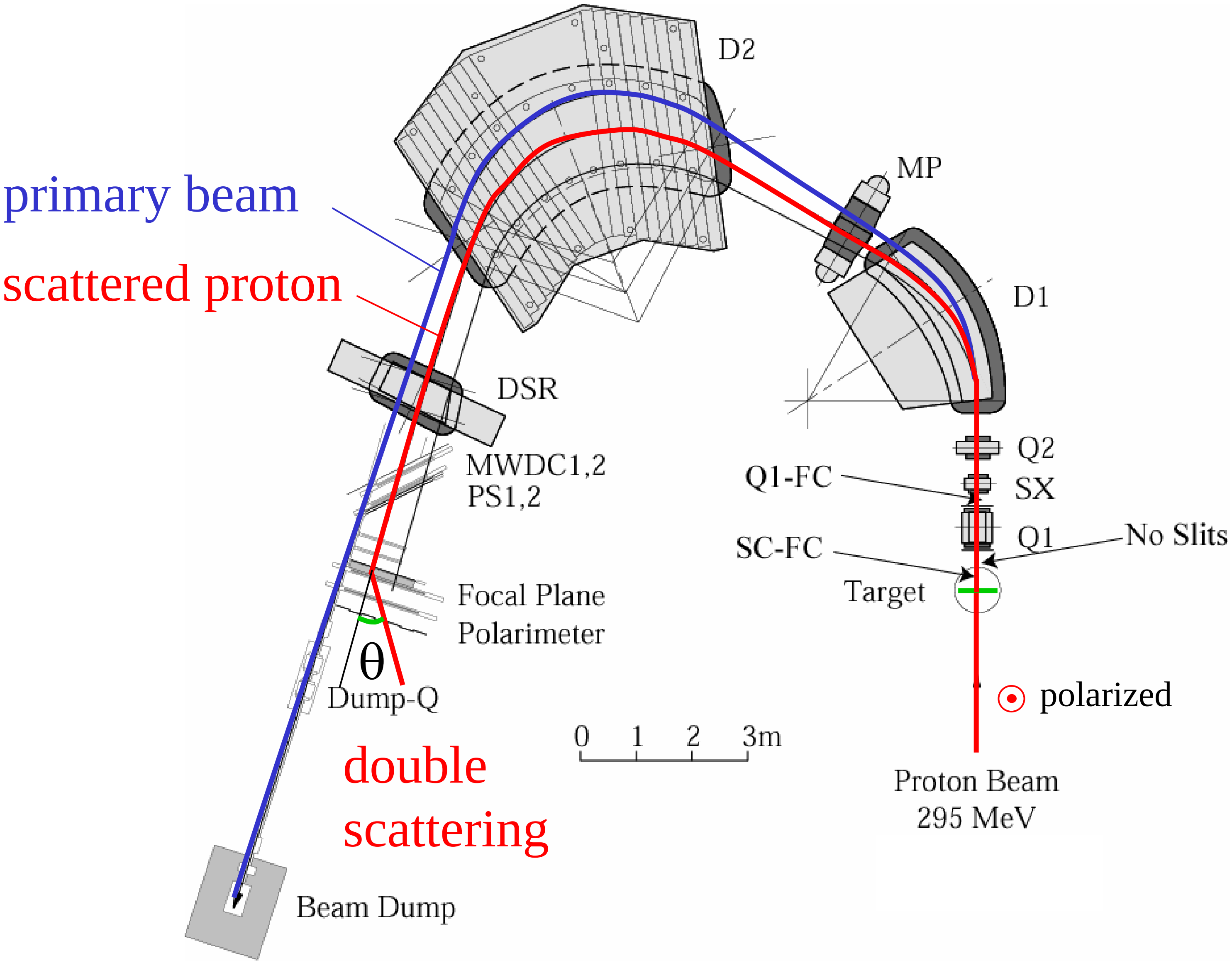

Grand Raiden in the 0deg Measurement Setup

in spin-transfer measurements

$$p_{y'} = \frac{1}{A_y}\frac{L-R}{L+R}$$

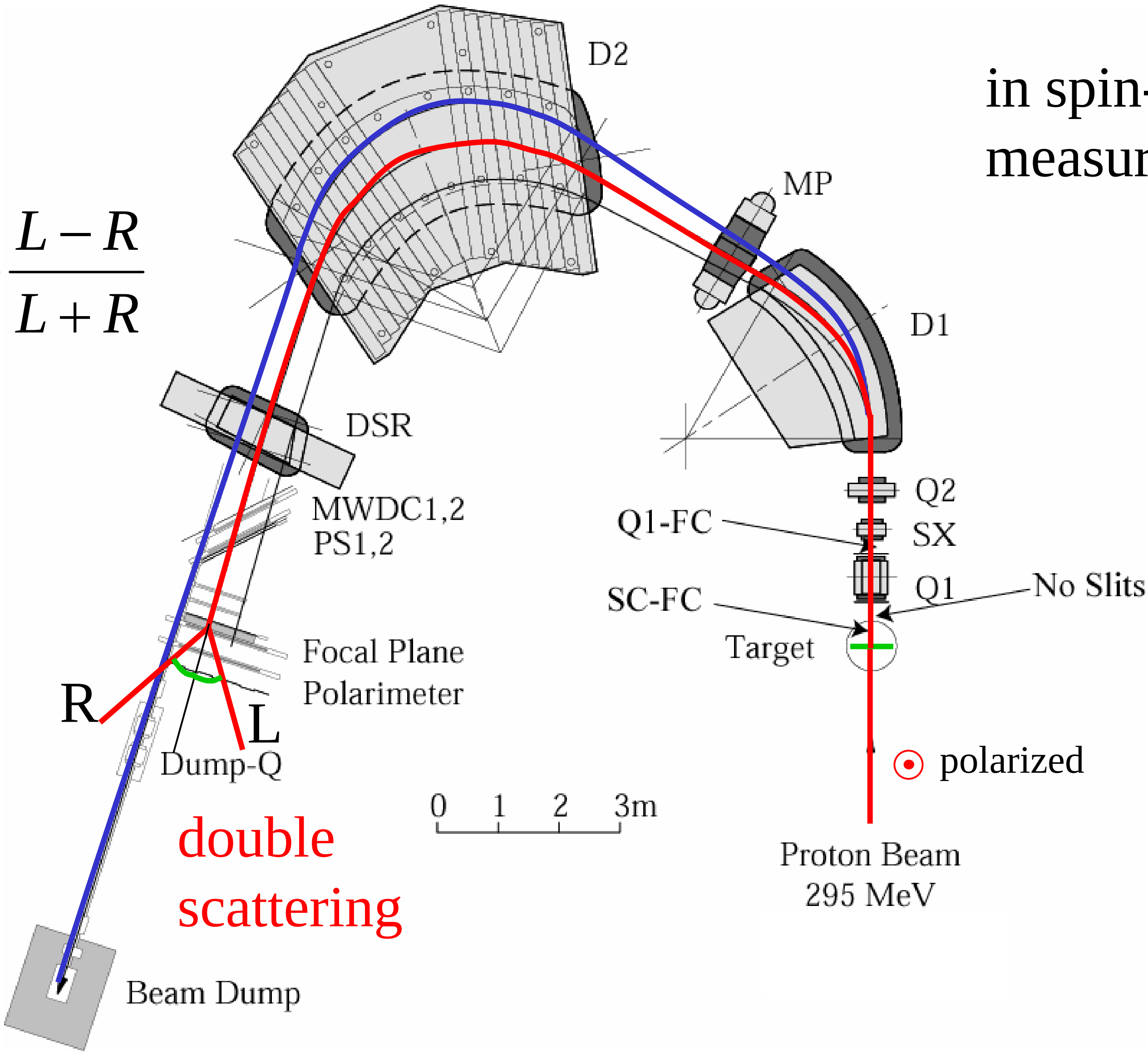

double scattering

Spectrometers in the 0-deg. experiment setup

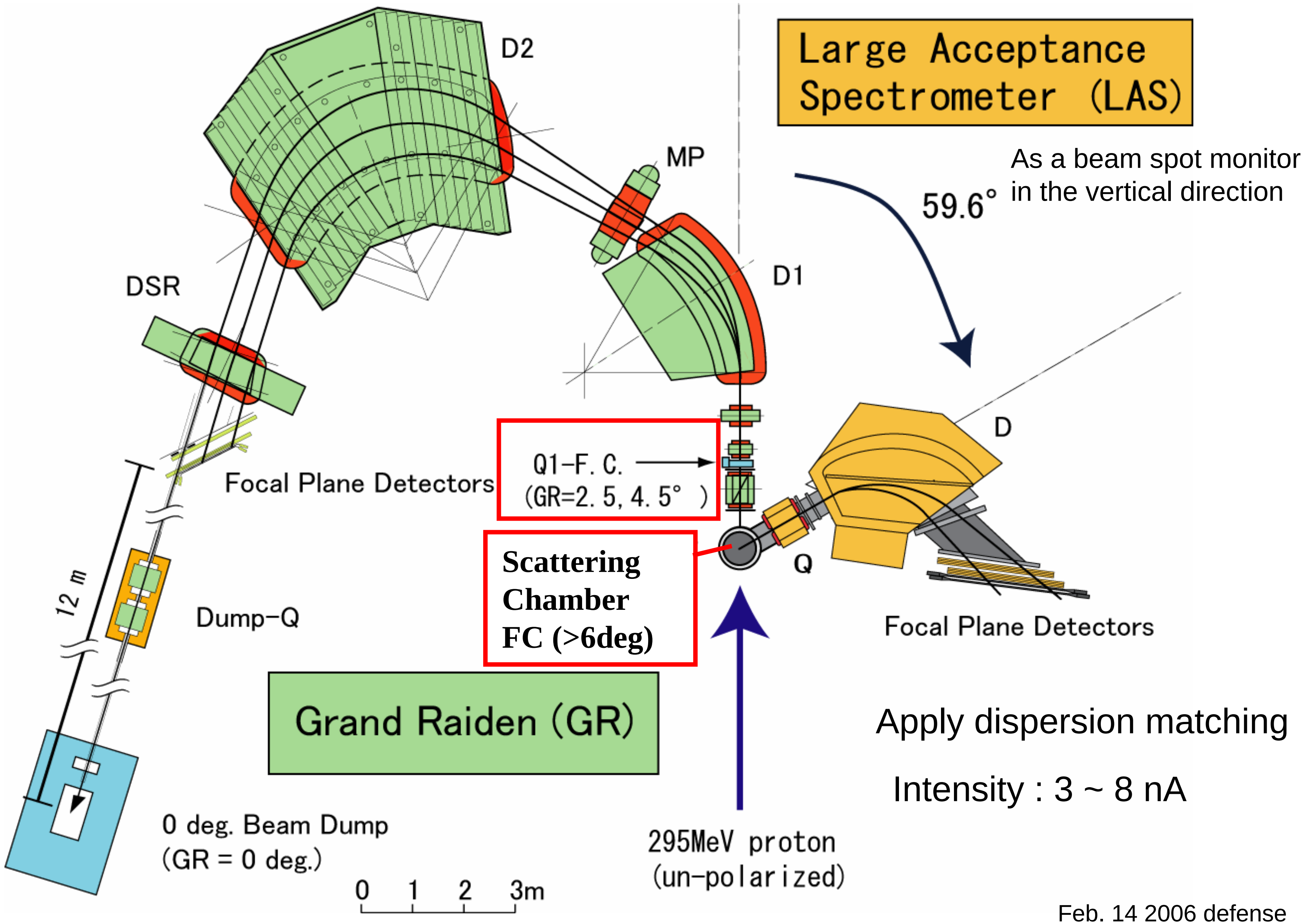

Apply dispersion matching

Intensity : 3 ~ 8 nA

Representative Specta

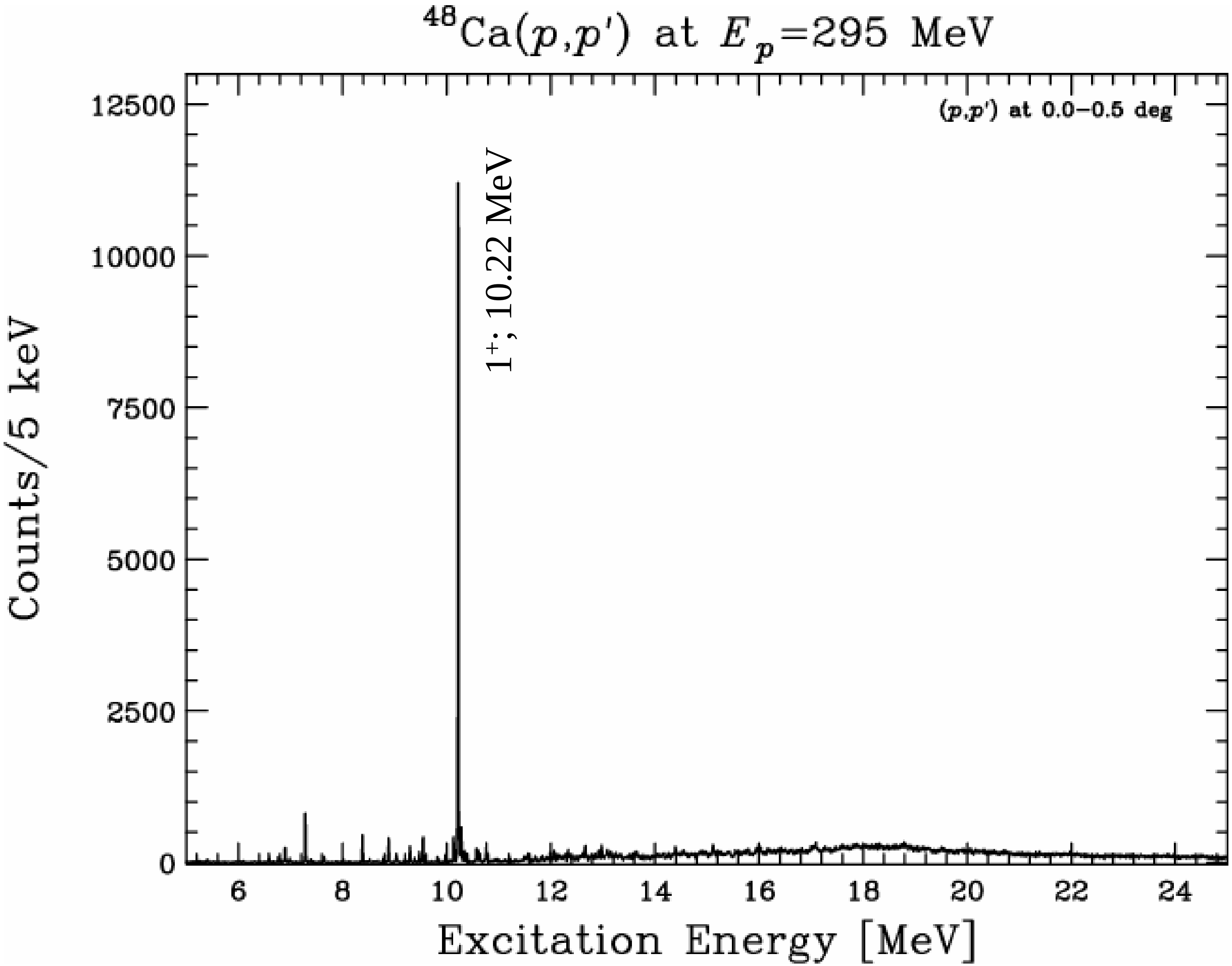

48Ca(p,p') at Ep=295 MeV
(p,p') at 0.0−0.5 deg
1+; 10.22 MeV
Counts/5 keV
Excitation Energy [MeV]
12500
10000
7500
5000
2500
0
6
8
10
12
14
16
18
20
22
24

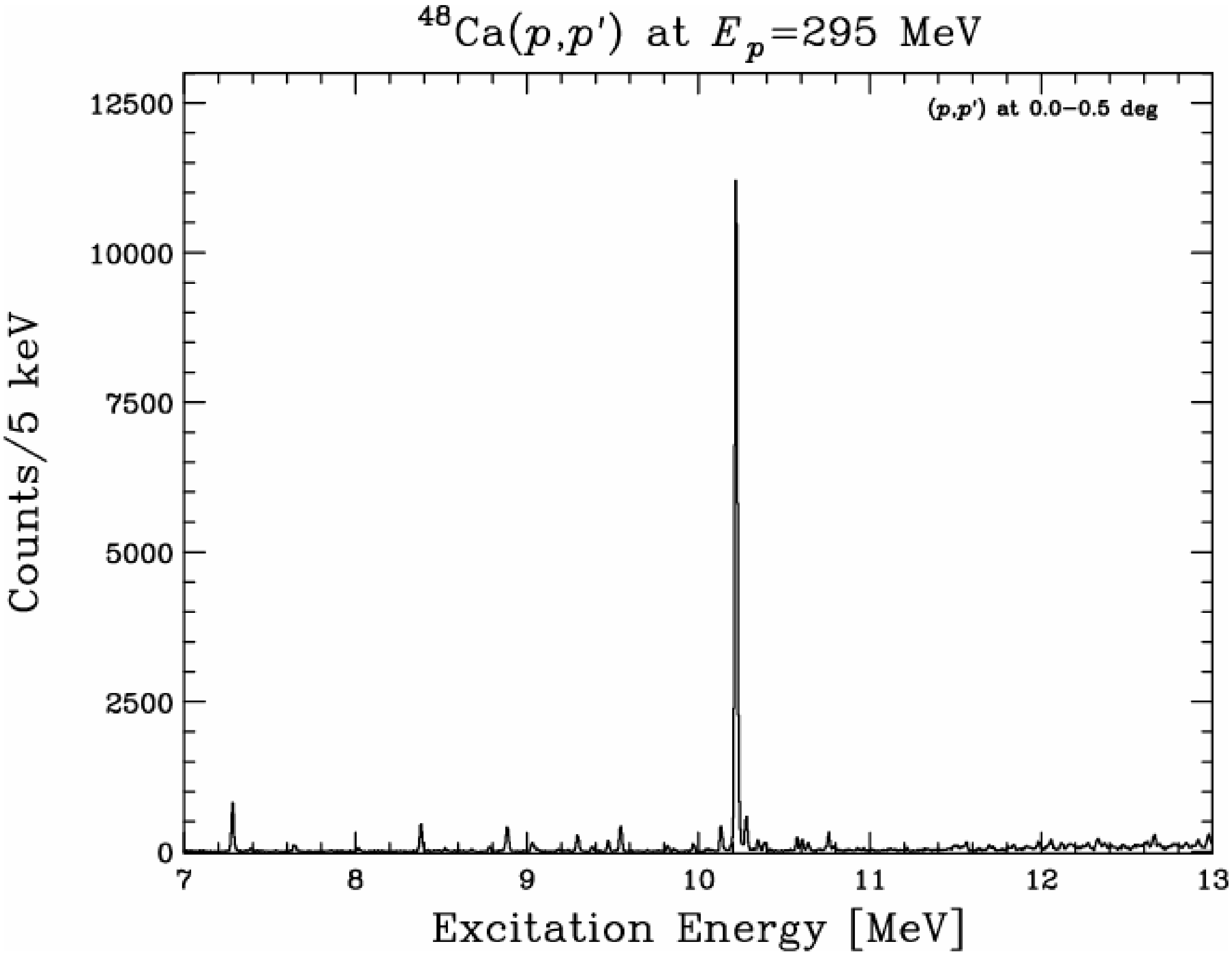

^{48}Ca(p,p') at E_p=295 MeV
(p,p') at 0.0–0.5 deg
Counts/5 keV
12500
10000
7500
5000
2500
0
7
8
9
10
11
12
13
Excitation Energy [MeV]

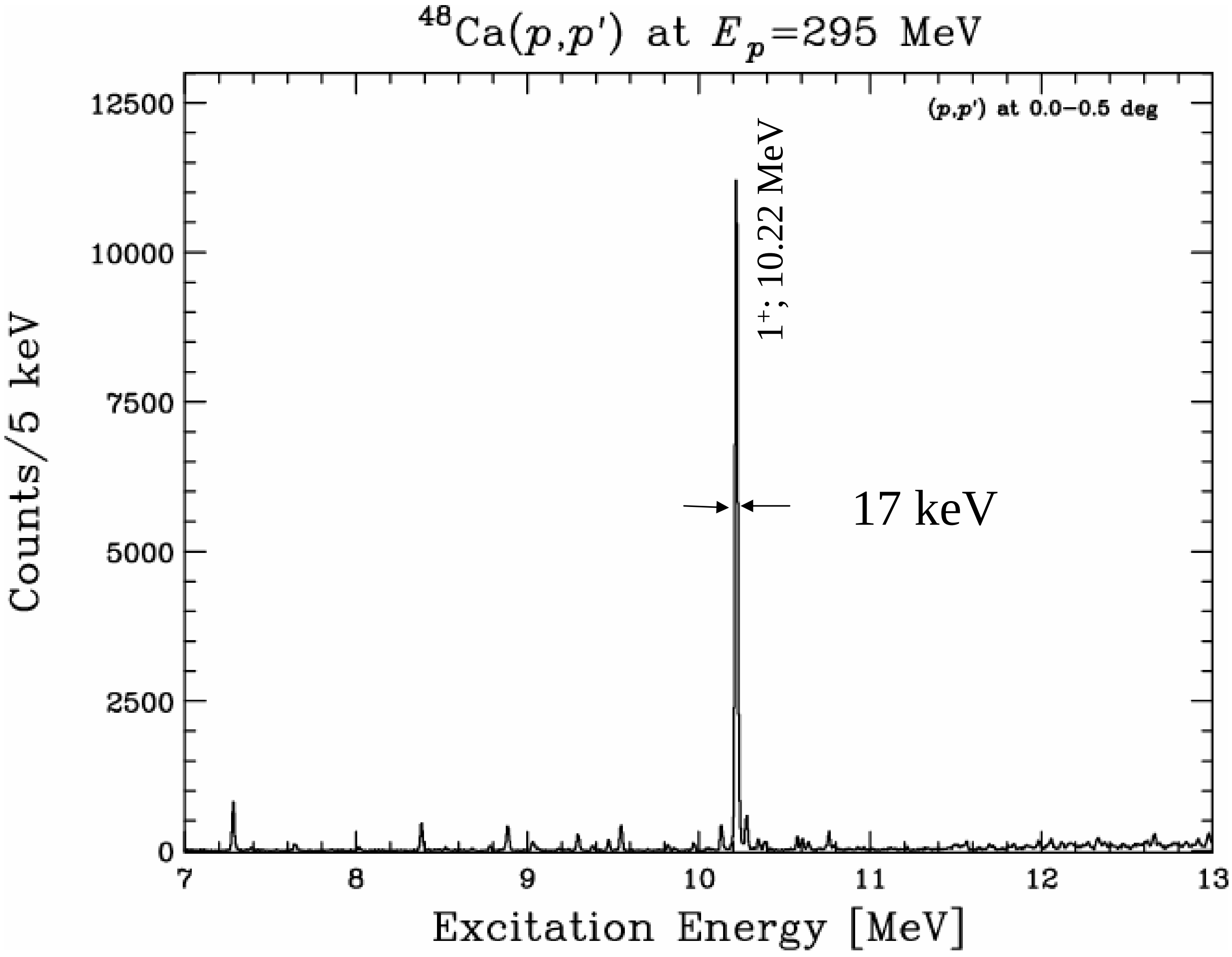

$^{48}Ca(p,p')$ at E_p=295 MeV
(p,p') at 0.0–0.5 deg
1+; 10.22 MeV
17 keV
Counts/5 keV
Excitation Energy [MeV]
12500
10000
7500
5000
2500
0
7
8
9
10
11
12
13

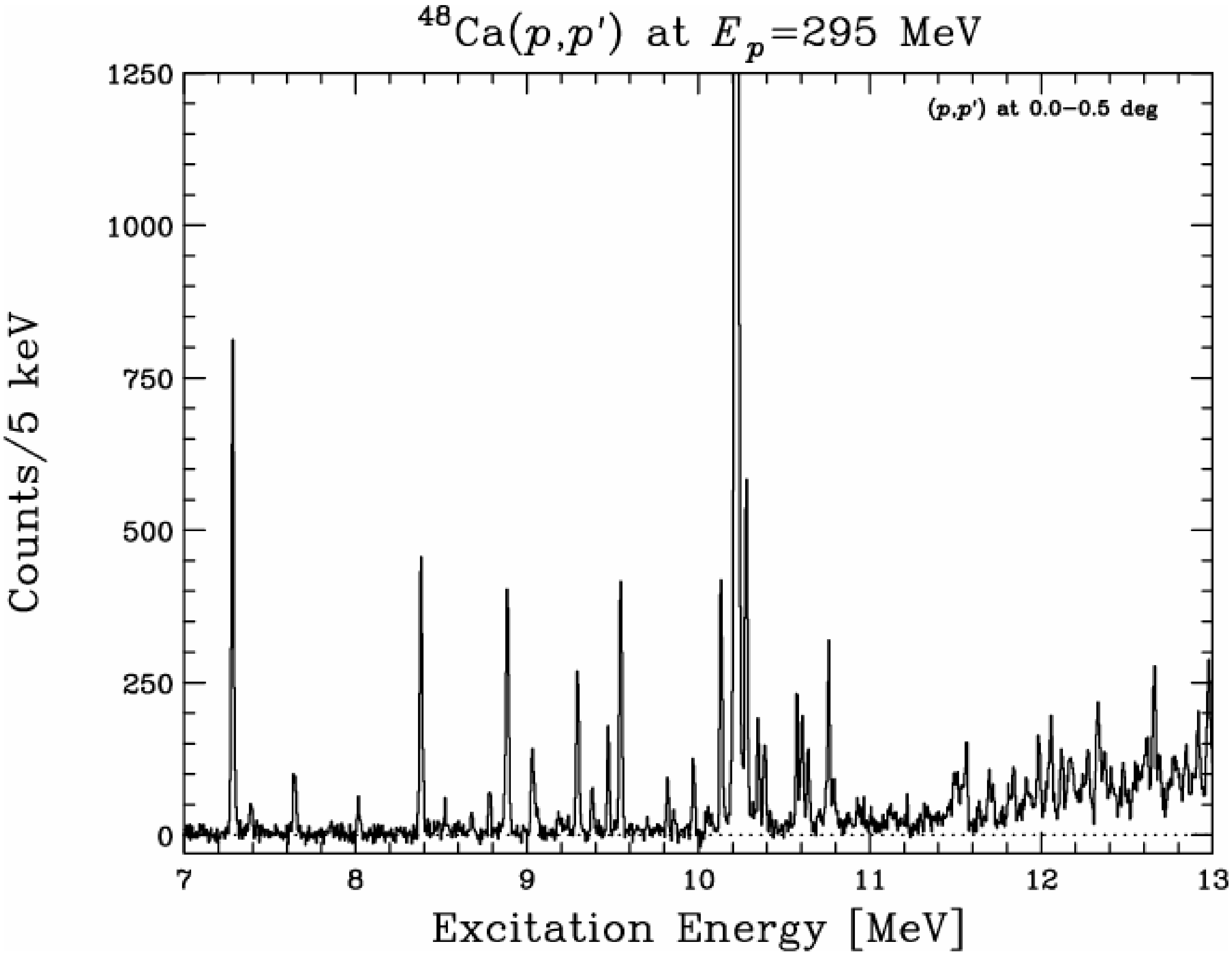

$^{48}Ca(p,p')$ at E_p=295 MeV
(p,p') at 0.0–0.5 deg
Counts/5 keV
Excitation Energy [MeV]
1250
1000
750
500
250
0
7
8
9
10
11
12
13

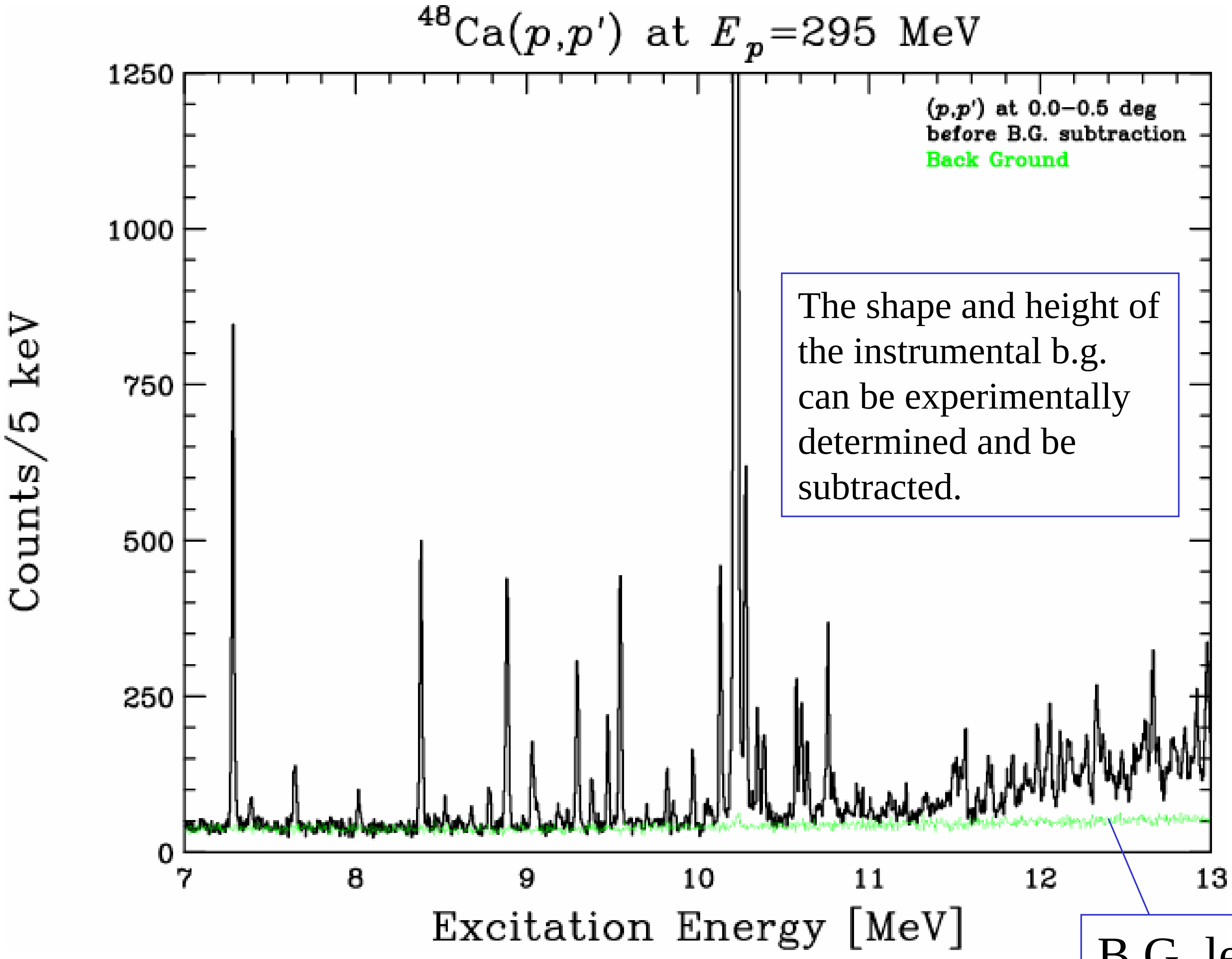

The shape and height of the instrumental b.g. can be experimentally determined and be subtracted.

B.G. level

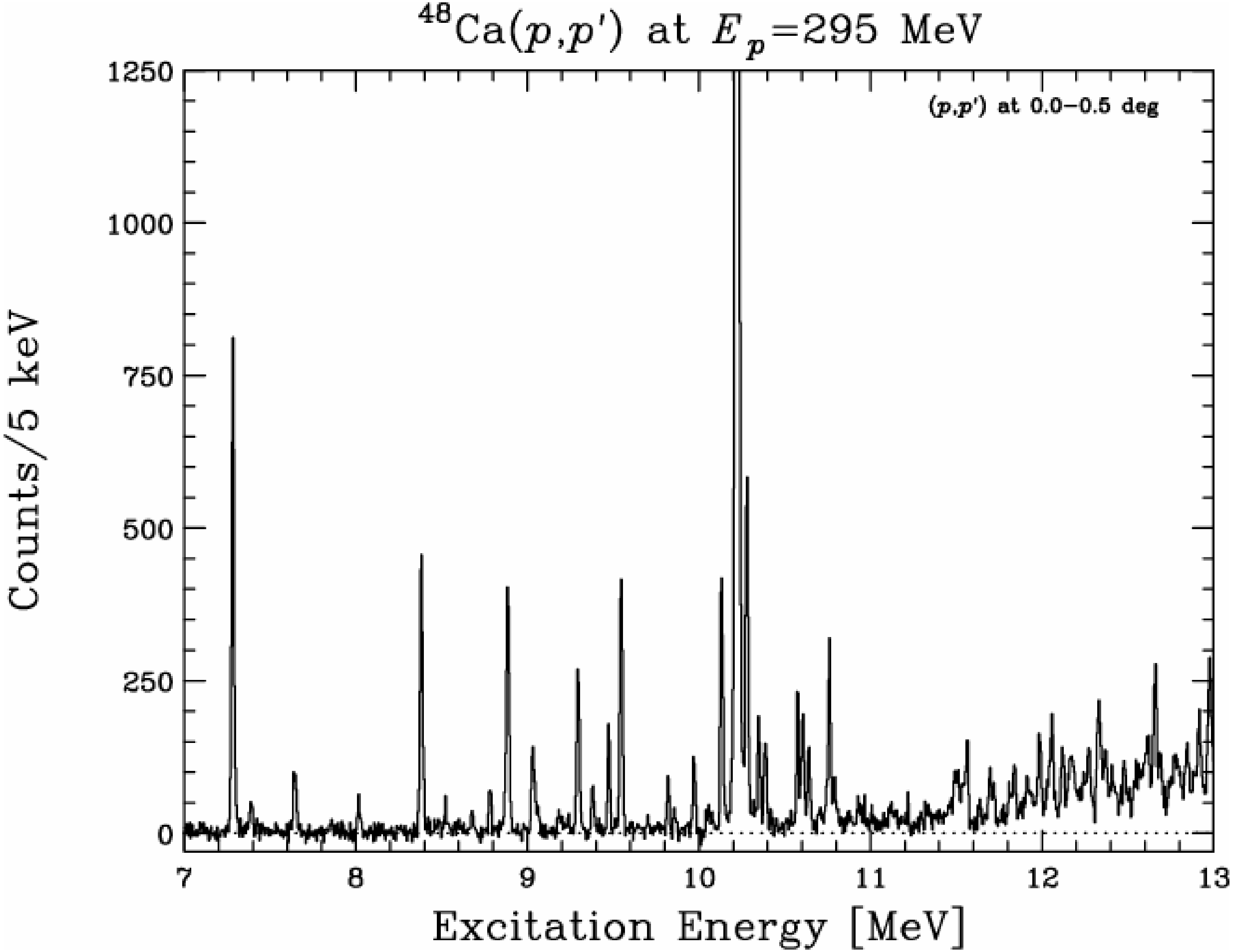

^{48}Ca(p,p') at E_p=295 MeV
(p,p') at 0.0–0.5 deg
Counts/5 keV
Excitation Energy [MeV]
0
250
500
750
1000
1250
7
8
9
10
11
12
13

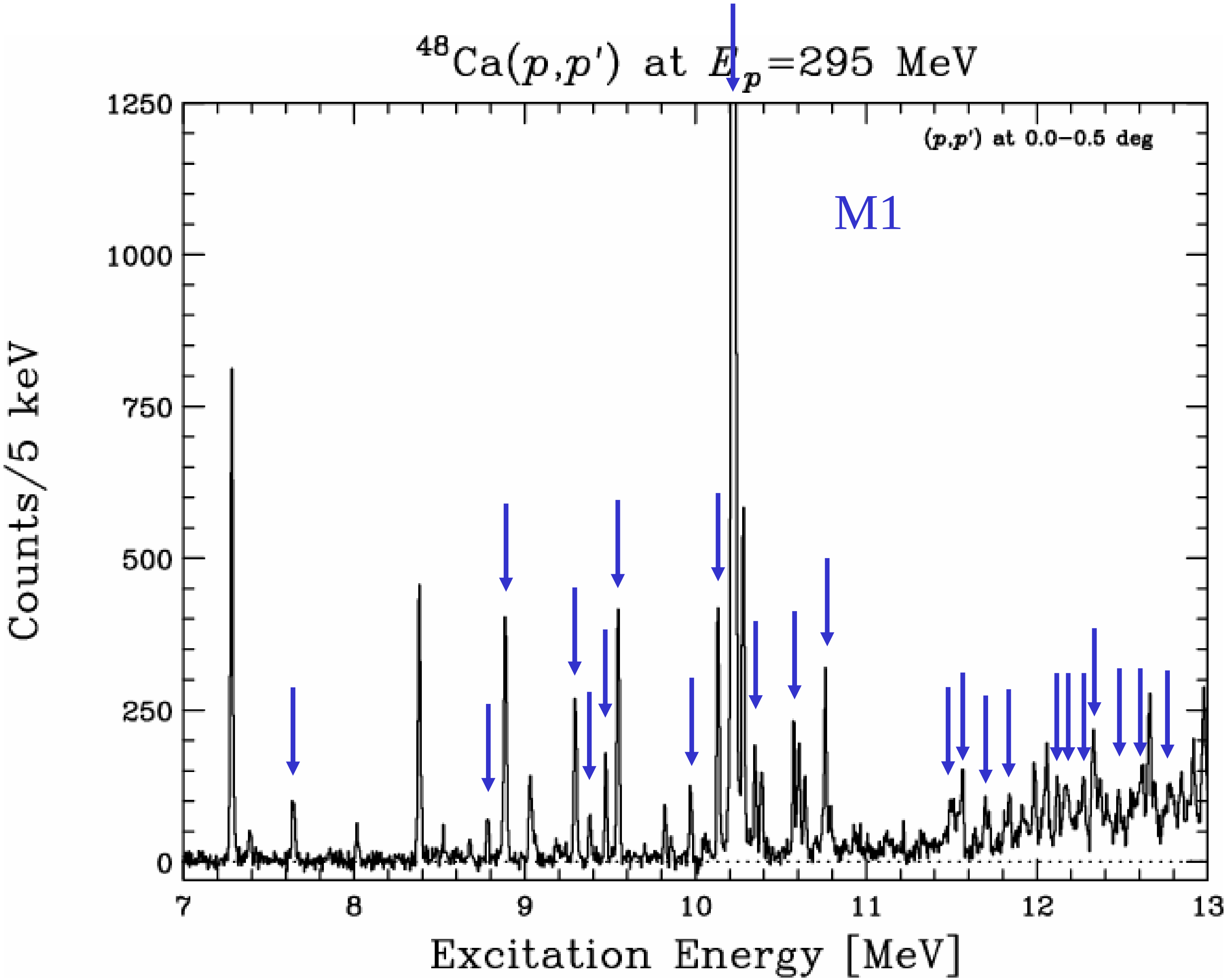

^{48}Ca(p,p') at E_p=295 MeV
(p,p') at 0.0–0.5 deg
M1
Counts/5 keV
1250
1000
750
500
250
0
7
8
9
10
11
12
13
Excitation Energy [MeV]

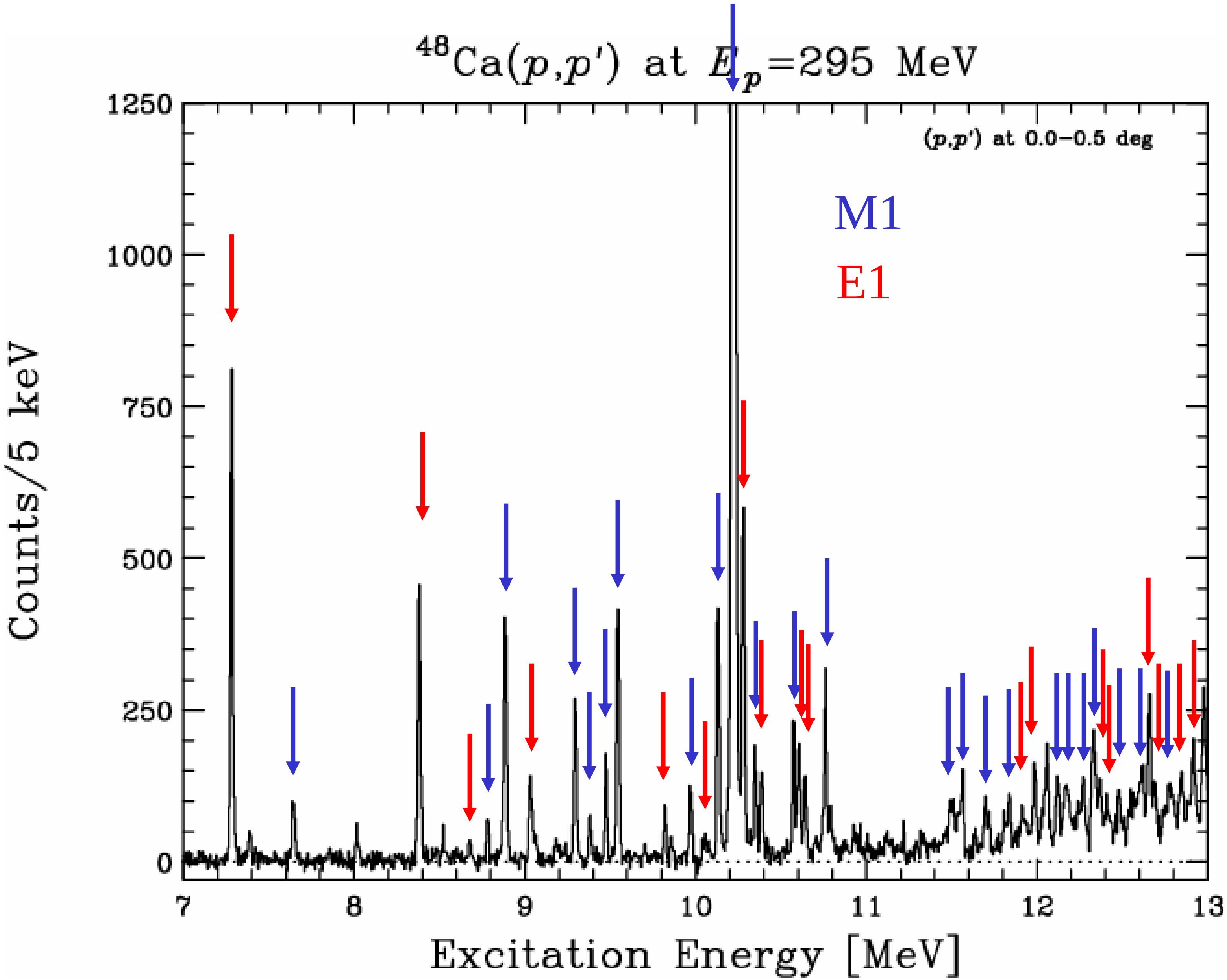

^{48}Ca(p,p') at E_p=295 MeV
(p,p') at 0.0−0.5 deg
M1
E1
Counts/5 keV
Excitation Energy [MeV]
0
250
500
750
1000
1250
7
8
9
10
11
12
13

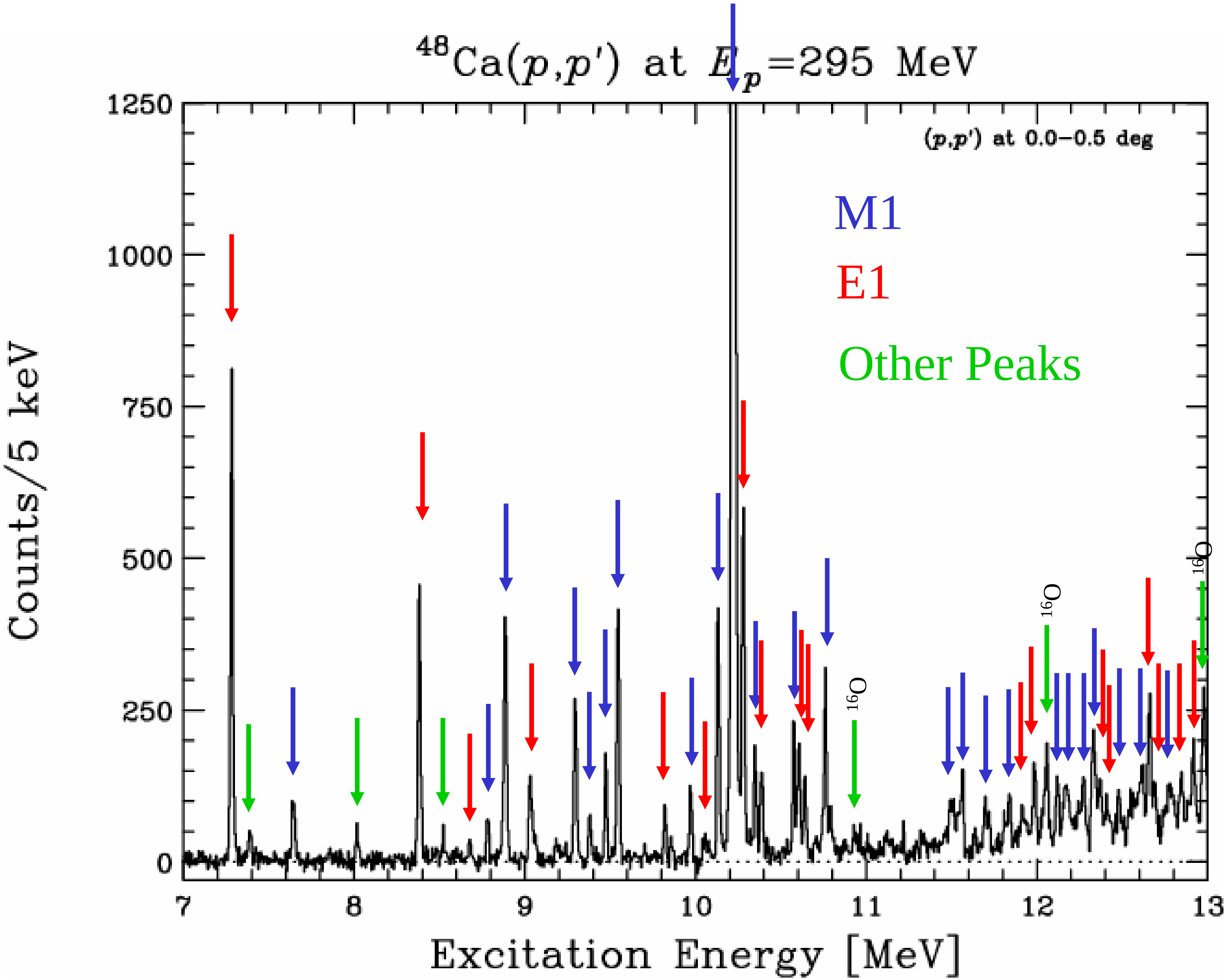

^{48}Ca(p,p') at E_p=295 MeV
(p,p') at 0.0−0.5 deg
M1
E1
Other Peaks
^{16}O
^{16}O
^{16}O
Counts/5 keV
Excitation Energy [MeV]
1250
1000
750
500
250
0
7
8
9
10
11
12
13

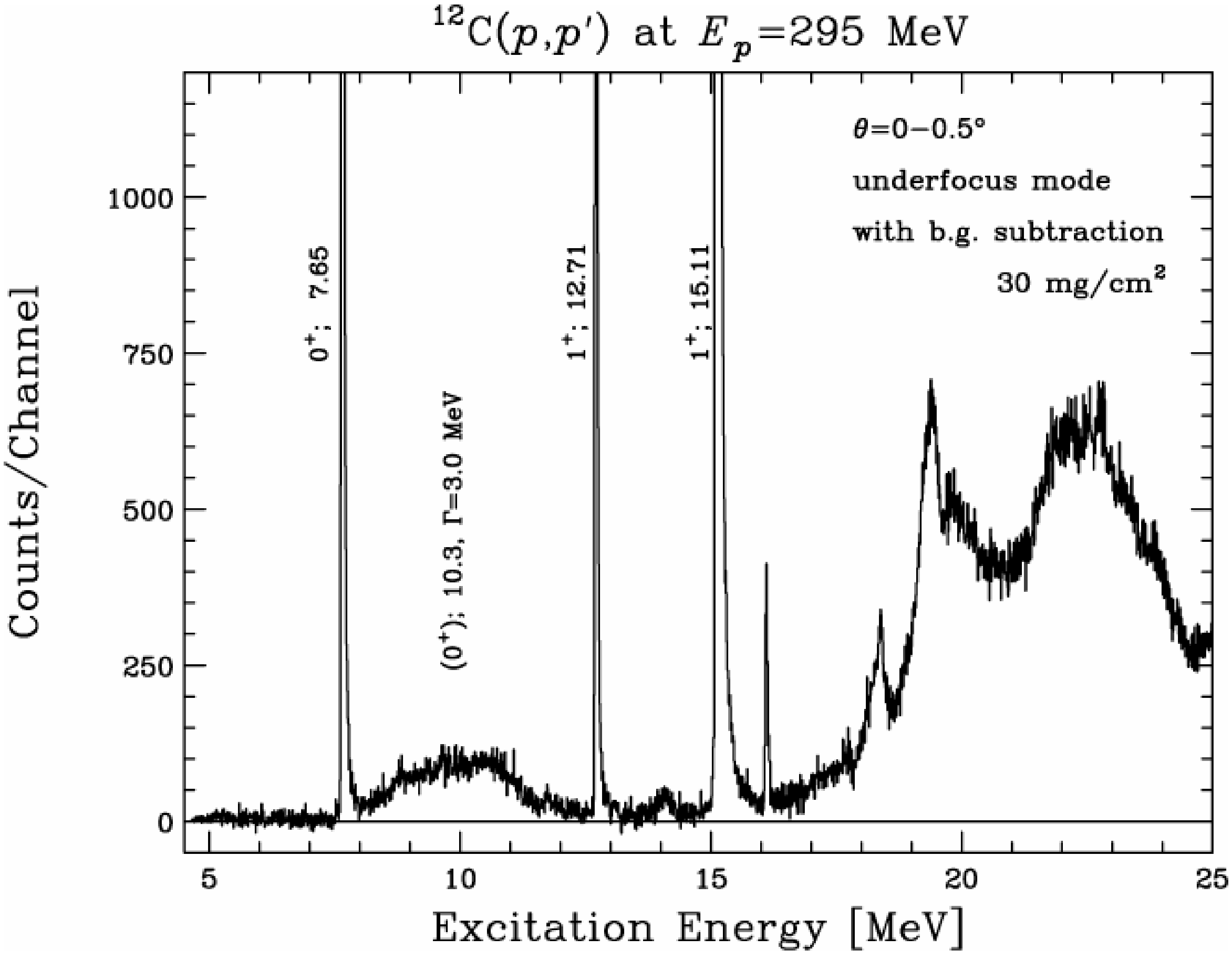

12C(p,p') at Ep=295 MeV
θ=0−0.5°
underfocus mode
with b.g. subtraction
30 mg/cm2
0+; 7.65
(0+); 10.3, Γ=3.0 MeV
1+; 12.71
1+; 15.11
Counts/Channel
0
250
500
750
1000
5
10
15
20
25
Excitation Energy [MeV]

Inelastic Scattering from ^{12}C

DWBA calc.
Cohen Kurath Wave Function
Franey Love Effective Interaction

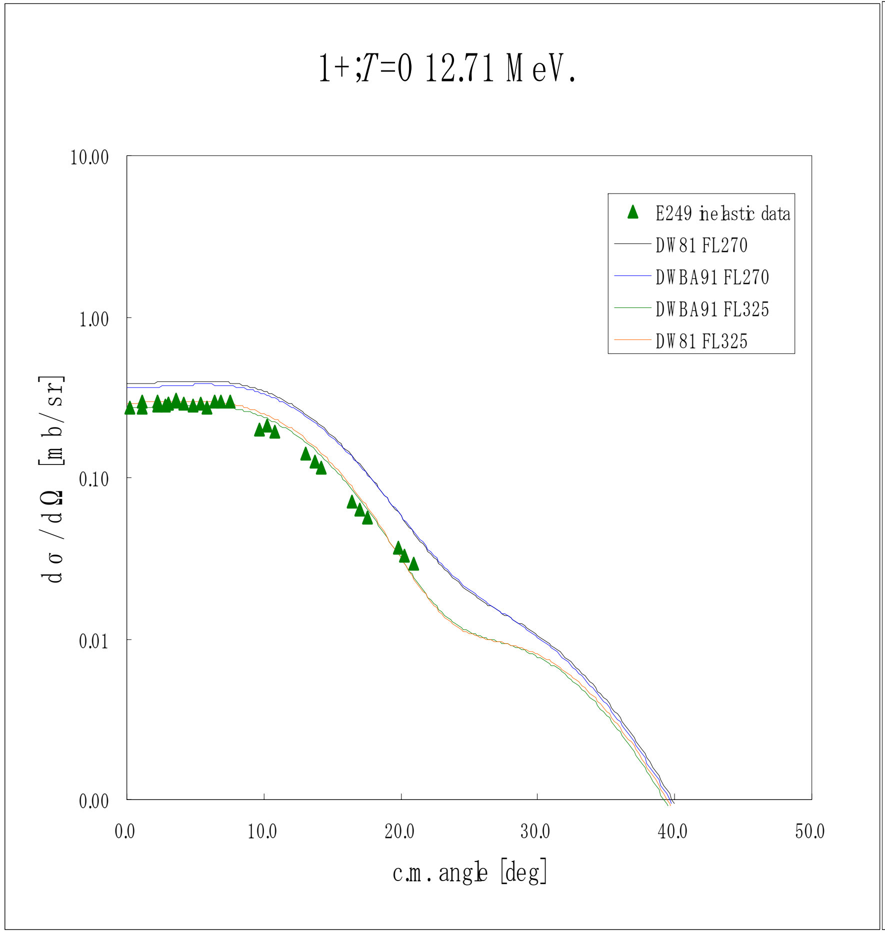

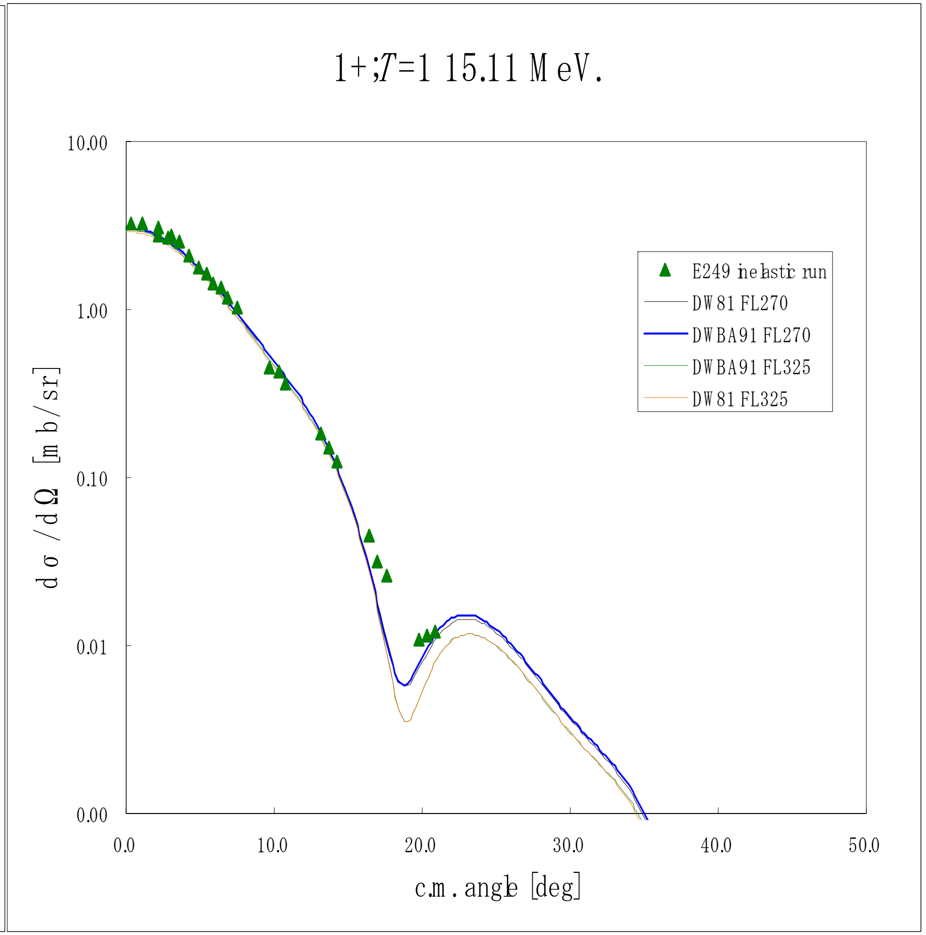

The angular distributions are well reproduced by the DWBA calculations for both T=0 and T=1.

Physics Motivations

Motivations

1. M1 excitation: $0^+ \longrightarrow 1^+$
   strength distribution and quenching for each T=0 and T=1 excitation over the sd-shell region

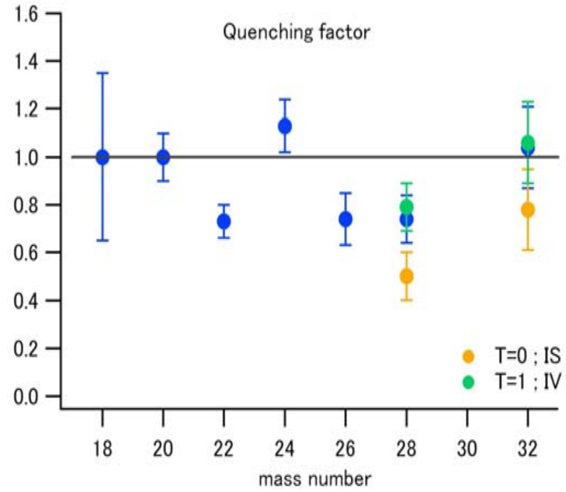

G.M. Crawley et al.,PRC39(1989)311

2. Missing M1 strength in 208Pb

(3. Fragmentation of the excitation strengths: giant resonances and M1 exciations)

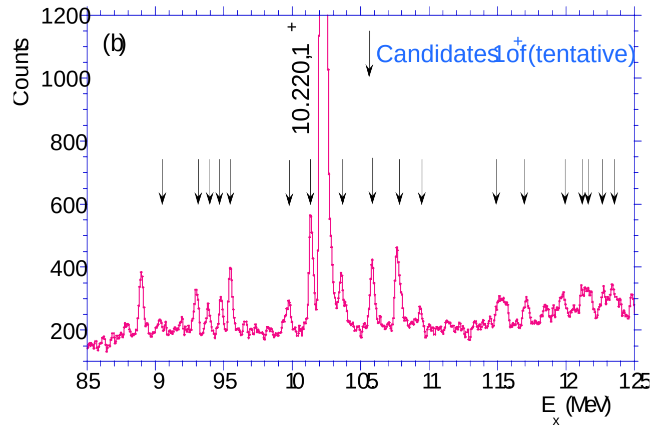

^{48}Ca(p,p') at IUCF at 0 deg., Y. Fujita *et al.*

Isoscalar and Isovector M1 strengths in the sd-shell region

Quenching of the GT strengths

Gamow-Teller (GT) quenching problem:
The observed GT strengths are systematically smaller the sum-rule value.

GT sum rule : $S_{\beta^-} - S_{\beta^+} = 3(N - Z)$

Quenching Factor

$$Q \equiv \frac{Strength(\exp.)}{Strength(theory)}$$

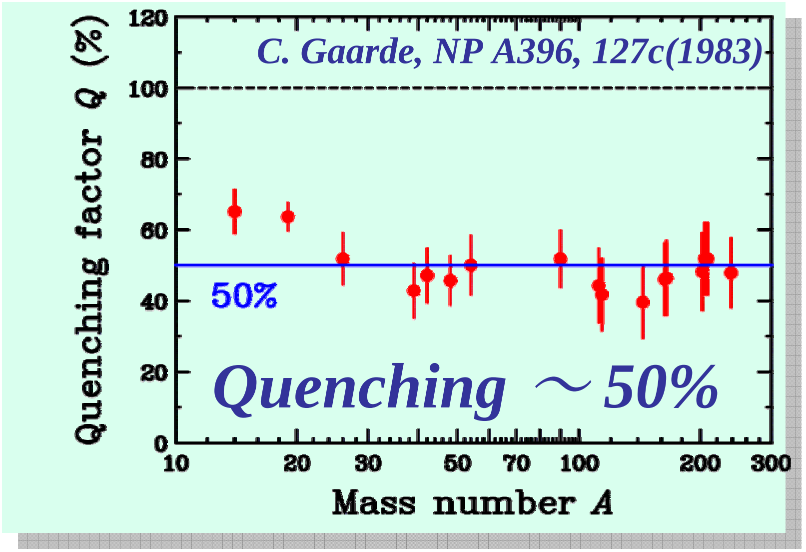

By sophisticated measurements and analysis of (p,n) and (n,p) reactions
50 → 90% of the strength was observed in ^{90}Zr upto E_x=50 MeV

T. Wakasa *et al*., PRC55(1997)2909 K. Yako *et al*., PLB615(2005)193

2 quenching schemes:
- Mixing of multi-particle multi-hole states ← dominant contribution
- Mixing of Δ-hole states

M1 excitations and analogous excitations

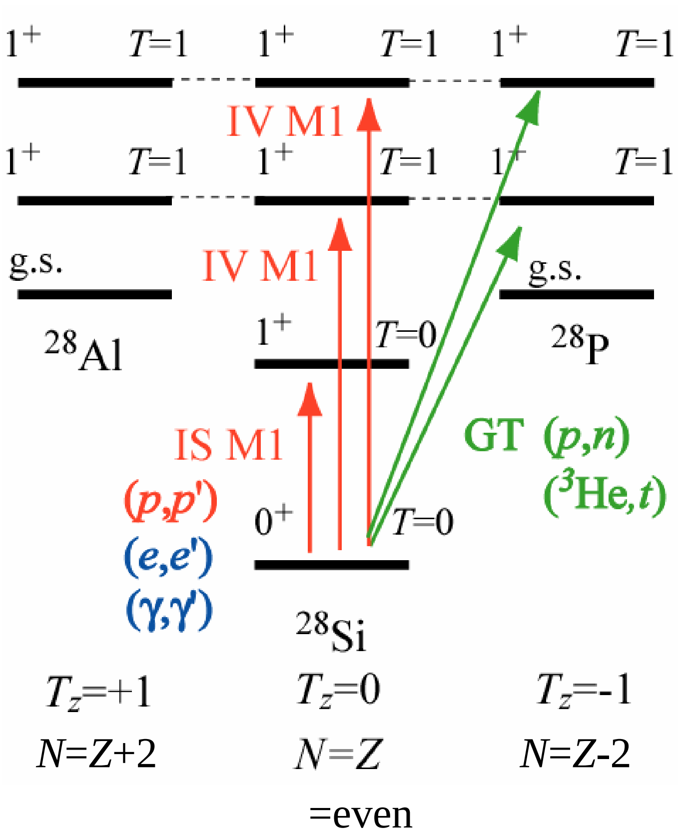

IS: Isoscalar $\Delta T=0$ σ

IV: Isovector $\Delta T=1$ $\sigma\tau$

Isovector (ΔT=1) M1 excitation is analogous to GT.

➡ Similar quenching is expected

Isoscalar (ΔT=0) M1 excitation: Δ-h mixing does not take place

➡ Is there any difference between isoscalar and isovector excitations?

Study of isoscalar/isovector M1 excitations over the sd-shell region

For all the N=Z even-even stable targets:
(isoscalar/isovector excitations do not mix to each other)

^{16}O, ^{20}Ne, ^{24}Mg, ^{28}Si, ^{32}S, ^{36}Ar, ^{40}Ca

^{16}O: Ice target (H_2O)
^{32}S: Cooled target (for preventing sublimation)
^{36}Ar: Gas target
^{20}Ne: Cooled gas target

Cooled target system

- H_2O, ^{32}S

Cooled by liq. N2

T. Kawabata *et al*., NIMA 459 (2001) 171.

10 mg/cm^2

Cooled gas target system

- Applicable for high-res. exp.（<30keV　at < 6 deg）
- Cooled by liq. N_2
- Gas recycling system

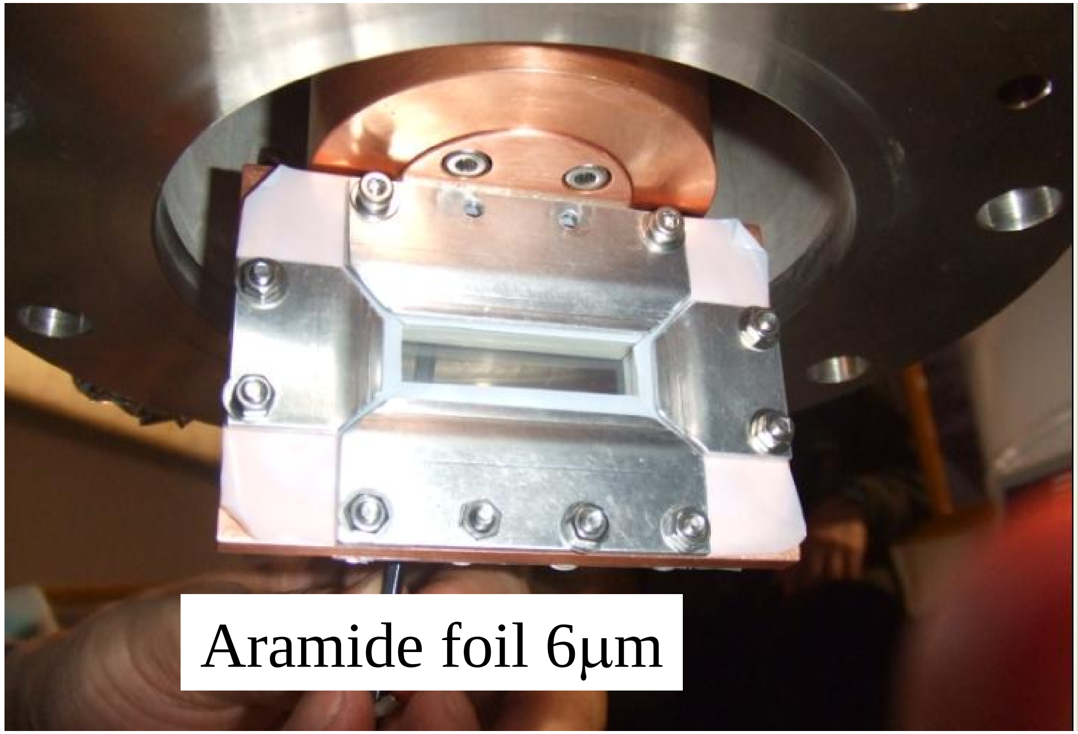

Inelastic Scattering from ^{28}Si at 0 degrees

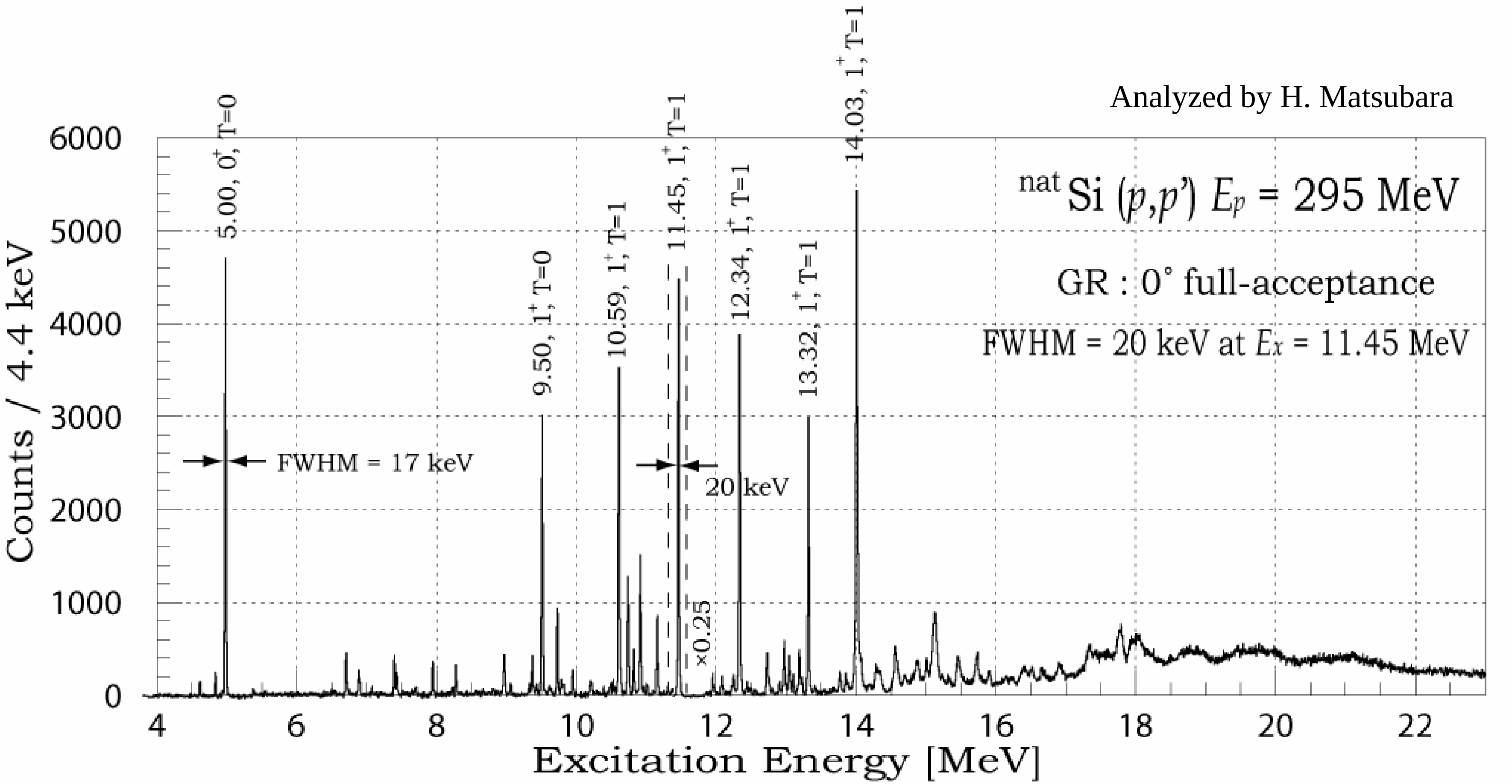

Angular Distribution of IS and IV 1^+ excitations

DWBA calculation

Trans. density : A. Willis et al., PRC 43(1991)5 (by OXBASH in sd shell only)

NN interaction. : Franey and Love, PRC31(1985)488. (325 MeV data)

Optical potential : K. Lin, M.Sc. thesis., Simon Fraser U. 1986.

Analyzed by H. Matsubara

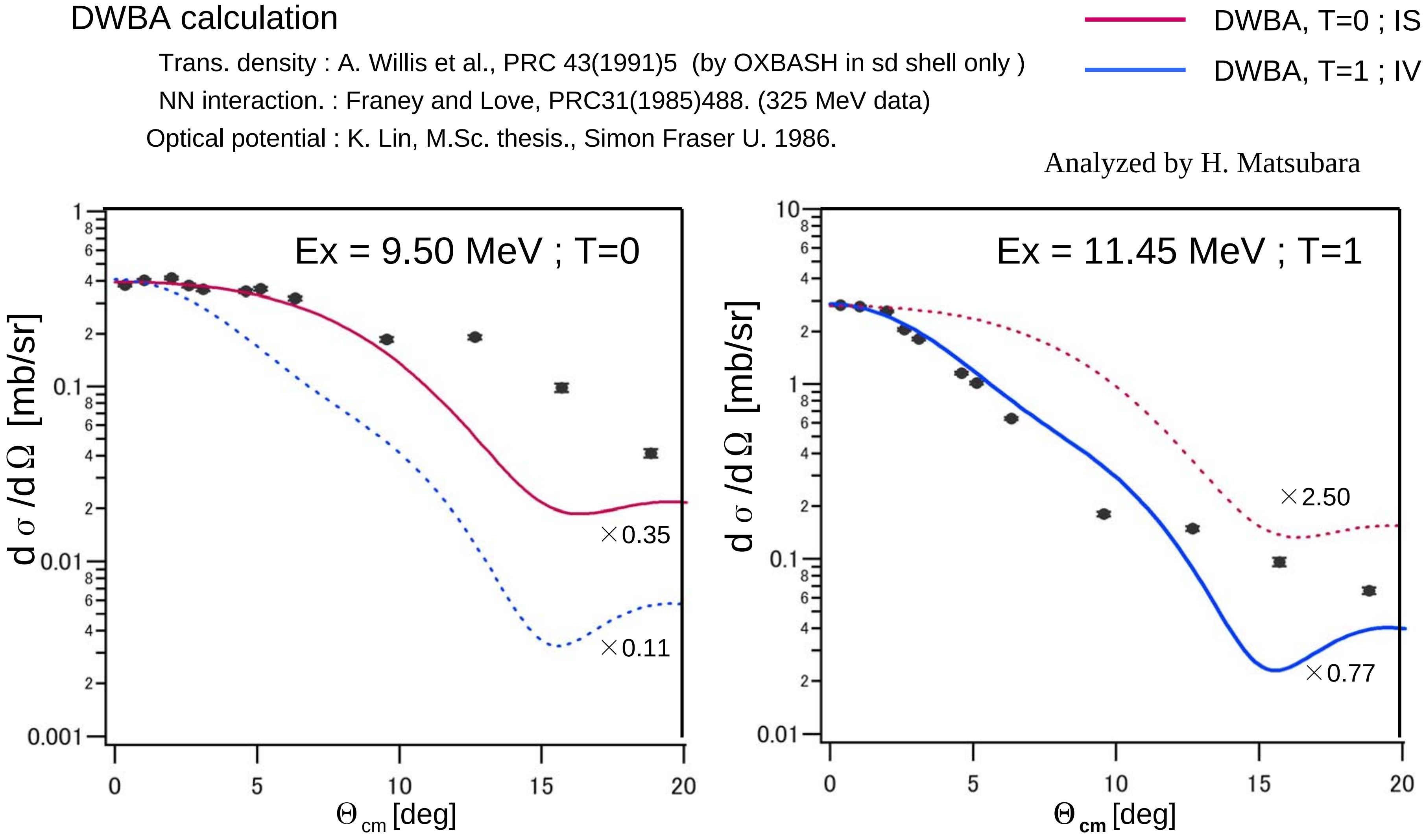

From angular distribution, isospin value is identified.

Other states identified as 1^+

1^+, T=0 states

1^+, T=1 states Analyzed by H. Matsubara

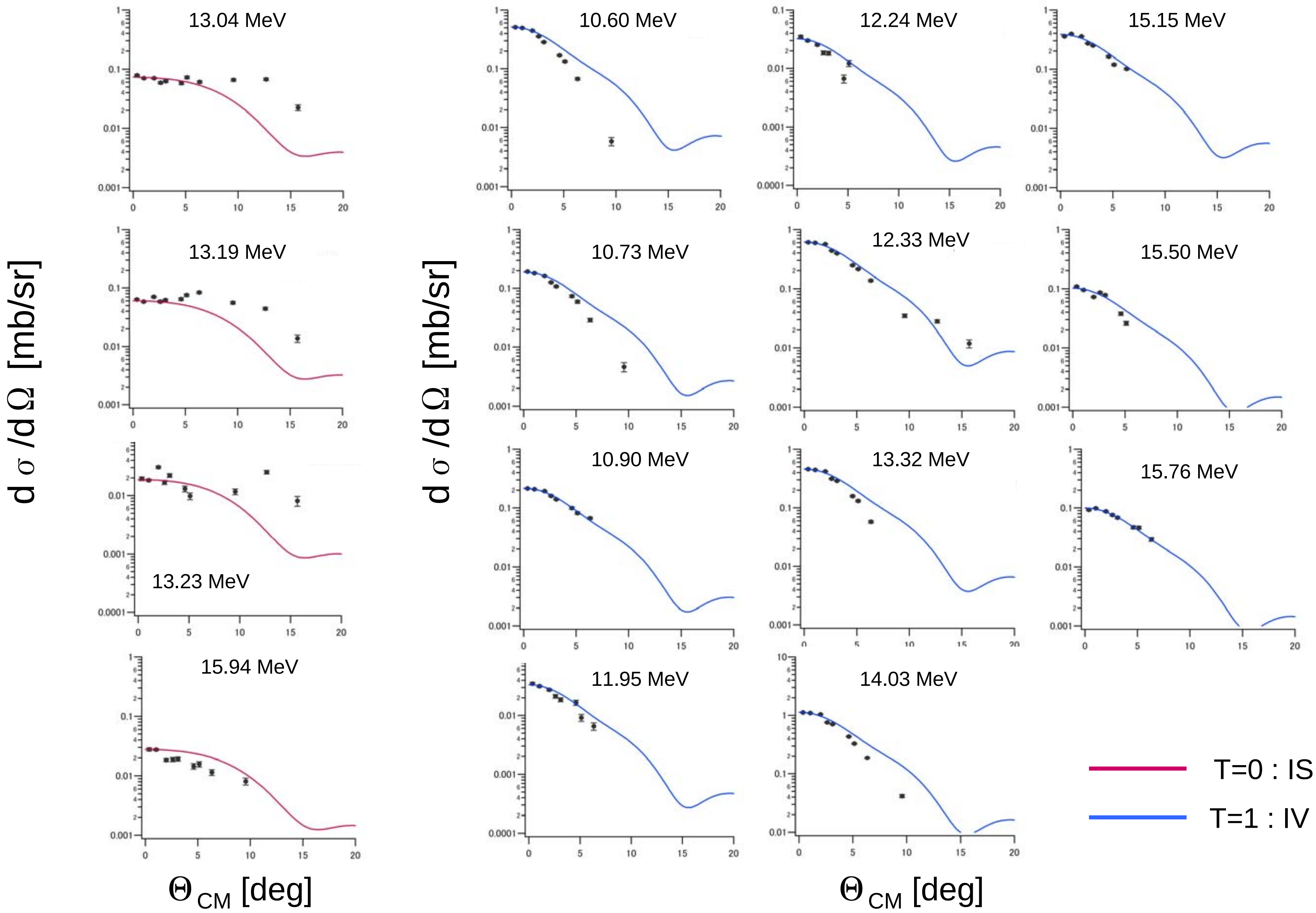

Strength distribution

preliminary

shell model calculation:
OXBASH + USD interaction

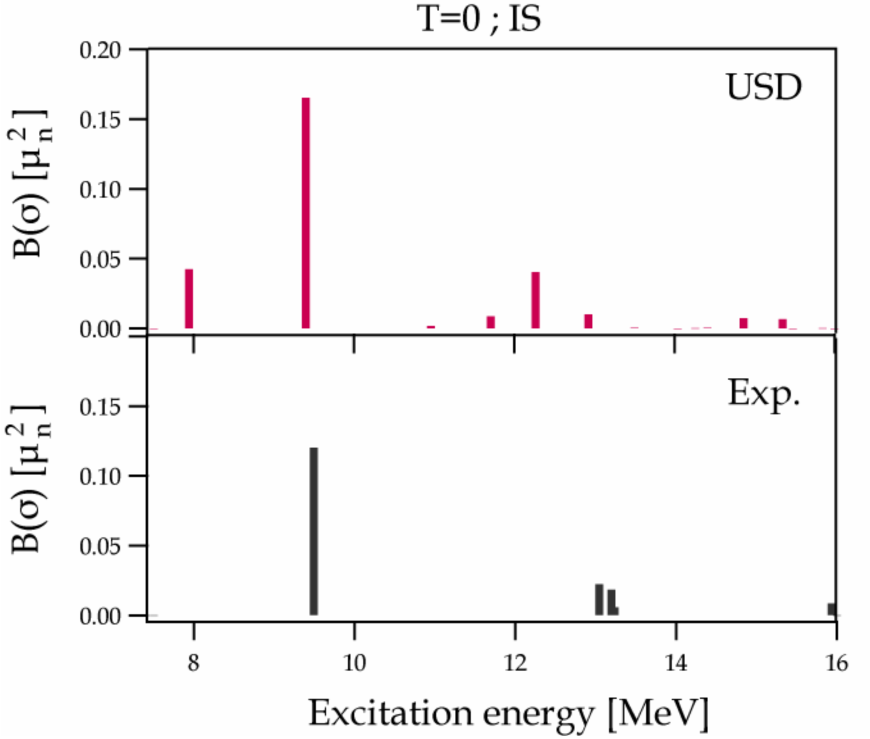

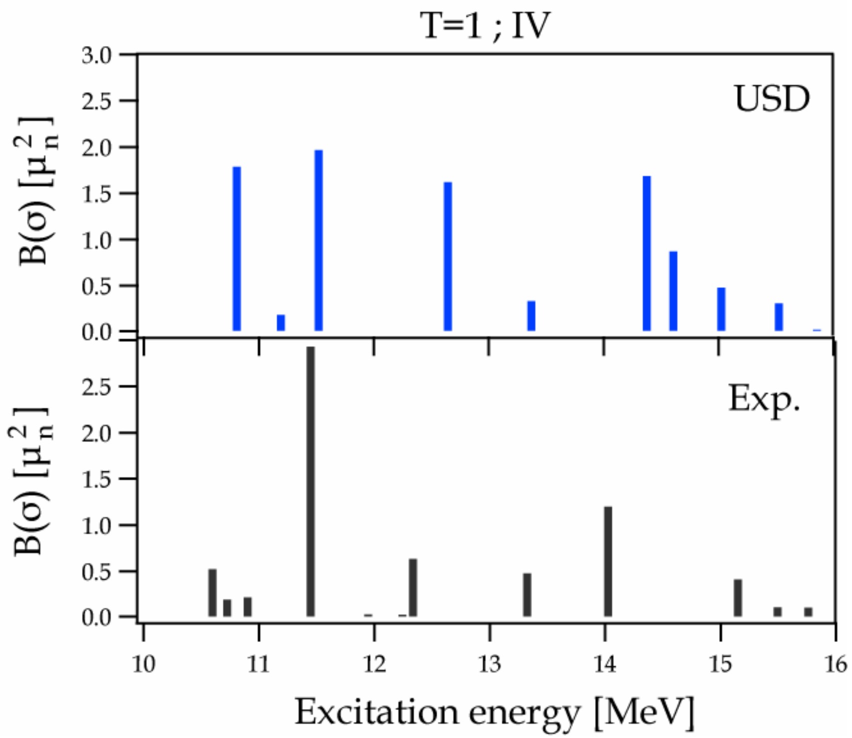

M1 strength in ^{28}Si

preliminary

Cumulative Sum

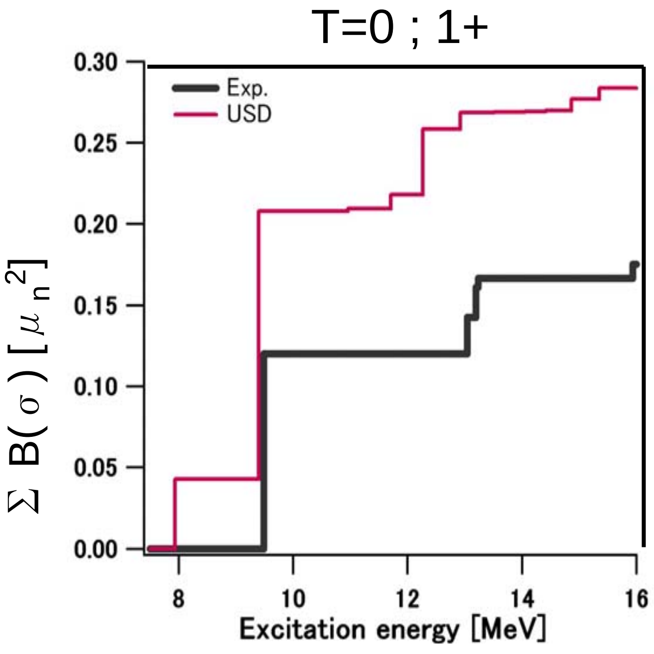

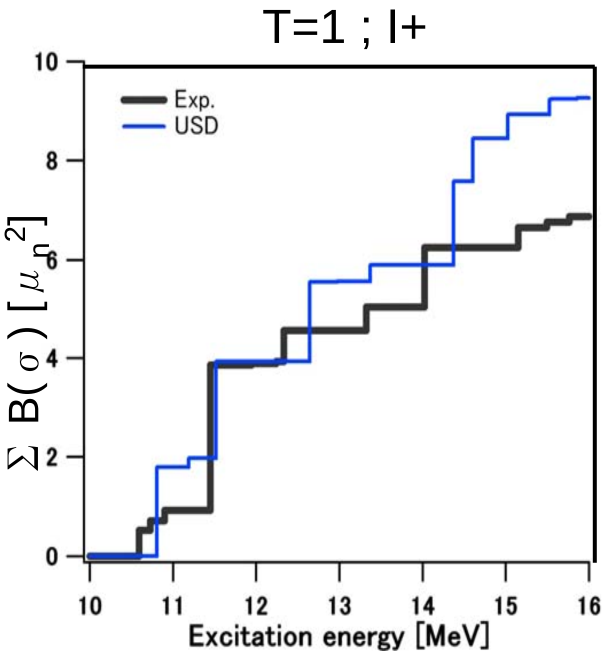

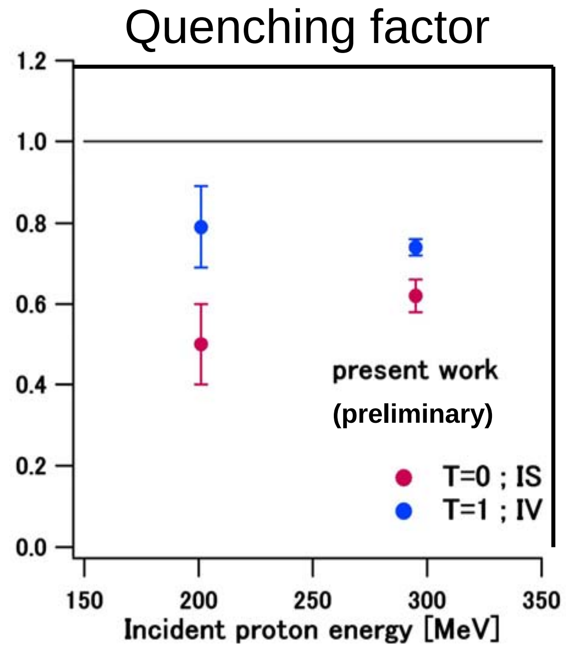

Followings should be checked more carefully.

- B(σ) is determined from dσ/dΩ(q=0) relying on the eff. interaction and DWIA calculation.

- Bare g-factor is used in the S.M. calculation.

$$Quenching\,Factor = \frac{\Sigma B(\sigma)_{\text{exp}}}{\Sigma B(\sigma)_{shell-\text{model}}}$$

Quenching factor for isovector M1 excitations (very preliminary)

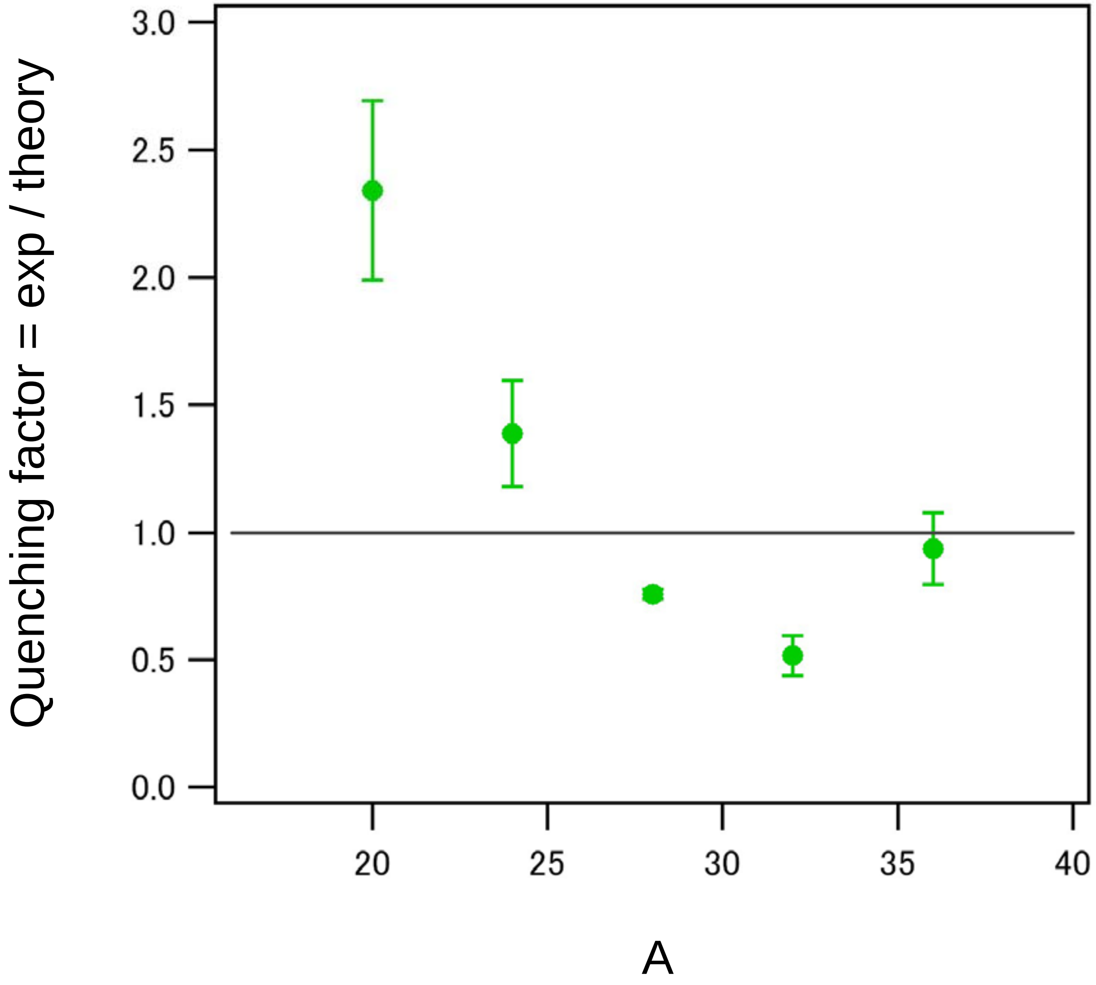

Theory: OXBASH USD, sd-shell, 0hw, free-g-factor

Missing *M1* strength in ^{208}Pb

Prediction of the M1 strengths in ^{208}Pb with 1*p*-1*h* basis

1*p*-1*h* excited states of protons $|\pi\{h_{9/2}\text{-}h_{11/2}^{-1}\}\rangle$ and neutrons $|\nu\{i_{11/2}\text{-}i_{13/2}^{-1}\}\rangle$ strongly couples to each other due to

- spin-orbit splittings of *p* and *n* orbits are similar
- orbital angular momentum l's are similar

and yield

- a lower-lying state at ~ 5.4 MeV with B(M1) ~ 1 μ_N^2
- a higher-lying state at ~ 7.5 MeV with B(M1) ~ 50 μ_N^2

in Tamm-Dancoff approximation.

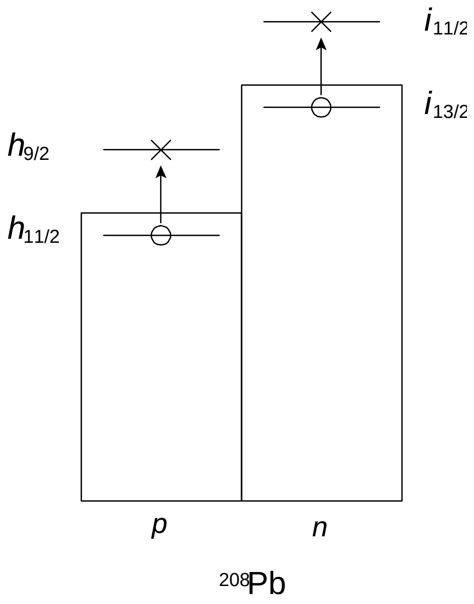

see *e.g.*
J.D. Vergados, Phys. Lett. 36B (1971) 12.
Bohr and Mottelson, Nuclear Structure vol II (1975)636.

Fragmentation of the M1 strengths in ^{208}Pb

The low-lying strength is considered to be exhausted by a state located at 5.846 MeV.

observed by (*p*,*p*') S.I. Hayakawa *et al*., PRL49(1982)1624, (e,e'), and (d,d').

The higher-lying strength is fragmented into many tiny states by mechanisms:

- core-polarization or g.s. correlation
- coupling to 2p-2h states
- coupling to Δ-h states
- meson exchange current

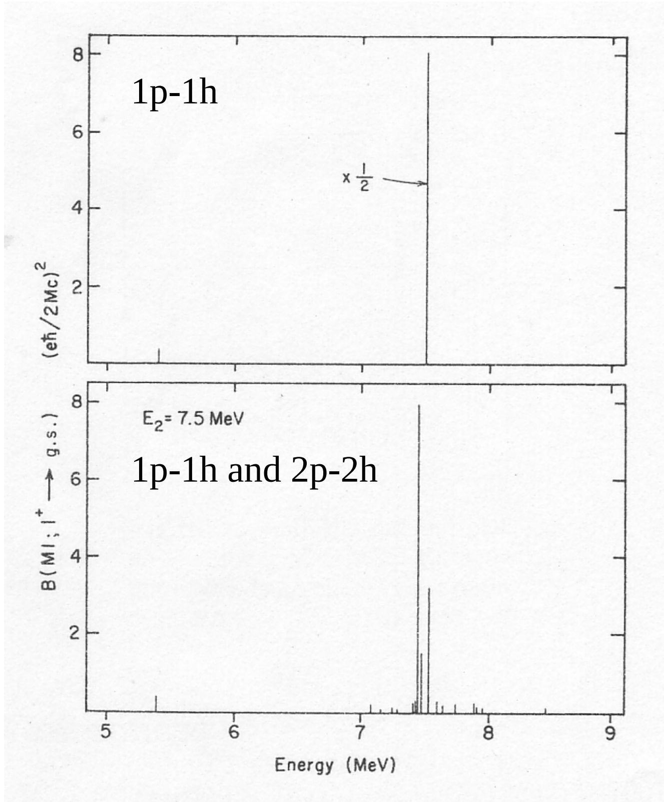

calc. by Lee and Pittel PRC11(1975)607.

Experimentally, only a strength of ~10 μ_N^2 has been observed (until 1988) comparing with theoretical predictions of ~10 μ_N^2 .

→ "Missing M1 strength in ^{208}Pb"

Prediction of the M1 strengths in ^{208}Pb

Many theoretical works have been done for reproducing the observed M1 strengths

- spreading by the coupling to 2p-2h states: 20% of reduction
- ground state correlation: 20% of reduction
- coupling to Δ-h states and MEC: 20% of reduction

If all these mechanisms additively contribute,

"the best that be expected from theoretical predictions is 20 μ_N^2"

I.S. Towner, Phys. Rep 155 (1987) 263.

Search for M1 strengths by experiments

Experimentally many reactions have been used to observe the M1 strengths:

^{208}Pb($\vec{\gamma}$,γ), ^{208}Pb(γ,$\vec{n}$), ^{207}Pb(*n*,*n*), ^{207}Pb(*n*,γ),

^{208}Pb(*e*,*e*'), and ^{208}Pb(*p*,*p*')

In 1988, R.M. Laszewsky et al. have identified

$8.8\mu_N^2$ below Sn by a ^{208}Pb($\vec{\gamma}$,γ) measurement.

In total the higher-lying strength became $15.6\mu_N^2$

which came closer to the "best" (smallest) theoretical prediction of $20\mu_N^2$.

The search for M1 strengths in ^{208}Pb over a large Ex range is important to experimentally determine the M1 strengths and their E_x distribution.

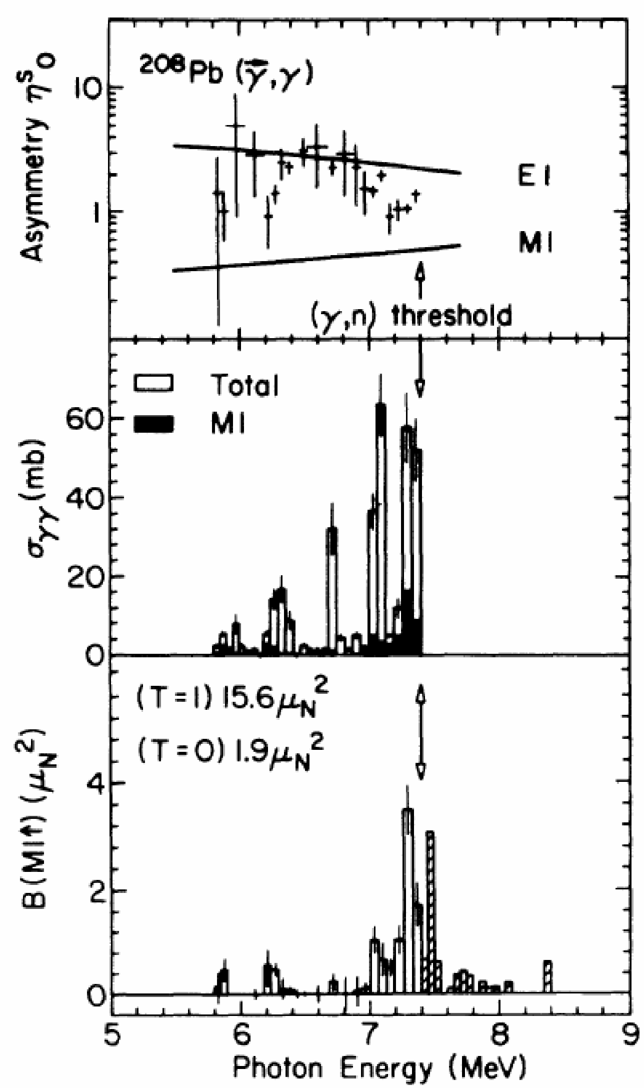

R.M. Laszewski et al, PRL61(1988)1710

Grand Raiden in the 0deg Measurement Setup

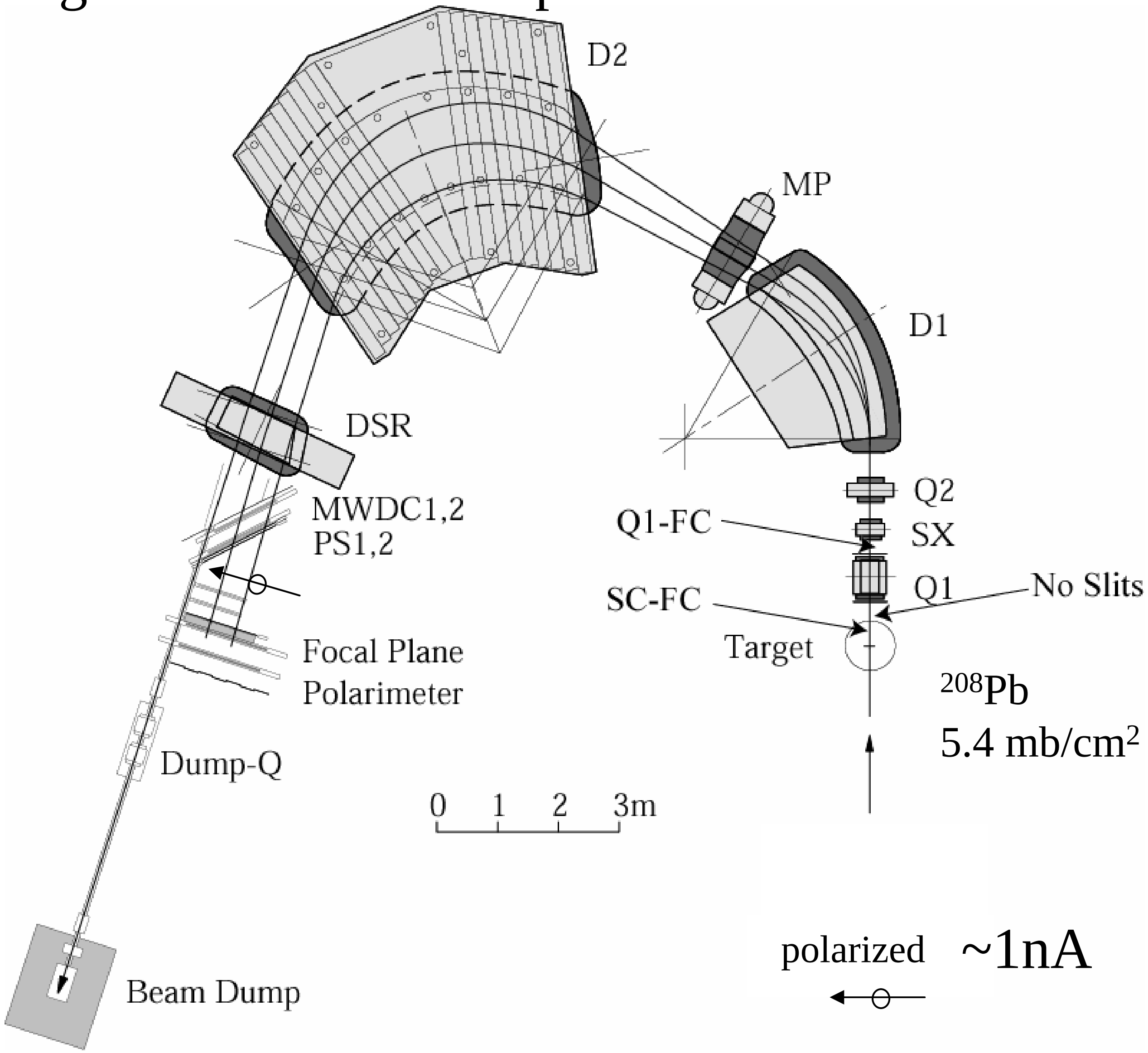

D_{LL} measurement is under preparation.

D_{NN} ($=D_{SS}$) Measurement

- ΔS can be model-independently extracted by measuring polarization transfer coefficients at 0° (ΔS decomposition of the strengths)

$$2D_{NN} + D_{LL} = \begin{cases} -1 \text{ for } \Delta S = 1 & \text{M1} \\ 3 \text{ for } \Delta S = 0 & \text{E1} \end{cases}$$

T.Suzuki, PTP103(2000)859

- E1 and M1 strengths can be decomposed

D_{NN} data have been taken.

D_{LL} measurement is scheduled in this year.

In the present stage, we need an assumption (D_{NN} = -0.24 for M1) for the decomposition.

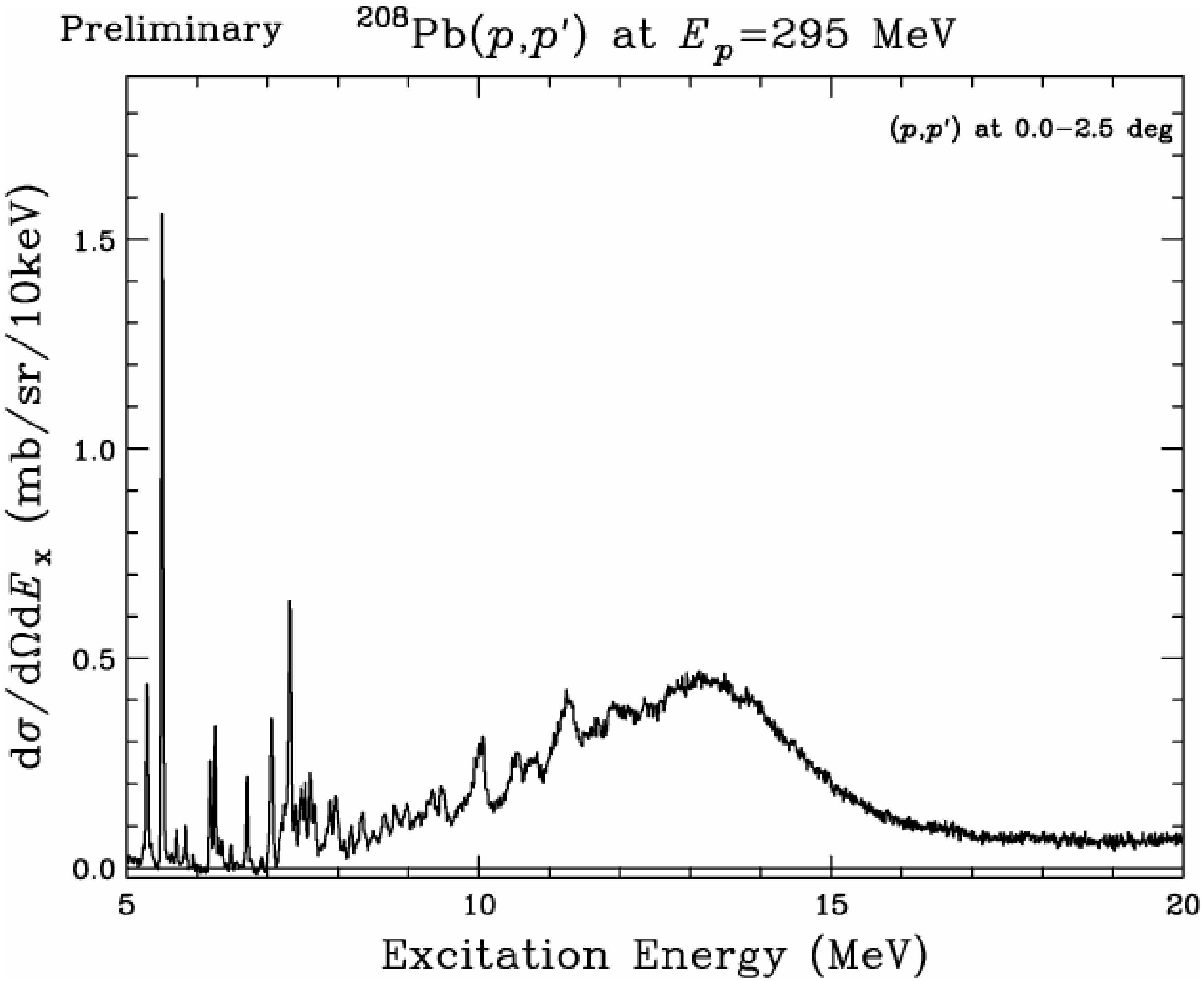
Preliminary
208Pb(p,p') at Ep=295 MeV
(p,p') at 0.0–2.5 deg
dσ/dΩdEx (mb/sr/10keV)
0.0
0.5
1.0
1.5
5
10
15
20
Excitation Energy (MeV)

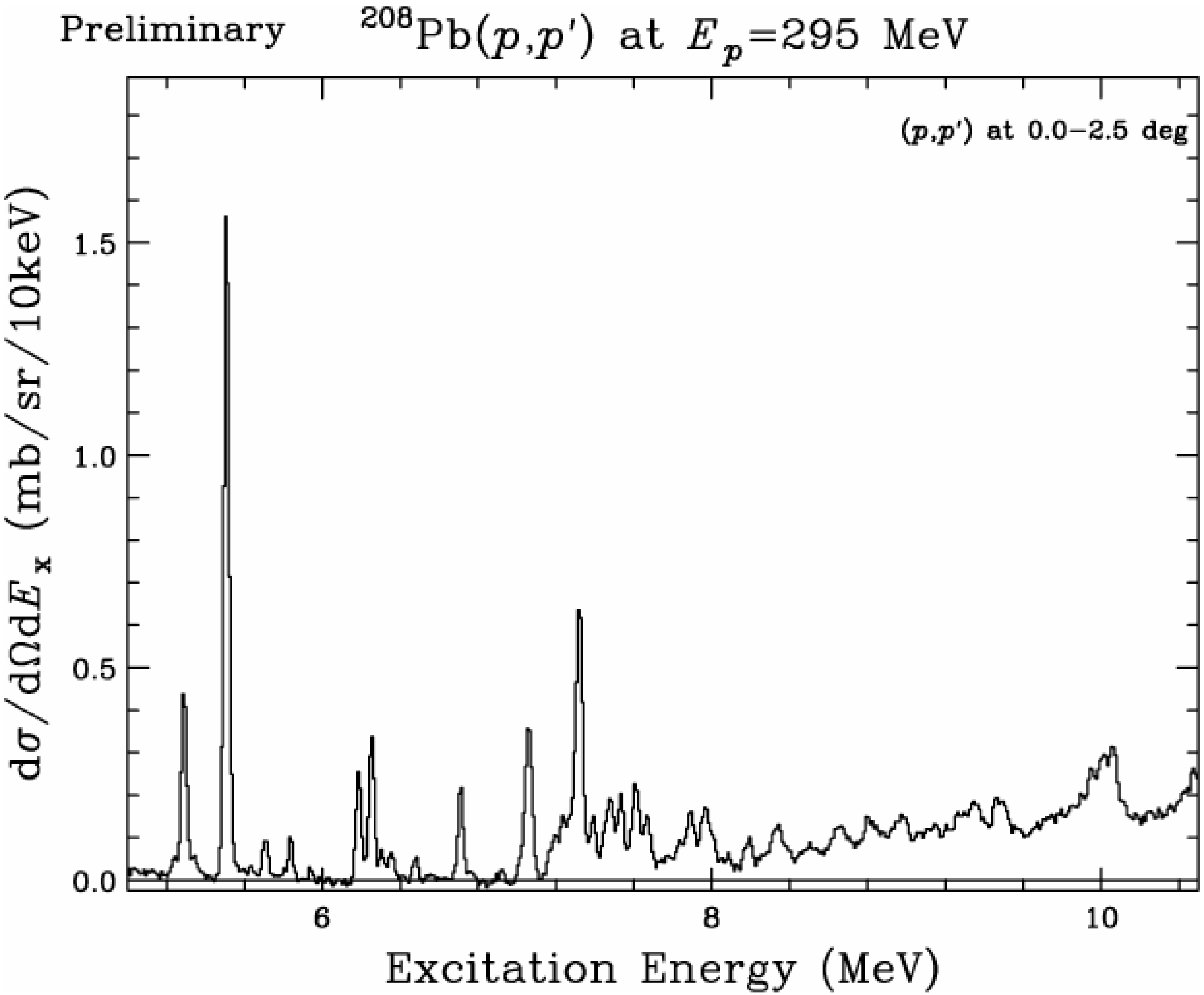
Preliminary
208Pb(p,p') at Ep=295 MeV
(p,p') at 0.0–2.5 deg
dσ/dΩdEx (mb/sr/10keV)
1.5
1.0
0.5
0.0
6
8
10
Excitation Energy (MeV)

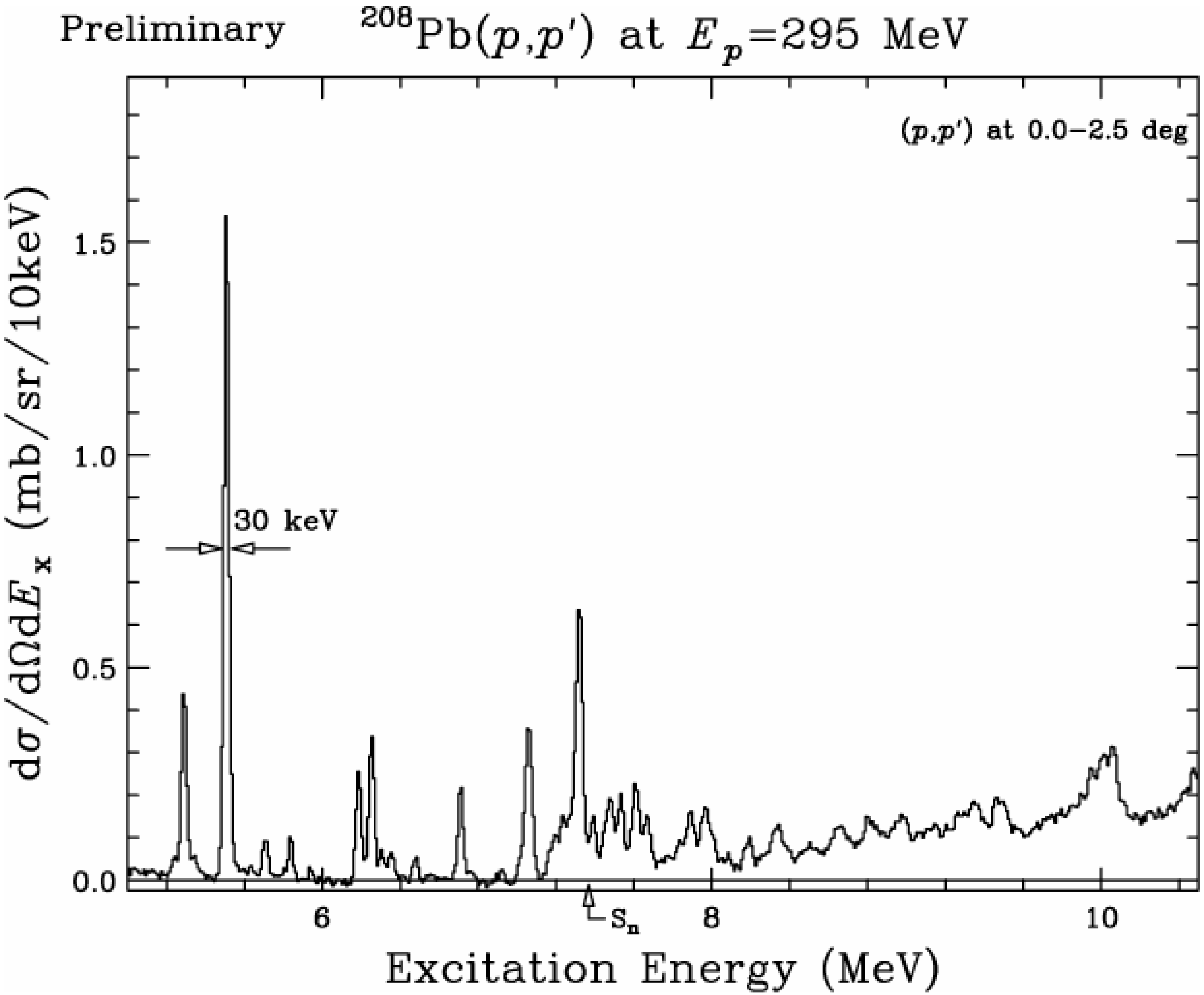
Preliminary
208Pb(p,p') at Ep=295 MeV
(p,p') at 0.0–2.5 deg
30 keV
dσ/dΩdEx (mb/sr/10keV)
0.0
0.5
1.0
1.5
6
8
10
Sn
Excitation Energy (MeV)

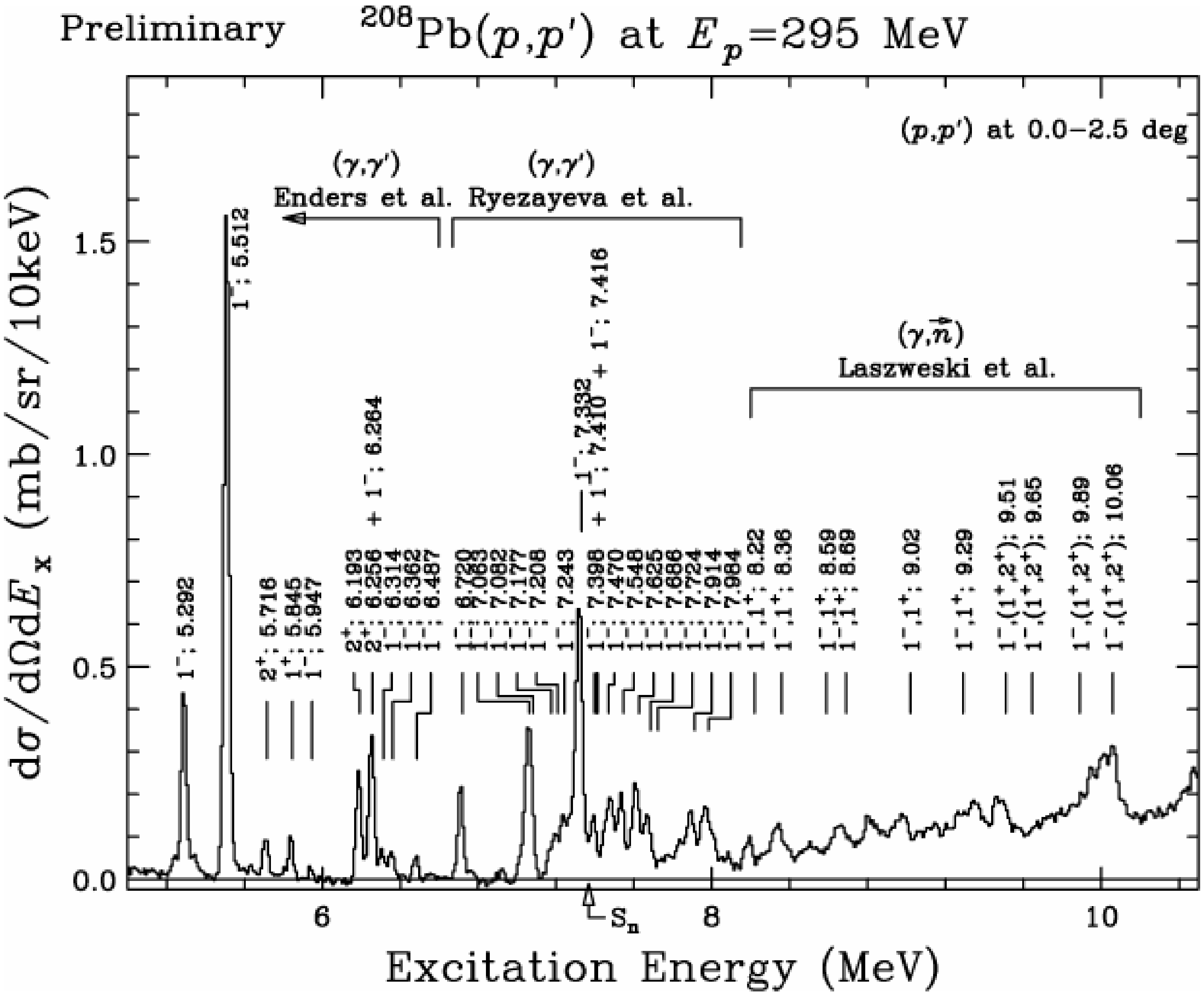
Preliminary
208Pb(p,p') at Ep=295 MeV
(p,p') at 0.0–2.5 deg
(γ,γ')
Enders et al.
(γ,γ')
Ryezayeva et al.
(γ,n)
Laszweski et al.
1−; 5.292
1−; 5.512
2+; 5.716
1+; 5.845
1−; 5.947
2+; 6.193
2+; 6.256
1−; 6.314
1−; 6.362
1−; 6.487
+ 1−; 6.264
1−; 6.720
1−; 7.063
1−; 7.082
1−; 7.177
1−; 7.208
1−; 7.243
1−; 7.332
1−; 7.398
1−; 7.470
1−; 7.548
1−; 7.625
1−; 7.686
1−; 7.724
1−; 7.914
1−; 7.984
+ 1−; 7.410 + 1−; 7.416
1−,1+; 8.22
1−,1+; 8.36
1−,1+; 8.59
1−,1+; 8.69
1−,1+; 9.02
1−,1+; 9.29
1−,(1+,2+); 9.51
1−,(1+,2+); 9.65
1−,(1+,2+); 9.89
1−,(1+,2+); 10.06
Sn
dσ/dΩdEx (mb/sr/10keV)
Excitation Energy (MeV)
0.0
0.5
1.0
1.5
6
8
10

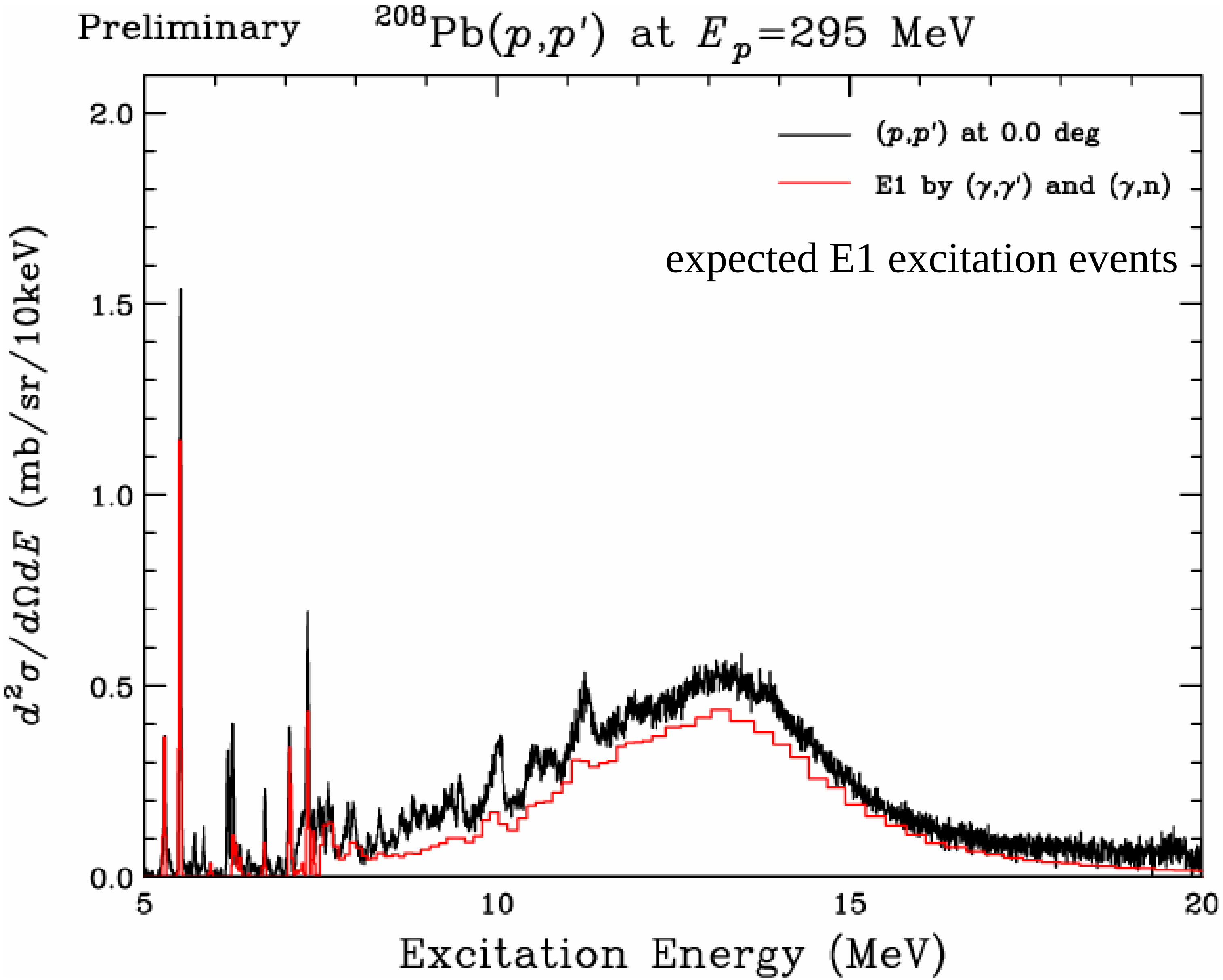
Preliminary
^{208}Pb(p,p') at E_p=295 MeV
(p,p') at 0.0 deg
E1 by (γ,γ') and (γ,n)
expected E1 excitation events
$d^2\sigma/d\Omega dE$ (mb/sr/10keV)
2.0
1.5
1.0
0.5
0.0
5
10
15
20
Excitation Energy (MeV)

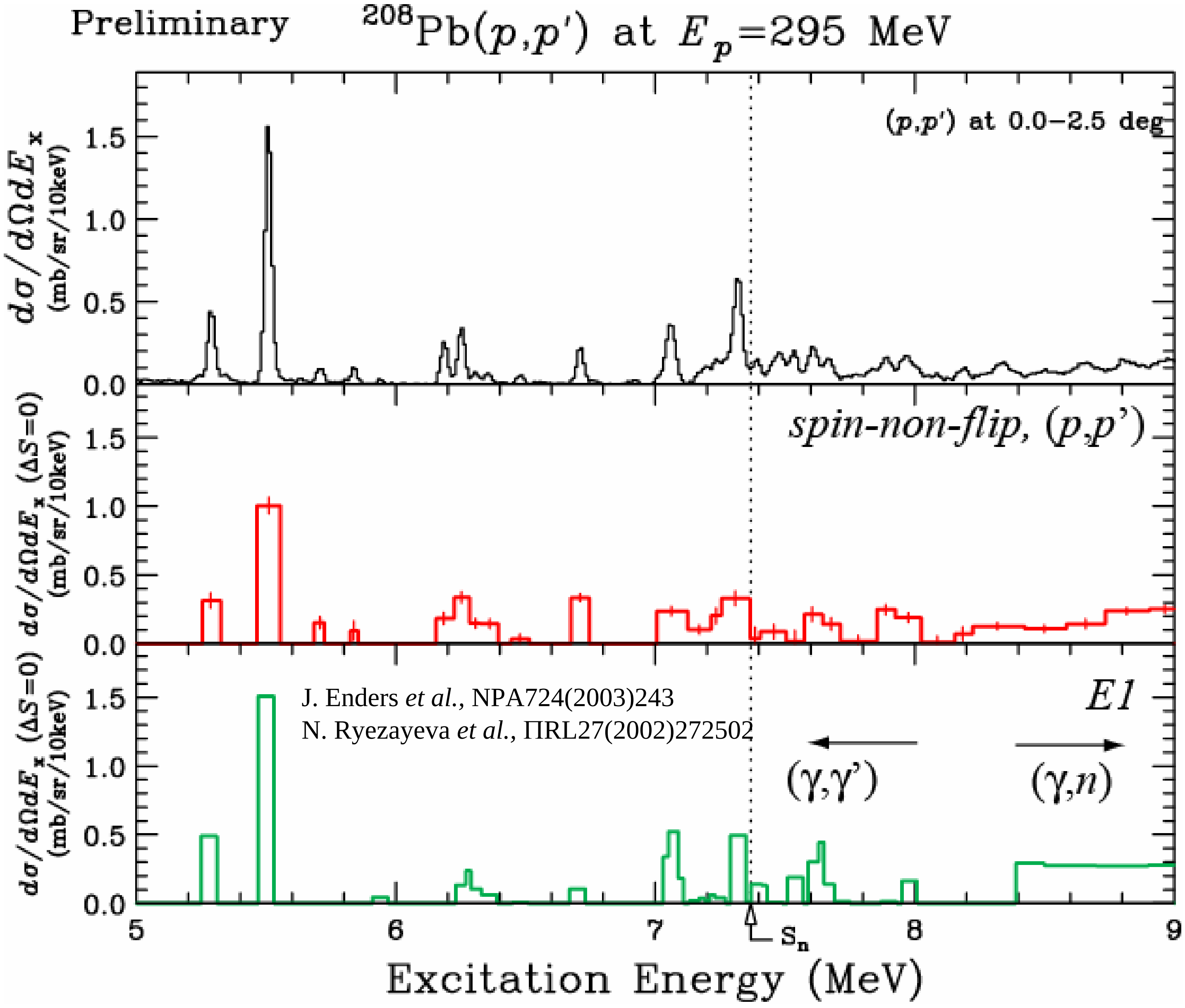
Preliminary
^{208}Pb(p,p') at E_p=295 MeV
(p,p') at 0.0–2.5 deg
spin-non-flip, (p,p')
E1
J. Enders et al., NPA724(2003)243
N. Ryezayeva et al., ПRL27(2002)272502
(γ,γ')
(γ,n)
$d\sigma/d\Omega dE_x$ (mb/sr/10keV)
$d\sigma/d\Omega dE_x$ (ΔS=0) (mb/sr/10keV)
0.0
0.5
1.0
1.5
5
6
7
8
9
S_n
Excitation Energy (MeV)

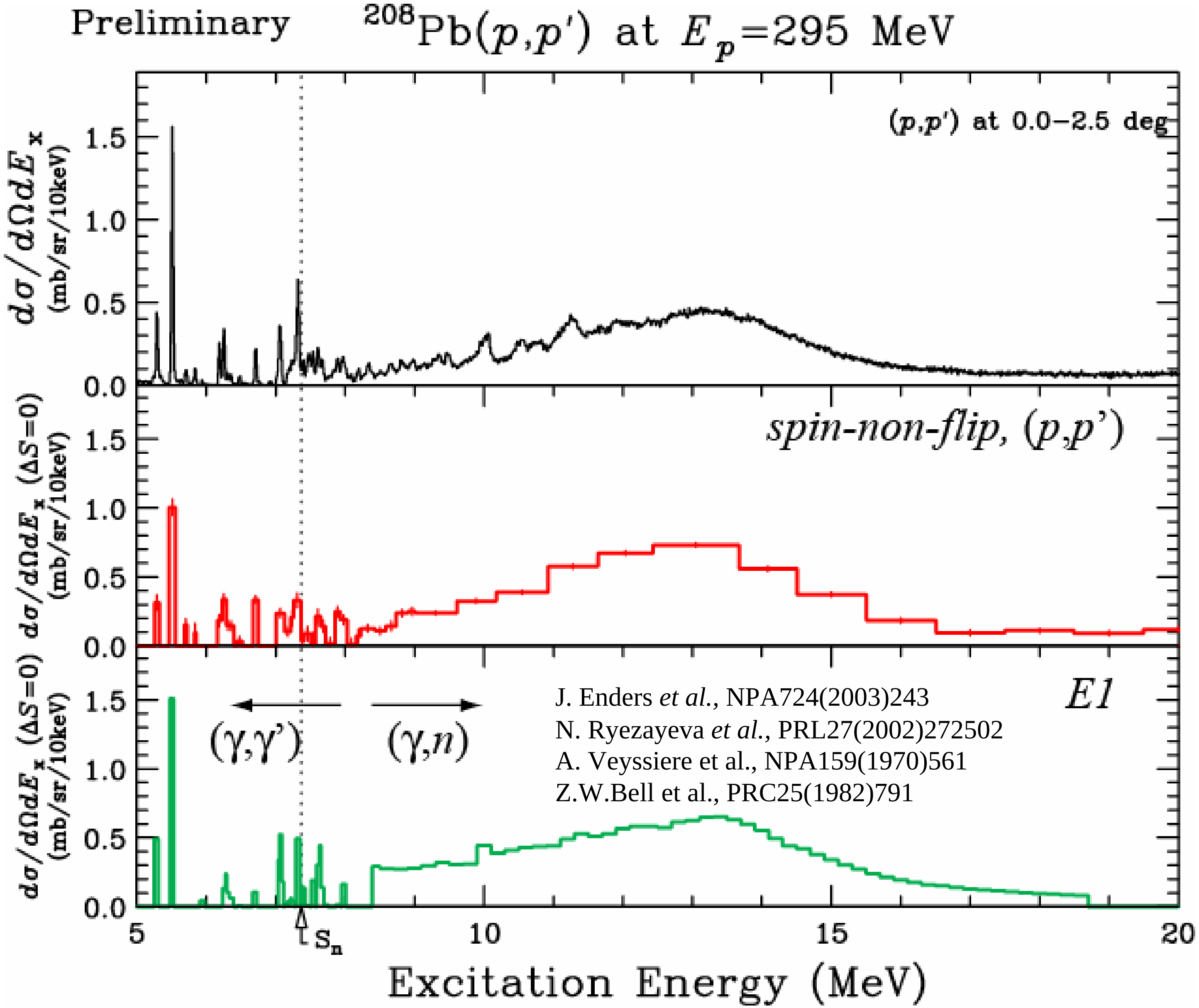

Preliminary
^{208}Pb(p,p') at E_p=295 MeV
(p,p') at 0.0–2.5 deg
spin-non-flip, (p,p')
E1
(γ,γ')
(γ,n)
J. Enders et al., NPA724(2003)243
N. Ryezayeva et al., PRL27(2002)272502
A. Veyssiere et al., NPA159(1970)561
Z.W.Bell et al., PRC25(1982)791
dσ/dΩdE$_x$ (mb/sr/10keV)
dσ/dΩdE$_x$ (ΔS=0) (mb/sr/10keV)
dσ/dΩdE$_x$ (ΔS=0) (mb/sr/10keV)
0.0
0.5
1.0
1.5
5
10
15
20
S$_n$
Excitation Energy (MeV)

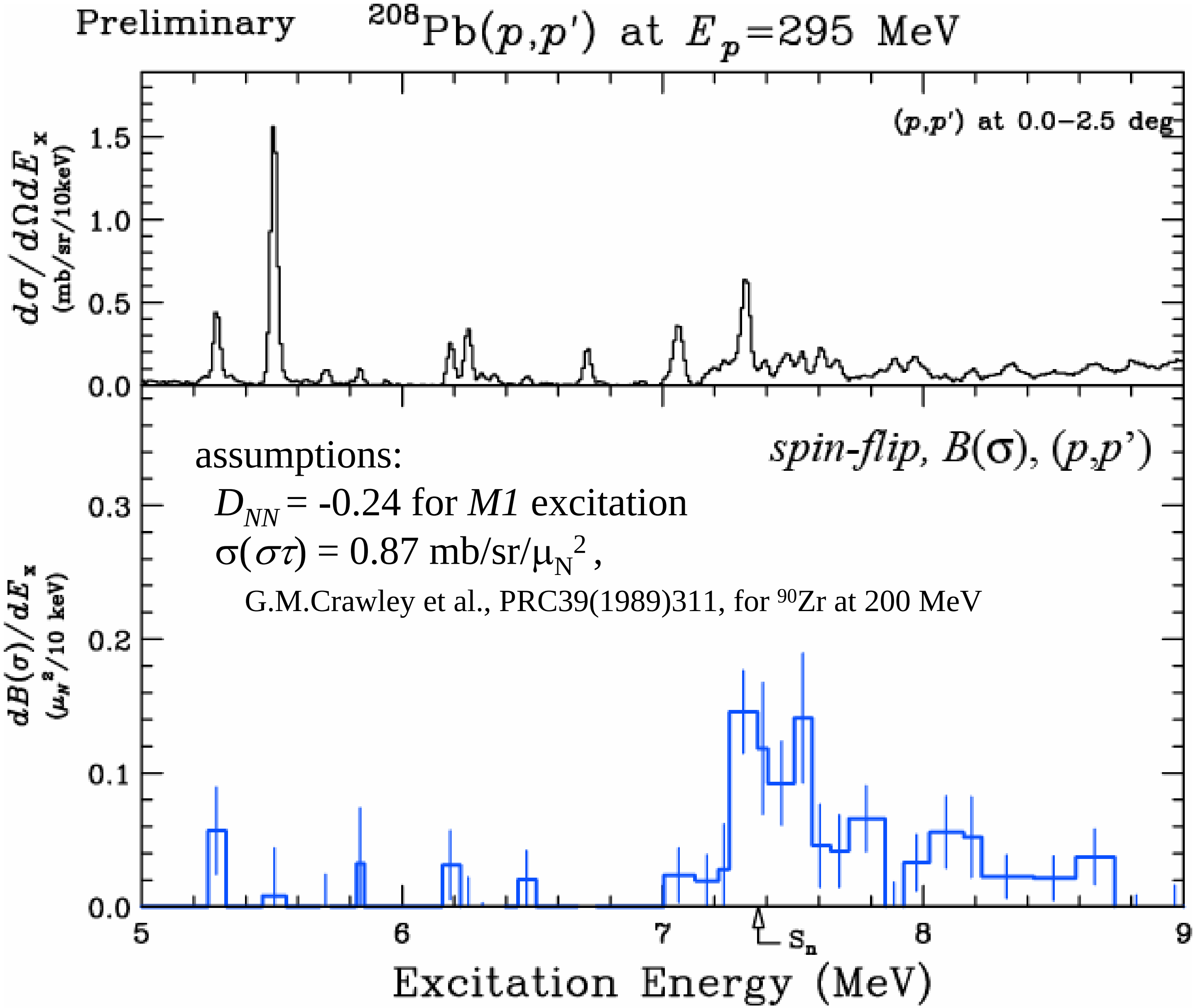
Preliminary
208Pb(p,p') at Ep=295 MeV
(p,p') at 0.0–2.5 deg
dσ/dΩdEx (mb/sr/10keV)
spin-flip, B(σ), (p,p')
assumptions:
DNN = -0.24 for M1 excitation
σ(στ) = 0.87 mb/sr/μN2 ,
G.M.Crawley et al., PRC39(1989)311, for 90Zr at 200 MeV
dB(σ)/dEx (μN2/10 keV)
Sn
Excitation Energy (MeV)

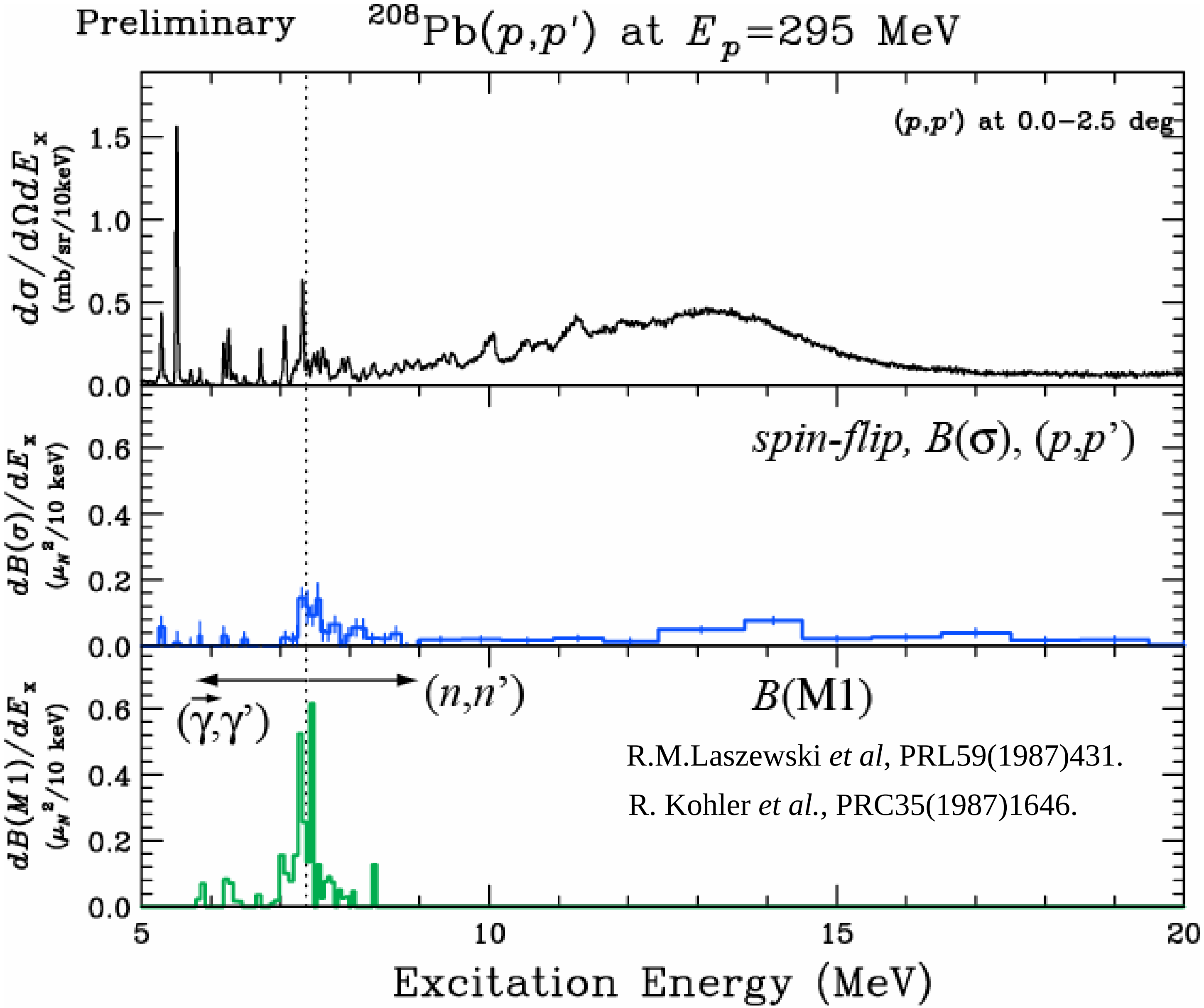

Preliminary
^{208}Pb(p,p') at E_p=295 MeV
(p,p') at 0.0–2.5 deg
dσ/dΩdE$_x$ (mb/sr/10keV)
spin-flip, B(σ), (p,p')
dB(σ)/dE$_x$ (μ_N^2/10 keV)
(n,n')
(γ,γ')
B(M1)
dB(M1)/dE$_x$ (μ_N^2/10 keV)
R.M.Laszewski et al, PRL59(1987)431.
R. Kohler et al., PRC35(1987)1646.
Excitation Energy (MeV)

Summary

- High-resolution (*p*,*p*') measurements at forward angles including zero degrees are established and are extensively performed.

  ^{12}C, sd-shell region, ^{48}Ca, ^{58}Ni, ^{208}Pb

- A lot of high-quality data are coming soon.

Thank you!

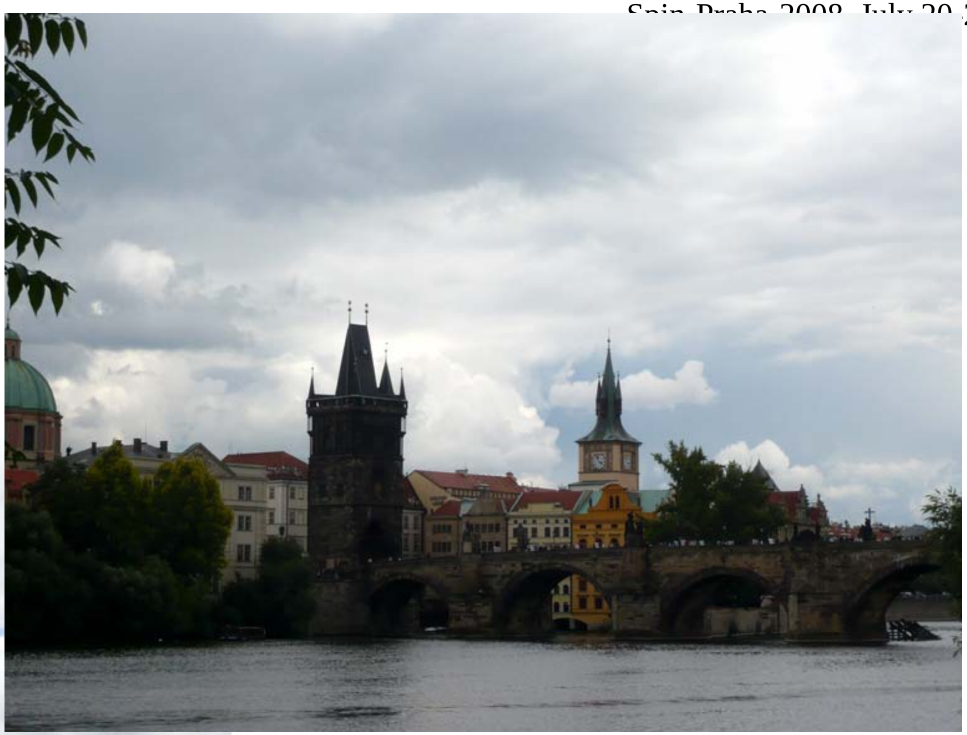

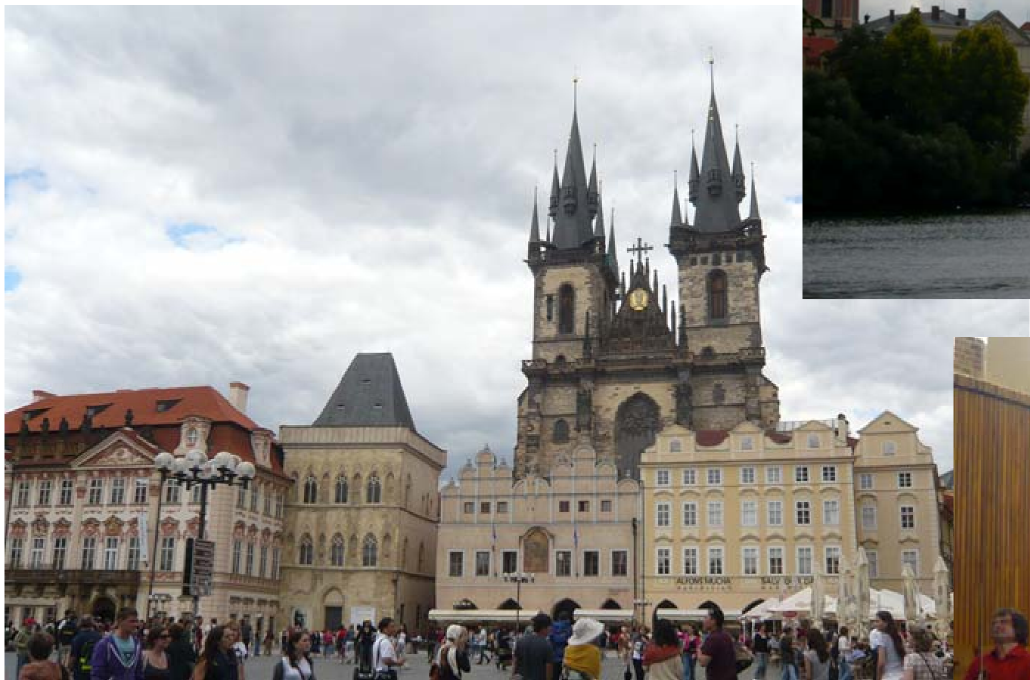

Fragmentation of Excitation Strengths

Fine Structure of the Gamow-Teller Resonances

$\Delta J^{\pi} = 1^{+}; \Delta T = 1$

The GT strength in ^{58}Cu has been resolved into many fragmented narrow peaks with widths of ~ 100 keV.

How can the
- fragmentation
- peak width

be explained by theories?

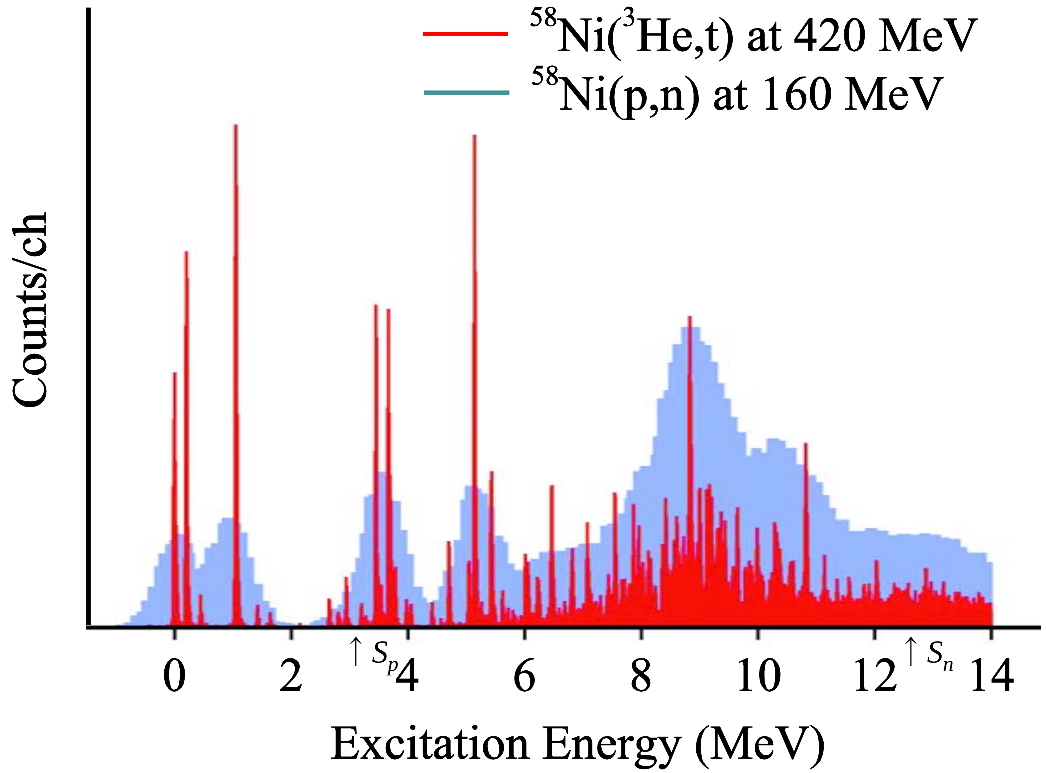

Y. Fujita *et al.*, EPJ A 13, 411 (2002)

Fine structure of the GDR in ^{28}Si

$\Delta J^{\pi}=1^{-}; \Delta T=1$

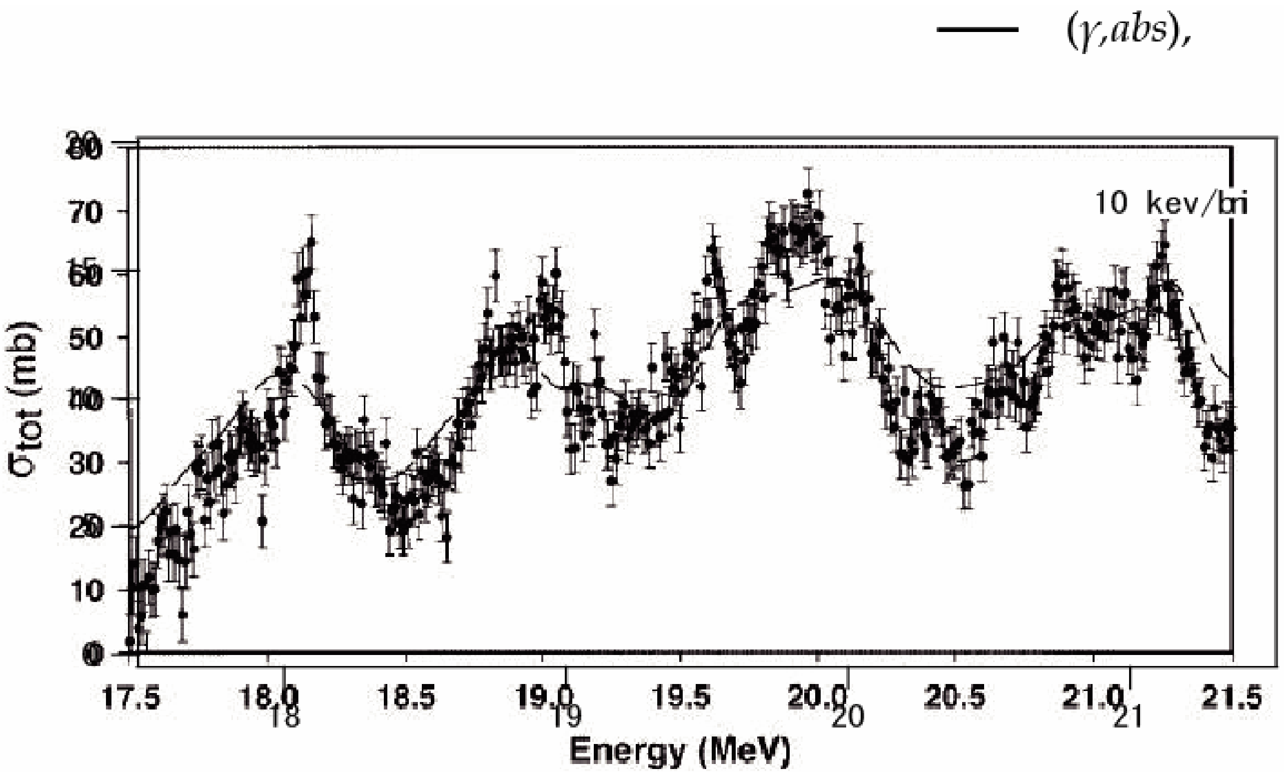

gamma absorption data: H. Harada et al., J. Nucl. Sci. Tech38_465(2001).

Fine structure of the GDR in ^{28}Si

Similar GDR fine structures are observed by different probes

$\Delta J^{\pi}=1^{-}; \Delta T=1$

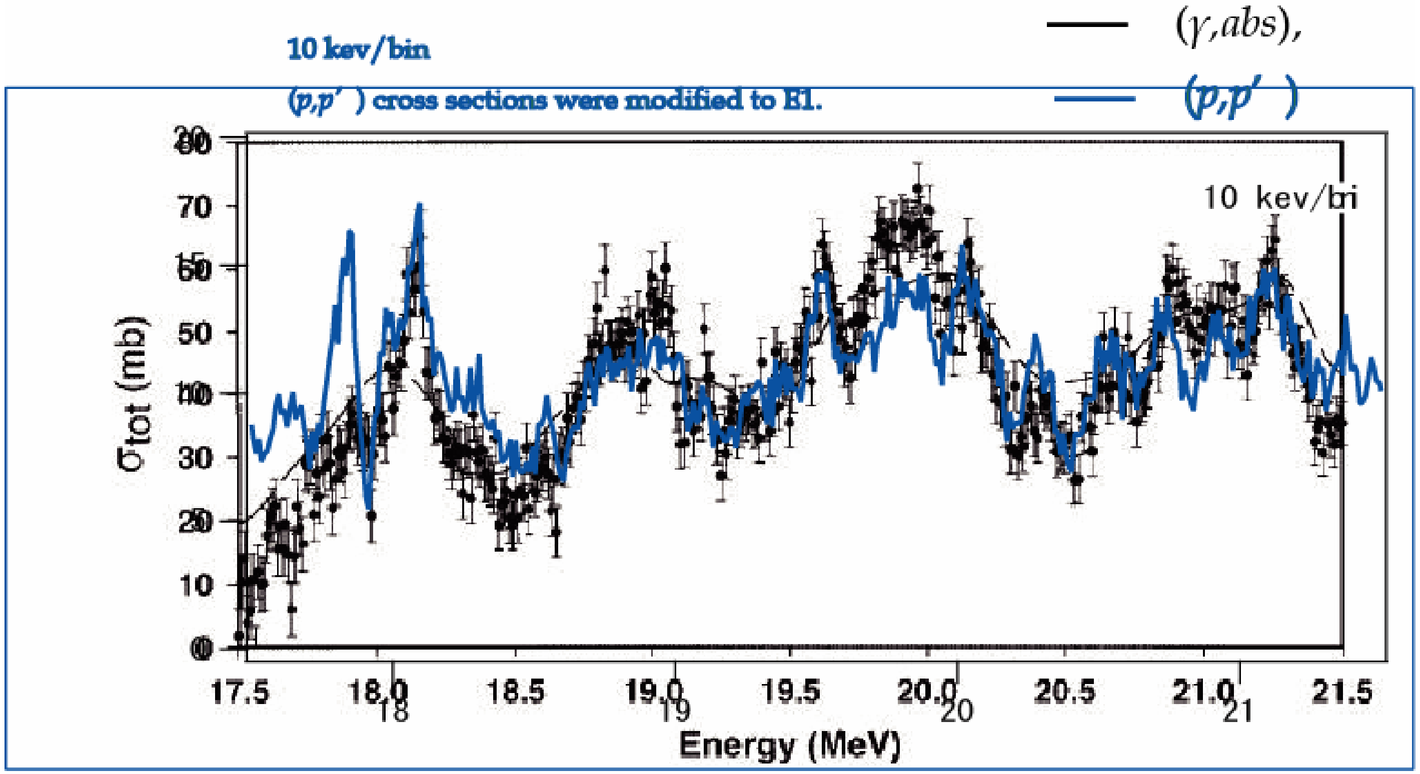

gamma absorption data: H. Harada et al., J. Nucl. Sci. Tech38_465(2001).
(*p*,*p*') data: from E249 at RCNP, H. Matsubara *et al*.
28Si: S_p=11.6 MeV, S_n=17.2 MeV

(p,p’) at 0deg RCNP-E299

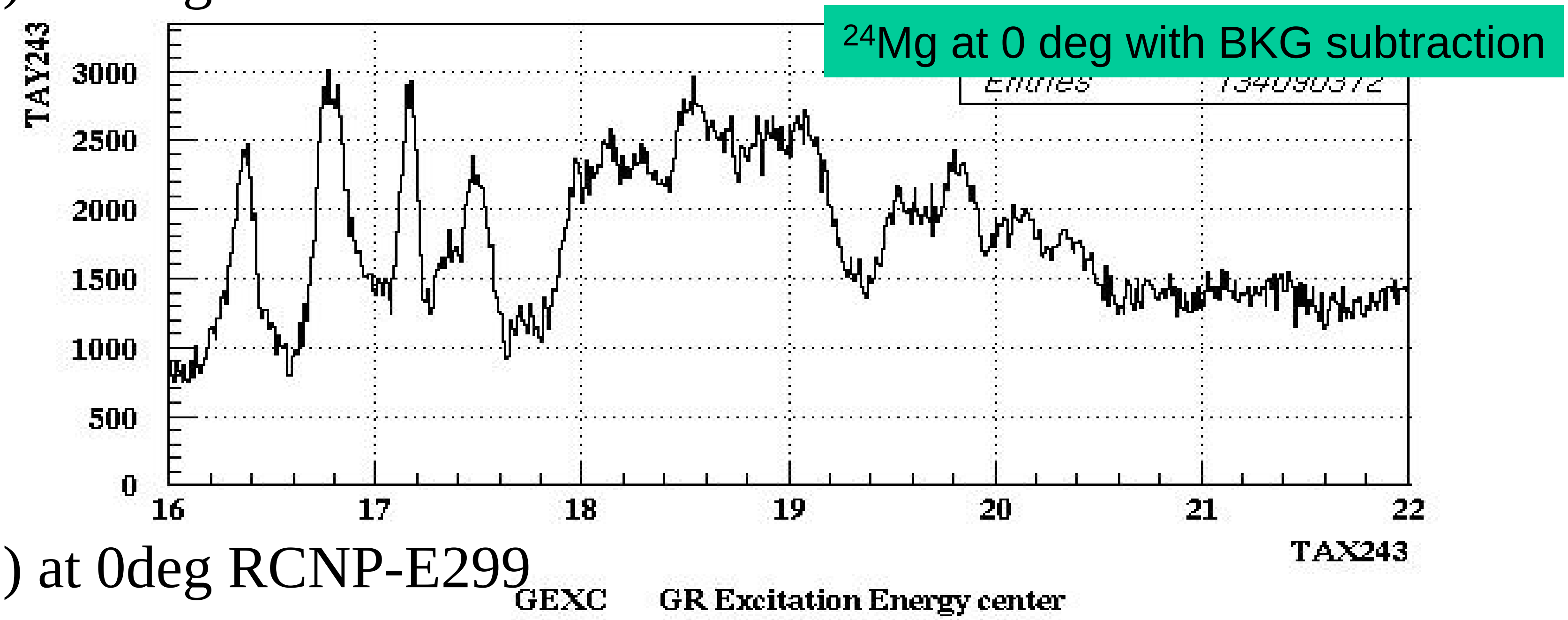

(p,p’) at 0deg RCNP-E299

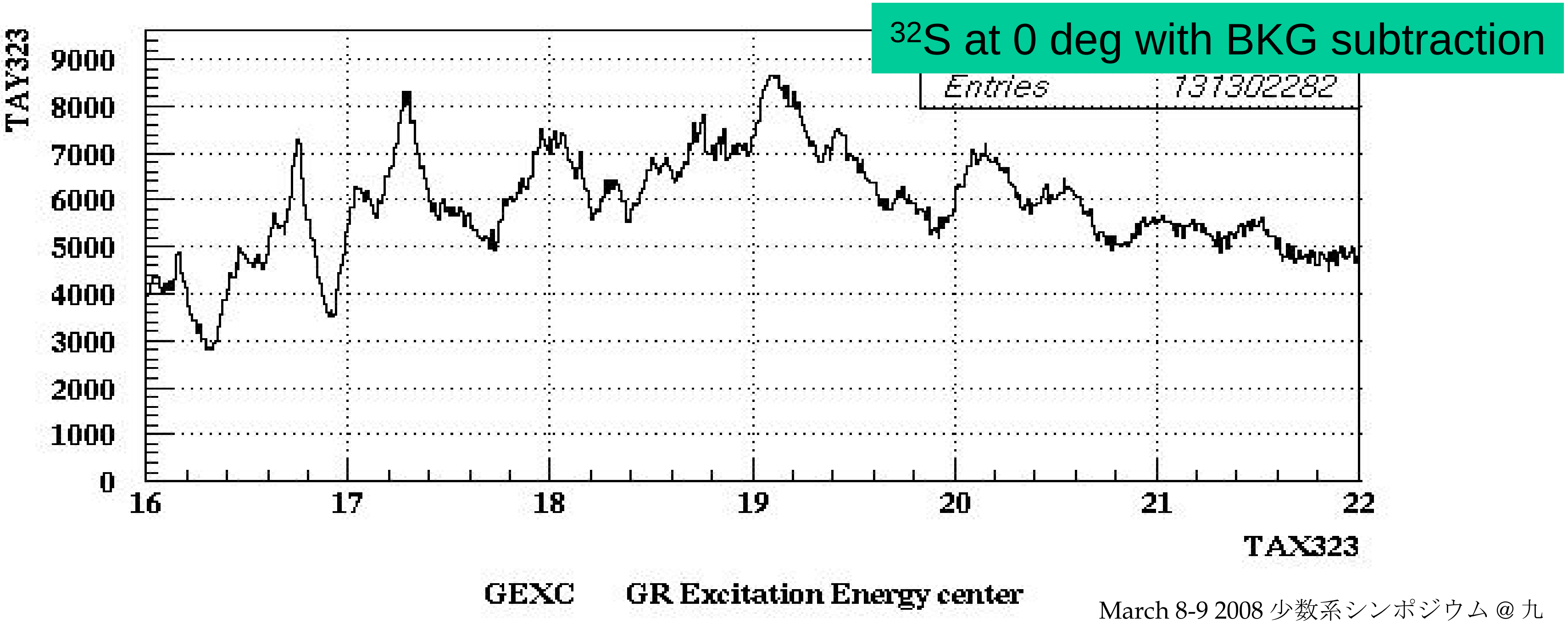

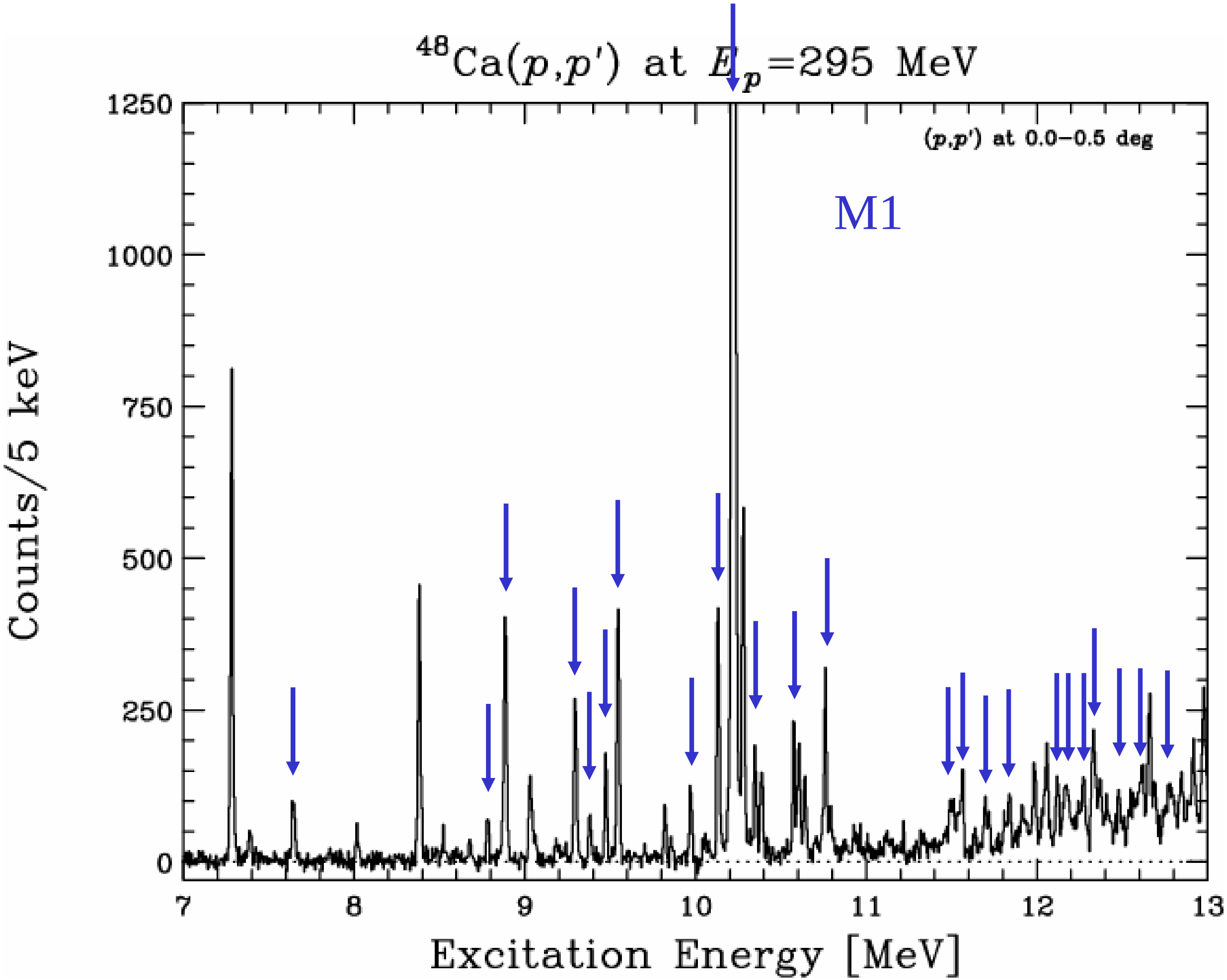

^{48}Ca(p,p') at E_p=295 MeV
(p,p') at 0.0–0.5 deg
M1
Counts/5 keV
1250
1000
750
500
250
0
7
8
9
10
11
12
13
Excitation Energy [MeV]

Strength distribution

preliminary

shell model calculation:
OXBASH + USD interaction

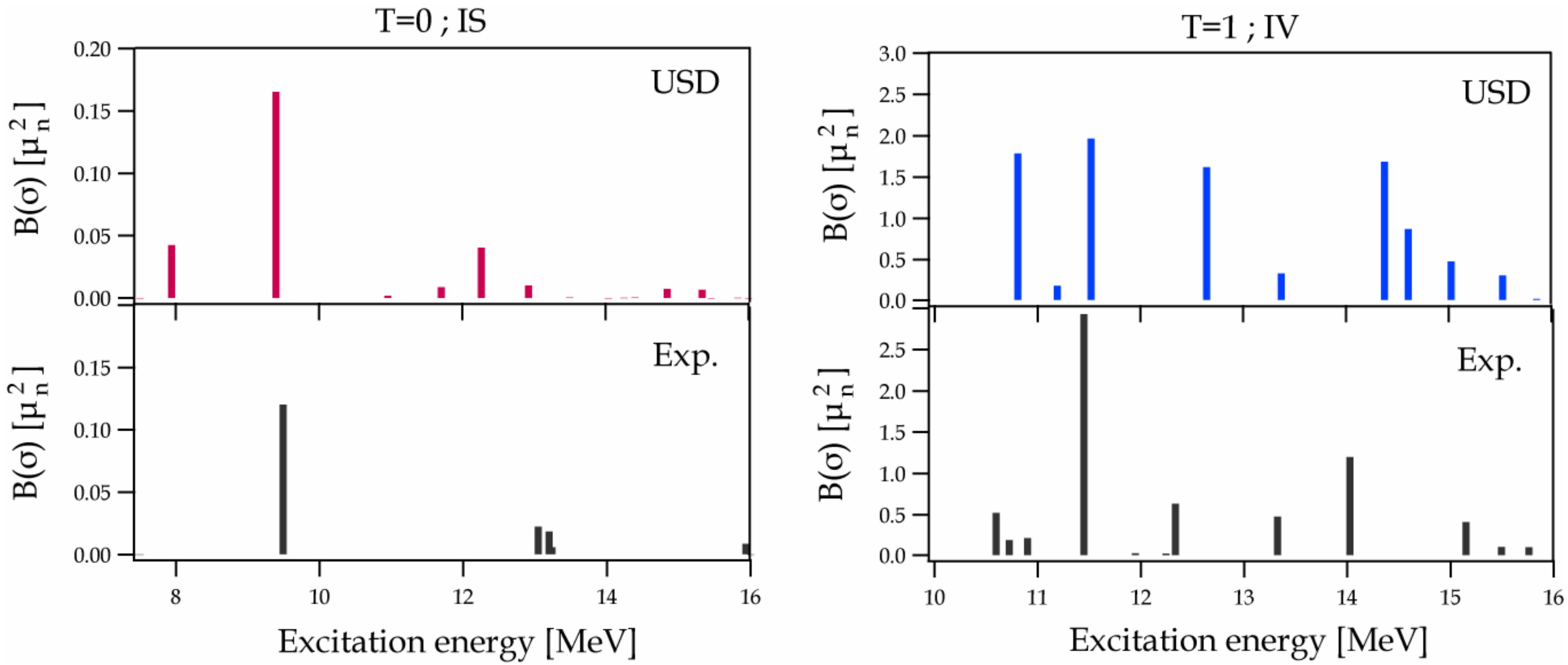

Exponential Slope of the B(σ) Strength Distribution

Data: RCNP-E249

Calc: OXBASH, *sd-shell*, 0hw

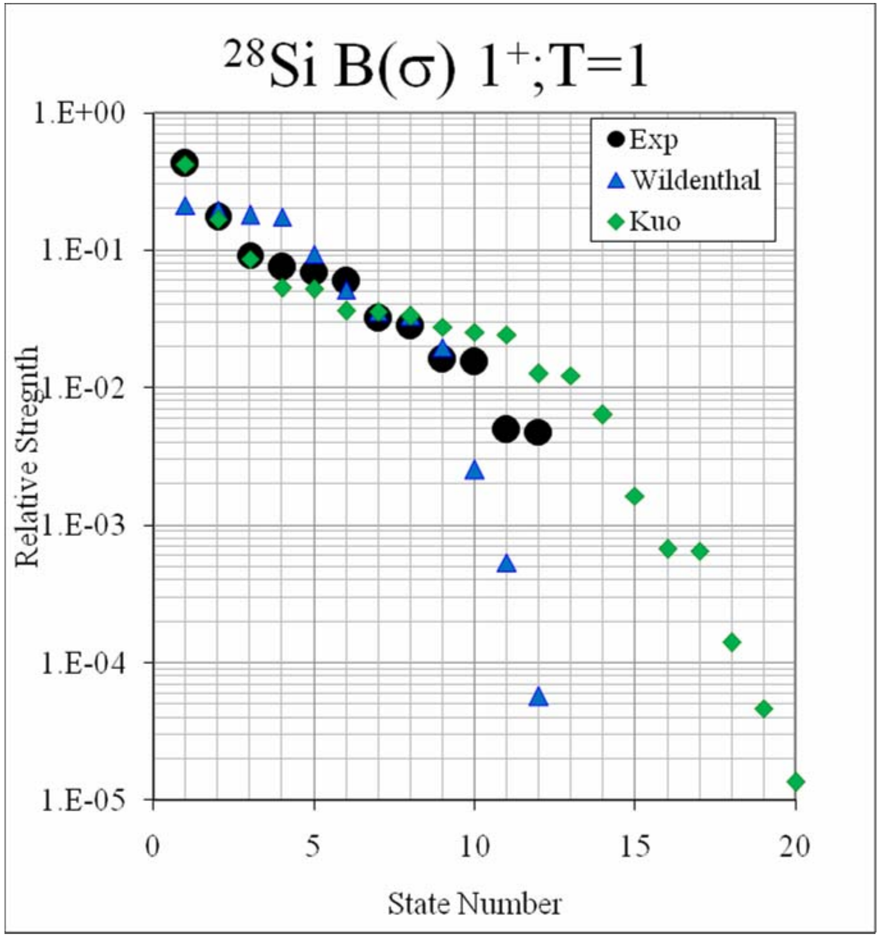

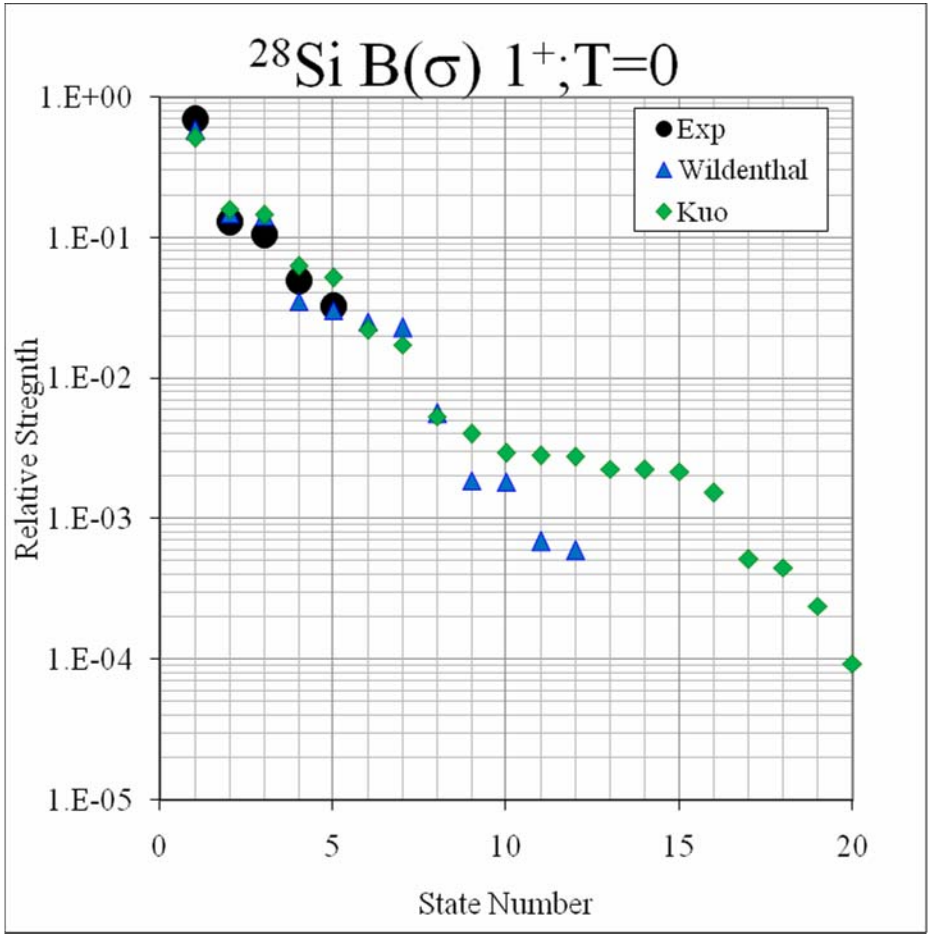

The property of fragmentation can be compared with theoretical calculations?

Backup Slides

Beam Tuning

- Beam energy spread was checked by ^{197}Au(p,p_0) elastic scattering in the achromatic transport mode

  40-60 keV (FWHM) at E_p=295 MeV

  It corresponds to a beam spot size of
  3~5 mm on target
  in the dispersive transport mode.

- Halo free beam tuning at 0 deg. (achro. beam)
  Single turn extraction of the AVF cyclotron

- Tuning of dispersion matching

  20 keV (FWHM) at E_p=295 MeV

It takes ~2 days for the beam tuning.

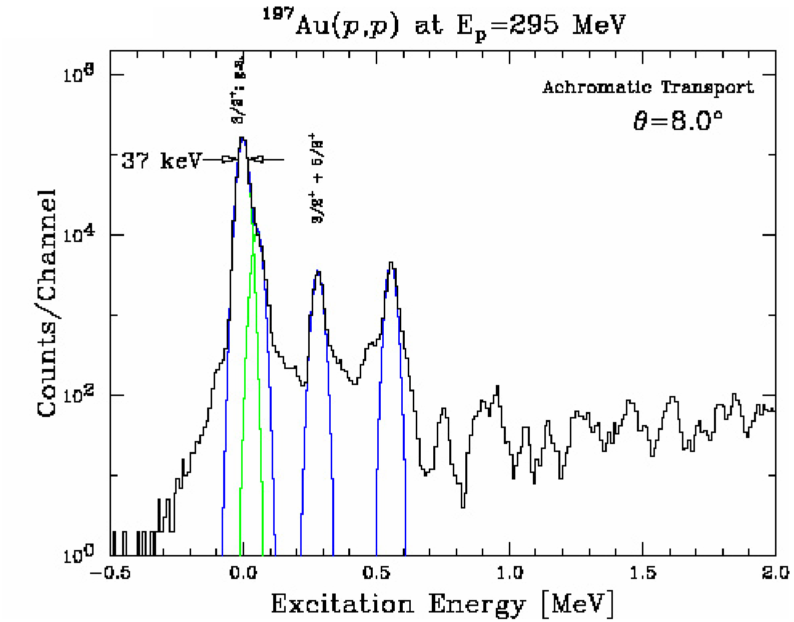

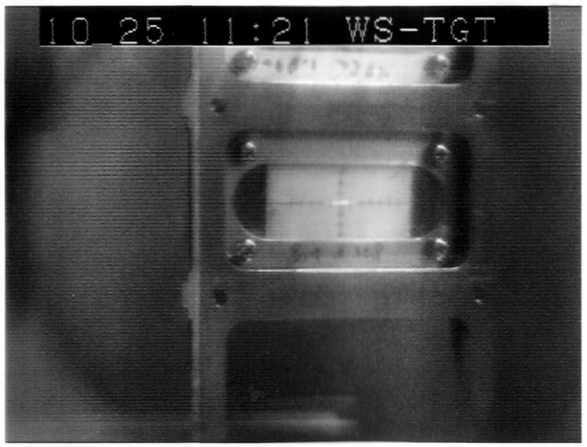

Beam spot in the dispersive mode

Background Subtraction

Vertical positions projected at the vertical focal plane were calculated.

Linear shape of the background in the Y position spectrum was assumed.

Background subtraction was applied by gating the Y position with true+b.g. and b.g. gates.

The background shape is well reproduced by this method.

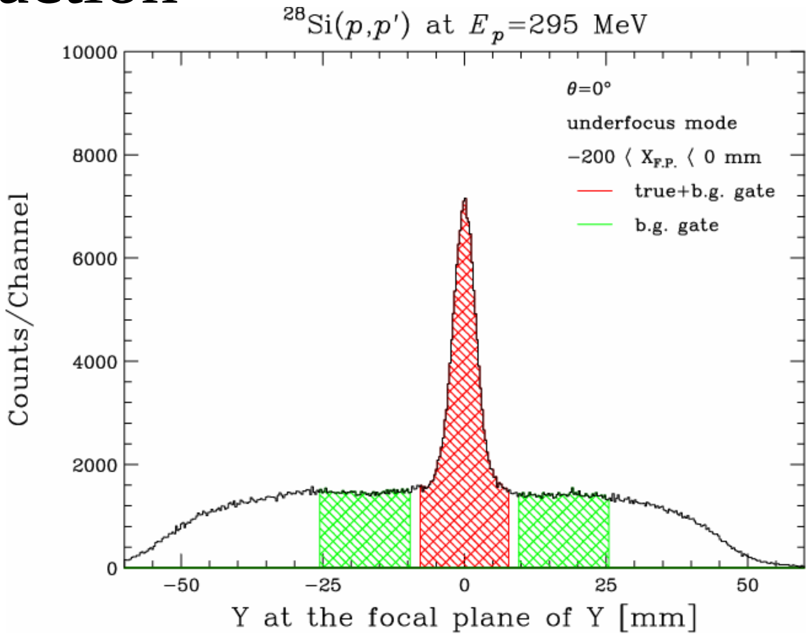

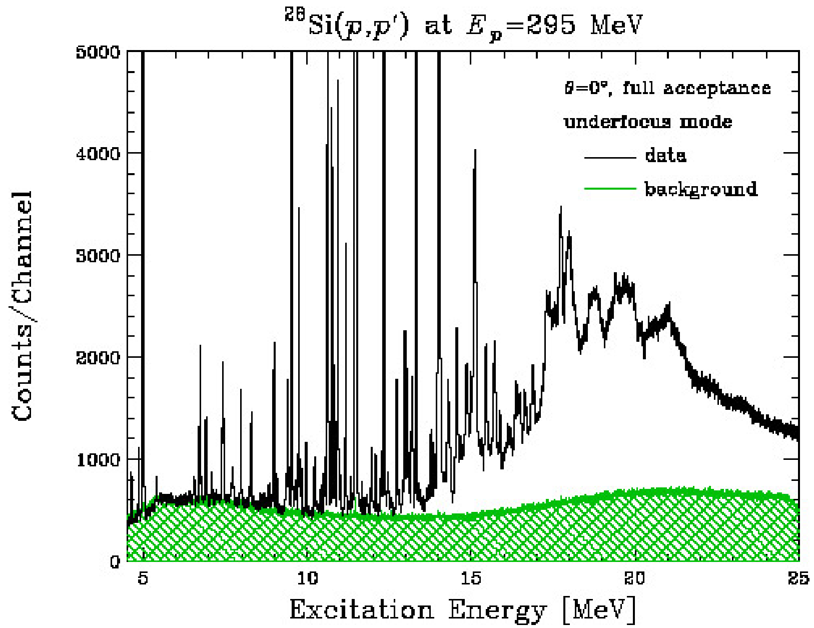

Research Center for Nuclear Physics (RCNP)

proton beam

E_p=295 MeV

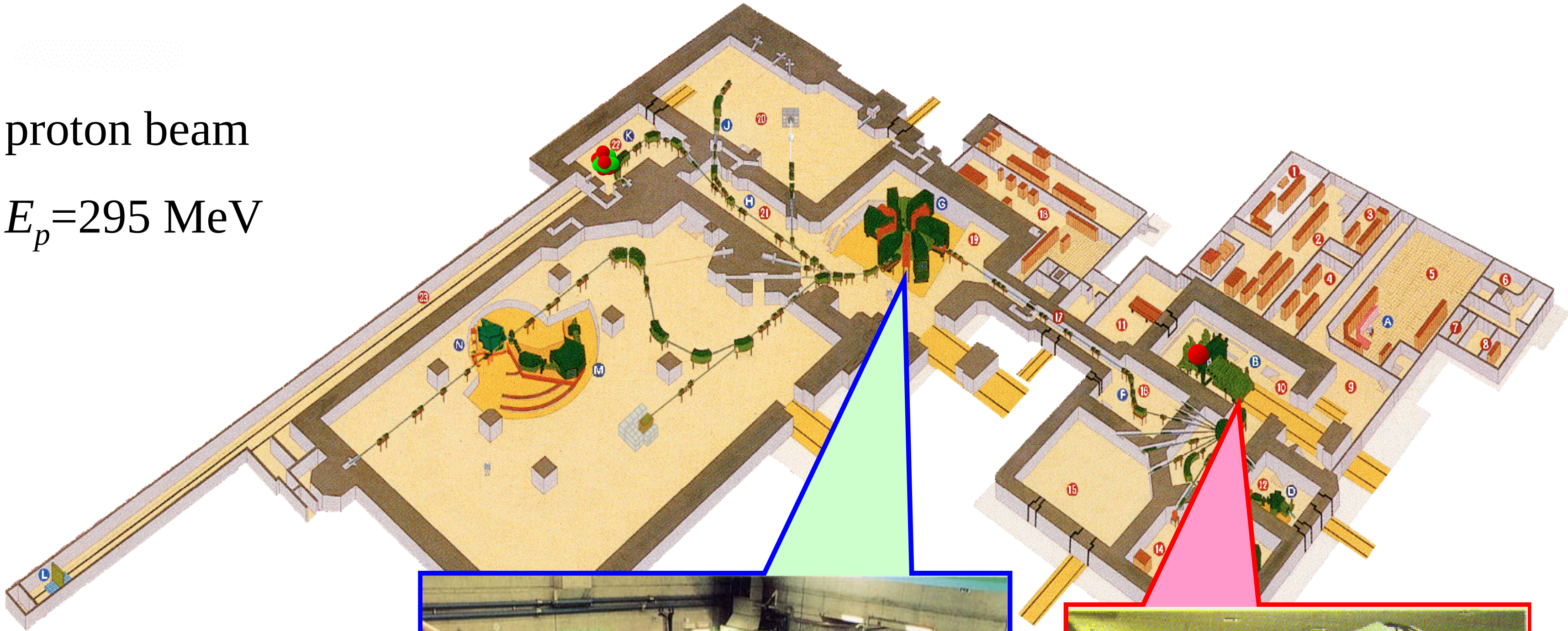

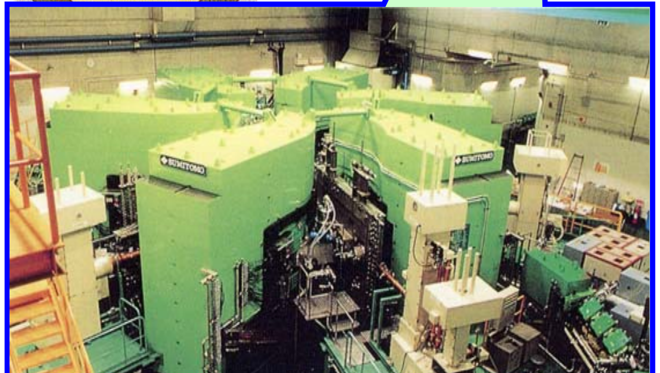

リングサイクロトロン(2,200t)

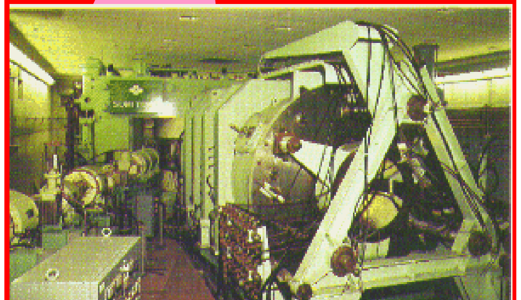

AVFサイクロトロン

Animation by T. Wakasa

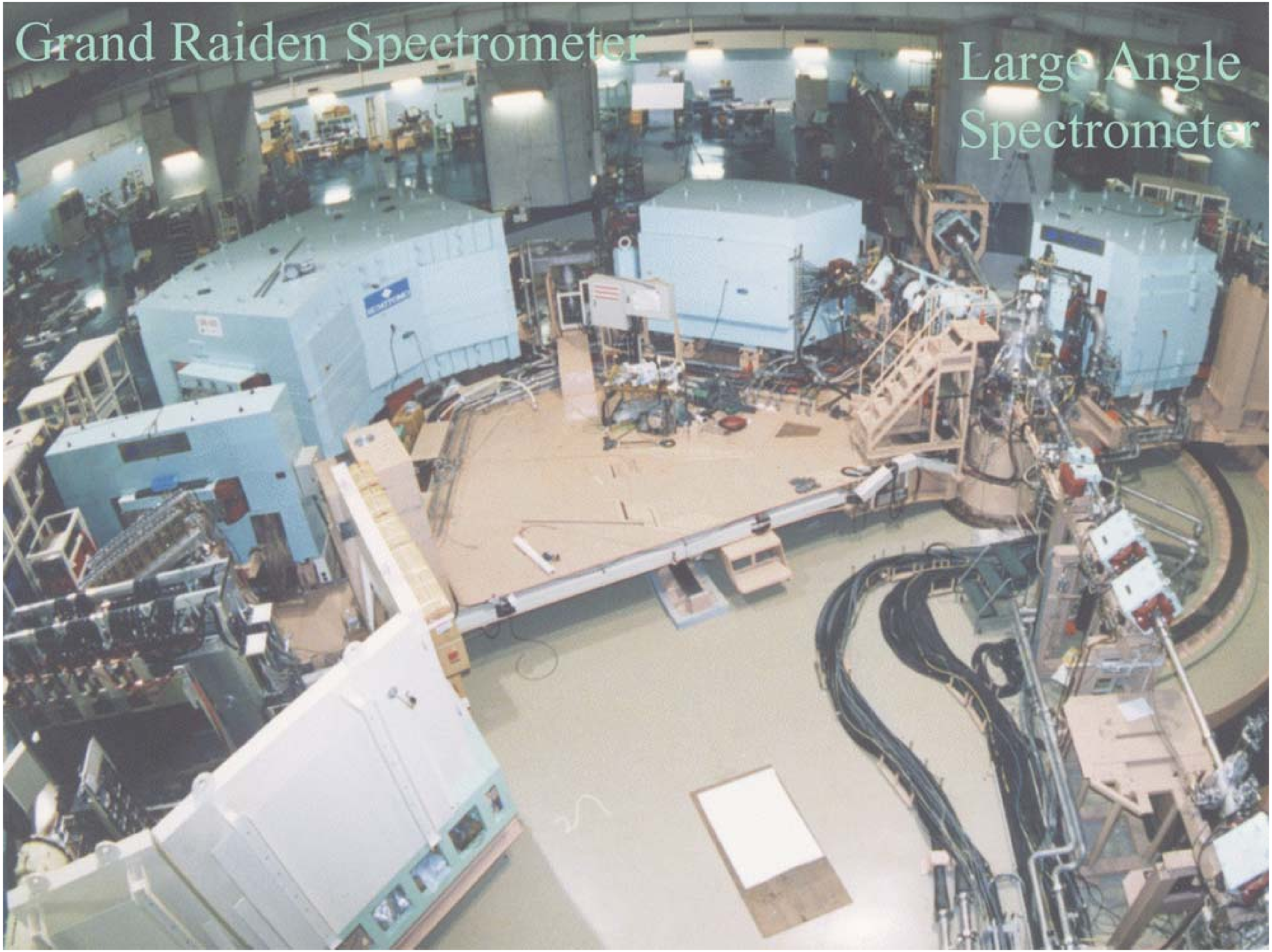
Grand Raiden Spectrometer
Large Angle Spectrometer

Research Center for Nuclear Physics (RCNP) Osaka University

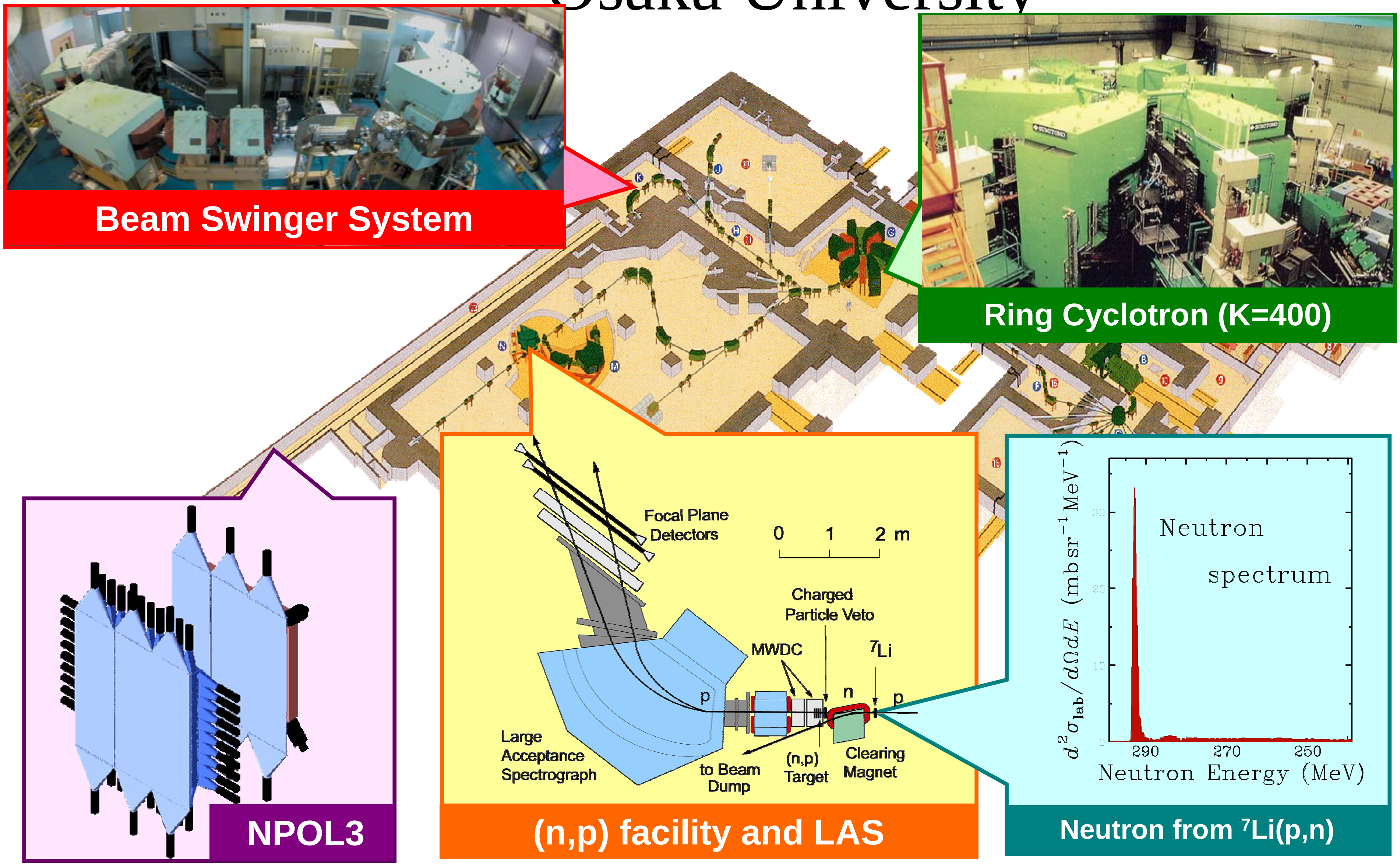

GT Strength B(GT) and Its Quenching

- GTGR :Predicted in 1963 by Ikeda, Fujii, Fujita (←Core Pol.)
  - Discovered in 1975
  - Systematic Studies in 1980s at IUCF
- GT strength B(GT) and σ(0°) of (p,n)
  - σ(0°) ∝ B(GT) ***(Proportionality)***
  - GT sum-rule
    - $S_{\beta-} - S_{\beta+} = 3(N-Z)$

Quenching Factor

$$Q \equiv \frac{S_{\beta^-} - S_{\beta^+}}{3(N-Z)}$$

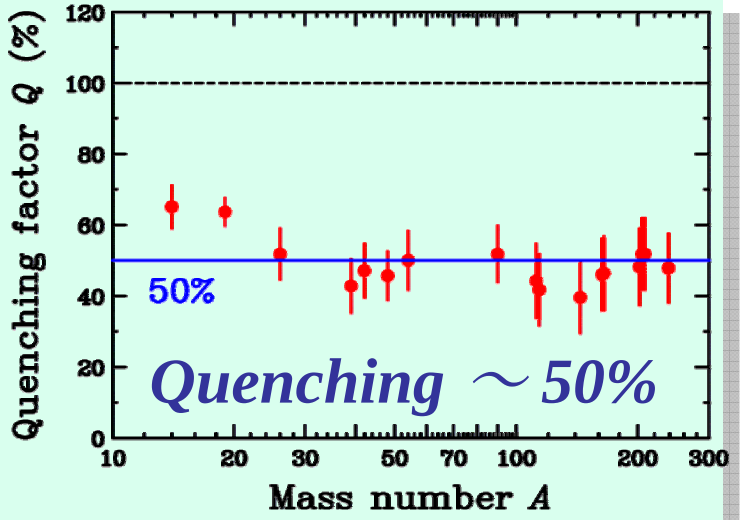

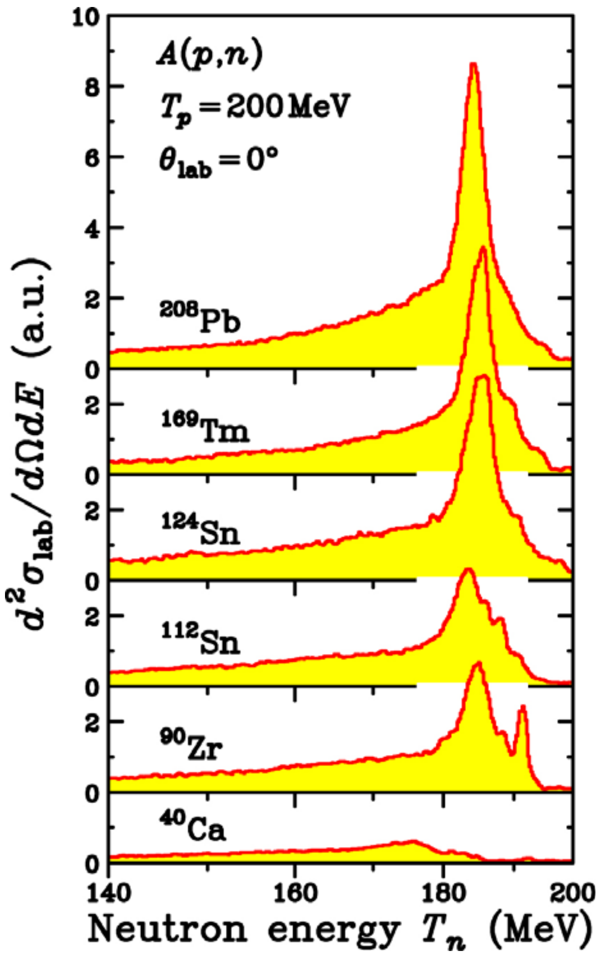

C. Gaarde, NP A396, 127c(1983)

Results of MDA for ^{90}Zr(p,n) & (n,p) at 300 MeV

(K.Yako et al.,PLB 615, 193 (2005))

- Multipole Decomposition (MD) Analyses
  - (p,n)/(n,p) data have been analyzed with the same MD technique
  - (p,n) data have been re-analyzed up to 70 MeV
- Results
  - (p,n)
    - Almost L=0 for GTGR region (No Background)
    - Fairly large L=0 (GT) strength up to 50 MeV excitation
  - (n,p)
    - L=0 strength up to 30MeV

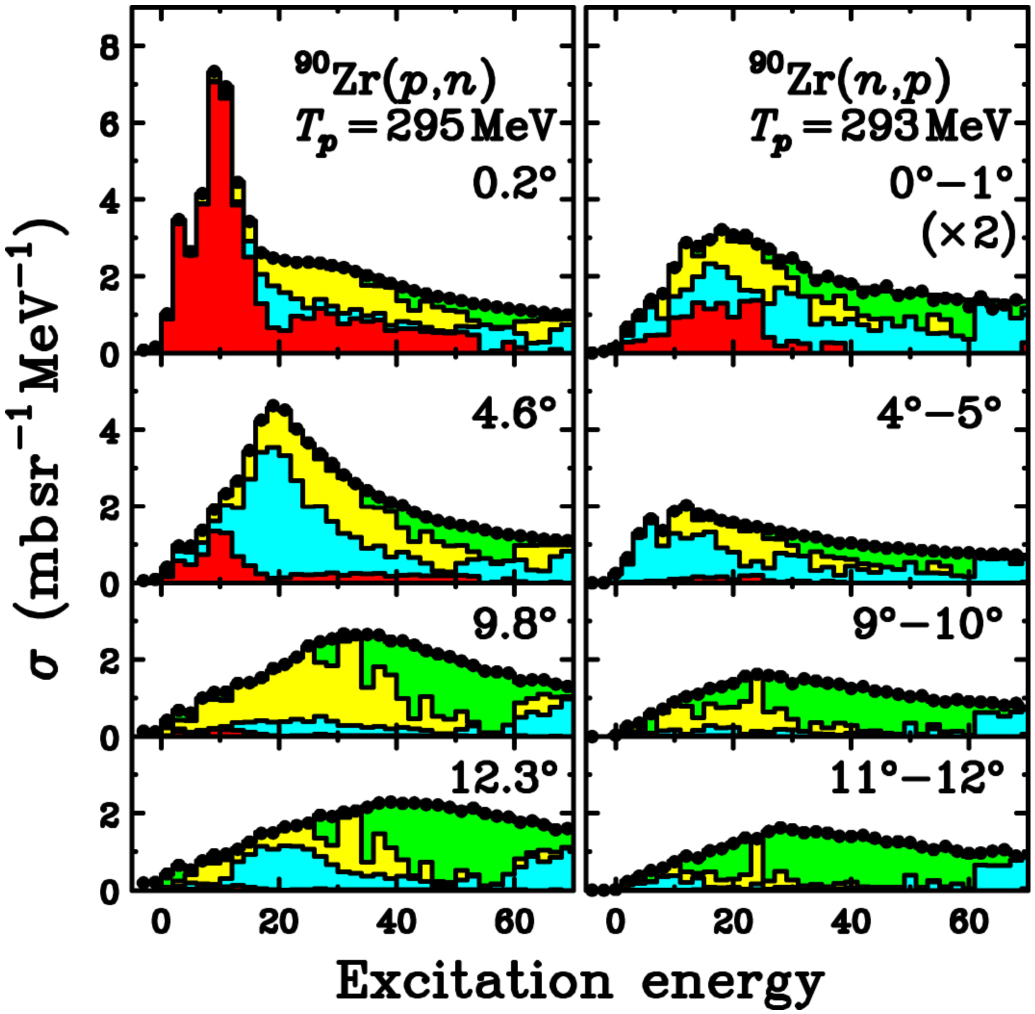

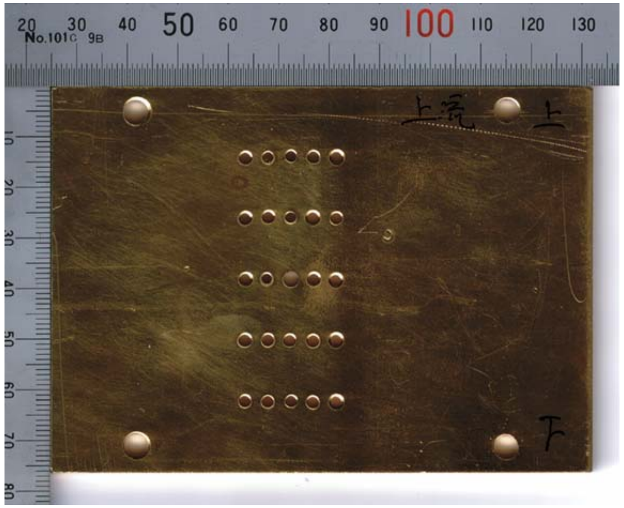

Reconstruction of scattering angles (sieve-slit analysis)

←

a sieve-slit was placed at the entrance of GR

B= +1.0%, X_{fp}= -460 mm,
E_x=~6 MeV at 0deg
$\Delta\phi$ = 0.5 deg, $\Delta\theta$ = 0.15 deg

Image at the focal plane

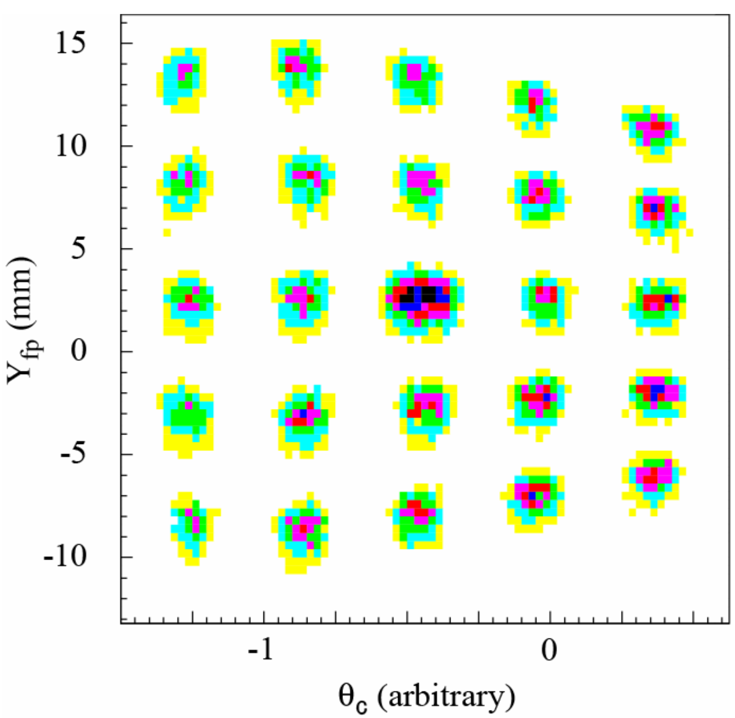

→

Reconstructed image

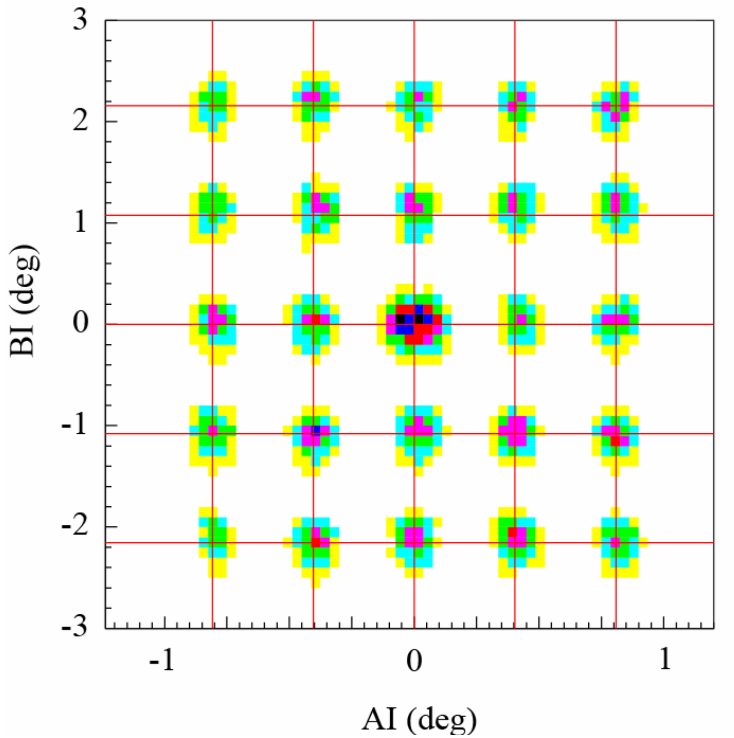

Targets and Angles

	0°	2.5°	4.5°	6°	9,12,15,18°	achrom. 0°	elastic	thickness (mg/cm^2)
^{nat}C	◎	◎	◎	◎	◎	◎	◎	30 (partly 1.1)
mylar	◎	◎	◎	—	—	—	—	10
$^{13}CH_2$	○	—	—	—	—	—	—	0.7
^{24}Mg	○	—	—	—	—	—	—	1.8
^{25}Mg	○	○	○	—	—	—	—	4.00
^{26}Mg	◎	◎	◎	◎	—	—	—	1.55
^{27}Al	○	—	—	—	—	—	—	1.8
^{28}Si	◎	◎	◎	◎	◎	◎	◎	1.86 (58.5 a part of elastic)
^{40}Ca	○	—	—	—	—	—	—	13
^{48}Ca	◎	◎	◎	—	—	—	—	1.9
^{58}Ni	◎	◎	◎	—	—	—	—	4
^{64}Ni	◎	◎	◎	—	—	—	—	4.7
^{90}Zr	△	—	—	—	—	—	—	1.0
^{120}Sn	△	—	—	—	—	—	—	2.6
^{208}Pb	◎	◎	◎	◎	—	—	—	5.2

○... measured, ◎... good statistics, △... poor statistics, —... not measured

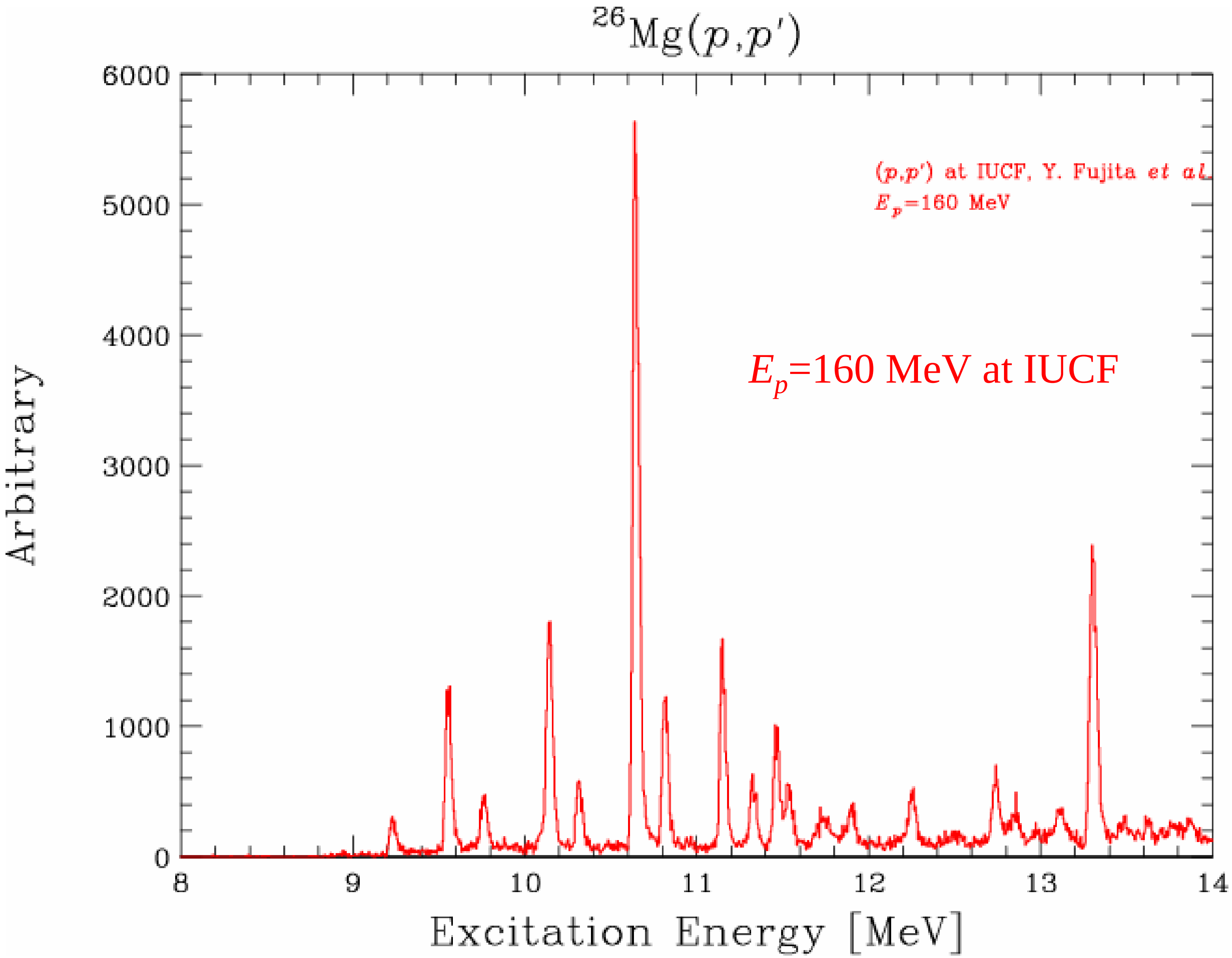

E_p=160 MeV at IUCF

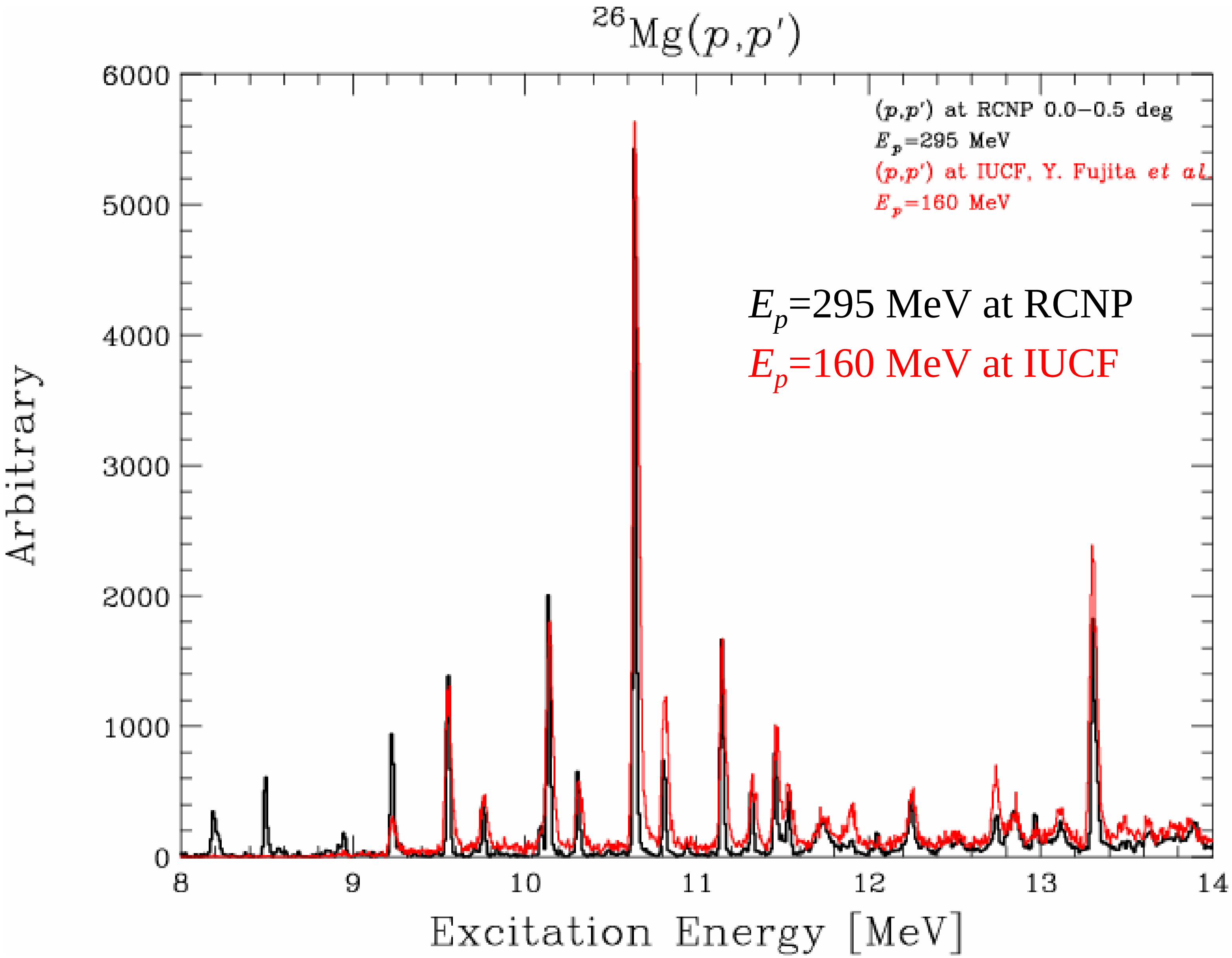
^{26}Mg(p,p')
(p,p') at RCNP 0.0−0.5 deg
Ep=295 MeV
(p,p') at IUCF, Y. Fujita et al.
Ep=160 MeV
E_p=295 MeV at RCNP
E_p=160 MeV at IUCF
Arbitrary
Excitation Energy [MeV]
0
1000
2000
3000
4000
5000
6000
8
9
10
11
12
13
14

Motivation

Merit of (*p*,*p*') scattering measurement at 0 deg. (1/2)

- $\Delta L=0$ excitations are favored at 0° (and Coulomb excitation of E1)
- ΔL information can be obtained from angular distribution of $d\sigma/d\Omega$ at forward angles.
- $d\sigma/d\Omega$ at 0° is approximately proportional to the relevant reduced matrix elements.

$$\frac{d\sigma}{d\Omega} = K \cdot N \cdot \left| J^{ST}(q) \right|^2 \cdot B^{ST}(q,\omega)$$

- ΔS is model-independently identified by measuring polarization transfer coefficients at 0° (ΔS decomposition of the strengths)

$$2D_{NN} + D_{LL} = \begin{cases} -1 \text{ for } \Delta S = 1 & \text{e.g. M1} \\ 3 \text{ for } \Delta S = 0 & \text{e.g. E1} \end{cases}$$

T.Suzuki, PTP103(2000)859

- High-resolution measurement (20 keV) is feasible.
- Other reaction data, *e.g.* (*d*,*d*'), (α,α'), (^{3}He, *t*), (γ,γ') and (*e*,*e*'), provide complementary information

Merit of (*p*,*p*’) scattering measurement at 0 deg. (2/2)

- Excitation strengths can be measured in a wide E_x range ($5<E_x<25$ MeV) by a “single-shot” measurement (missing-mass spectroscopy)
  - independent of the decay channel
  - flat and high detection efficiency
  - total width (or total excitation strength)
- Comparison with (*e*,*e*’)
  - complimentary:
    B(σ) by (*p*,*p*’) ⇔ *B*(*M1*) by (*e*,*e*’)
  - no radiative tail
  - large cross-section
  - reaction mechanism is not “very well-known”

Sensitivity to B(M1) of various probes

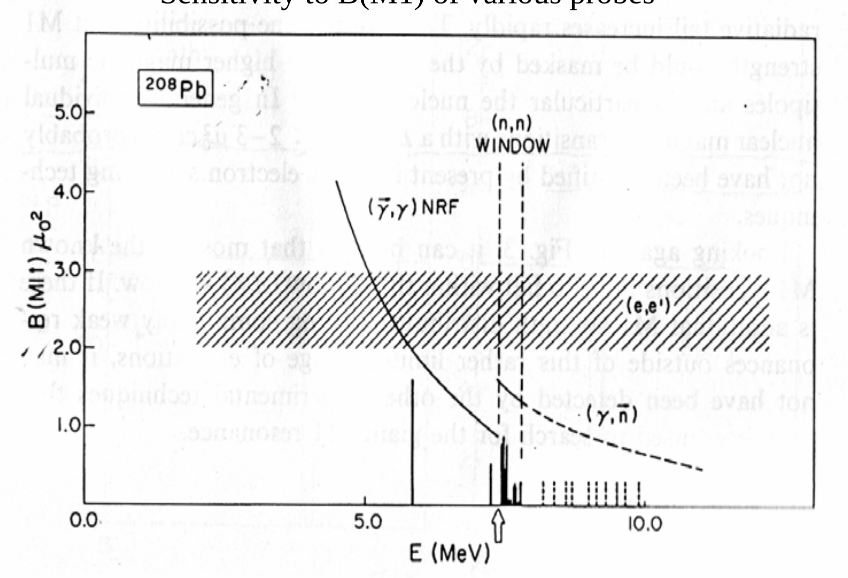

R.M. Laszewski and J. Wambach, Comments Nucl. Part. Phys. 14 (1985) 321.

Demerits

- Reduction of instrumental B.G. is essential
  ... requires a high-quality halo-free beam and beam stability
- Absolute normalization of the strength is not very straightforward

Analysis

Detailed calibrations have been mostly finished.

- Calibration of the scattering angle, solid angle.
  $\Delta\theta \sim 0.5\text{-}0.6^{\circ}$
- Calibration for high energy-resolution data.
  $\Delta E \sim 20$ keV
- Background subtraction
  works well
- Absolute cross sections and continuous angular distribution
  from 0 deg to large angles

M1 operator and reduced transition strength

see *e.g.* Y. Fujita et al., PRC67(2003)064312

GT transition:

$$O(GT) = \sigma \cdot \tau$$

$$B(GT) = c\left|\langle f \left| (\sigma \cdot \tau) \right| i \rangle\right|^2$$

orbital-part spin-part

isoscalar isovector

M1 transition:

$$O(M1) = g_\ell^{IS}\ell + g_s^{IS}\sigma + g_\ell^{IV}\ell\cdot\tau + g_s^{IV}\sigma\cdot\tau$$

$$B(M1) = c'\left|\langle f \left| \left(g_\ell^{IS}\ell + g_s^{IS}\sigma + g_\ell^{IV}\ell\cdot\tau + g_s^{IV}\sigma\cdot\tau\right) \right| i \rangle\right|^2$$ EM probes

$$B(\sigma) = c'\left|\langle f \left| \left(g_s^{IS}\sigma\right) \right| i \rangle\right|^2$$ IS-M1 by (*p*,*p*')

$$B(\sigma) = c'\left|\langle f \left| \left(g_s^{IV}\sigma\cdot\tau\right) \right| i \rangle\right|^2$$ IV-M1 by (*p*,*p*')

→ (*p*,*p*') and EM probes are complementray.

Motivation

1. Systematic study of M1 strengths and their quenching

Gamow-Teller (GT) quenching problem:

The observed GT strengths are systematically smaller the sum-rule value.

GT sum rule : $S_{\beta^-} - S_{\beta^+} = 3(N - Z)$

60 → 90% of the strength is observed in ^{90}Zr upto E_x=50 MeV

T. Wakasa *et al*., PRC55(1997)2909 (*p*,*n*) reaction

K. Yako *et al*., PLB615(2005)193 (*n*,*p*) reaction

How about M1 strengths? $\sigma, \sigma\tau$ Common with GT

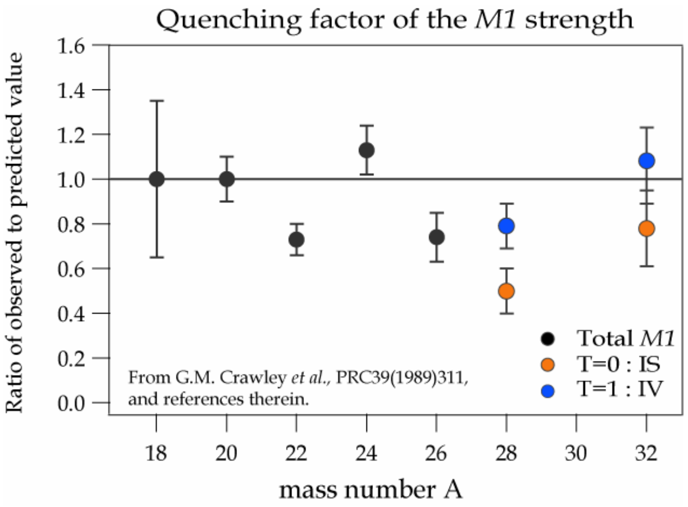

G.M. Crawley *et al*., PRC39(1989)311

Quenching is observed in T=0,1 M1 strengths in ^{28}Si.

N. Anantaraman *et al*.,PRL52(1984)1409

Almost no quenching is observed in ^{24,26}Mg, ^{28}Si, ^{32}S for the sum of *T*=0 and *T*=1 strengths.

G.M. Crawley *et al*.,PRC39(1989)311

High quality data are required.

2. Mechanism of Fragmentation of M1 Strengths.

- Many candidates of fragmented M1 strengths in ^{48}Ca were found. ^{48}Ca(*p*,*p*') at IUCF at the foot of the prominent 1^+ peak at 10.22 MeV.

- Several small M2 and M1 strengths have been identified from the ^{48}Ca(*e*,*e*') data at Darmstadt and Mainz

  W. Steffen NPA404(1983)413.
  P. von Nuemann-Cosel *et al*., PRL82(1999)1105.

^{48}Ca(*p*,*p*') at IUCF at 0 deg. analyzed by Y. Fujita *et al*.

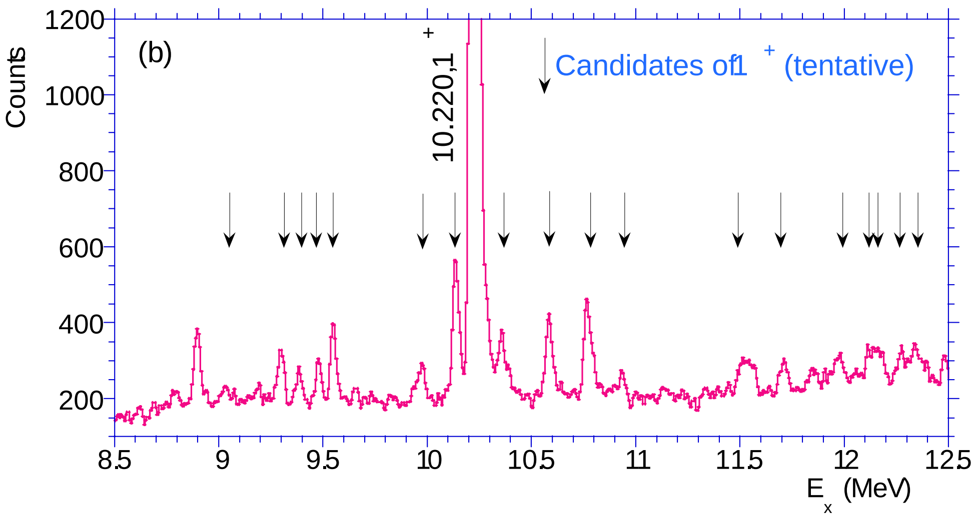

N. Ryezayeva et al.,
PRL89(2002)272502

3. New or exotic type of excitations in nuclei

Vortex type excitations in nuclei?

⟶ Candidates found by Darmstadt (γ,γ’) group by using Quasi-particle Phonon Model

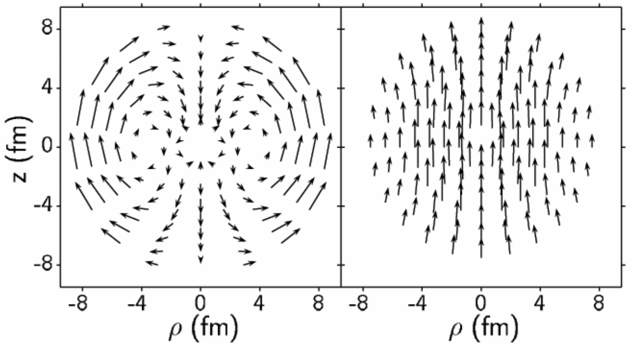

FIG. 4. The QPM prediction for the velocity distributions of $E1$ excitations at $E_x = 6.5$–10.5 MeV (left) and $E_x > 10.5$ MeV (right) in ^{208}Pb.

4. Nuclear matrix element of inelastic scattering

→ Origin of elements (nucleosynthesis)

(ν,ν’) processes in supernovae

Search for toroidal E1 excitations in ^{208}Pb

Prediction of toroidal E1 excitation in ^{208}Pb by Quasi-particle Phonon Model (QPM) calculations around 6.5-10.5 MeV.

QPM is known to well reproduce the E1 distribution measured by ^{208}Pb(γ,γ).

By measuring angular distributions of dσ/dΩ and other observables for Coulomb E1 excitations might provide (indirect) evidence of the toroidal E1 mode excitation.

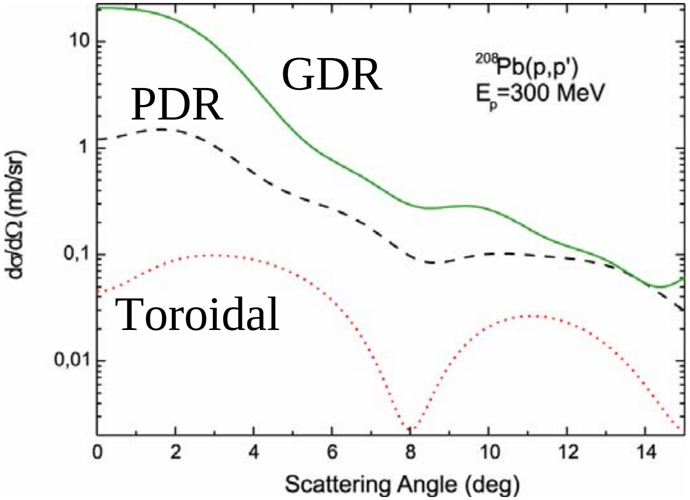

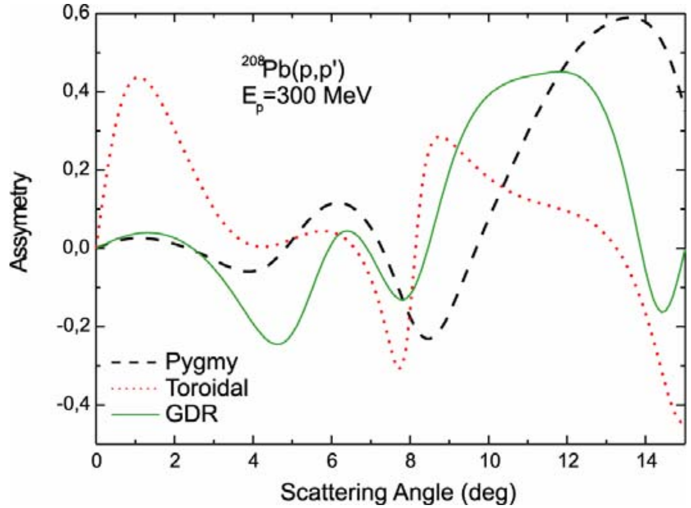

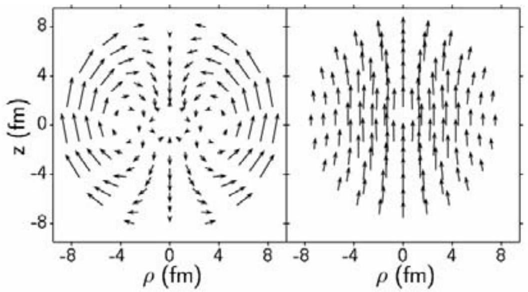

FIG. 4. The QPM prediction for the velocity distributions of $E1$ excitations at $E_x = 6.5$–10.5 MeV (left) and $E_x >$ 10.5 MeV (right) in ^{208}Pb.

N. Ryezayeva et al., RL89(2002)272502

DWBA calc. by P. von Neuman-Cosel et al.

using QPM wave function and Love-Franey int.

Search for M1 strengths by experiments

Experimentally many reactions have been used to observe the M1 strengths:

^{208}Pb($\vec{\gamma}$,γ), ^{208}Pb(γ,$\vec{n}$), ^{207}Pb(*n*,*n*), ^{207}Pb(*n*,γ),

^{208}Pb(*e*,*e*'), and ^{208}Pb(*p*,*p*')

In 1988, R.M. Laszewsky et al. have identified

$8.8\mu_N^2$ below Sn by a ^{208}Pb($\vec{\gamma}$,γ) measurement.

In total the higher-lying strength became $15.6\mu_N^2$

which came closer to the "best" (smallest) theoretical prediction of $20\mu_N^2$.

Still the search for M1 strengths in ^{208}Pb is an important job to experimentally determine the M1 strengths and their E_x distribution.

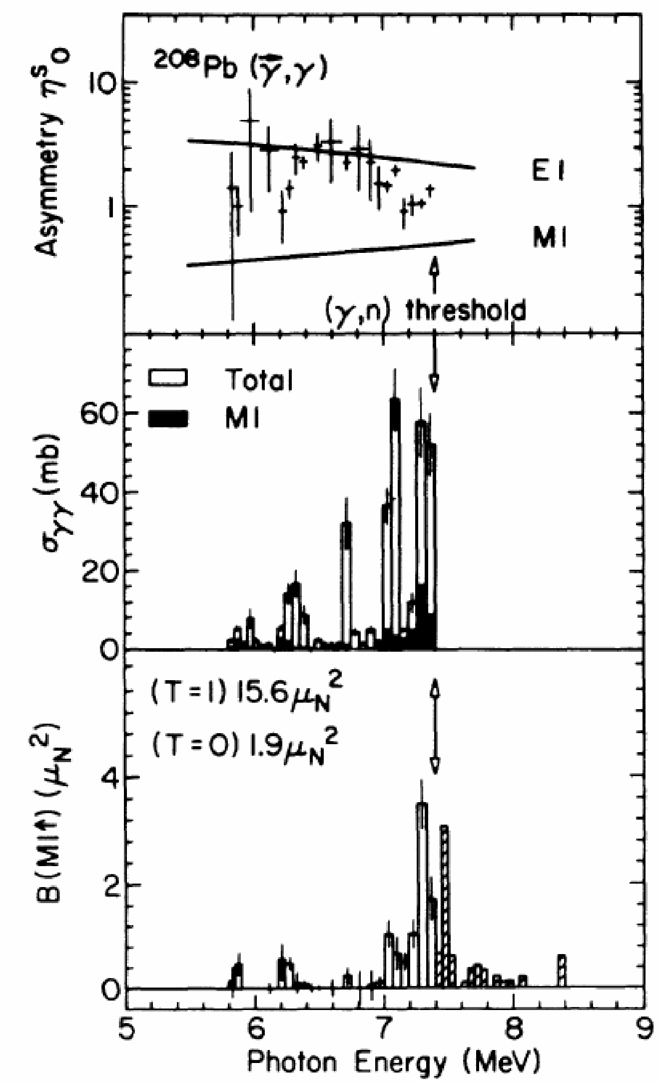

R.M. Laszewski et al, PRL61(1988)1710

(*p*,*p*') scattering measurement at 0 deg (1/2)

M1

- $\Delta L=0$ excitations are favored at 0° (+ Coulomb excitation, E1)
- ΔL information can be obtained from angular distribution of $d\sigma/d\Omega$ at forward angles.
- $d\sigma/d\Omega$ at 0° is approximately proportional to the relevant reduced matrix elements.

$$\frac{d\sigma}{d\Omega} = K \cdot N \cdot \left| J^{ST}(q) \right|^2 \cdot B^{ST}(q,\omega)$$

B(σ)

- ΔS is model-independently identified by measuring polarization transfer coefficients at 0° (ΔS decomposition of the strengths)

T.Suzuki, PTP103(2000)859

$$D_{SS} + D_{NN} + D_{LL} \; (= 2D_{NN} + D_{LL}) = \begin{cases} -1 \text{ for } \Delta S = 1 & \text{e.g. M1} \\ 3 \text{ for } \Delta S = 0 & \text{e.g. Coulomb Excitation of E1} \end{cases}$$

- High-resolution measurement (20 keV) is possible.
- Other reaction data, *e.g.* (*d*,*d*'), (α,α'), (^{3}He, *t*), (γ,γ') and (*e*,*e*'), provide complementary information

(p,p') scattering measurement at 0 deg. (2/2)

- Excitation strengths can be measured in a wide E_x range ($5<E_x<25$ MeV) by a "single-shot" measurement (missing-mass spectroscopy)
  - independent of the decay channel
  - high and flat detection efficiency
  - total excitation strength

- Comparison with (e,e')
  - complementary:
    $B(\sigma)$ by (p,p') ⇔ $B(M1)$ by (e,e')
  - no radiative tail
  - large cross-section
  - reaction mechanism is not "very well-known"

Sensitivity to B(M1) of various probes

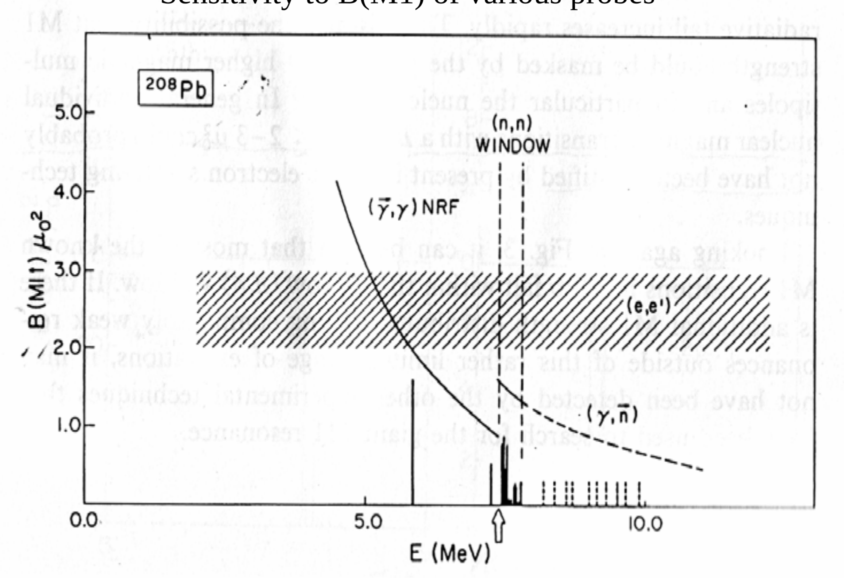

R.M. Laszewski and J. Wambach, Comments Nucl. Part. Phys. 14 (1985) 321.

Demerits

- Reduction of instrumental B.G. is essential
  ... requires a high-quality halo-free beam and beam stability
- Absolute normalization of the strength is not straightforward

Experiment

Data Reduction

Sieve Slit Calibration (Scattering Angle)

calib. by H. Matsubara

Sieve slit data by using

^{58}Ni(p, p_0) reaction at 16°

Horizontal scattering angle resolution:

$\Delta\theta$ = 0.15 deg

Vertical scattering angle resolution depends on the F.P. position

$\Delta\phi$ = 0.5 deg at lower E_x.

0.8 deg at higher E_x.

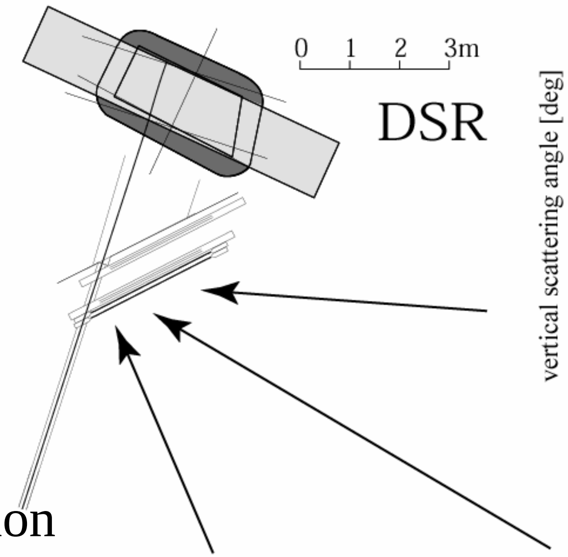

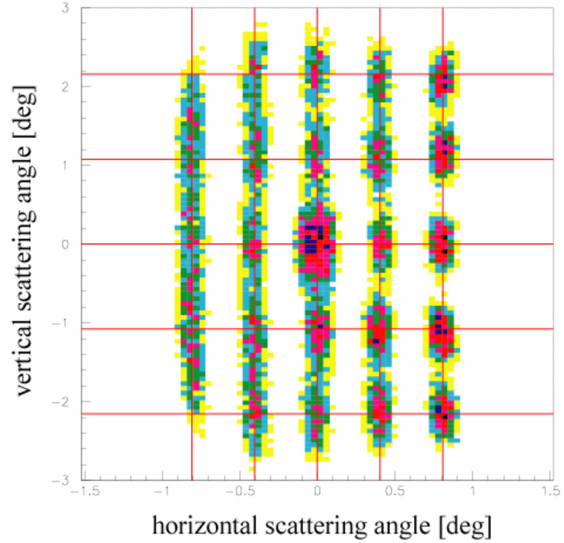

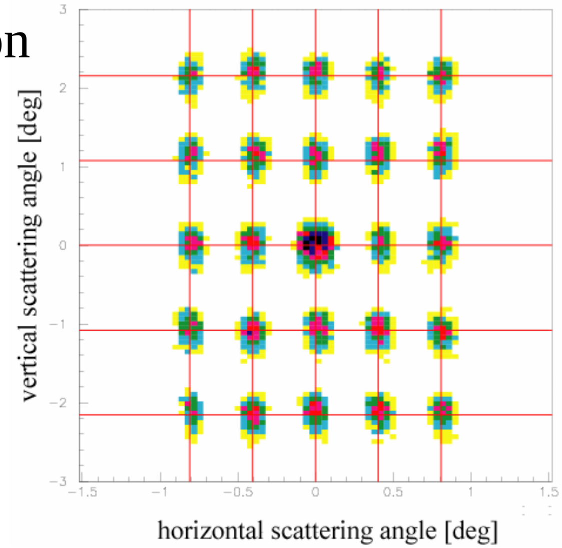

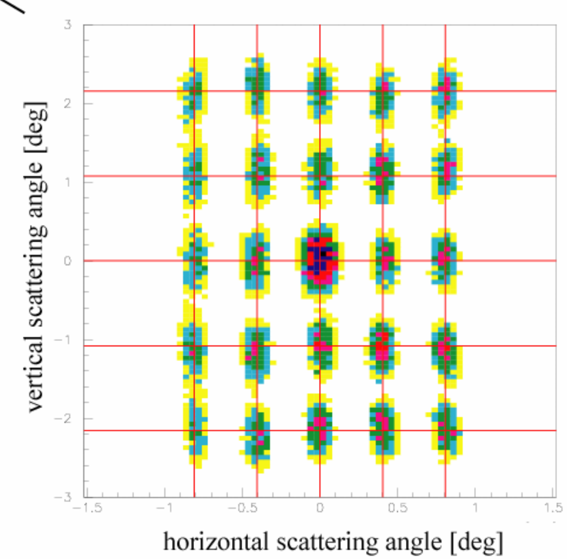

Calibration of the aberation of GR

calib. by H. Matsubara

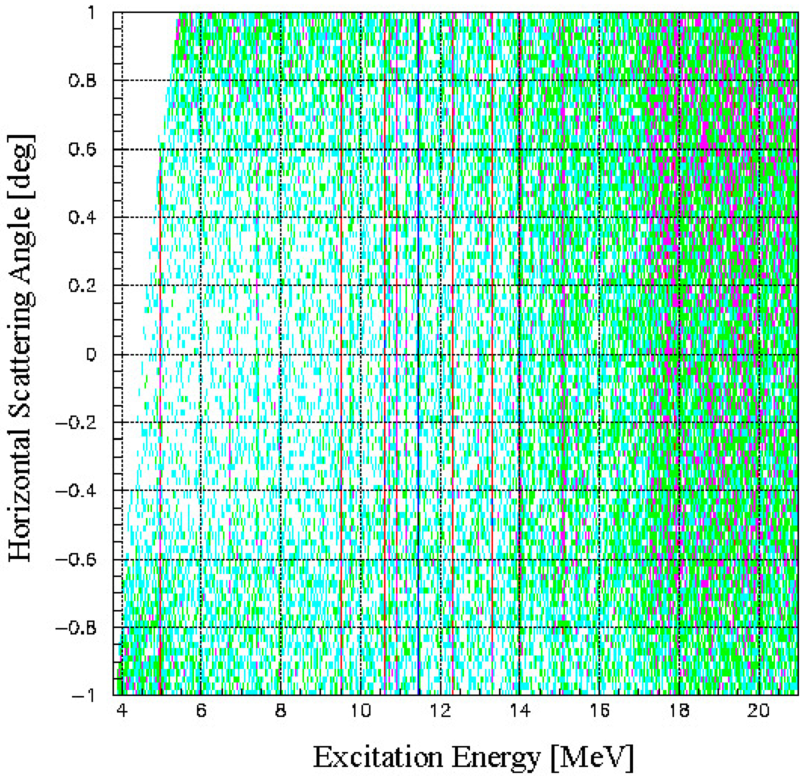

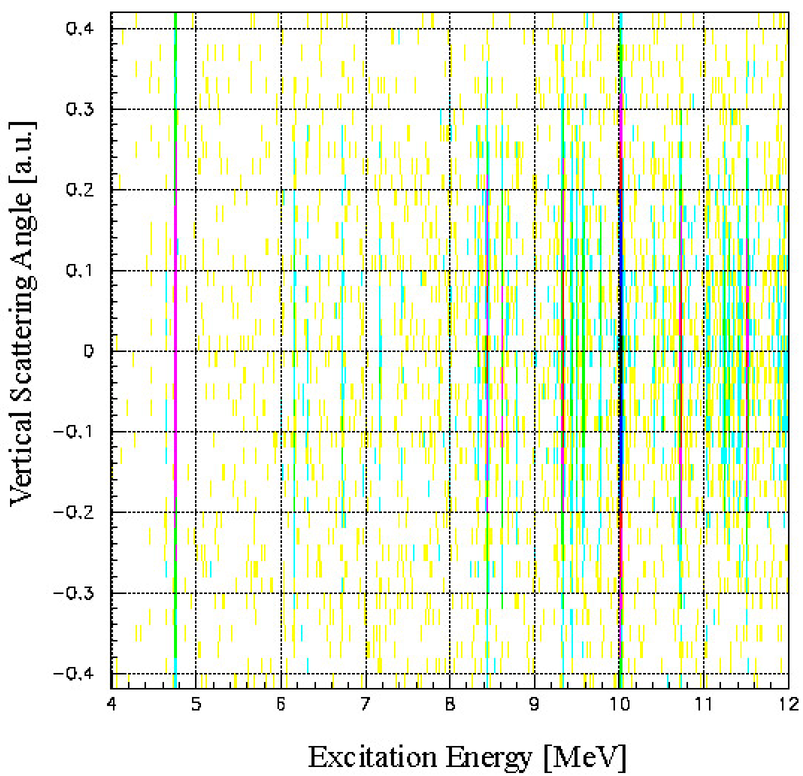

Aberation of the ion optics of GR was calibrated as the energy resolution of discrete peaks becomes better.

Sieve Slit Calibration (Scattering Angle)

Calibration of vertical scattering angle is very sensitive to the vertical beam position.

The vertical beam position was monitored by the LAS spectrometer during the experiment by measuring quasielastic scattering from the target.

This effect will be included in the analysis of the scattering angle (not yet).

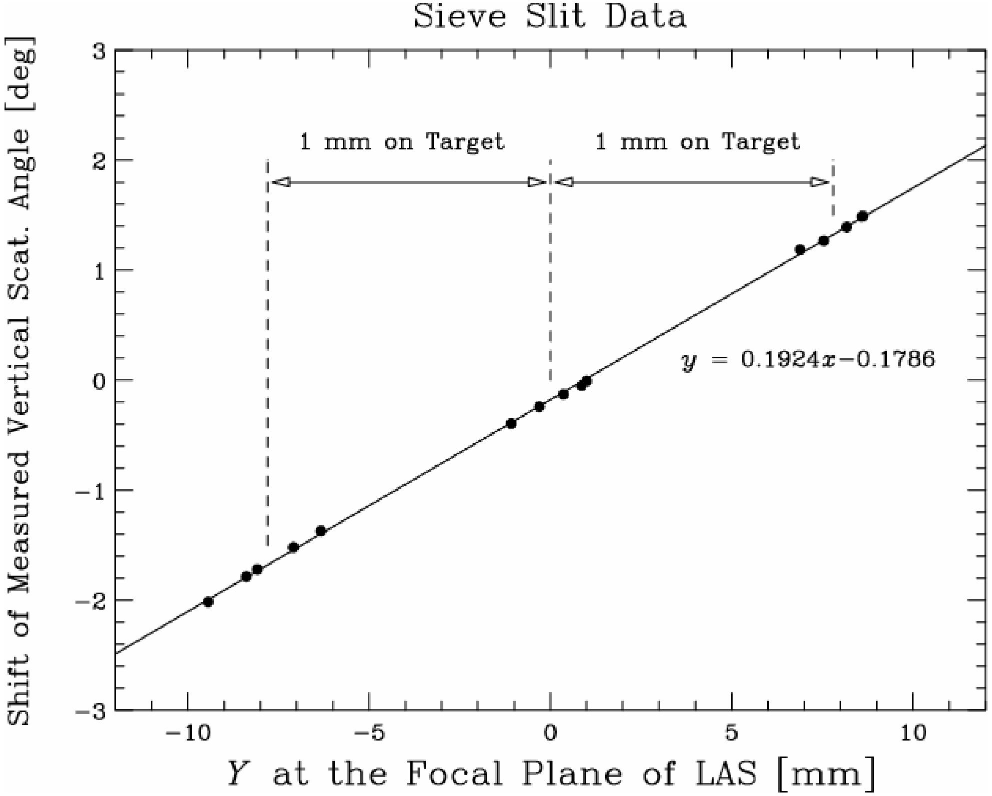

Sieve slit data taken with various displaced beam spot on the target

Y: -1, 0, 1 mm

X: -8, -4, 0, 4, 8 mm

Background Subtraction

One of possible solutions:

→ Shift the Y_{fp} (and correspondingly ϕ_{fp}) before any calculation and apply completely the same analysis procedure as well as gates for getting b.g. spectrum

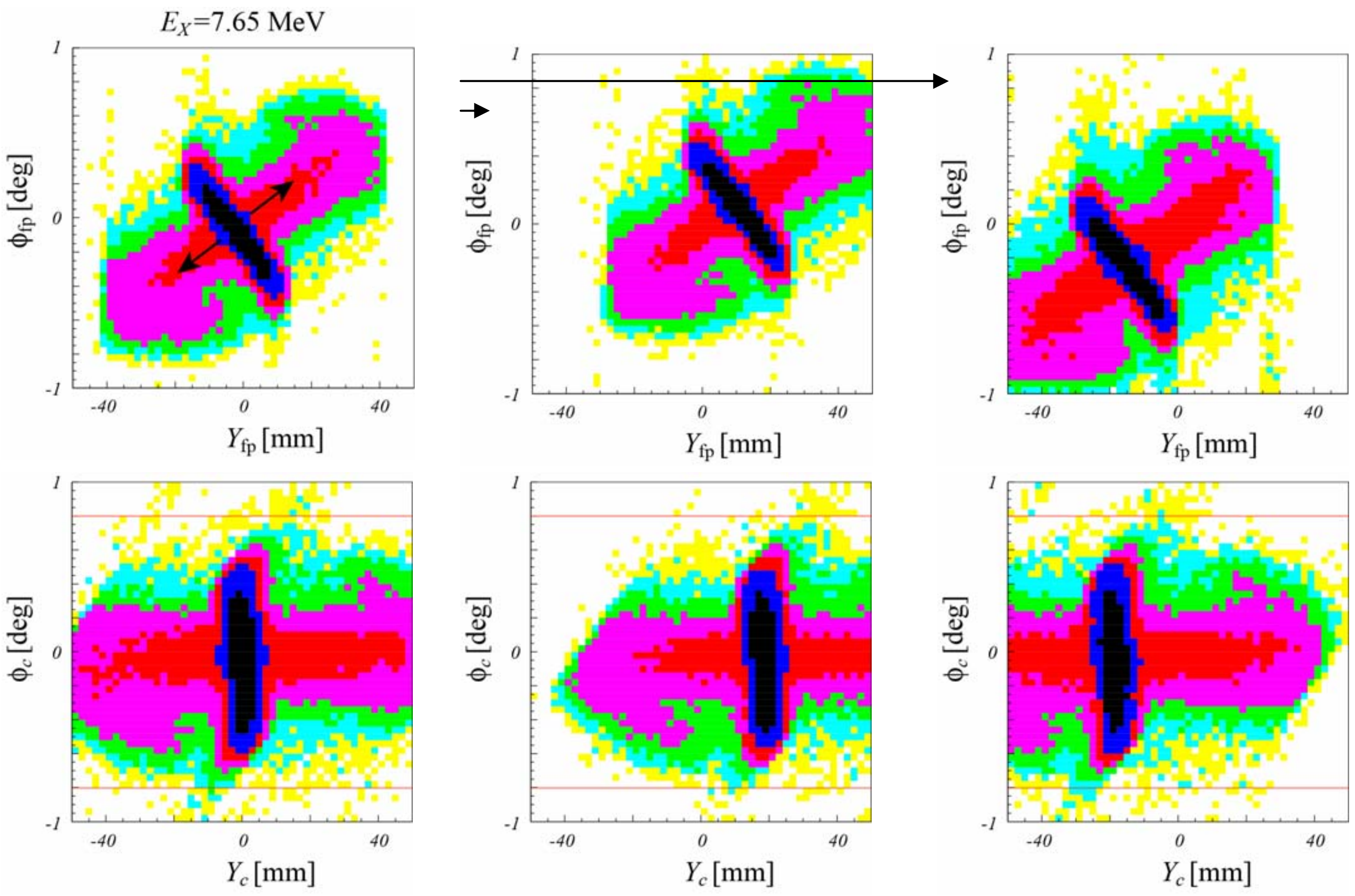

Tilted

Background Subtraction

Gated by ϕ_c

and projected onto Y_c

after applying Scattering

angle gate

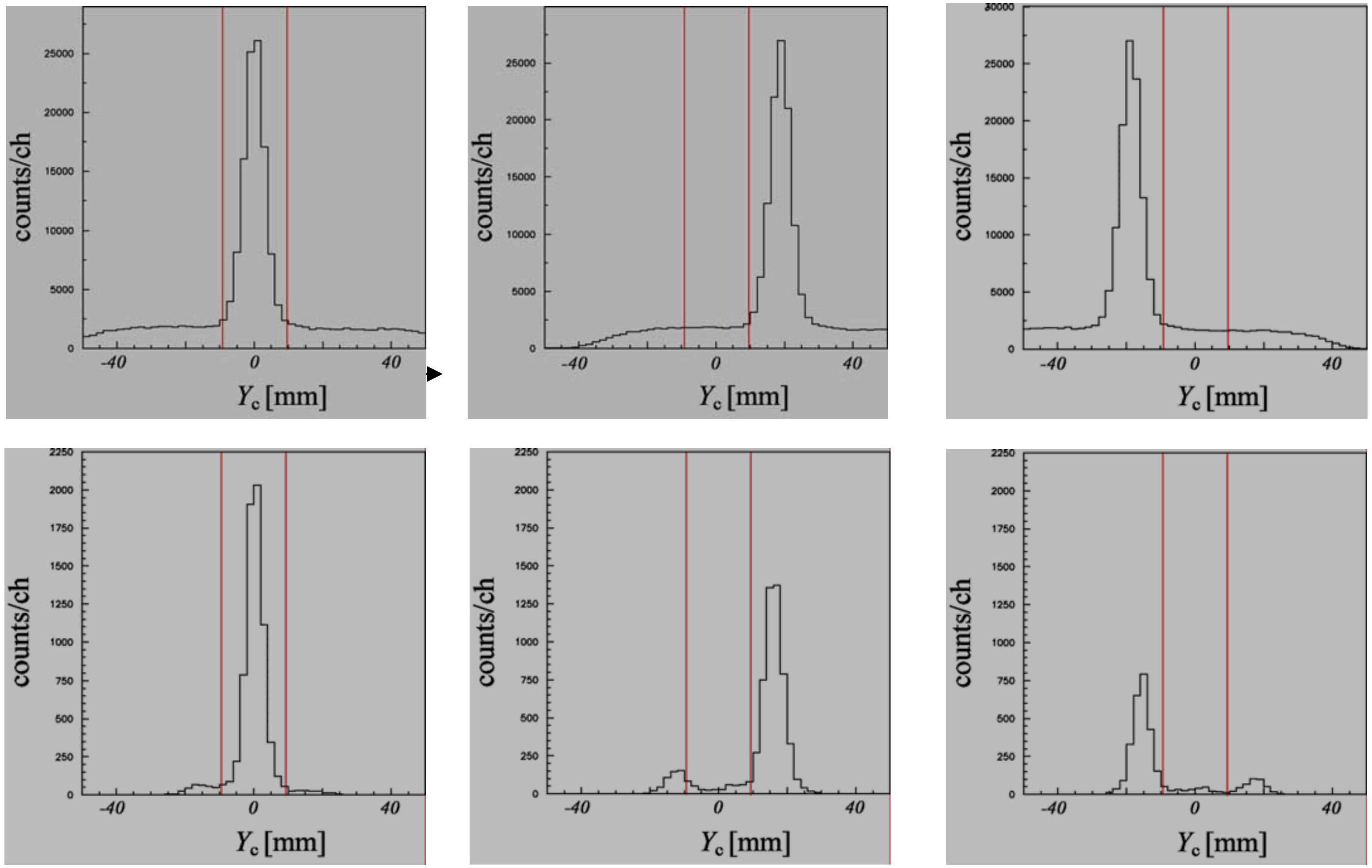

Background Subtraction

It looks working good (even better than previous works?), but still requires more careful checks.

Comment:

Once a smooth b.g. shape is obatined, it is better to fit the b.g. shape by some smooth function and subtract it from true+b.g. spectrum for reducing statistical uncertainty especially in the case S/N is not very good.

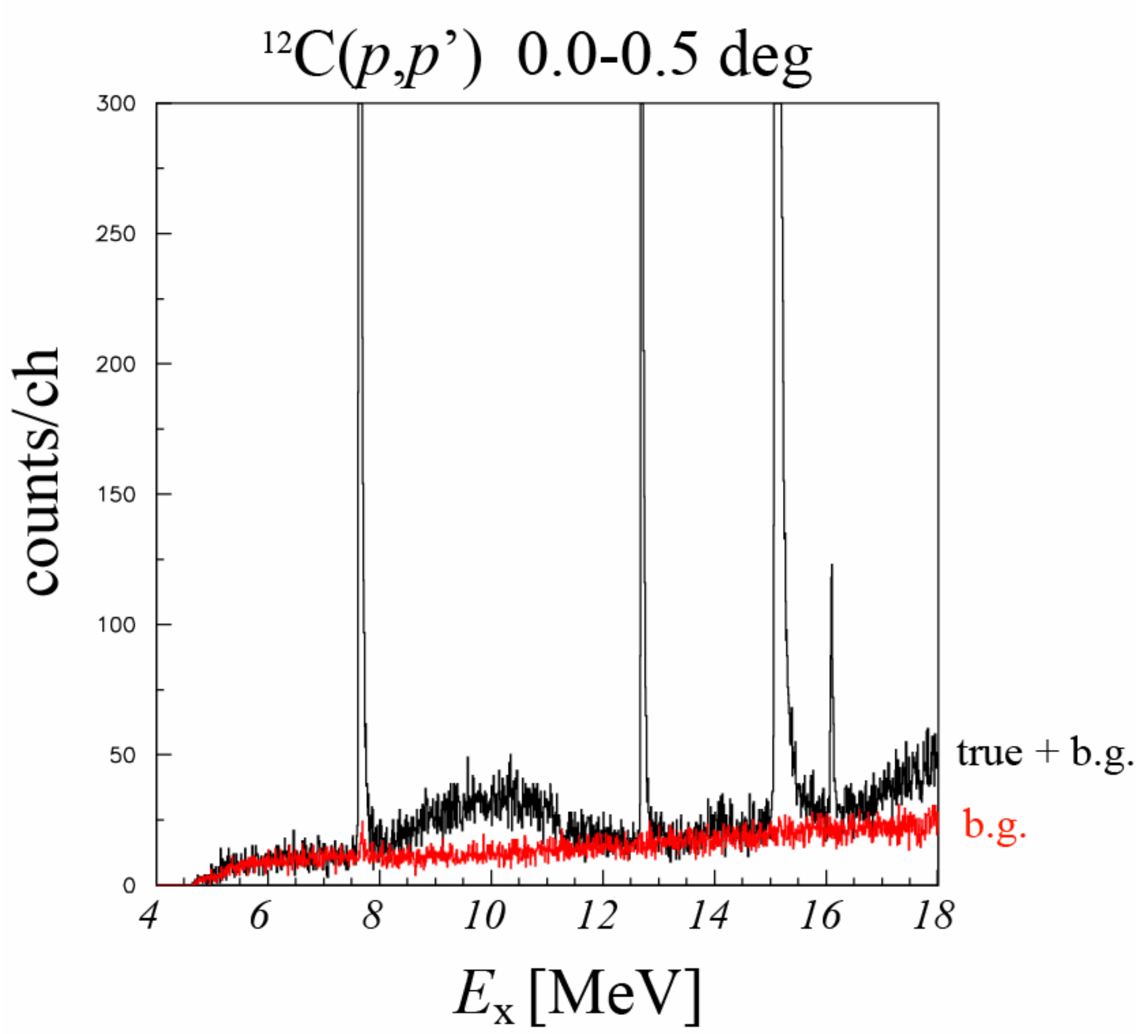

Analysis

Systematic study of the unit cross section is required

$$\frac{d\sigma}{d\Omega}(q,\omega) = \hat{\sigma}_{T=0,1} \; F(q,\omega) \; B(\sigma)$$

q : momentum transfer
ω : energy transfer

$\hat{\sigma}_{T=0,1}$: unit cross section for B(σ)
F(q, ω) : kinematical factor
B(σ) : spin-flip excitation strength

present step

1) To determine the unit cross section by DWBA calculations relying on effective interaction and optical potential.

2) Calibration of the unit cross section against b-decay *ft* values on the assumption of charge symmetry (only for *T*=1)
^{12}C, ^{26}Mg, ...

3) Calibration against electro-magnetic probes: (γ,γ') and (*e*,*e*')
(*p*,*p*') --- B(σ) ⇔ B(M1) --- electro magnetic probes
can be well calibrated?

should be studied as a next step

→ Systematic study is to be done

Systematic study of the unit cross section is required

$$\frac{d\sigma}{d\Omega}(q,\omega) = \hat{\sigma}_{T=0,1} \ F(q,\omega) \ B(\sigma)$$

q : momentum transfer
ω : energy transfer

$\hat{\sigma}_{T=0,1}$: unit cross section for $B(\sigma)$
$F(q,\omega)$: kinematical factor
$B(\sigma)$: spin-flip excitation strength

present step

1) To determine the unit cross section by DWBA calculations relying on effective interaction and optical potential.

2) Calibration of the unit cross section against b-decay *ft* values on the assumption of charge symmetry (only for *T*=1)

^{12}C, ^{26}Mg, ...

3) Calibration against electro-magnetic probes: (γ,γ') and (*e*,*e*')

(*p*,*p*') --- B(σ) ⇔ B(M1) --- electro-magnetic probes can be well calibrated?

Spectra

Spectra

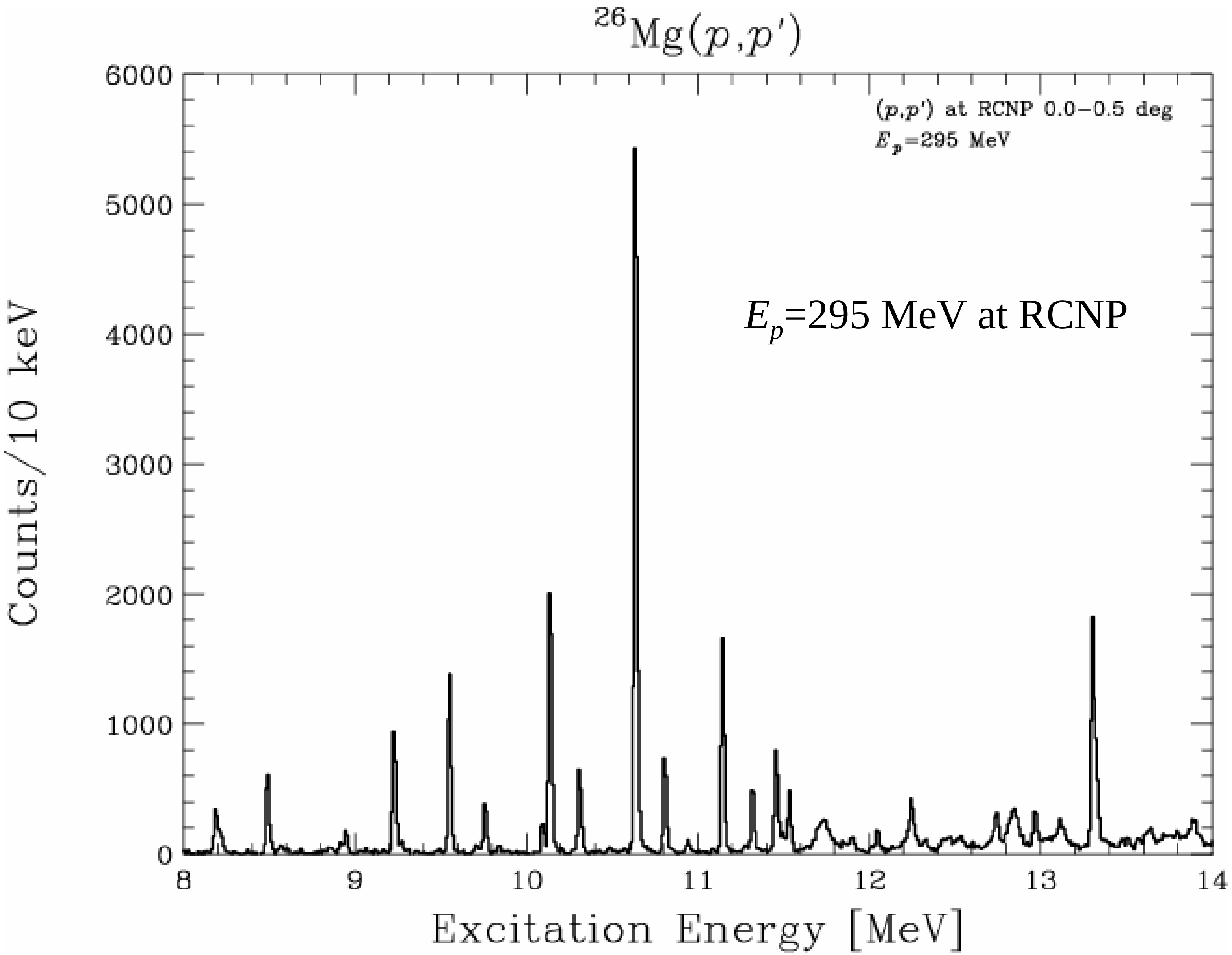

E_p=295 MeV at RCNP

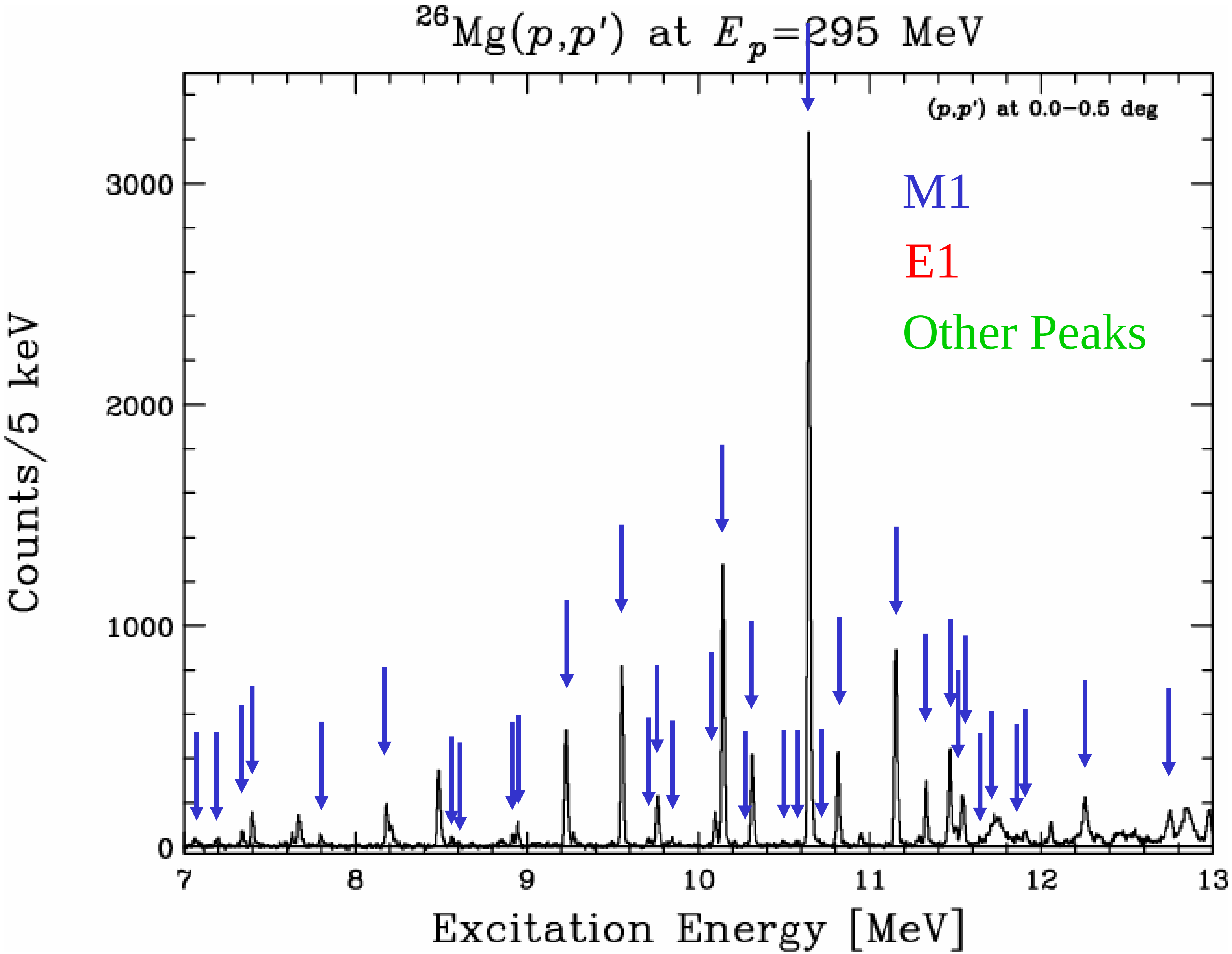

26Mg(p,p') at Ep=295 MeV
(p,p') at 0.0−0.5 deg
M1
E1
Other Peaks
Counts/5 keV
3000
2000
1000
0
7
8
9
10
11
12
13
Excitation Energy [MeV]

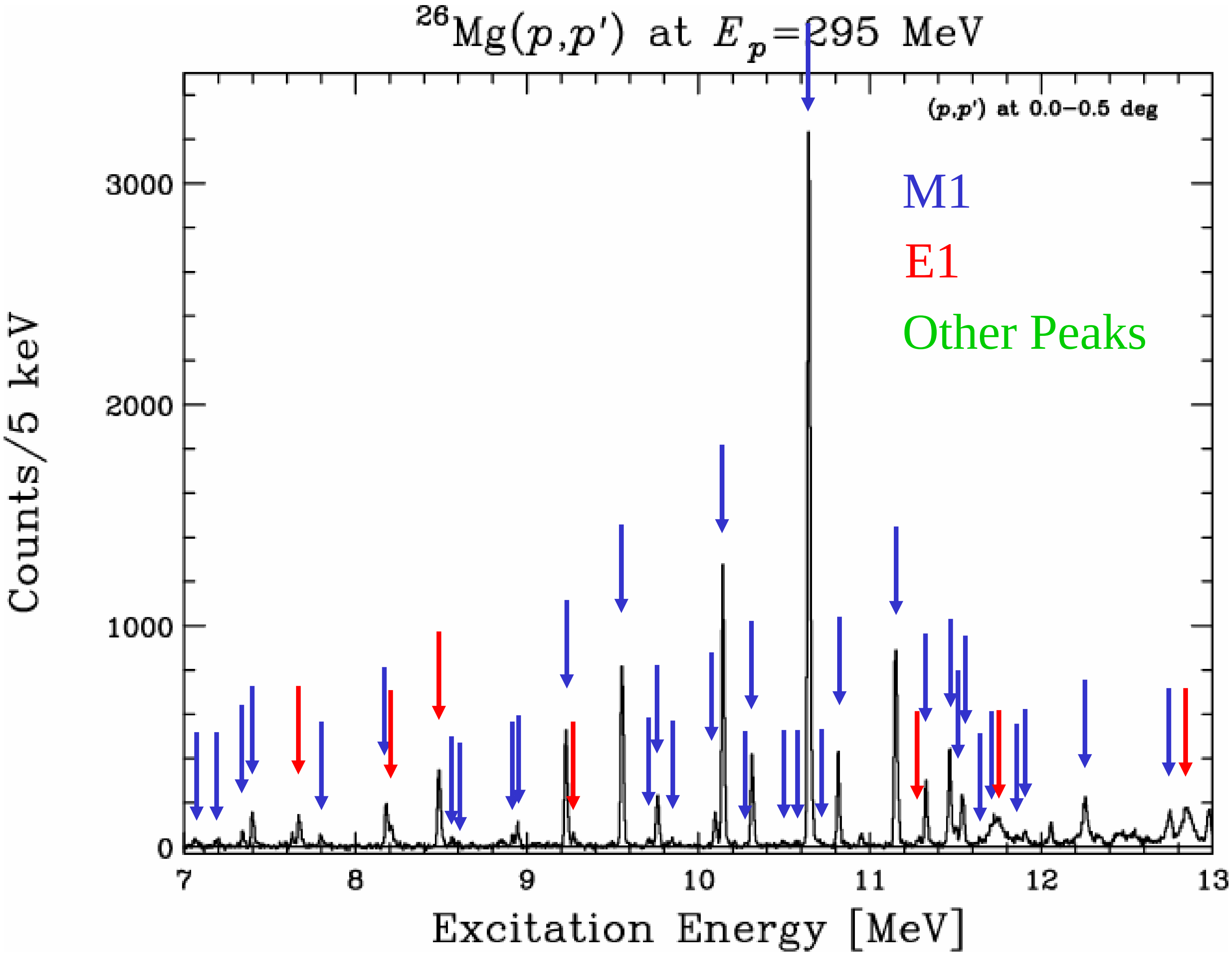

^{26}Mg(p,p') at E_p=295 MeV
(p,p') at 0.0–0.5 deg
M1
E1
Other Peaks
Counts/5 keV
0
1000
2000
3000
7
8
9
10
11
12
13
Excitation Energy [MeV]

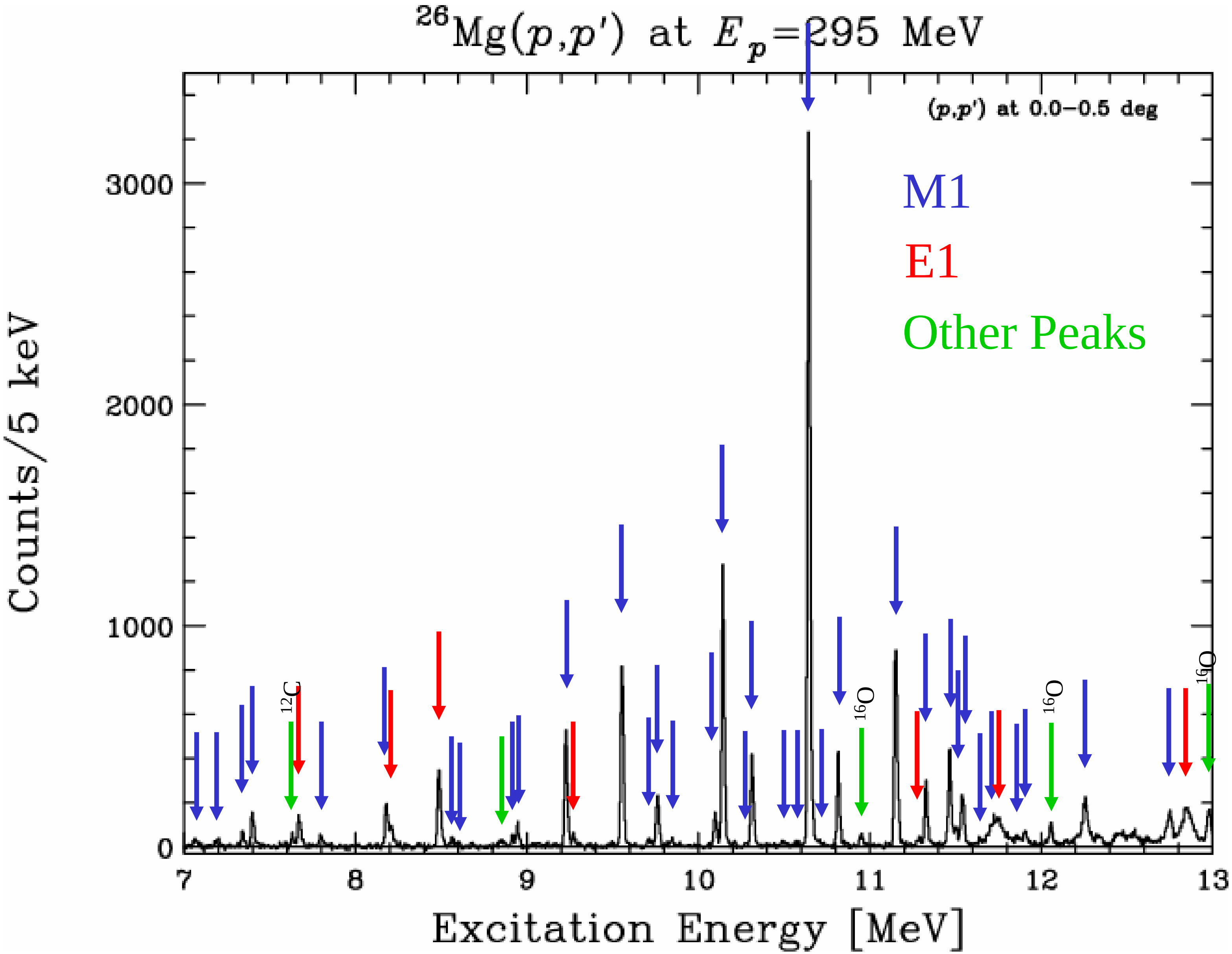
^{26}Mg(p,p') at E_p=295 MeV
(p,p') at 0.0–0.5 deg
M1
E1
Other Peaks
Counts/5 keV
Excitation Energy [MeV]
^{12}C
^{16}O
^{16}O
^{16}O
0
1000
2000
3000
7
8
9
10
11
12
13

G.M. Crawley et al, PRC39(1989)311, at Orsay

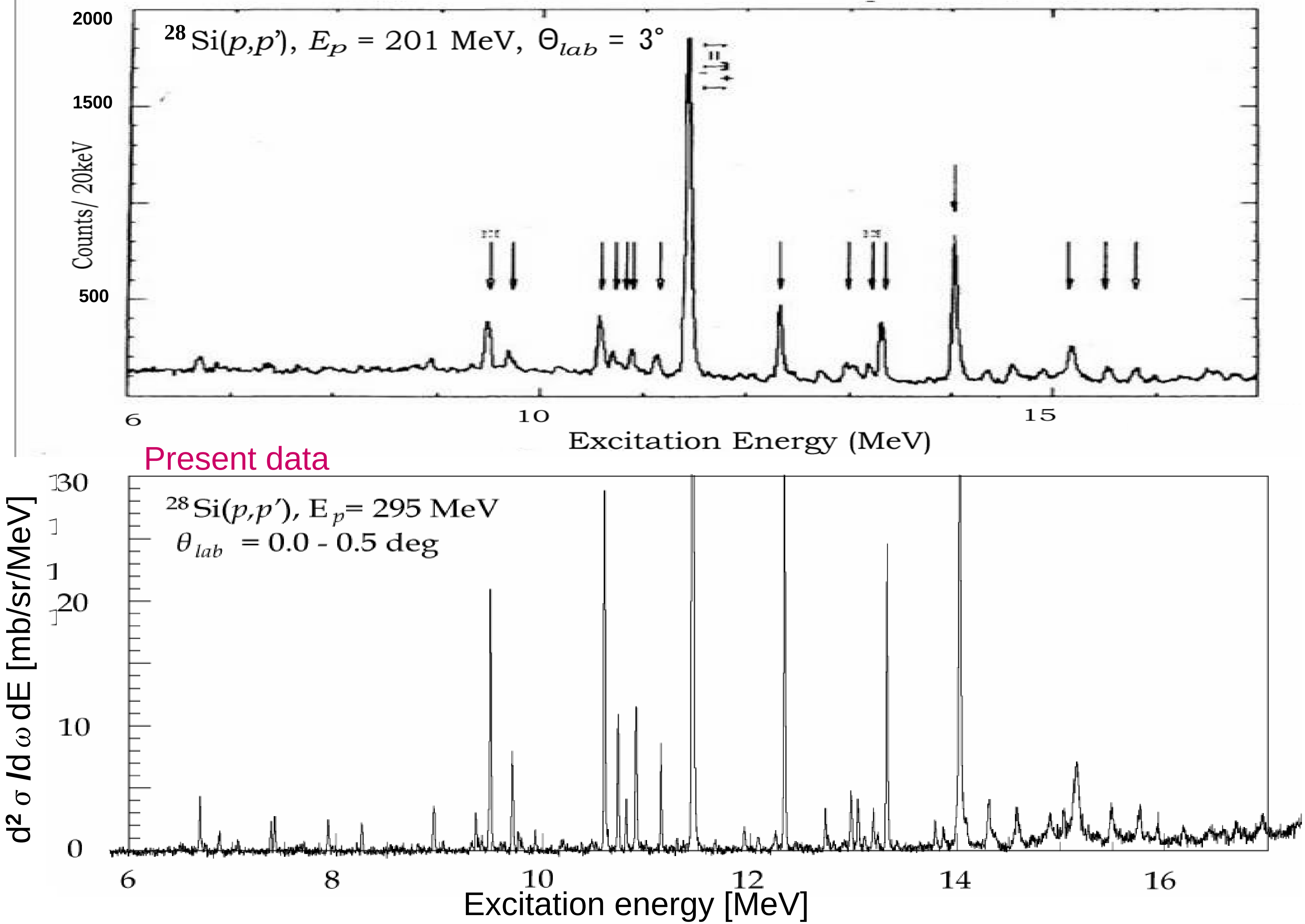

$^{40}Ca(p, p')$

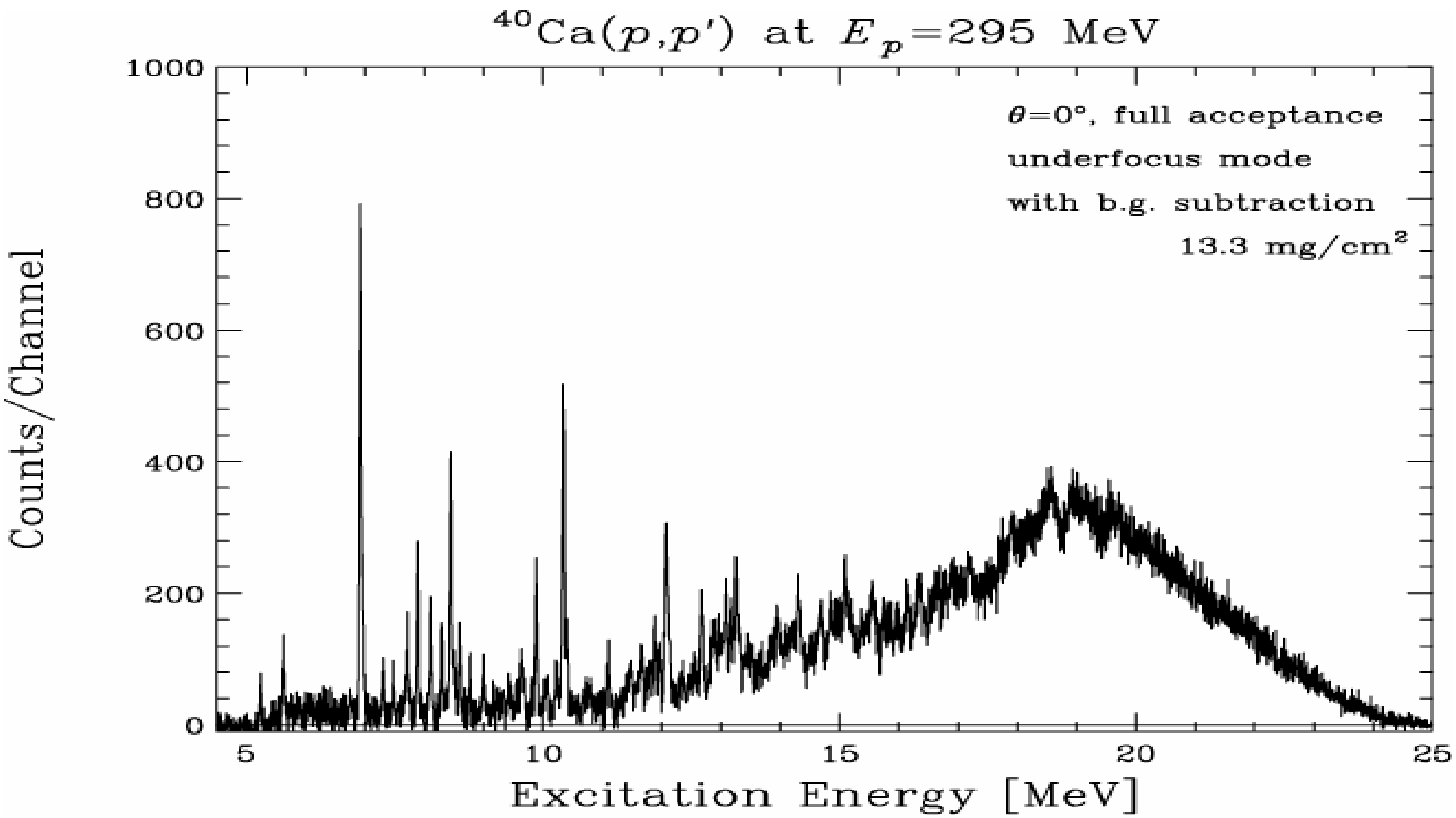

40Ca(p,p') at Ep=295 MeV
θ=0°, full acceptance
underfocus mode
with b.g. subtraction
13.3 mg/cm2
Counts/Channel
Excitation Energy [MeV]
0
200
400
600
800
1000
5
10
15
20
25

G.M. Crawley *et al*, PLB127(1983)322; (p,p') at Orsay, E_p=201 MeV

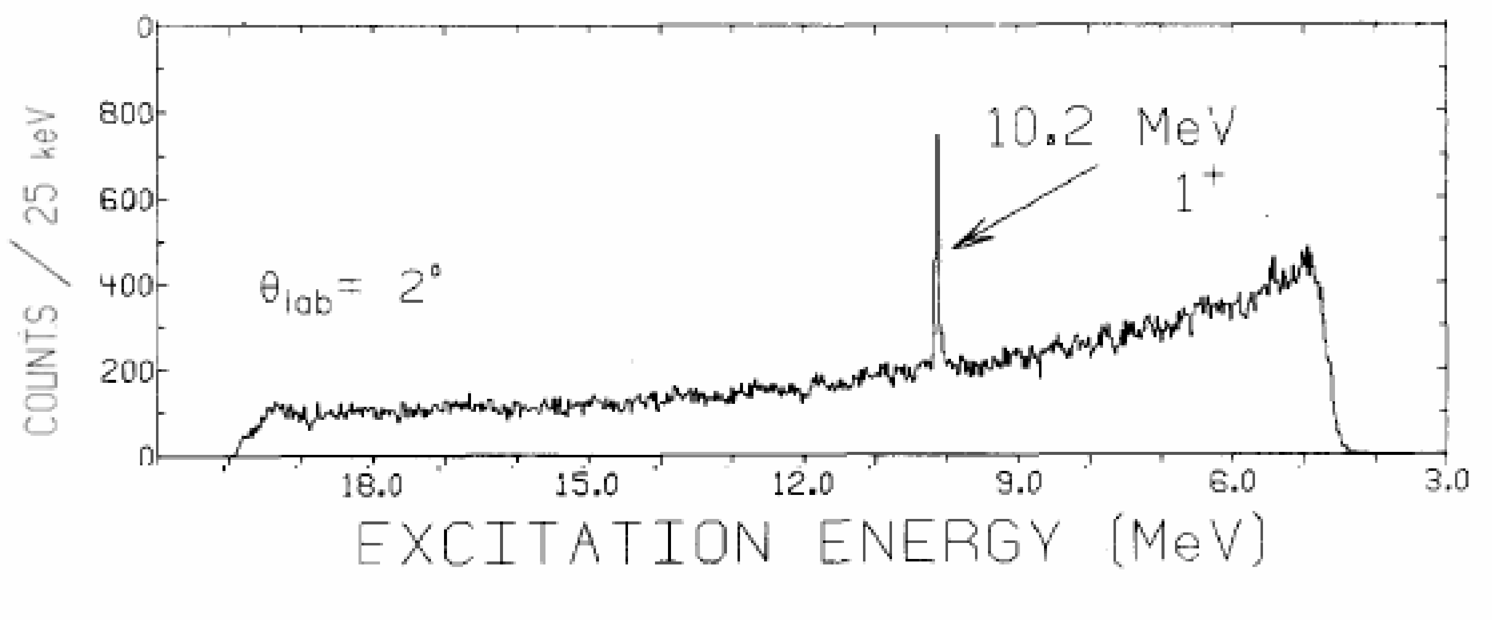

7 of the states identified by (e,e') : observed.
11 of them: not observed
8 additional peaks were observed

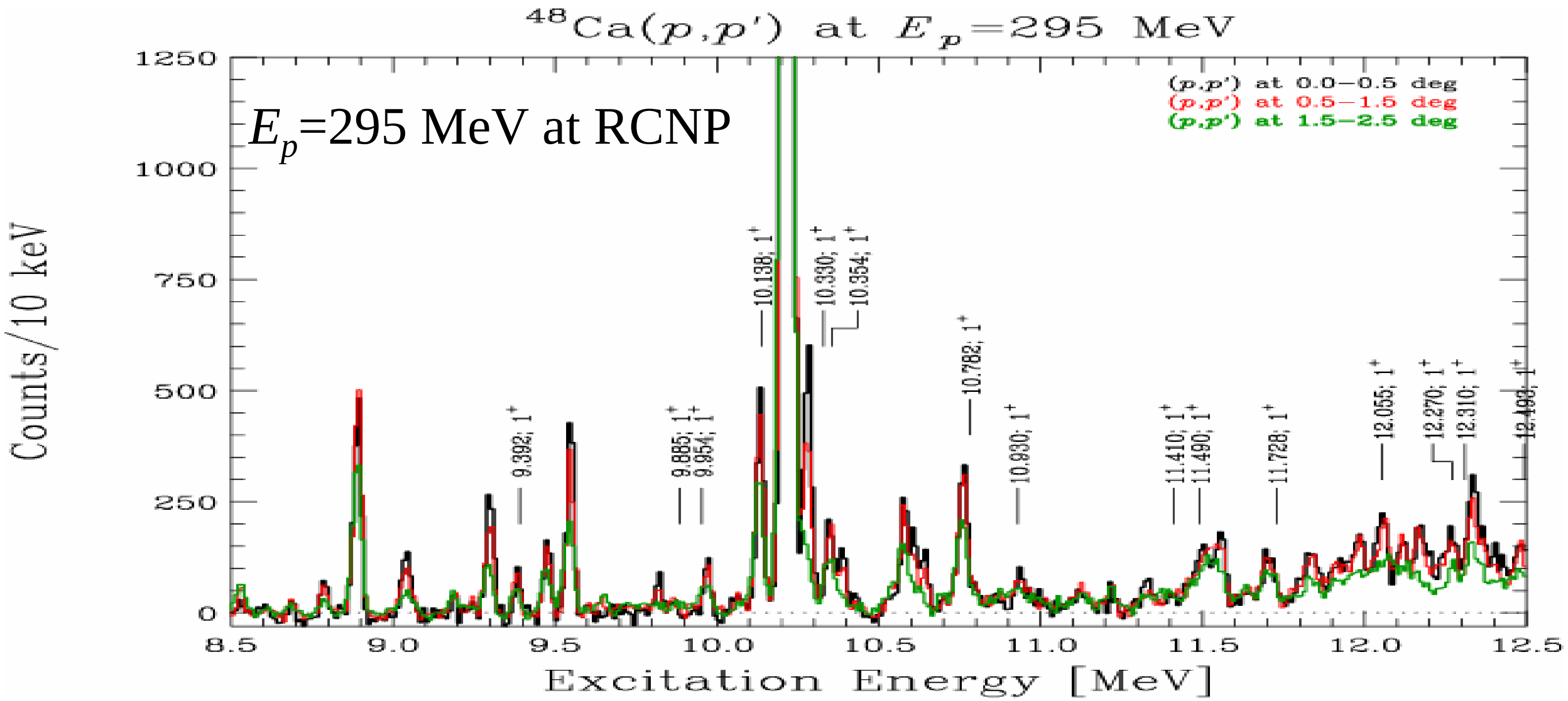

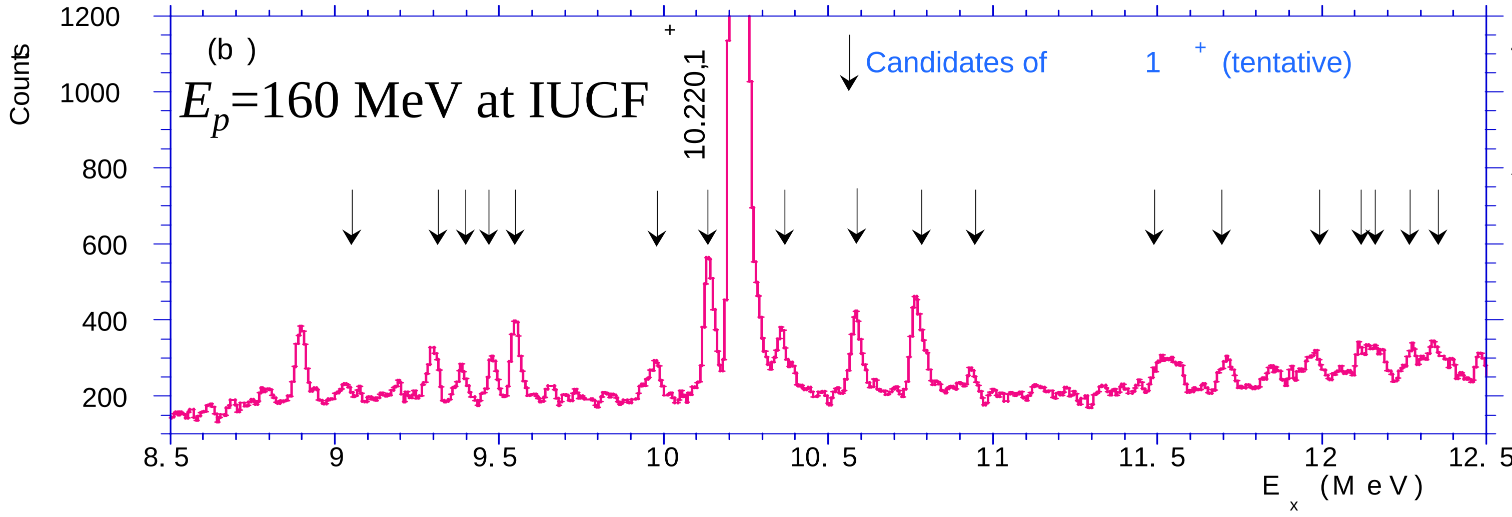

^{48}Ca(*p*,*p*')
IUCF at 160 MeV
0 deg.
Y. Fujita *et al.*

W. Steffen *et al*, NPA404(1983)413; (*e*,*e*') at Darmstadt and Mainz

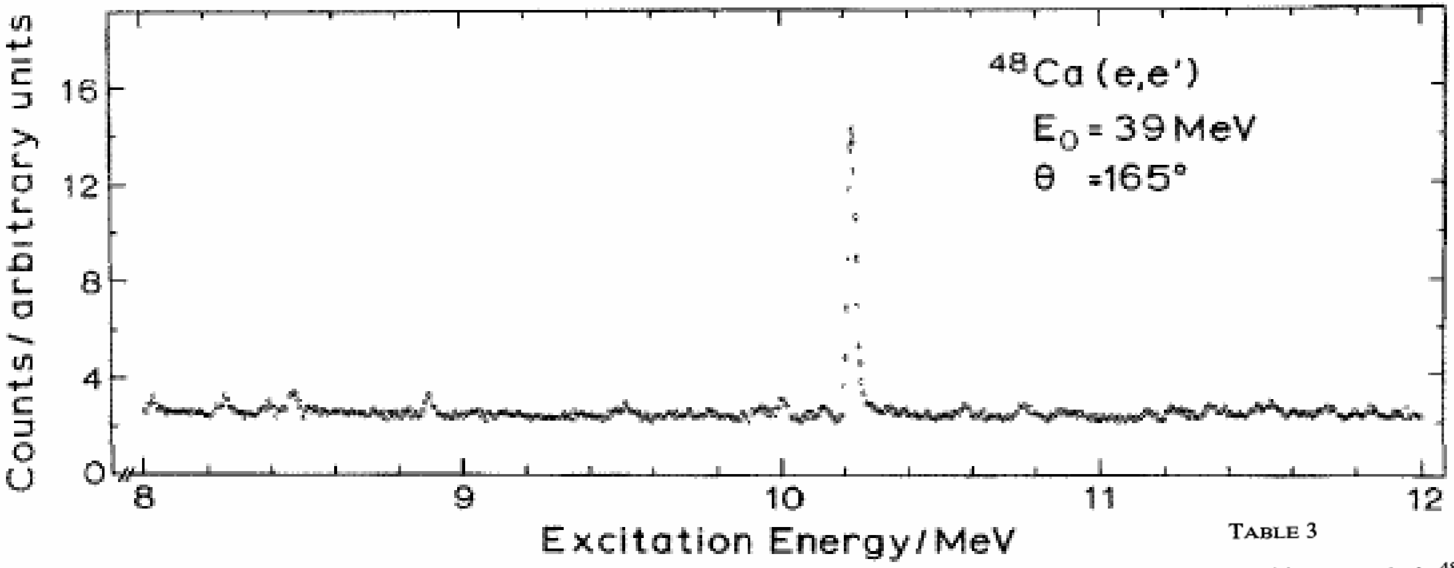

TABLE 3

M1 ground-state transition strengths in ^{48}Ca between $E_x \approx$ 7.7–12.7 MeV

E_x (MeV)	$B(M1, k)\uparrow$ (μ_N^2)
7.696	<0.05
8.150	<0.05
9.392	<0.07
9.885	<0.09
9.954	<0.10
10.138	0.12 ± 0.03
10.225	3.9 ± 0.3
10.330	0.09 ± 0.04
10.354	0.08 ± 0.04
10.782	0.12 ± 0.04
10.930	0.05 ± 0.02
11.410	<0.09
11.490	0.15 ± 0.03
11.728	0.12 ± 0.04
12.055	0.08 ± 0.03
12.270	0.10 ± 0.05
12.310	0.11 ± 0.03
12.493	0.09 ± 0.04
12.700	0.10 ± 0.05

They identified ~19 1^+ states though it is very ambiguous.

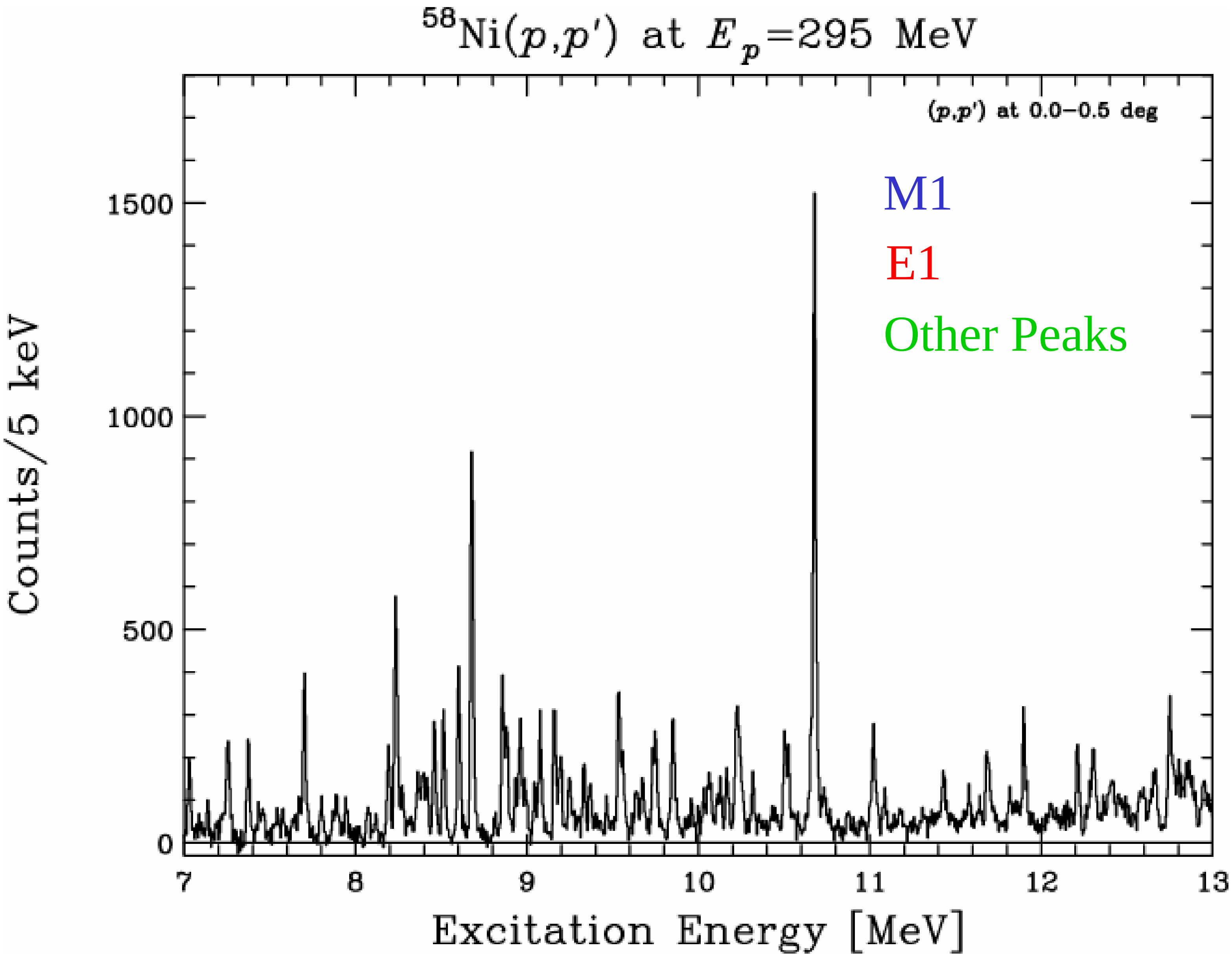

^{58}Ni(p,p') at E_p=295 MeV
(p,p') at 0.0–0.5 deg
M1
E1
Other Peaks
Counts/5 keV
0
500
1000
1500
7
8
9
10
11
12
13
Excitation Energy [MeV]

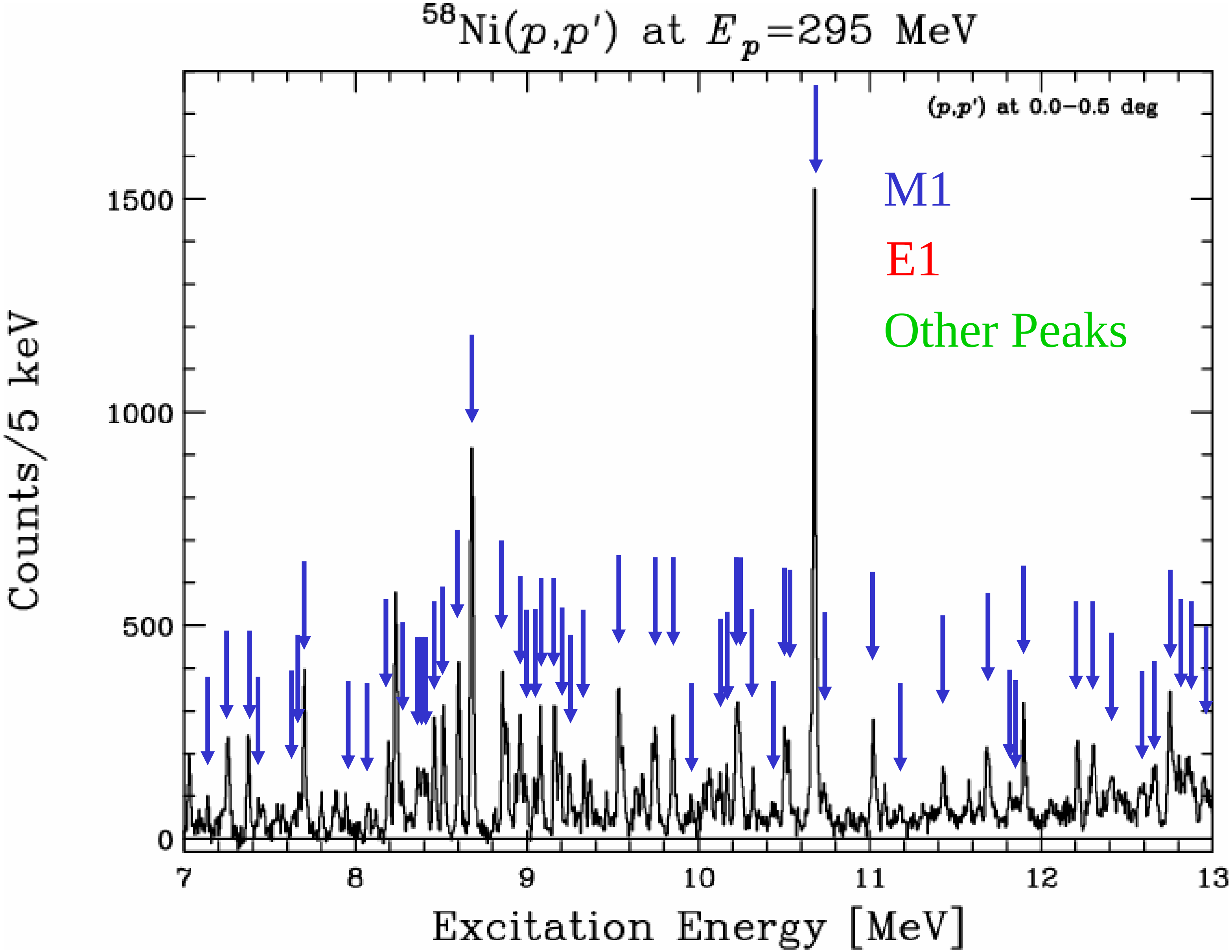

^{58}Ni(p,p′) at E_p=295 MeV
(p,p′) at 0.0–0.5 deg
M1
E1
Other Peaks
Counts/5 keV
Excitation Energy [MeV]
0
500
1000
1500
7
8
9
10
11
12
13

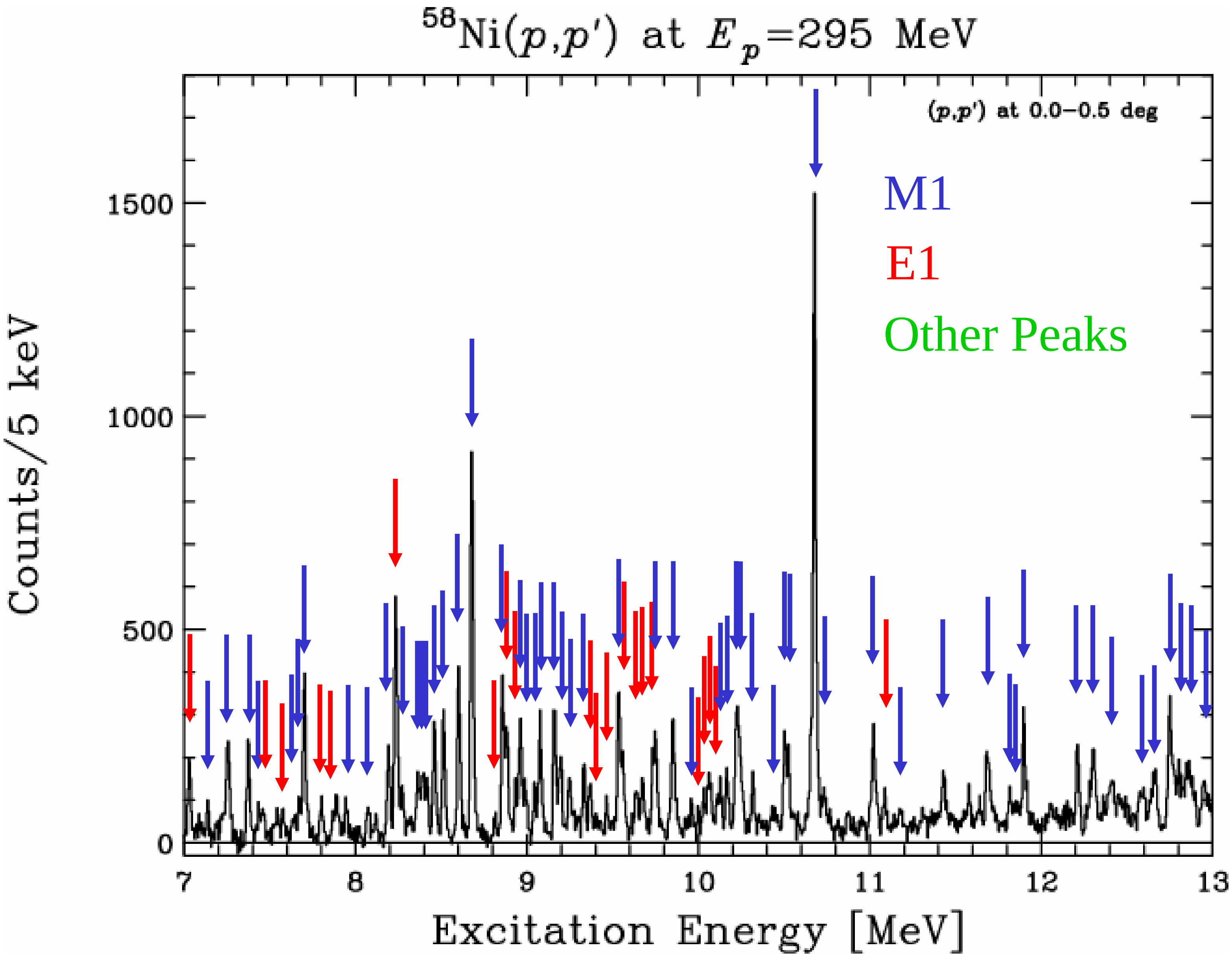

^{58}Ni(p,p') at E_p=295 MeV
(p,p') at 0.0–0.5 deg
M1
E1
Other Peaks
Counts/5 keV
0
500
1000
1500
7
8
9
10
11
12
13
Excitation Energy [MeV]

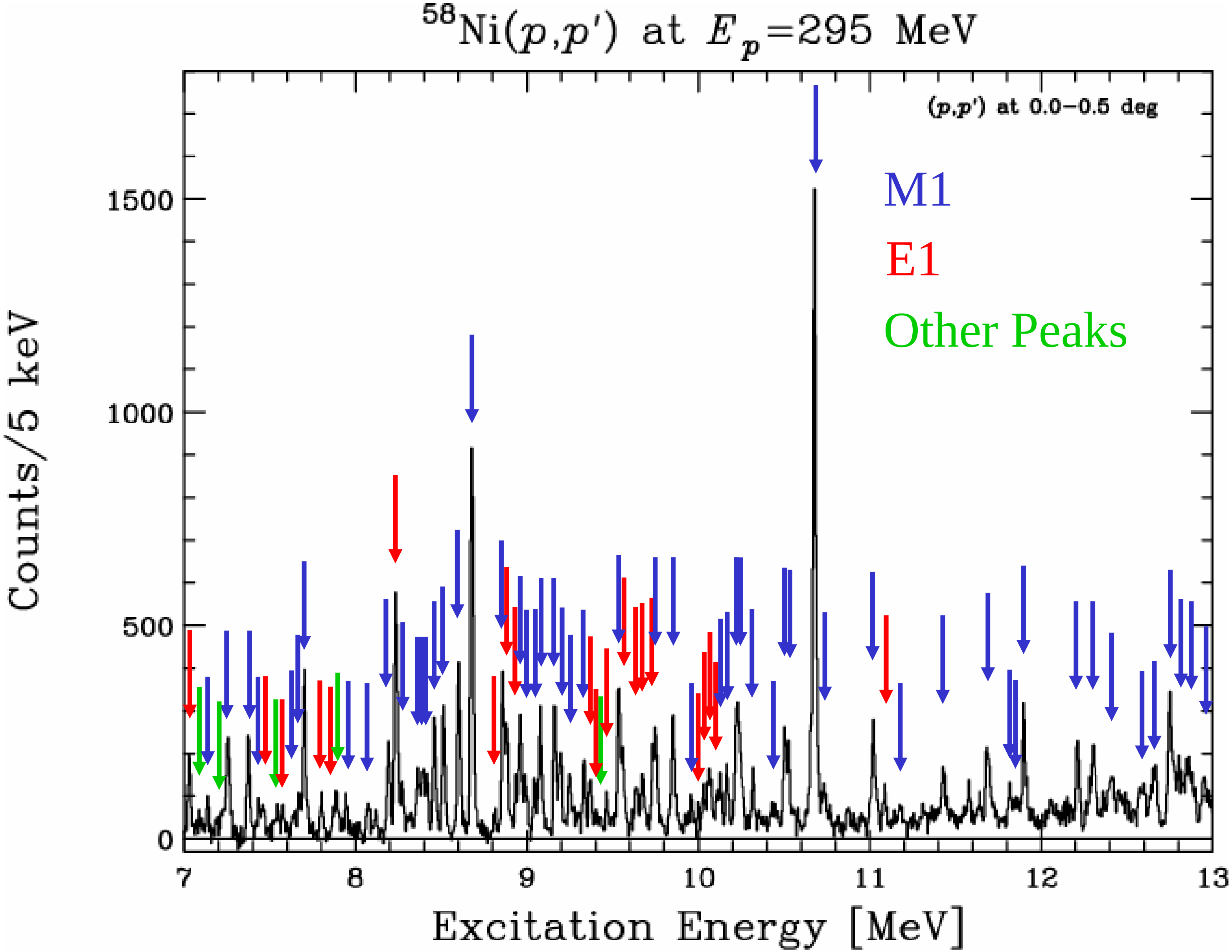

^{58}Ni(p,p') at E_p=295 MeV
(p,p') at 0.0–0.5 deg
M1
E1
Other Peaks
Counts/5 keV
0
500
1000
1500
7
8
9
10
11
12
13
Excitation Energy [MeV]

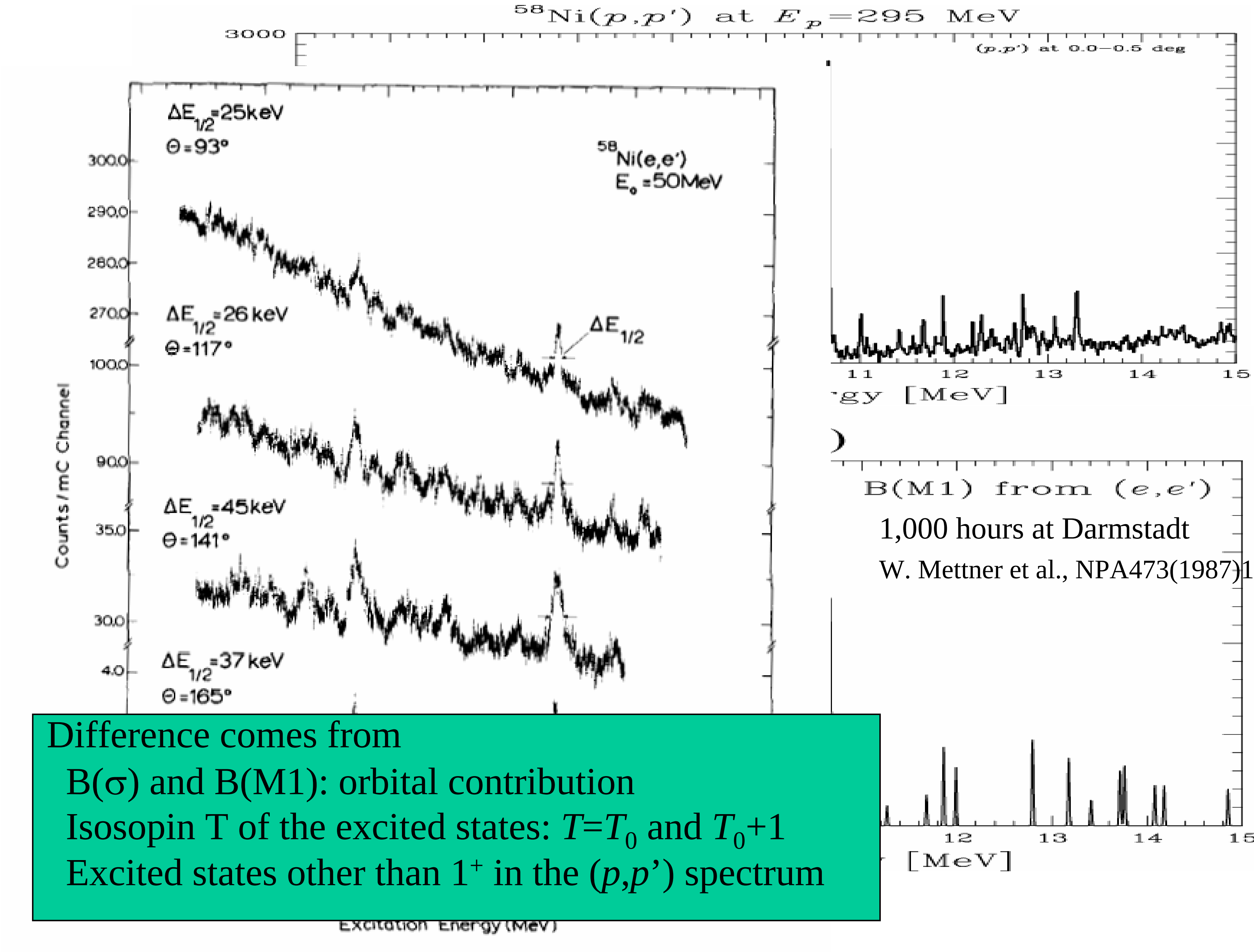

1,000 hours at Darmstadt

W. Mettner et al., NPA473(1987)160.

Difference comes from

- B(σ) and B(M1): orbital contribution
- Isosopin T of the excited states: T=T_0 and T_0+1
- Excited states other than 1^+ in the (*p*,*p*') spectrum

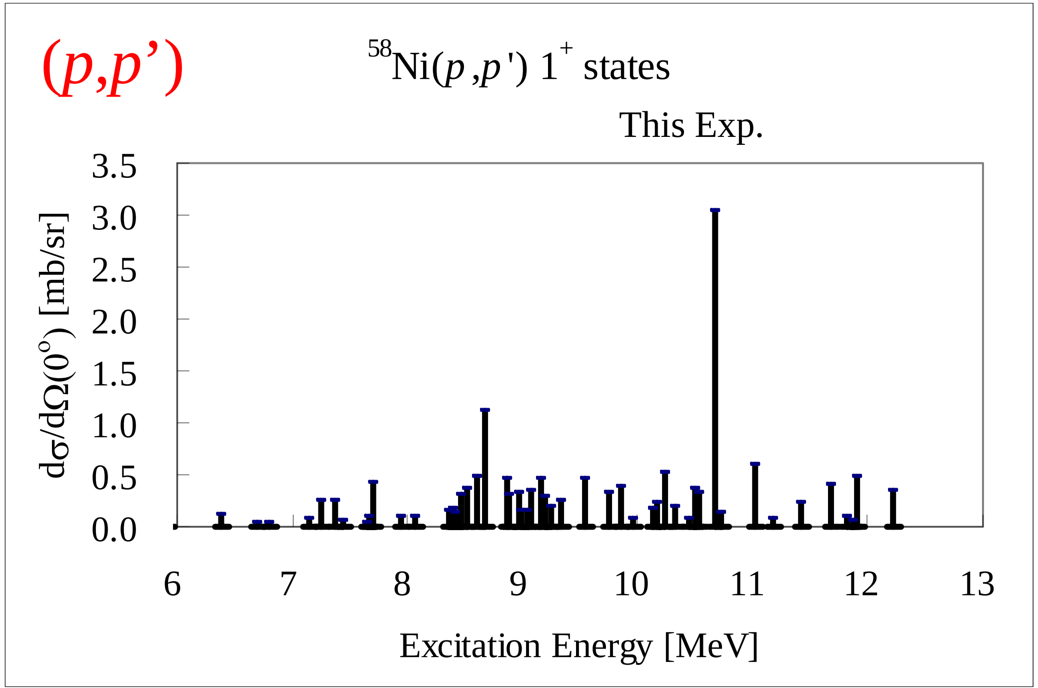

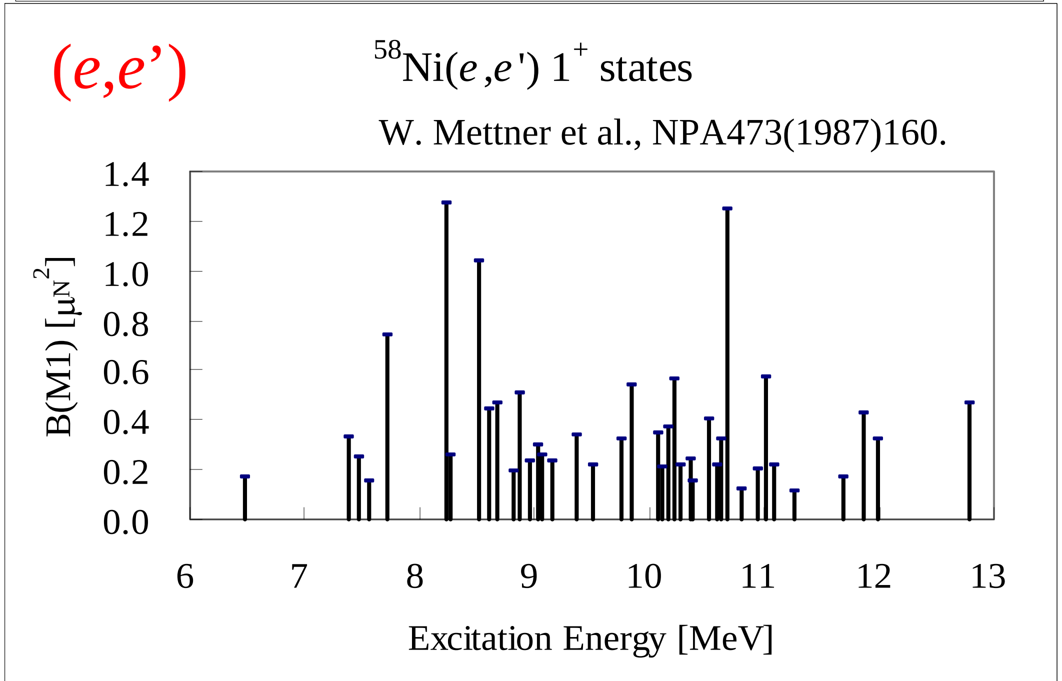

Differences come from:
orbital par of the M1 operator

↓

Extraction of general trend by checking the orbital contribution in each state.

B(σ): (p,p')
B(M1): EM probes
orbital part: combination

^{64}Ni(p, p')

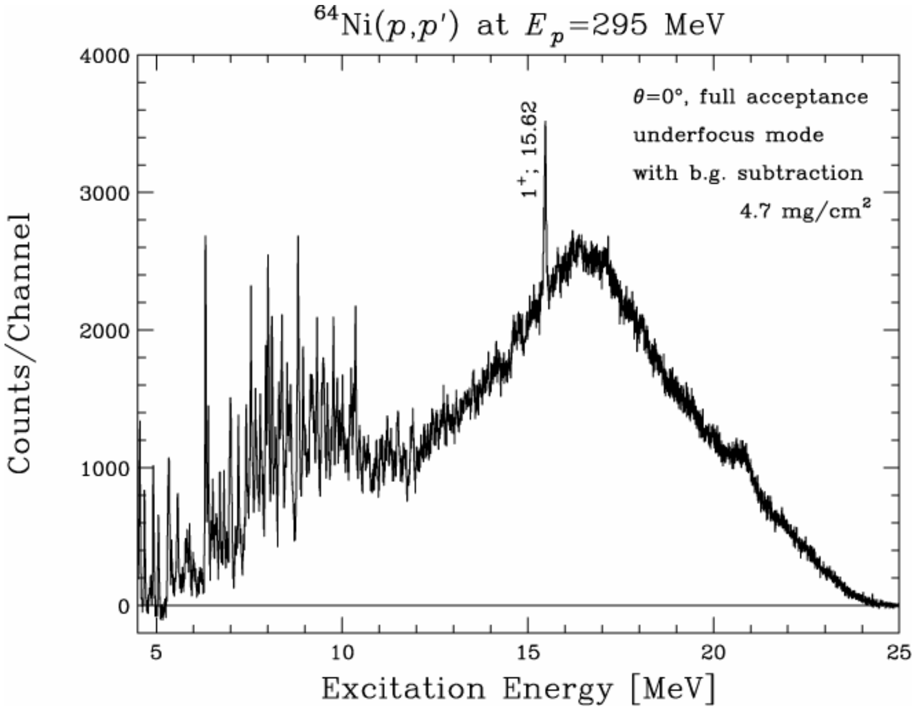

^{64}Ni(p,p') at E_p=295 MeV
θ=0°, full acceptance
underfocus mode
with b.g. subtraction
4.7 mg/cm²
1⁺; 15.62
Counts/Channel
Excitation Energy [MeV]

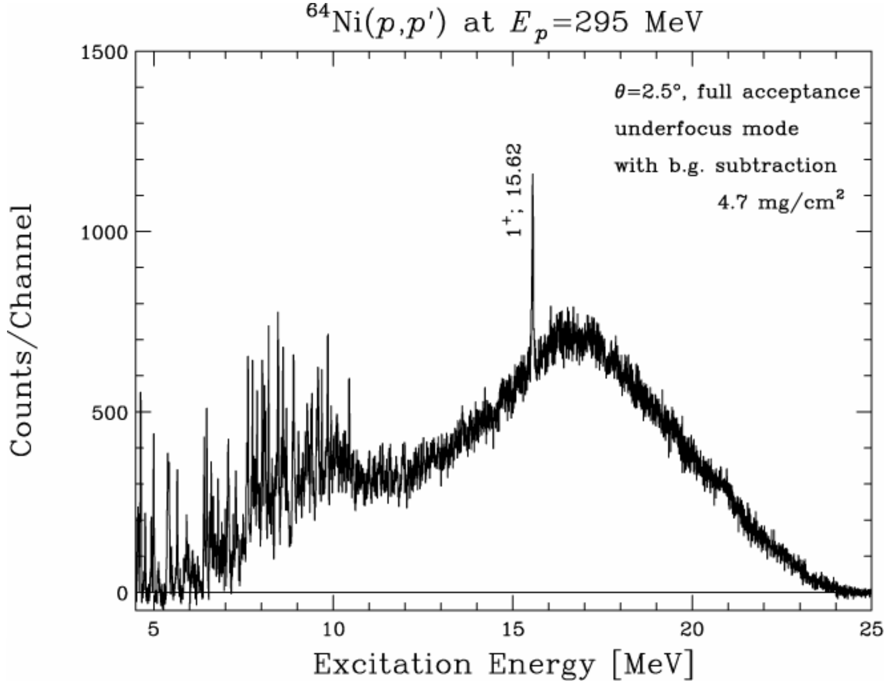

^{64}Ni(p,p') at E_p=295 MeV
θ=2.5°, full acceptance
underfocus mode
with b.g. subtraction
4.7 mg/cm²
1⁺; 15.62
Counts/Channel
Excitation Energy [MeV]

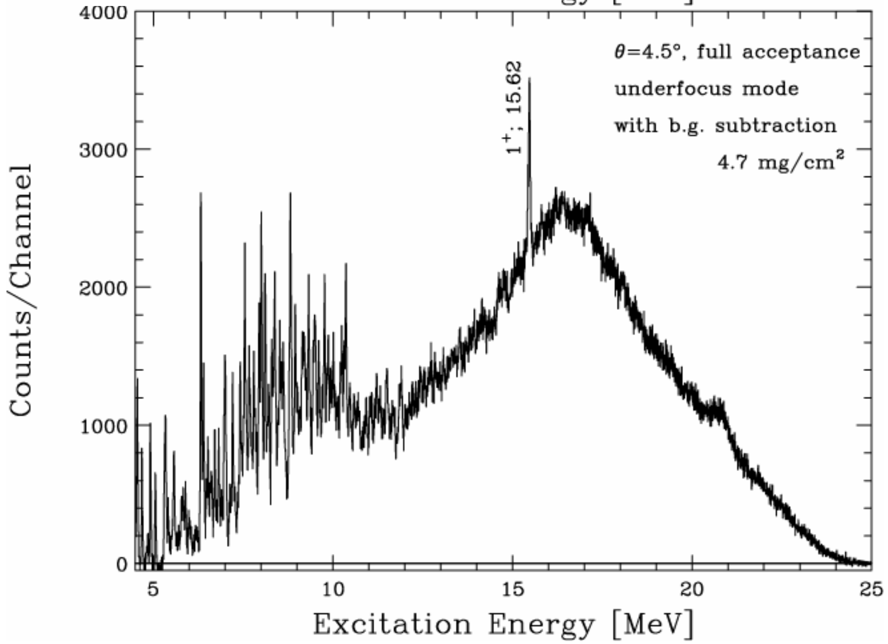

θ=4.5°, full acceptance
underfocus mode
with b.g. subtraction
4.7 mg/cm²
1⁺; 15.62
Counts/Channel
Excitation Energy [MeV]

$^{90}Zr(p, p')$

G.M. Crawley et al,

PRC26(1982)87

at 200 MeV and 4 deg

present data

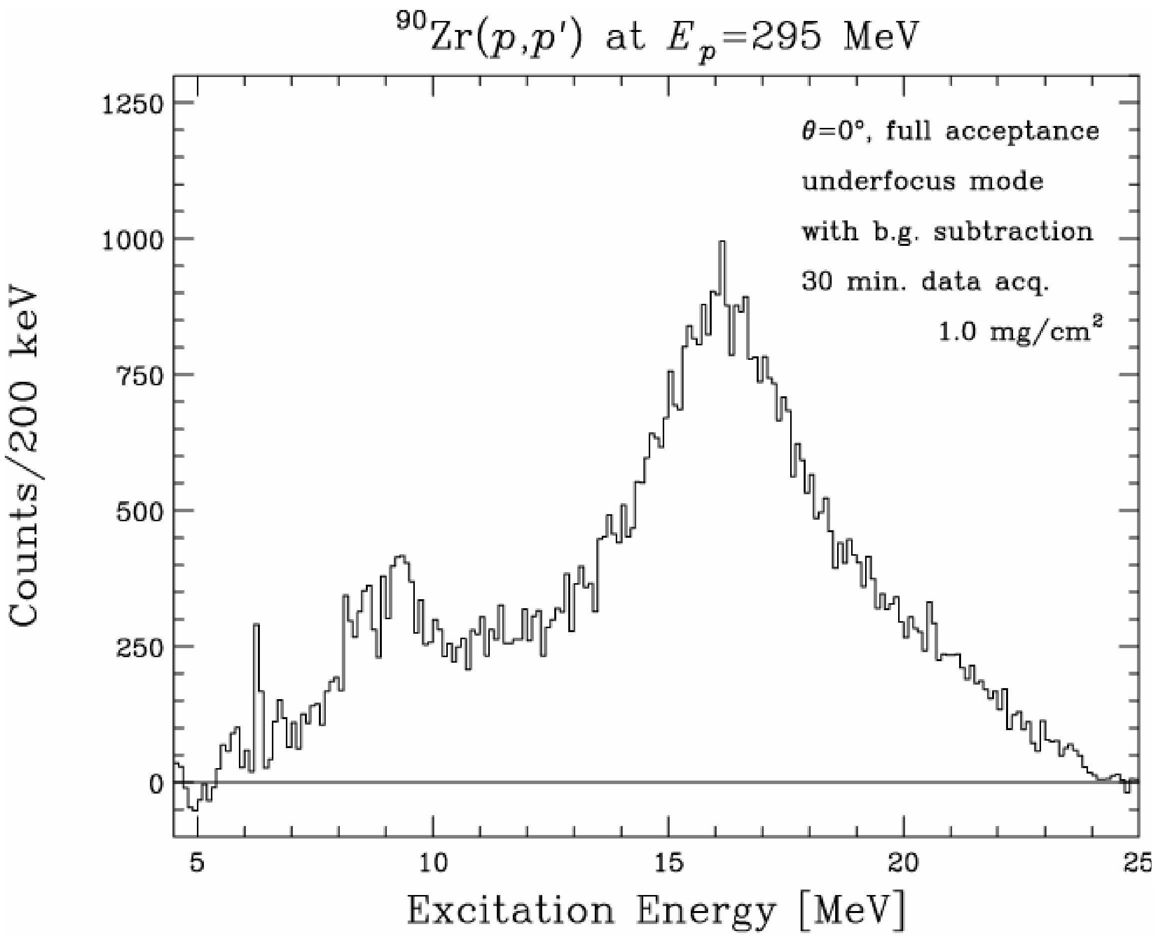

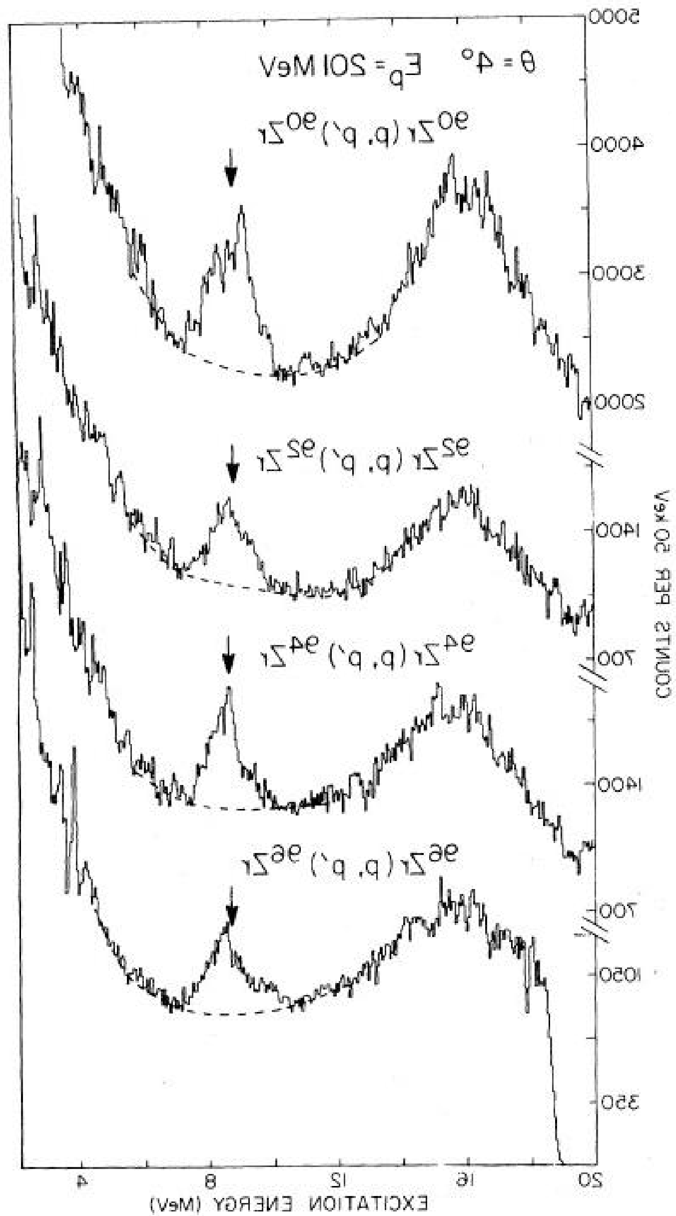

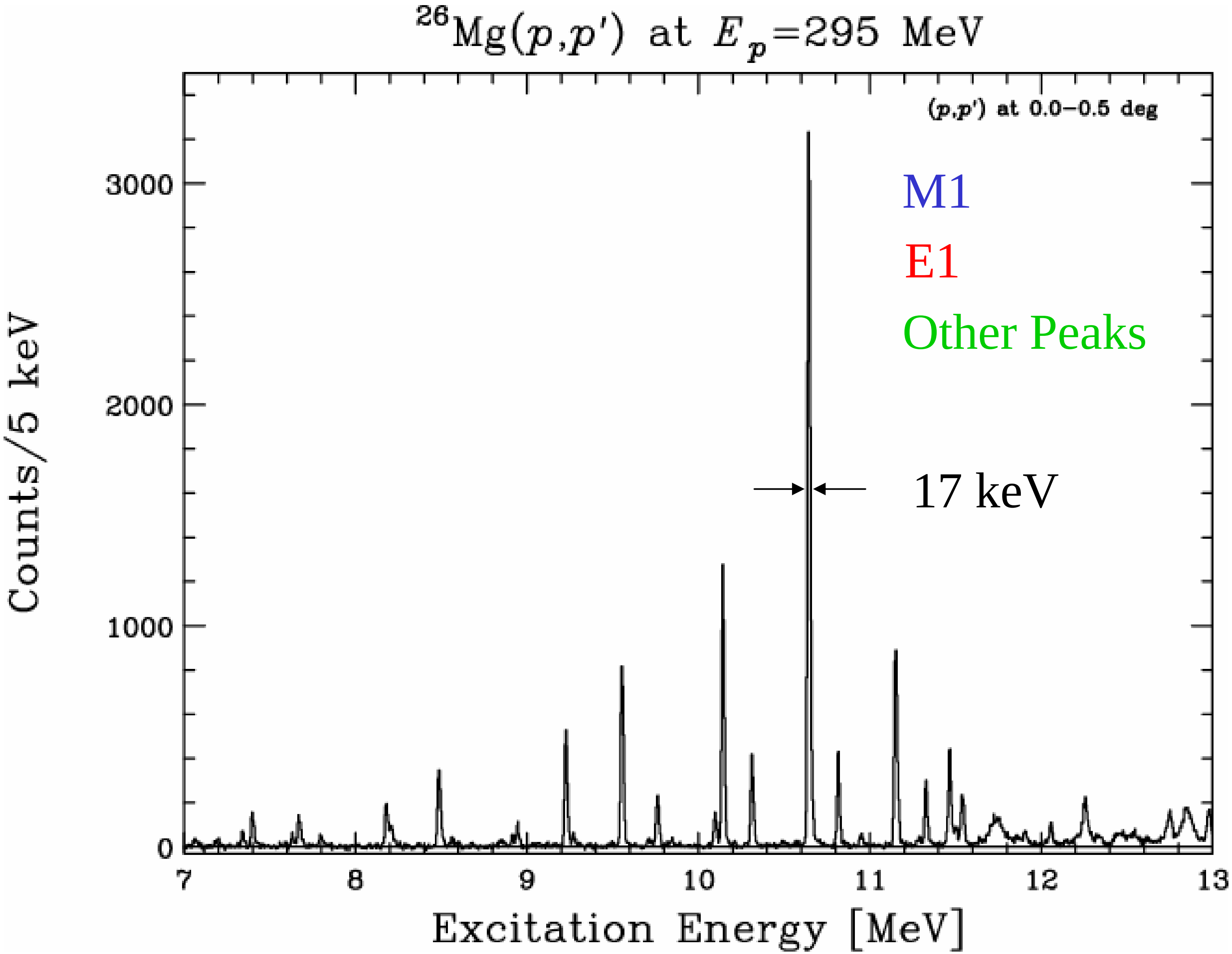
^{26}Mg(p,p') at E_p=295 MeV
(p,p') at 0.0–0.5 deg
M1
E1
Other Peaks
17 keV
Counts/5 keV
0
1000
2000
3000
7
8
9
10
11
12
13
Excitation Energy [MeV]

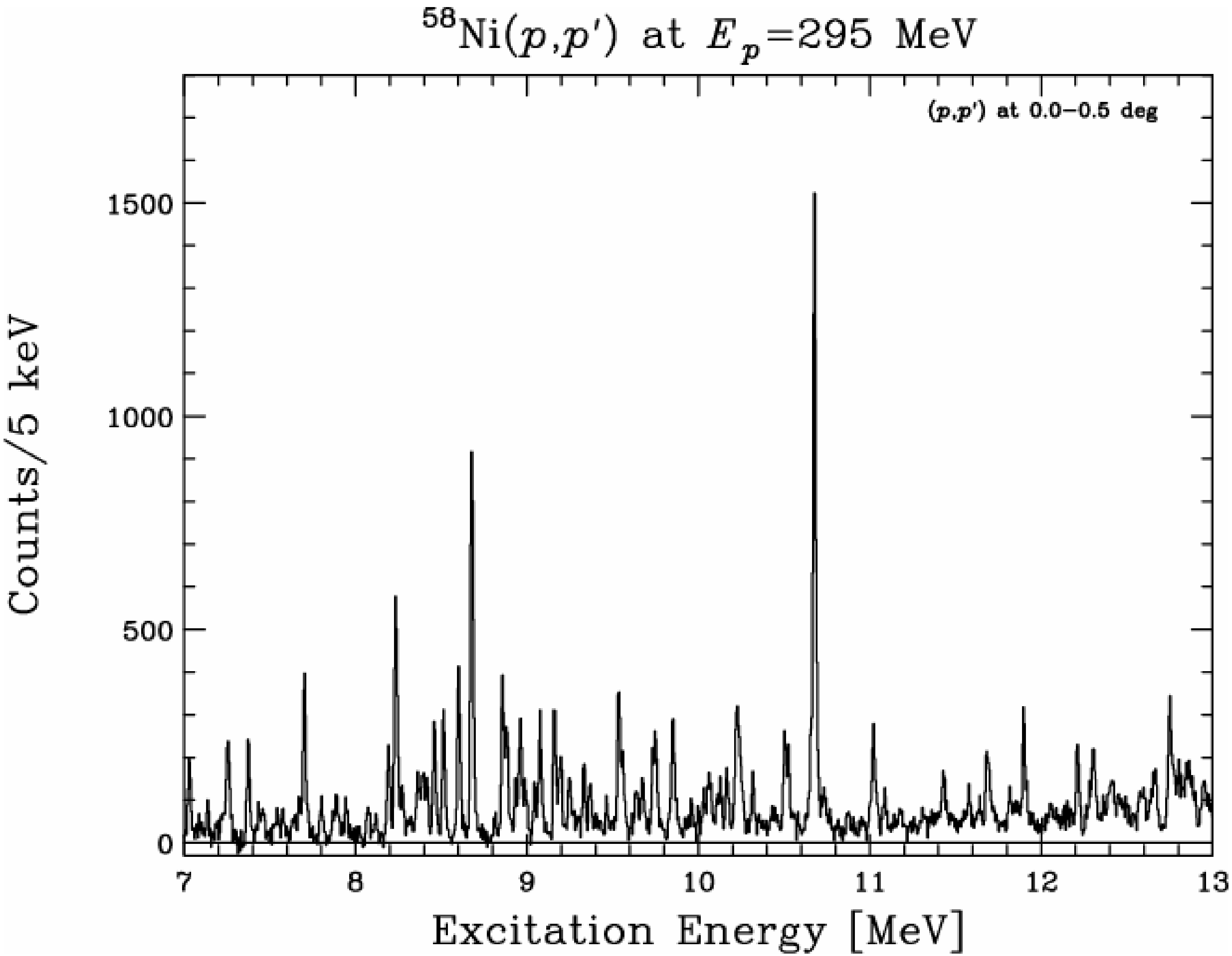

^{58}Ni(p,p') at E_p=295 MeV
(p,p') at 0.0–0.5 deg
Counts/5 keV
0
500
1000
1500
7
8
9
10
11
12
13
Excitation Energy [MeV]

Discussion

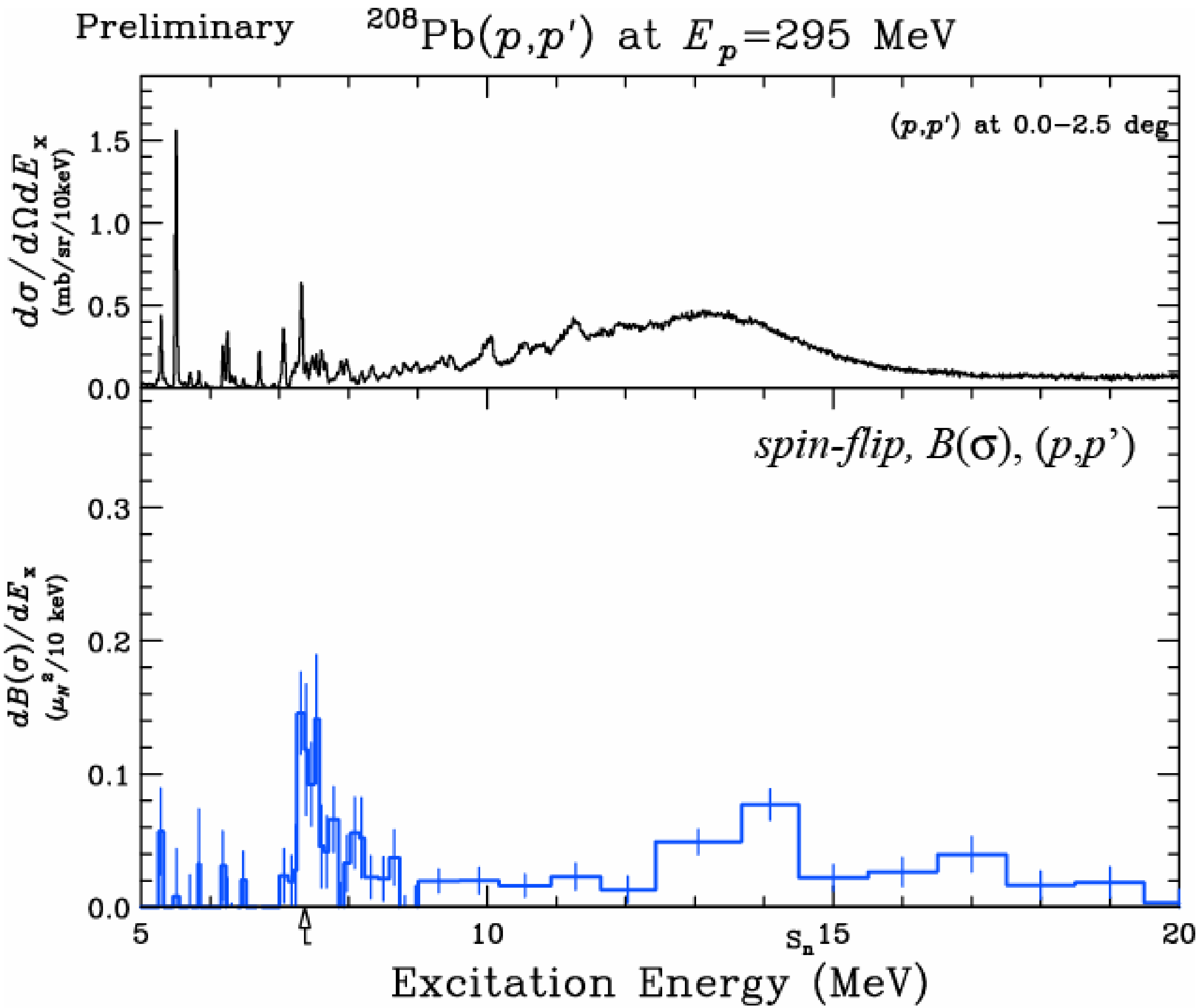
Preliminary
208Pb(p,p') at Ep=295 MeV
(p,p') at 0.0−2.5 deg
dσ/dΩdEx (mb/sr/10keV)
1.5
1.0
0.5
0.0
spin-flip, B(σ), (p,p')
dB(σ)/dEx (μN²/10 keV)
0.3
0.2
0.1
0.0
5
10
Sn 15
20
Excitation Energy (MeV)

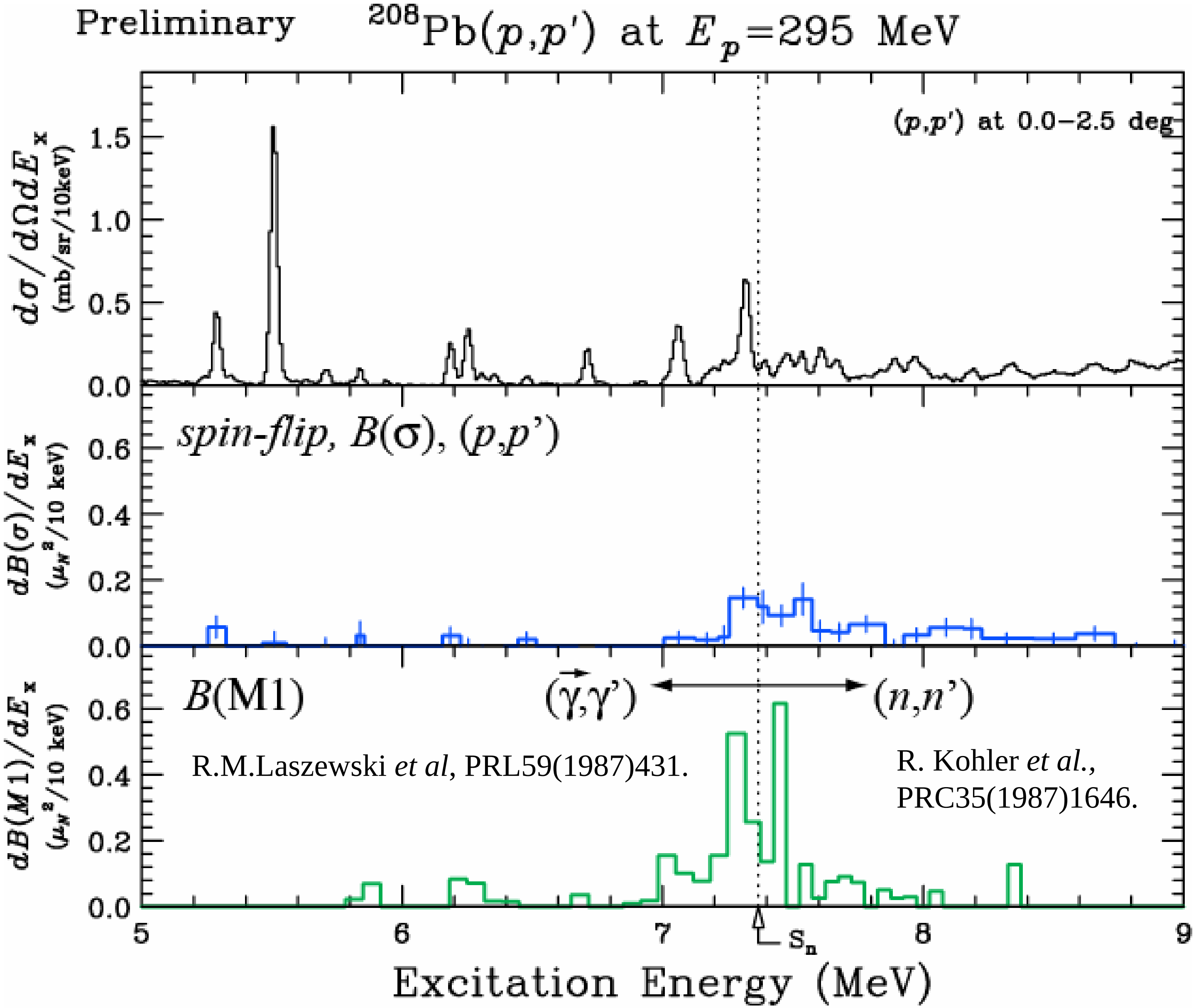

Preliminary
208Pb(p,p') at Ep=295 MeV
(p,p') at 0.0–2.5 deg
dσ/dΩdEx (mb/sr/10keV)
spin-flip, B(σ), (p,p')
dB(σ)/dEx (μN²/10 keV)
B(M1)
(γ,γ')
(n,n')
R.M.Laszewski et al, PRL59(1987)431.
R. Kohler et al., PRC35(1987)1646.
dB(M1)/dEx (μN²/10 keV)
Sn
Excitation Energy (MeV)

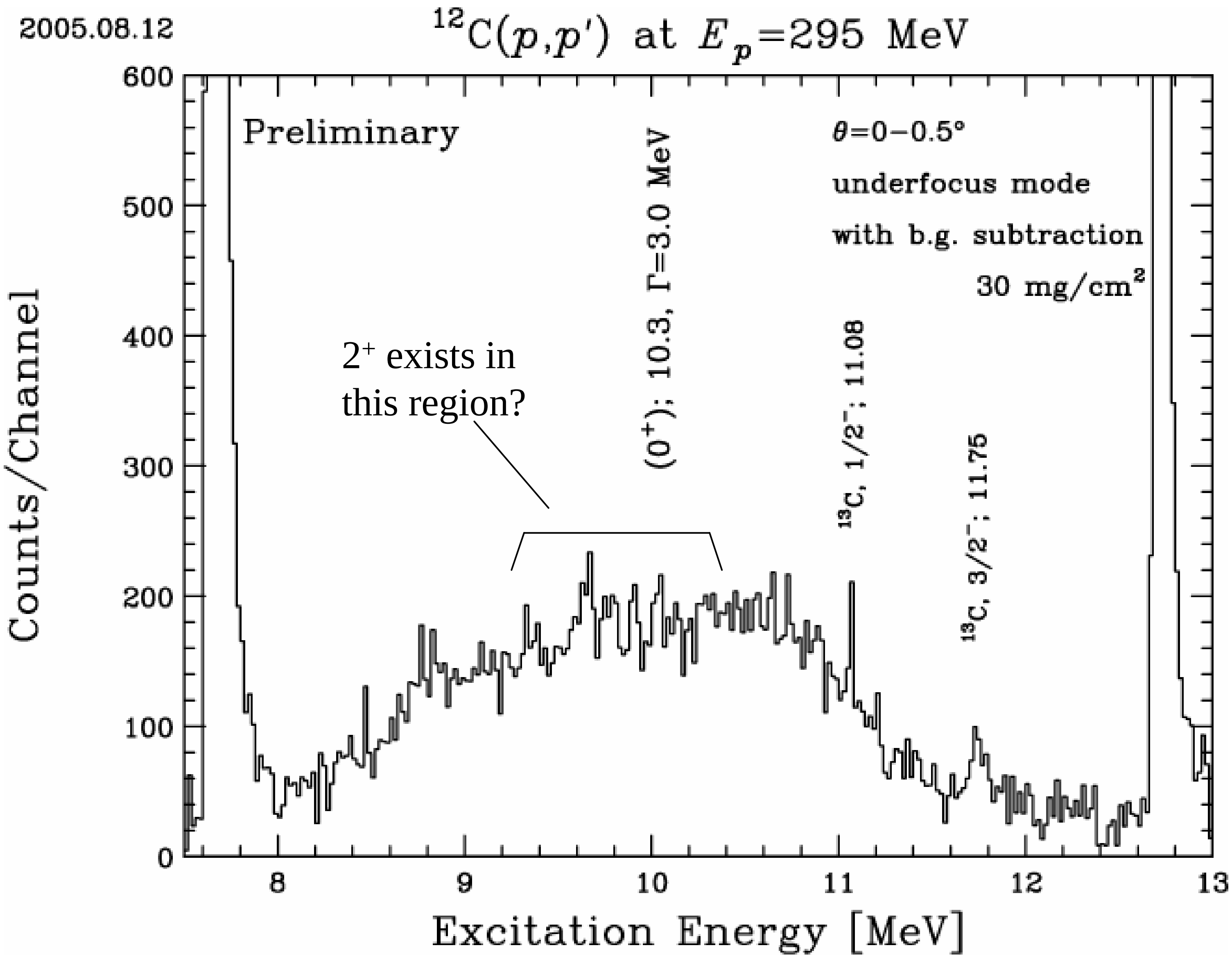
2005.08.12
$^{12}C(p,p')$ at E_p=295 MeV
Preliminary
θ=0−0.5°
underfocus mode
with b.g. subtraction
30 mg/cm²
(0⁺); 10.3, Γ=3.0 MeV
¹³C, 1/2⁻; 11.08
¹³C, 3/2⁻; 11.75
2⁺ exists in
this region?
Counts/Channel
Excitation Energy [MeV]
0
100
200
300
400
500
600
8
9
10
11
12
13

Inelastic Scattering from ^{12}C at 8-12 MeV region

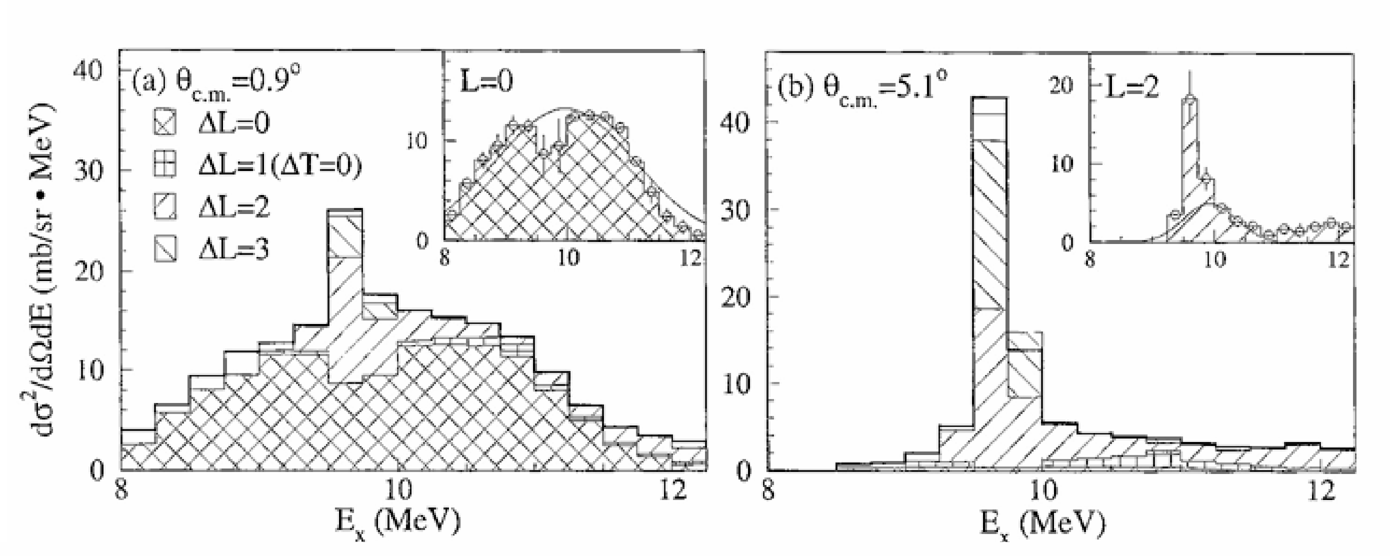

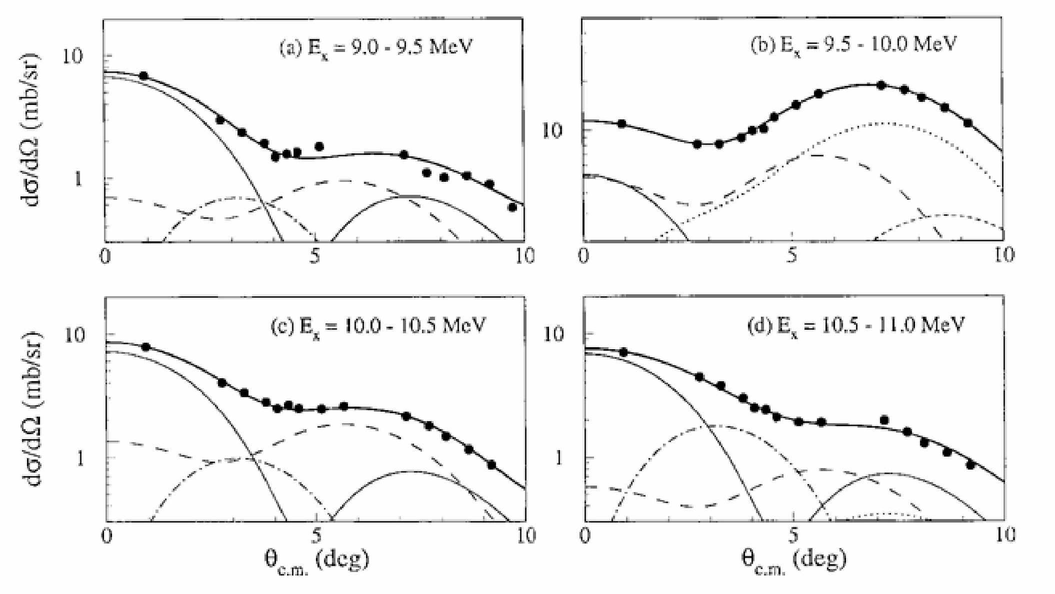

$^{12}C(\alpha,\alpha')$ at 400 MeV,

M. Itoh et al.,
NPA738(2004)268.

Inelastic Scattering from ^{12}C at 8-12 MeV region

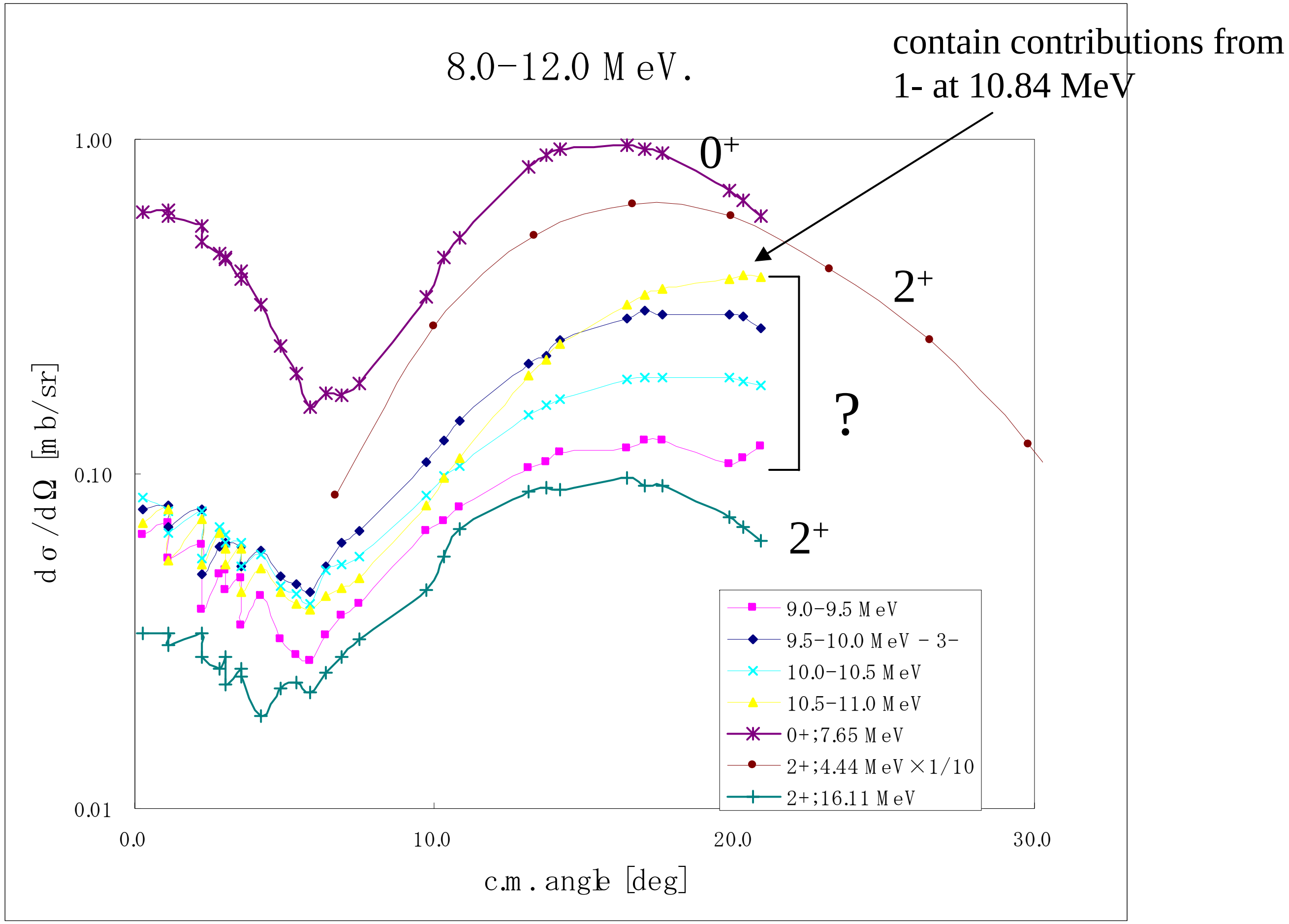

The angular distribution need to be analyzed carefully.

At present, I cannot draw any preliminary conclusion. DWBA calculations are required.

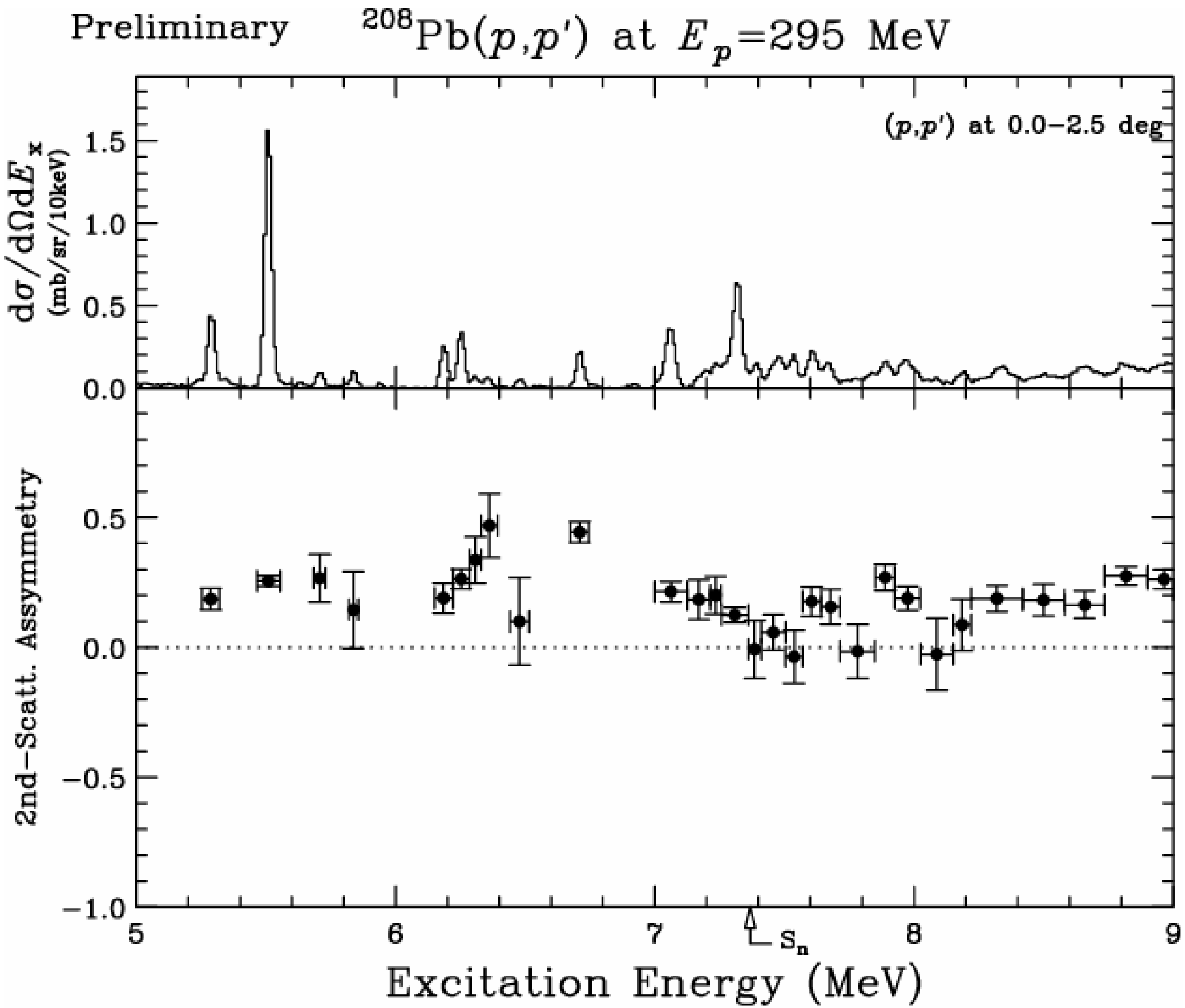
Preliminary
208Pb(p,p') at Ep=295 MeV
(p,p') at 0.0–2.5 deg
dσ/dΩdEx (mb/sr/10keV)
0.0
0.5
1.0
1.5
2nd–Scatt. Assymmetry
−1.0
−0.5
0.0
0.5
5
6
7
8
9
Sn
Excitation Energy (MeV)

Decomposition of M1 and E1 Excitations

After completing the experiment, we use the following model-independent relation at 0 deg

T.Suzuki, PTP103(2000)859

$$D_{SS} + D_{NN} + D_{LL} = \begin{cases} -1 \text{ for } \Delta S = 1 & \text{e.g. M1} \\ 3 \text{ for } \Delta S = 0 & \text{e.g. Coulomb-Excited E1} \end{cases}$$

$$(= 2D_{NN} + D_{LL})$$

The D_{LL} measured is not done yet.

Thus, here we use an approximation of

$$D_{NN} = \begin{cases} -0.24 \text{ for } \Delta S = 1 \\ 1 \quad \text{ for } \Delta S = 0 \end{cases}$$

← c.f. T.Wakasa, M. Dozono *et al.*, for $^{12}C(p,n)^{12}N$(g.s) at 300 MeV

to extract spin-flip strength.

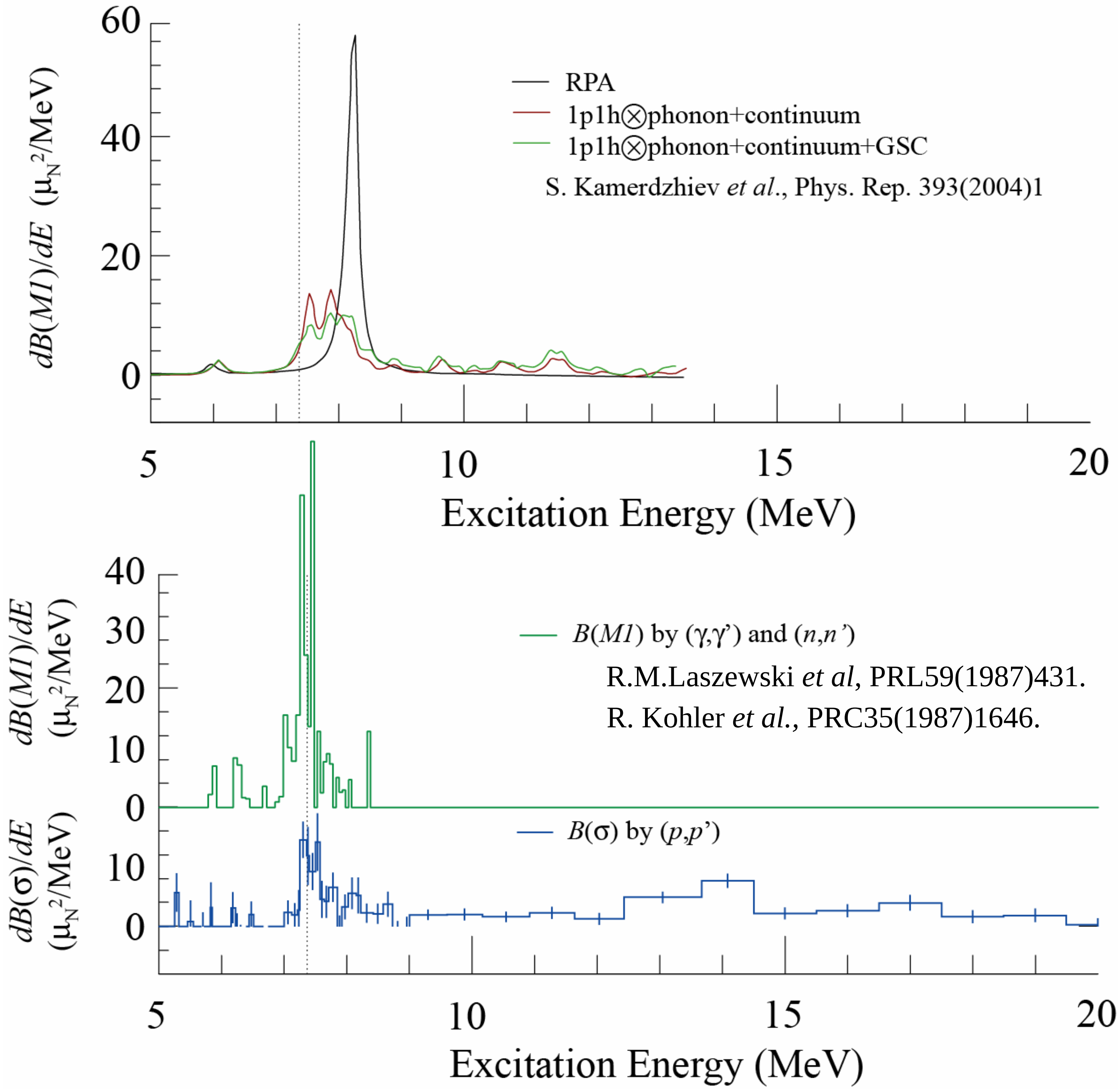

dB(M1)/dE (μN2/MeV)
RPA
1p1h⊗phonon+continuum
1p1h⊗phonon+continuum+GSC
S. Kamerdzhiev et al., Phys. Rep. 393(2004)1
Excitation Energy (MeV)
dB(M1)/dE (μN2/MeV)
B(M1) by (γ,γ') and (n,n')
R.M.Laszewski et al, PRL59(1987)431.
R. Kohler et al., PRC35(1987)1646.
dB(σ)/dE (μN2/MeV)
B(σ) by (p,p')
Excitation Energy (MeV)

Comparison of B(E1) Strength Distribution

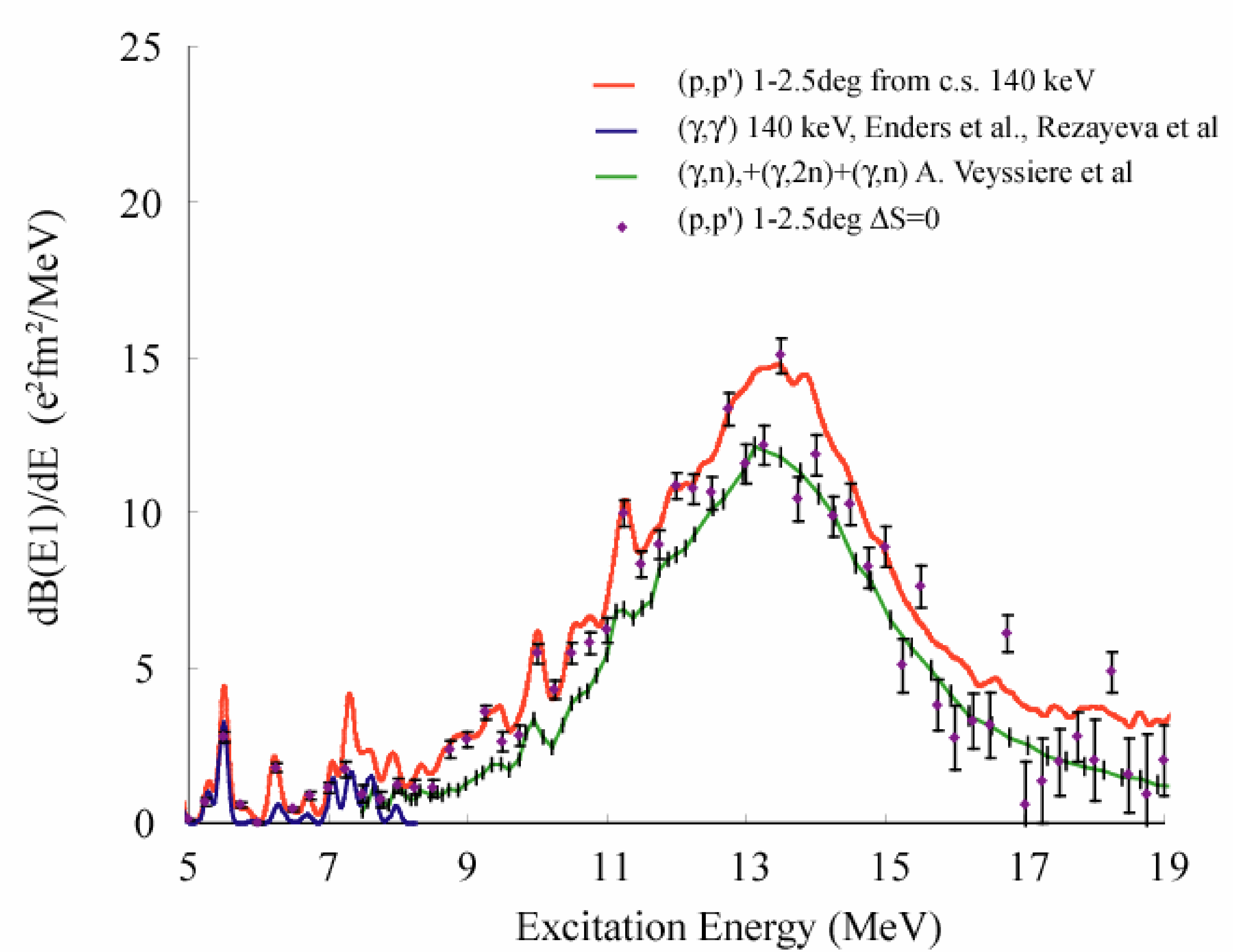

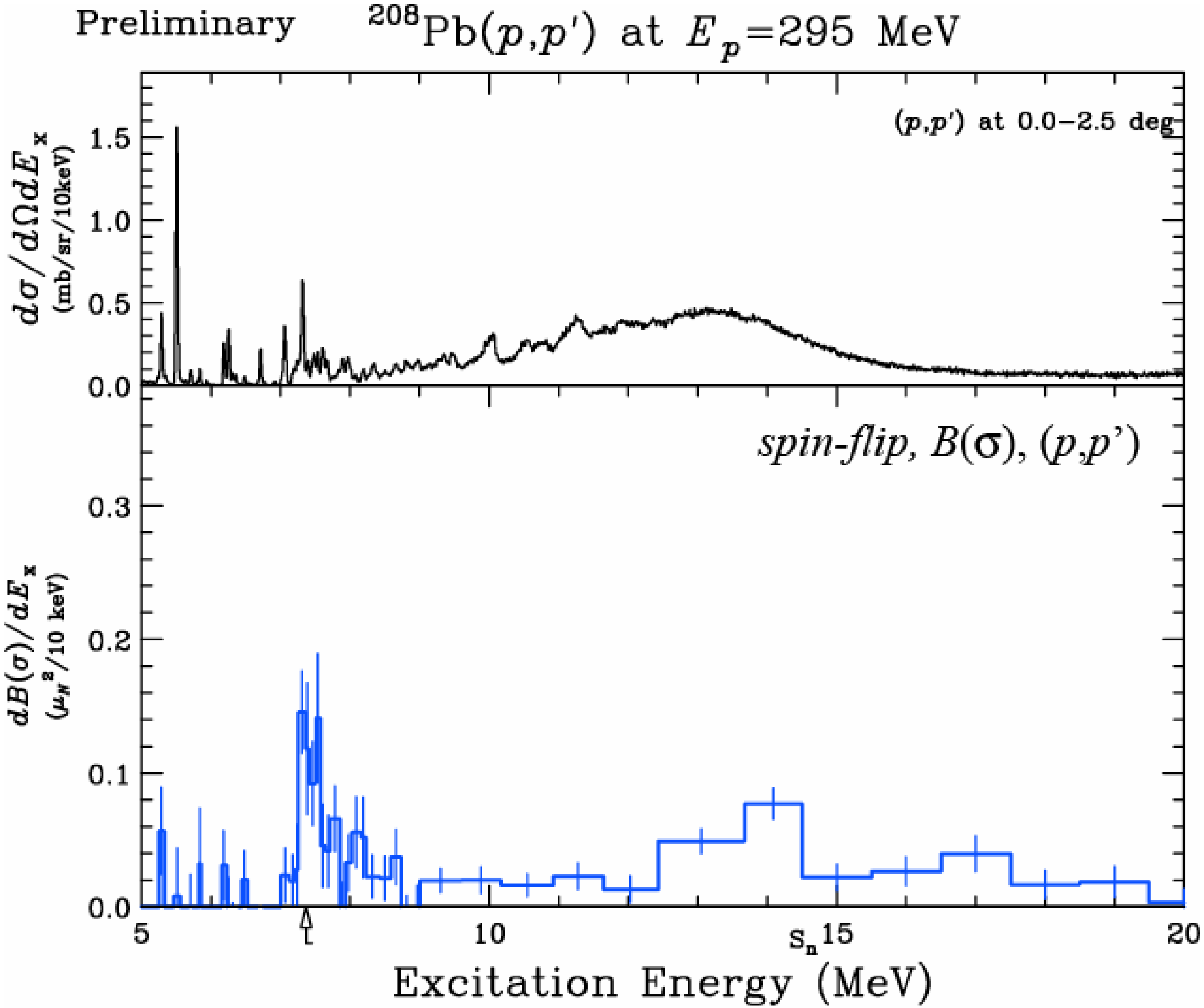

Preliminary
^{208}Pb(p,p') at E_p=295 MeV
(p,p') at 0.0–2.5 deg
$d\sigma/d\Omega dE_x$ (mb/sr/10keV)
1.5
1.0
0.5
0.0
spin-flip, $B(\sigma)$, (p,p')
$dB(\sigma)/dE_x$ (μ_N^2/10 keV)
0.3
0.2
0.1
0.0
5
10
S_n 15
20
Excitation Energy (MeV)

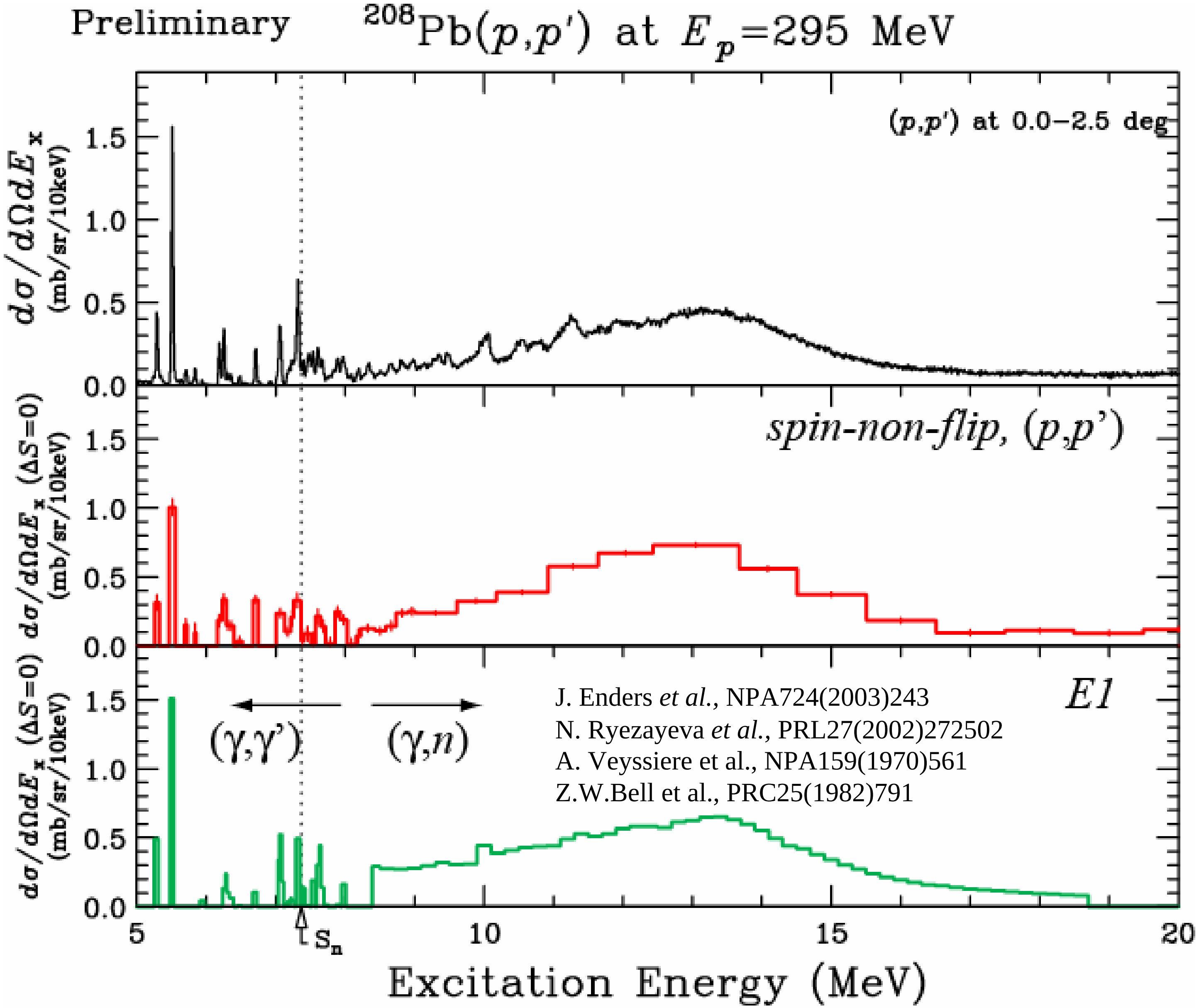
Preliminary
208Pb(p,p') at Ep=295 MeV
(p,p') at 0.0–2.5 deg
spin-non-flip, (p,p')
E1
(γ,γ')
(γ,n)
J. Enders et al., NPA724(2003)243
N. Ryezayeva et al., PRL27(2002)272502
A. Veyssiere et al., NPA159(1970)561
Z.W.Bell et al., PRC25(1982)791
dσ/dΩdEx (mb/sr/10keV)
dσ/dΩdEx (ΔS=0) (mb/sr/10keV)
Sn
Excitation Energy (MeV)
0.0
0.5
1.0
1.5
5
10
15
20

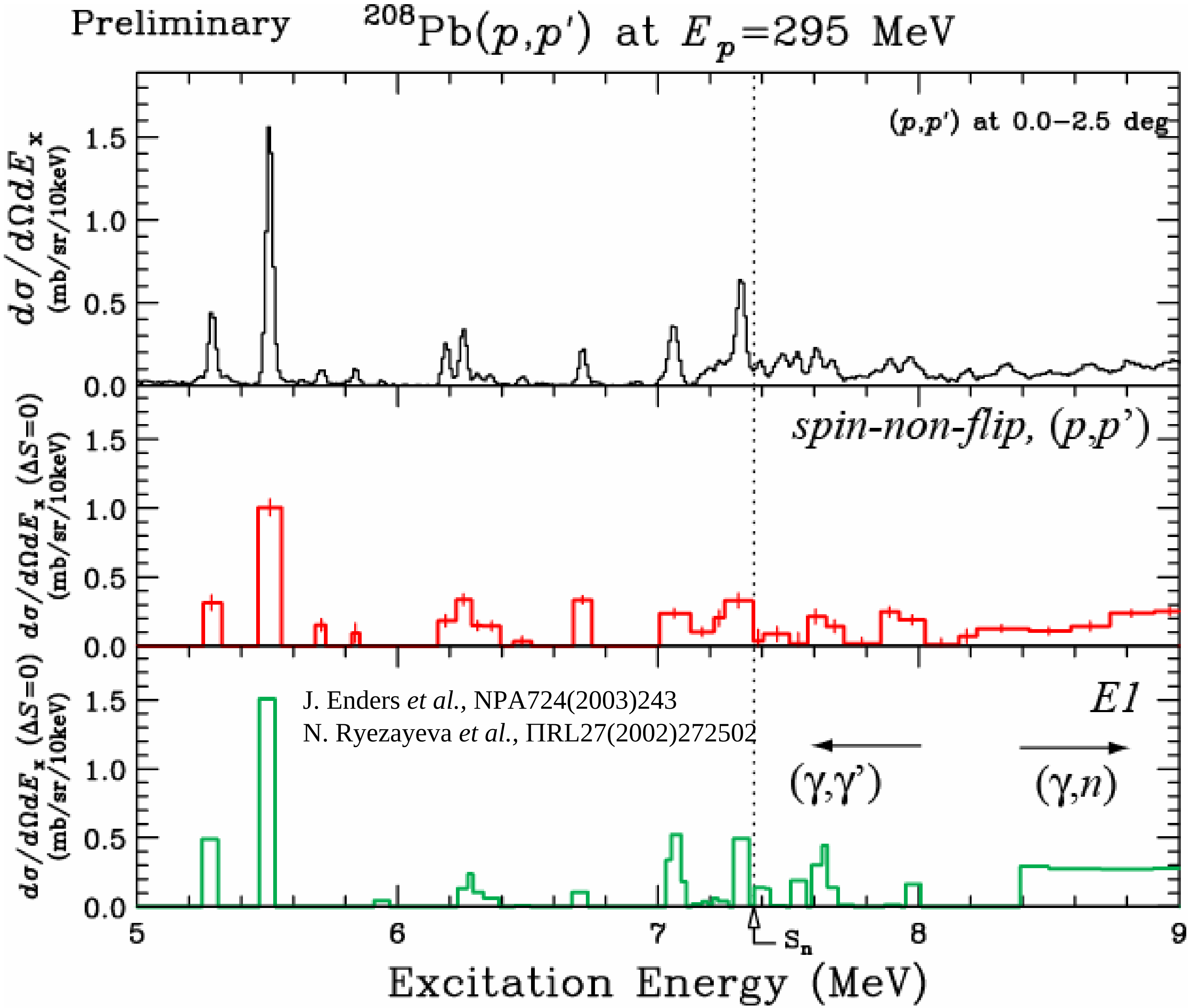
Preliminary
208Pb(p,p') at Ep=295 MeV
(p,p') at 0.0–2.5 deg
dσ/dΩdEx (mb/sr/10keV)
spin-non-flip, (p,p')
dσ/dΩdEx (ΔS=0) (mb/sr/10keV)
E1
J. Enders et al., NPA724(2003)243
N. Ryezayeva et al., ПRL27(2002)272502
(γ,γ')
(γ,n)
Sn
Excitation Energy (MeV)
0.0
0.5
1.0
1.5
5
6
7
8
9

Comparison with B(E1) Strength Distribution

preliminary

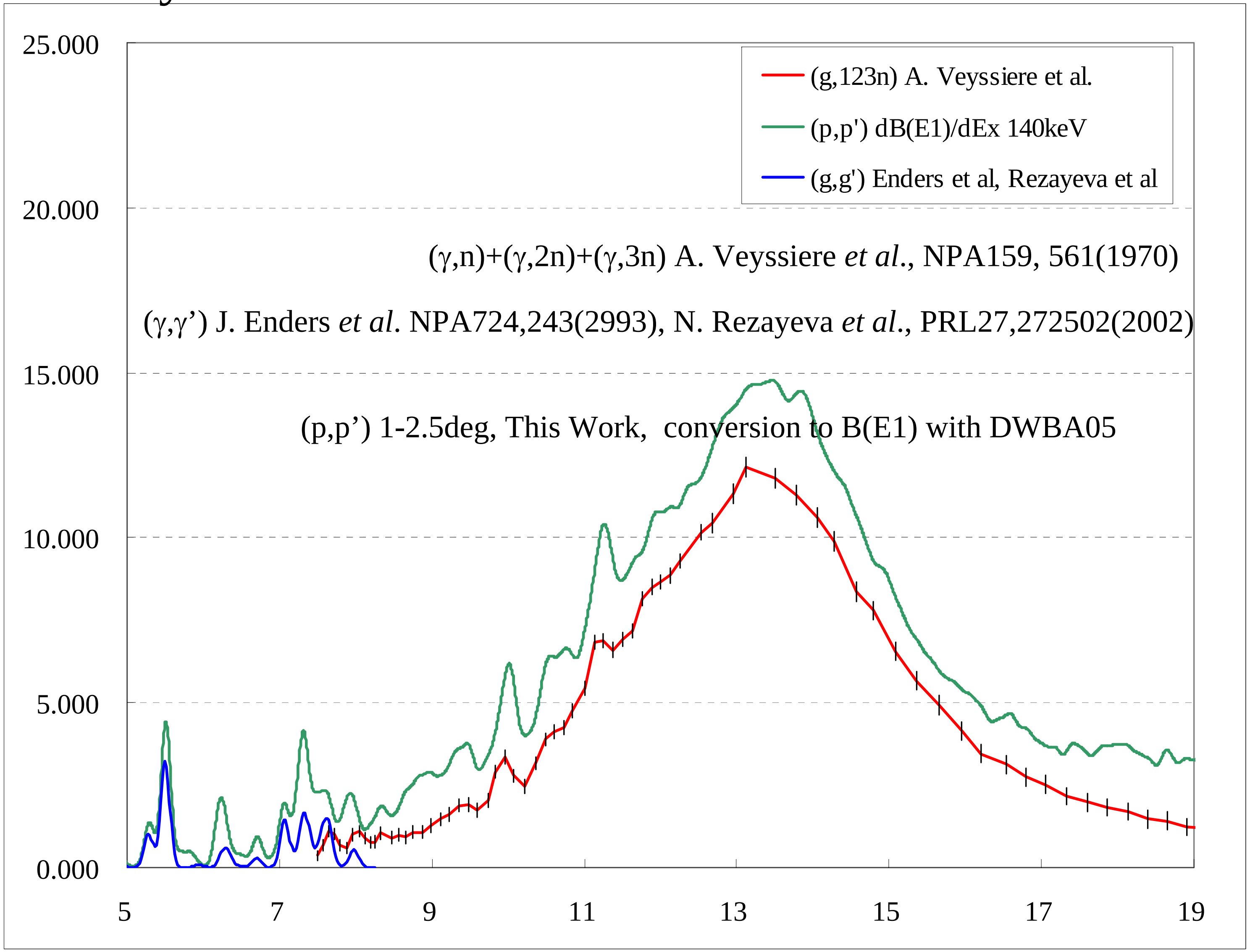

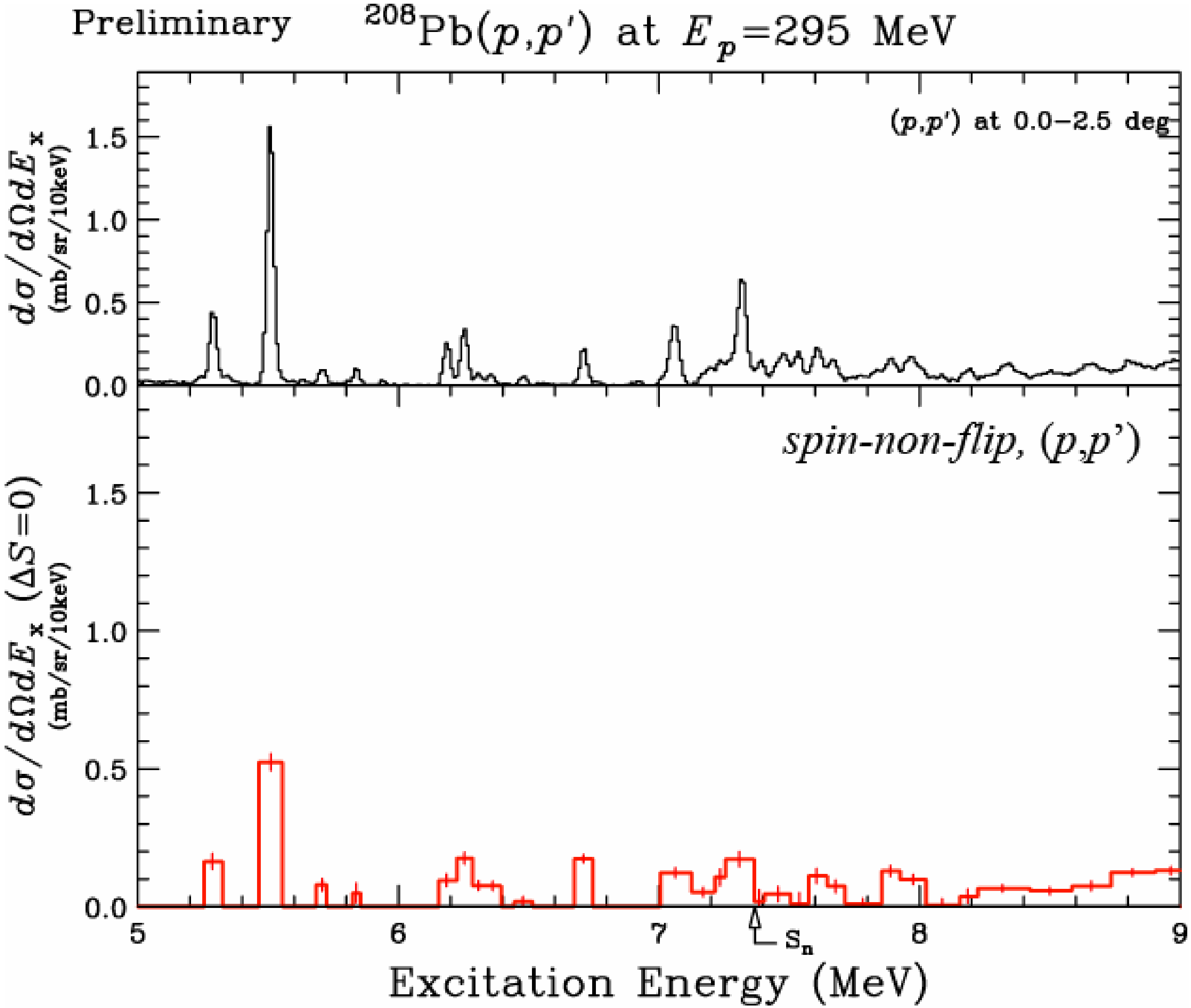
Preliminary
208Pb(p,p') at Ep=295 MeV
(p,p') at 0.0–2.5 deg
dσ/dΩdEx (mb/sr/10keV)
spin-non-flip, (p,p')
dσ/dΩdEx (ΔS=0) (mb/sr/10keV)
0.0
0.5
1.0
1.5
5
6
7
8
9
Sn
Excitation Energy (MeV)

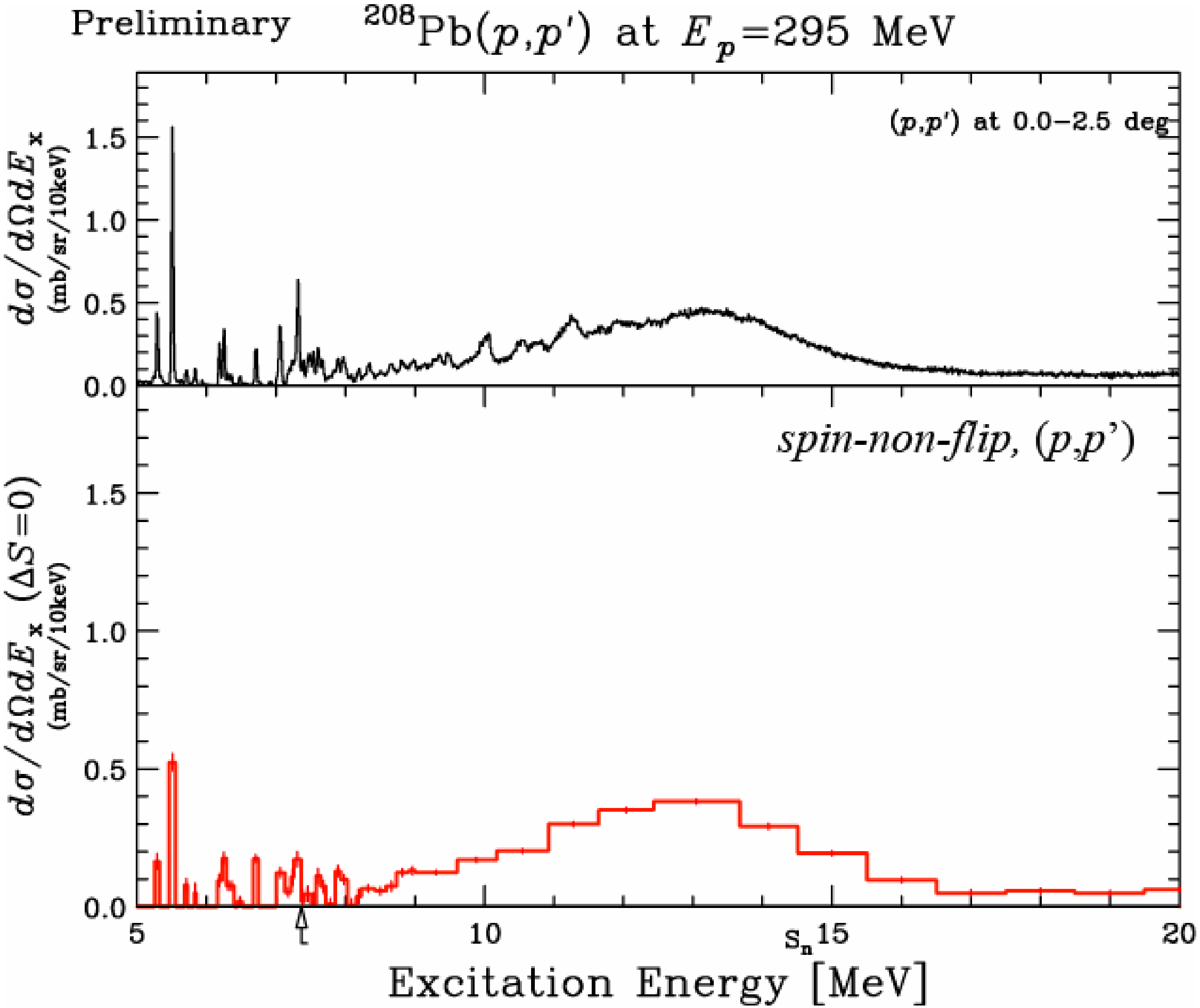

Preliminary
^{208}Pb(p,p') at E_p=295 MeV
(p,p') at 0.0–2.5 deg
$d\sigma/d\Omega dE_x$ (mb/sr/10keV)
spin-non-flip, (p,p')
$d\sigma/d\Omega dE_x$ (ΔS=0) (mb/sr/10keV)
1.5
1.0
0.5
0.0
5
10
S_n 15
20
Excitation Energy [MeV]

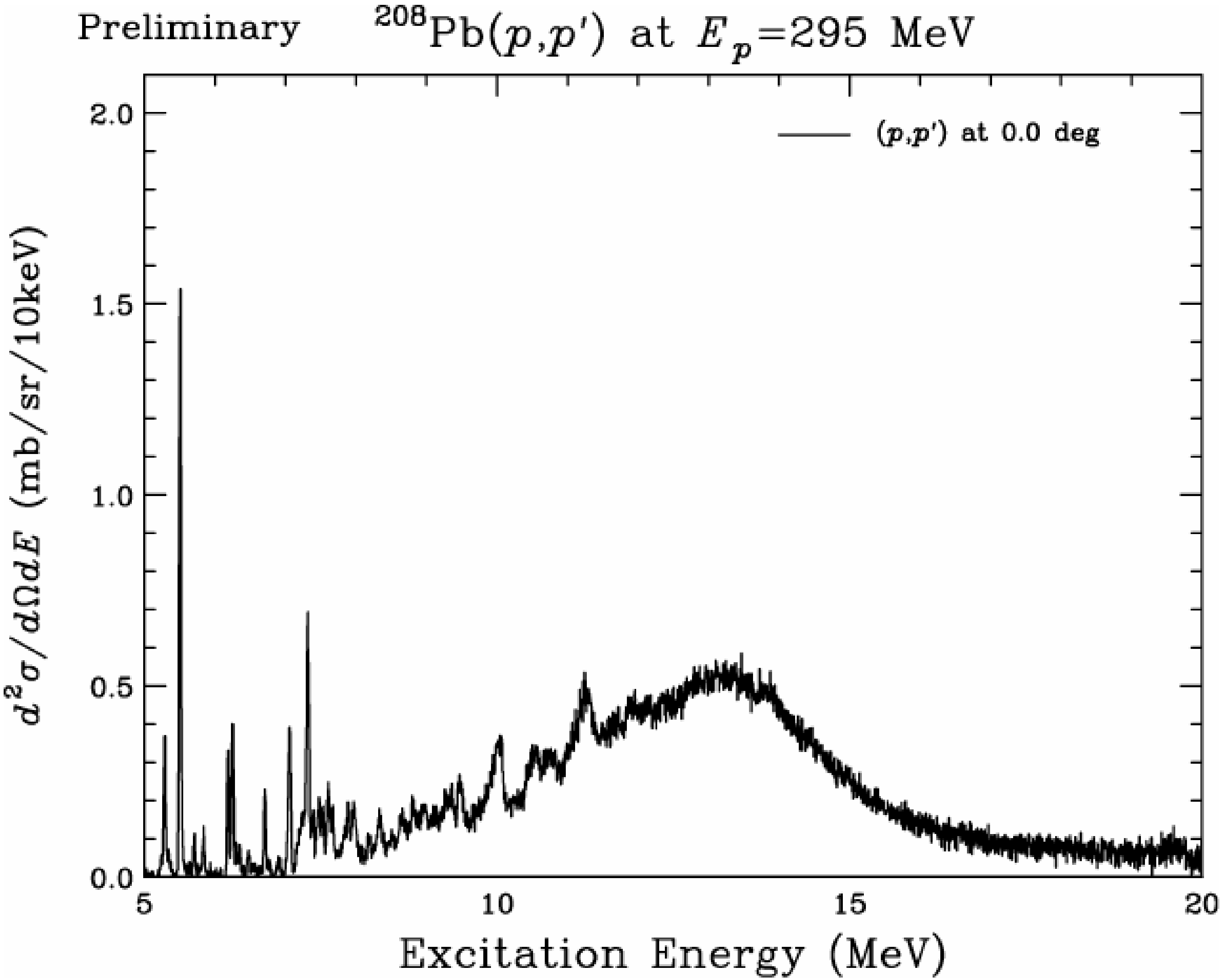
Preliminary
208Pb(p,p') at Ep=295 MeV
(p,p') at 0.0 deg
d2σ/dΩdE (mb/sr/10keV)
2.0
1.5
1.0
0.5
0.0
5
10
15
20
Excitation Energy (MeV)

Comparison of B(E1) Strength Distribution

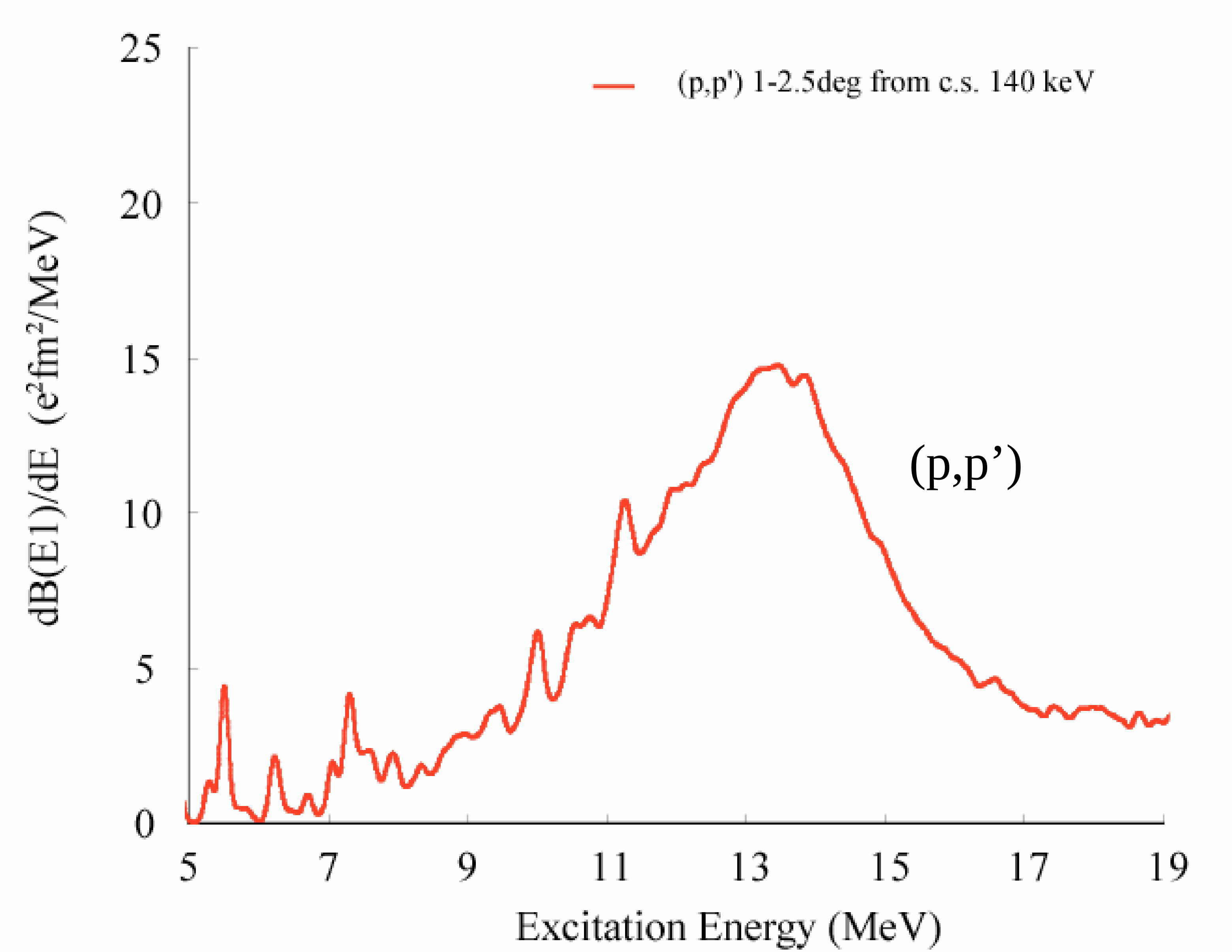

Comparison of B(E1) Strength Distribution

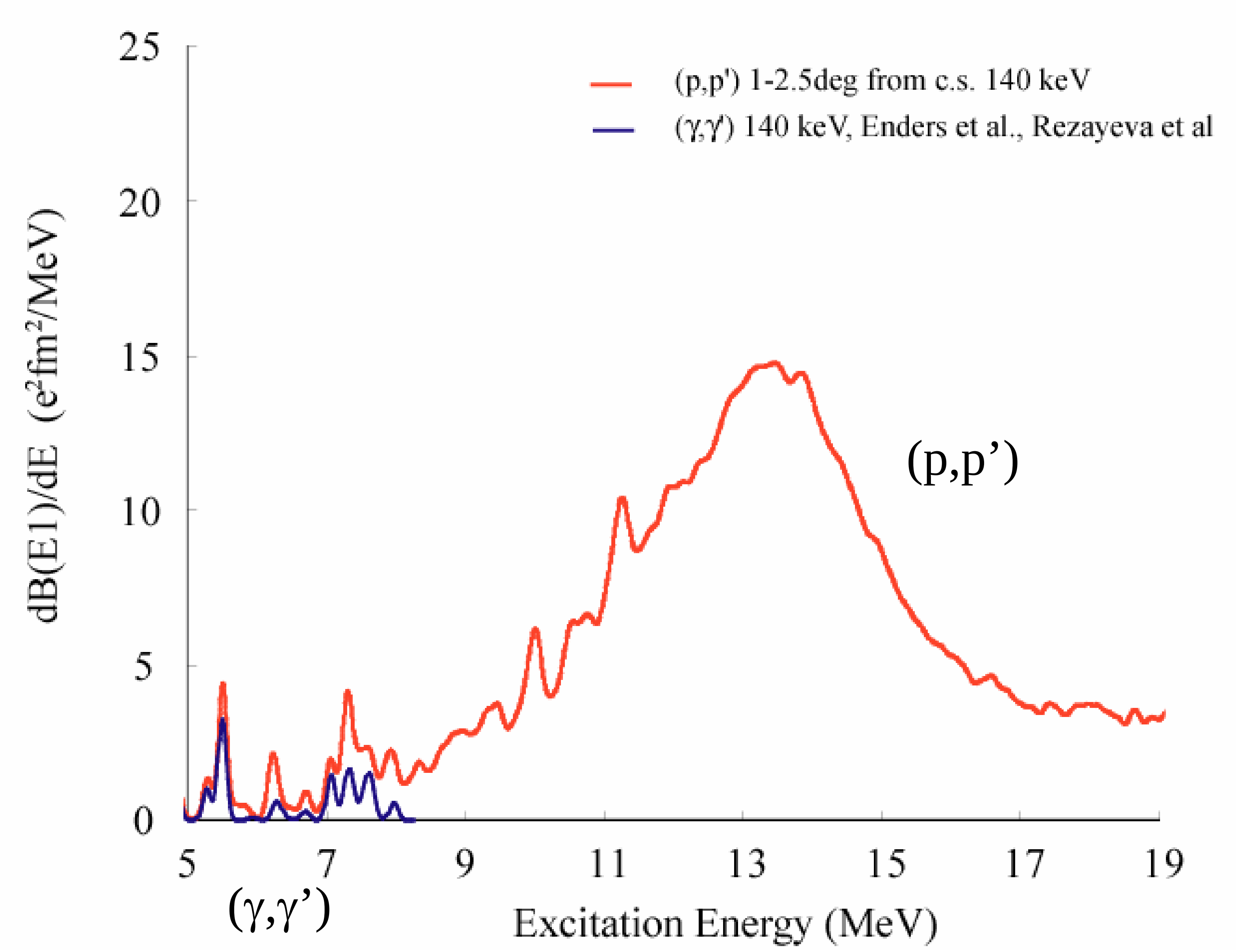

Comparison of B(E1) Strength Distribution